MICROTUBULE ORGANIZATION

IN INTERNODAL CELLS OF

CHARACEAN ALGAE

BY

GEOFFREY OLIVER WASTENEYS

A THESIS SUBMITTED FOR THE DEGREE OF

DOCTOR OF PHILOSOPHY

OF THE AUSTRALIAN NATIONAL UNIVERSITY

NOVEMBER, 1988

Fig. 1.1. A young shoot of *Nitella tasmanica* grown for several days in the presence of the microtubule inhibitor oryzalin. The abnormal growth of these cells as spheres rather than as cylinders dramatically illustrates the importance of microtubules in plant cell morphogenesis.

STATEMENT

All research reported in this thesis
is original and my own,
except where acknowledgement is given,
and has not been submitted
for any other degree.

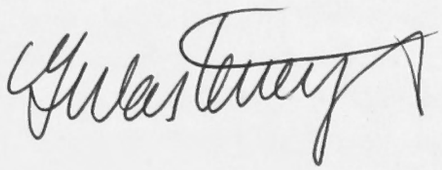

G. O. Wasteneys

This thesis is dedicated to the memory of my Grandfather,

Professor Hardolph Wasteneys,

for his valuable contributions to the field of Biochemistry,

for inspiring many others in similar pursuits,

and in recognition of his early years spent in Australia.

ACKNOWLEDGEMENTS

It has been a pleasure to be part of the Plant Cell Biology Group (formerly Developmental Biology) at the Research School of Biological Sciences. For this I am especially grateful to Brian Gunning who - despite a winter storm - flew in to snow-bound Ottawa for a few hours one day in February 1984 to tell me about his research group in Canberra. As one of my supervisors, he has provided helpful advice throughout the project. In particular, I would like to thank him for assistance with various software packages which provided an interesting diversion and for reading and commenting on parts of this manuscript.

My principal supervisor, Richard Williamson, provided an attractive research proposal and an excellent system to work with. I have greatly enjoyed our many worthwhile discussions throughout the project; his input was fundamental for the project's success. I also thank Richard for incredible expediency in reading this manuscript and for his "soft pencil" comments.

Adrienne Hardham was probably responsible for getting me interested in plant cells as far back as 1979. While demonstrating hand sectioning in a second year plant anatomy lab she was horrified by my roller skiing blisters and this incident led to an enduring friendship centered around cross country skiing and plant cells. In her capacity as advisor, Adrienne has readily dropped what ever she happened to be doing in order to discuss important revelations concerning cortical microtubules. In particular I wish to thank her for advice on thesis preparation and for commenting on that all important concluding chapter.

One of the highlights of this thesis is its quantitative approach. Meaningful presentation of many months worth of accumulated data required someone with a special talent for computing, especially for data transfer between incompatible systems. I am therefore greatly indebted to Michael Savage for his contribution of skill, time and energy to various aspects of this project. I am also grateful for his interest, encouragement and for the use of his computer.

Peter Jablonsky was responsible for tubulin purification and biotinylation procedures and for carrying out the turbidimetric assays. Having a resident biochemist and volleyball coach has been a great asset.

There are many others who have been of tremendous assistance, both during the course of research and in the preparation of this thesis. Some of them include: Ursula Hurley, for teaching me the famous perfusion technique and for accompanying me on numerous fishing trips for *Nitella*; Janet Gorst, for advice and encouragement throughout thesis preparation and for being an understanding tennis partner; Franz Grolig for help with electrophoresis work and for sharing ideas, new methods and an office; Jean Perkin, for showing me how to run gels; Brenda Ballentyne, for teaching me the ins and outs of Mass-11; Cathy Busby for advice on photographic plate preparation; Sally Stowe, for help with image analysis and for finally disposing of the Kontron; George Weston, for help with electron microscopy; Maureen Whittaker, Garry Hanson and James Whitehead of the photography unit for reproduction of photographic plates; Pat Wilkinson for organizing my financial matters - in spite of having an office decorated from floor to ceiling with paper work; Jadwiga Duniec, for Mowiol preparation; Jan Elliott for providing antibody supernatants; Ross Cunningham, for statistics advice; Dave Brown and Daina Simmonds for helpful discussions during the preparation of the manuscript; Anne Cleary for sharing her ideas on cell "corners"; John Harper, Ros Hoggart and Dave McCurdy for advice on thesis preparation; Mary Webb for careful proof-reading and finally, Moira Galway, for taking time during her holiday to read Chapter 5 and for many provocative conversations.

ABSTRACT

This thesis details an investigation of microtubule organization in a convenient experimental model - the giant internodal cells of the characean algae.

Two locally available, indigenous Australian charophytes, *Nitella tasmanica* and *Chara corallina* were chosen for this work. The internodal cells of these species were found to be particularly well suited for such studies on account of their large size, which allows an accurate growth assessment to be made and also makes them amenable to manipulations and microscopical examination. Their uniform and predictable growth as highly elongated cylinders implies an anisotropic wall texture which, in turn, may be governed by a highly ordered array of sub-plasmalemmal microtubules.

Immunoblotting extracts of internodal cells with a variety of antibodies verified the presence of tubulin, the major component protein of microtubules. An immunofluorescence technique, utilizing vacuolar perfusion was refined so that the distribution and arrangement of microtubules could be determined. This method enabled microtubules to be observed with a high degree of resolution, sufficient for quantitative analysis.

Microtubules were detected predominantly in the cortical cytoplasmic region between the chloroplast layer and the plasma membrane. Microtubules were also detected under the chloroplast layer, in the subcortical region occupied by the prominent actin cables and to some extent also associated with the numerous endoplasmic nuclei. Alignment of the subcortical microtubules in the same direction as the actin cables suggests some association between the two cytoskeletal elements. Anti-actin immunofluorescence also detected ring-like structures associated with nuclei but there was no evidence for any association between these elements and microtubules. Actin filaments were not observed in association with the cortical microtubule array.

In young, rapidly elongating cells, cortical microtubules were predominantly aligned perpendicular to the long axis. Microtubules were still present in older, non-growing cells but lacked any preferred orientation. Production of inner wall replicas for electron microscopy showed that the most recently deposited wall microfibrils had similar

arrangement to cortical microtubules in the same cells, that is, with transverse alignment in elongating cells and an apparently random organization in non-growing cells.

Using immunofluorescence and an image analyzer, the length and orientation of microtubules in *Nitella* internodal cells fixed at known stages of growth was described quantitatively. Microtubules were generally more numerous and of greater mean length in growing cells than in non-growing cells. The microtubules of the youngest, rapidly-growing cells, however, were shorter than those of older, more slowly growing cells. They also showed little sign of overlapping with other microtubules suggesting that maintenance of transverse orientation need not depend on intertubule cross-bridging. The median orientation of microtubules in young, rapidly growing cells was found to be truly transverse with respect to the cell's long axis and unrelated to the helix described by its major cytoplasmic features (the chloroplasts, actin cables and the direction of cytoplasmic streaming). The dispersal of microtubules about this angle gradually increased as the relative growth rate declined, supporting the view that microtubule orientating mechanisms may be regulated by the rate of cell growth. Non-growing cells had a slight preponderance of longitudinal microtubules that was most pronounced just after growth cessation.

A comparison of cortical microtubules in *Chara corallina* and *Nitella tasmanica* internodal cells showed a similar organization at most stages of development but considerable differences were detected during the period of growth cessation. Instead of increased dispersal of microtubules about the transverse axis as observed during this transition period in *Nitella*, *Chara* microtubules retained their local parallel order but became variously oriented in different regions of the cell such that the array became a mosaic of transversely-, obliquely- and longitudinally-aligned regions. The two cell types showed nearly identical morphogenetic development so the difference in microtubule organization may represent a diversity in alignment mechanisms.

The dynamics of microtubule assembly and alignment was assessed by following the reestablishment of the cortical array of *Nitella* internodal cells after inhibitor-induced disassembly. The plant tubulin-specific dinitroaniline herbicide oryzalin proved effective

for these experiments. Recovery was analyzed both qualitatively and quantitatively for young, rapidly elongating cells. This detailed analysis suggested that assembly and alignment may be separate processes and that the survival of some transversely-aligned microtubules is unnecessary for the reestablishment of transverse orientation. Comparing recovery in cells at different stages of development showed that the mechanism that operates to align microtubules transversely is only active in growing cells.

Microtubule assembly during recovery from oryzalin treatments occurred principally in the cortex but assembly was also detected in the endoplasm. Anti-tubulin-specific labelling of sites on the surface of nuclei suggested that microtubule-initiating material may be found at these locations. A semi-*in vitro* assay of microtubule assembly sites was subsequently carried out by perfusing *Nitella* internodal cells - depleted of their endogenous microtubule proteins - with tubulin purified from sheep brain tissue. Tubulin was supplied in a buffer that would only support microtubule assembly in the presence of specialized assembly-promoting sites or material. This procedure resulted in microtubule assembly in both the cortex and endoplasm, suggesting that initiating factors are present in both locations. This verified, for the first time, the existence of assembly promoting elements in plant cells.

The results described in this thesis are incompatible with some of the models that have previously been put forward to explain how the cortical microtubule arrays of plant cells could be organized. These aspects are highlighted in the concluding discussion and some alternate proposals are presented.

List of Abbreviations

ADP	Adenosine diphosphate
AMP	Adenosine monophosphate
ATP	Adenosine triphosphate
Ac-	acetylated
BSA	bovine serum albumin
CTP	cytidine triphosphate
DEAE	diethylaminoethyl
DMSO	dimethylsulfoxide
DNA	deoxyribonucleic acid
EDTA	ethylene diamine tetra-acetic acid
EGTA	ethylene glycol bis(β-aminoethylether) N, N, N',N'-tetraacetic acid
FITC	fluorescein isothiocyanate
GA	glutaraldehyde
GDP	guanosine diphosphate
glu-	detyrosinated (tubulin)
GTP	guanosine triphospate
h	hour
HeLa	line of human neoplastic (cervical) epithelial cells
HMW	high molecular weight
IgG	immunoglobulin g
kD	kilodalton
LMW	low molecular weight
l	liter
M	molar
M_r	relative molecular mass
mf	microfibril
MAb	monoclonal antibody
MAP	microtubule-associated protein
MT	microtubule
MTAB	microtubule assembly promoting buffer
MTOC	microtubule organizing center
MW	molecular weight
NAB	non-assembly buffer
O	oneiromancer
PAGE	polyacrylamide gel electrophoresis
PBS	phosphate buffered saline
PE	phycoerythrin
P_i	inorganic orthophosphate
PIPES	piperazine-N,N'-bis (2-ethane-sulphonic acid)
PS	perfusion solution
RNA	ribonucleic acid
SA	streptavidin
SDS	sodium dodecyl sulfate
TTC	tubulinyl-tyrosine carboxypeptidase
TTL	tubulinyl-tyrosine ligase
tyr-	tyrosinated
UTP	uridine triphosphate
UV	ultra violet

TABLE OF CONTENTS

CHAPTER 1

MICROTUBULE ORGANIZATION AND PLANT CELL DEVELOPMENT

IN PERSPECTIVE

1.1 PREAMBLE

Microtubule (MT) organization is relevant to several aspects of plant cell morphogenesis, from the demarcation of future division planes to the regulation of cell shape. Organization of MTs into parallel arrays near the plasma membrane is believed to coordinate a similar pattern of cellulose microfibril (mf) deposition which constrains the expansion of the cell wall in predominantly one direction. This process is fundamental in the growth of cells with specific shapes and ultimately contributes to the morphology of the particular tissue, organ and organism.

Major changes in emphasis in the field of MT research have resulted from a recently improved understanding of MT assembly and disassembly. These concepts provide an essential background for any study on MT organization but have not yet featured in the current models on how cortical MTs are organized in plant cells. Instead, these models are dependent on structural evidence from electron microscopy (reviewed by Gunning & Hardham 1982) and more recently from fluorescence microscopy (reviewed by Lloyd 1987). The primary objective of this introductory chapter is to outline the current concepts on MT assembly behaviour - with especial consideration for the most recent studies - as no such review is presently available. Plant MT research is also briefly discussed in terms of the organization of cortical arrays which are implicated in cell wall deposition and morphogenesis.

1.2 MICROTUBULE ORIGIN AND FUNCTION

The emergence of the nucleus in cells one billion years ago probably marked the beginning of MTs as they are known today. It is thought that the first eukaryotic MTs may have arisen through associations of proto-eukaryotes with spirochete bacteria, prokaryotes that possess MTs with tubulin-like subunits (Margulis *et al.* 1978). How spirochete MTs could have been acquired is not

completely clear. It has been suggested that if spirochetes were phagocytosed but not digested by their proto-eukaryote "hosts", their MTs could have become utilized in various cellular processes (Kunicki-Goldfinger 1980). Undulipodia (flagella and cilia) are thought to have developed from MTs and MTOCs already present and functioning in eukaryotic cells (Pickett-Heaps 1974; Cavalier-Smith 1975, 1978) or alternatively to have arisen through symbiosis between spirochetes and host cells (Margulis *et al.* 1979, 1981). Recently, Szathmary (1987) has proposed that cytoplasmic MTs may have been incorporated into proto-eukaryotic cells from phagocytosed spirochetes (Kunicki-Goldfinger 1980) whilst undulipodial MTs may have developed in a separate event from ectosymbiotic spirochetes.

From the time that MTs were first recognized as ubiquitous elements of eukaryotic cells (Slautterback 1963), many diverse functions - primarily of a motile nature - have been recognized. Locomotor functions of MTs include flagellar and ciliar activity, ameboid movement by bulk flow of cytoplasm and tissue cell movement. MTs are also involved in intracellular traffic regulation including meiotic and mitotic movement of chromosomes, endo- and exocytosis, positioning and transport of organelles, pigment distribution in melanophores, axonal transport in nerve cells and cytoplasmic streaming. Finally, MTs are involved in morphogenetic functions including the determination of division planes (in cytokinesis) and the establishment, maintenance and modification of cell shape and polarity.

1.3 PROPERTIES OF MICROTUBULES

1.3.1 Structure

Cytoskeletal elements can be identified from electron micrographs according to their appearance and size. In contrast to micro- and intermediate filaments whose diameters measure approximately 6 and 10 nm respectively, MTs appear as

hollow cylinders that are between 19 and 27 nm (McEwen & Edelstein 1980) in diameter (30 nm when X-ray diffraction analysis is used; Mandelkow *et al.* 1977), with a wall thickness between 5 and 7 nm. MT length, as determined from *in vitro* (Bonne & Pantaloni 1982) and *in vivo* measurements (Hardham & Gunning 1978; Bray 1979; Tsukita & Ishihawa 1981; Lloyd 1982) is generally in the order of 5 to 20 μm. The wall consists of a helical array of tubulin protofilaments, aligned in parallel; protofilaments can be distinguished in electron micrographs when tannic acid is included in the fixative (Mizuhira & Futaesaku 1972). The number of protofilaments per MT - easily determined from MT profiles - is commonly 13 but there are many exceptions both *in vitro* and *in vivo* (see review by Unger *et al.* 1986). MT-associated proteins (MAPs) adhere to the outer MT wall and can assume various configurations. A clear zone of at least 10nm separates MTs even when they are organized in bundles. This exclusion zone could be caused by electrostatic repulsion between tubulin of adjacent MTs or may be due to associated proteins projecting from the MT surface.

1.3.2 Tubulin

Tubulin, the major subunit protein of eukaryotic MTs, was first recognized for its binding affinity with colchicine, an alkaloid derived from the higher plant *Colchicum autumnale*. Colchicine was recognized for its anti-mitotic effect as early as 1889 (Pernice 1889; for historical review see Dustin 1984), a property that led to its use in karyotyping (Tjio & Levan 1956) and the production of polyploid plants (Blakeslee 1937). Interestingly, other colchicine-mediated effects such as shape changes in plant cells (Gorter 1945) appear to have received relatively little attention. Spindle fiber proteins were thus obvious binding sites for colchicine and this was confirmed by Taylor (1965) who suggested MTs could be the target. Isolation and characterization of a "colchicine-binding" protein (Borisy & Taylor 1967 a & b) and the discovery that the same protein was found in many non-

mitotic cells (Weisenberg *et al.* 1968) implicated MTs (by then recognized as ubiquitous organelles of diverse function - Slautterback 1963) as the source. The acceptance that the "colchicine-binding protein" was microtubular in origin (Shelanski & Taylor 1967) led to the adoption of the name "tubulin" (Mohri 1968).

Tubulin, is in fact a dimer with the α and β moieties present in MTs in equimolar amounts. α- and β-tubulin combine to form heterodimers, the functional units of MT assembly. These in turn link in series to form linear chains of alternating α- and β-tubulins known as protofilaments. The two tubulins have up to 50% homology in amino acid sequence (Ponstingl *et al.* 1983) which suggests that they are derived from a common ancestral protein. They are also similar in size; a molecular weight of about 50 kD has been determined from amino acid sequencing (Lemischka & Sharp 1982; Valenzuela *et al.* 1981). β-tubulin, with 445 amino acids has slightly greater mobility in SDS-PAGE (Bryan & Wilson 1971) than α-tubulin (450 amino acids) but the reverse occurs with plant tubulins (Morejohn & Fosket 1986). The carboxy terminal end of both α- and β-tubulin is extremely acidic, a feature that may be important for the binding of associated proteins (which are basic) and cations. In addition to specific sites that are involved in linkages within (longitudinal) and between (lateral) protofilaments, tubulins have binding sites for various agents influencing assembly including guanine nucleotides and MAPs (Vera *et al.* 1988) and also for MT poisons such as colchicine. Although the tubulins are remarkably conserved throughout evolution, many organisms possess several isoforms of both α- and β-tubulin. The functional implications of this phenomenon are discussed in section 1.4.10.

1.3.3 Microtubule-Associated Proteins

Microtubule-associated proteins (MAPs) and tubulin are related stoichiometrically and will co-purify through repeated cycles of assembly and disassembly *in vitro* (Borisy *et al.* 1975; Stearns & Brown 1979). MAPs are basic

molecules that adhere to the outer surface of the MT wall; they comprise a significant proportion (about 15 to 25%) of the overall MT structure (Hyams 1982). In some cases they form projections that may be involved in the spatial distribution of MTs or in cross-linking MTs with membranes, organelles, other cytoskeletal components (microfilaments, intermediate filaments and myosin) and other MTs. The role of MAPs in MT assembly and stability is discussed in section 1.4.9.

Just as tubulins have many isoforms, it is logical that MAPs could also show variations necessary for specialized MT properties in certain organisms and cell cycle-dependent functions. The potential variation of MAPs among different organisms is therefore very large. To date, MAPs have been characterized mainly in higher animal cells; the ubiquity of these particular MAPs in other organisms is therefore uncertain. MAPs may be isolated from MT protein extracts by high salt treatments and DEAE-Sephadex or phosphocellulose chromatography and categorized according to molecular weight. Accordingly, mammalian MAPs are divided into three major groups: the high molecular weight (HMW) MAPs (more than 200 kD), the low molecular weight (LMW) MAPs (28 to 30 kD) and the Tau fraction (58 to 65 kD). Two HMW MAPs have been characterized most extensively. MAP-1 (345 kD) is an elongated molecule that forms side arms *in vitro* (Vallee 1982) and is suggested to be a MT-membrane cross-linker. MAP-2 is a doublet molecule (286 and 271 kD) that is L-shaped, with the short arm connecting to and the long arm projecting from the MT wall. MAP-2 is credited with many functions including the interaction of MTs with micro- and intermediate filaments (Sattilaro *et al.* 1981; Griffith & Pollard 1982; Pollard *et al.* 1984; Yamauchi & Purich 1987; Yamauchi & Fujisawa 1988) and MT stabilization (Berkowitz & Wolff 1981; Schliwa *et al.* 1981). It binds strongly to phospholipids (Murthy *et al.* 1985) - which suggests that it may also be involved in the cross-linking of MTs to the plasma membrane - and it also appears to be phosphorylated

by protein kinases. The LMW MAPs probably are associated with MAP 1 and may modulate its function in the promotion of MT assembly (Vallee 1982). The Tau fraction consists of 5 proteins of similar molecular weight. They are elongated molecules that appear to be involved in MT assembly (Fellous *et al.* 1977; Weingarten *et al.* 1975; Murphy & Borisy 1975), stability (Berkowitz & Wolff 1981; Schliwa *et al.* 1981) and in cross-linking MTs with actin filaments (Griffith & Pollard 1982).

Some MT-binding proteins are ATP-sensitive and may be involved in motile processes. Dynein, for example, mediates mechanochemical interaction between adjacent subfibers of outer doublets of cilia and flagella, resulting in inter-MT sliding. A 300 kD protein with dynein-like properties has also been isolated from brain cell extracts (Koszka *et al.* 1987). It has been suggested that this protein could represent a cytoplasmic dynein variant. Kinesin is a 110 kD polypeptide that generates force along MTs in one direction (Vale *et al.* 1985a, 1985b; Porter *et al.* 1987; Saxton *et al.* 1988) and may be involved in axonal transport. A HMW polypeptide, designated HMW4 (Hollenbeck & Chapman 1986) could be responsible for axonal transport in conjunction with kinesin.

Several novel MAPs have recently been isolated from brain tissue (Parysek *et al.* 1984; Huber *et al.* 1986; Riederer *et al.* 1986; Koszka *et al.* 1987) and also from other sources (Gard & Kirschner 1987; Vale & Toyoshima 1988). At least three tubulin-binding proteins have been detected in extracts of mung bean (P. P. Jablonsky, personal communication). One of these is a 125 kD polypeptide that is implicated in the bundling of MTs (Cyr & Palevitz, in press). The other two are of low molecular weight, one in the 70 to 75 kD range, another is a dimeric polypeptide of 66 kD (33 kD monomers). It has been speculated that this latter MAP may have MT organizing properties (see section 1.6). Whether any plant MAPs resemble the MAPs characterized in mammalian tissue is uncertain but Jablonsky has recently isolated a polypeptide with MT binding properties from

Chara using SDS-PAGE purification that appears to have a molecular weight greater than 150 kD.

1.4 MICROTUBULE ASSEMBLY

1.4.1 Nucleation and Condensation

The formation of MTs involves the polymerization of tubulin subunits in concert with associated proteins in a complex process that can be divided into two major steps, nucleation and condensation. Nucleation is a slow reaction involving the coming together of tubulin subunits accompanied by associated proteins to provide a MT 'seed', capable of further end-wise addition of subunits by the second condensation reaction. Nucleation may also be used somewhat confusingly to refer to the growth of MTs from existing MT seeds or from non-MT nucleating sites (the so called MT organizing centers of many cells). In this case, the initiation of assembly will occur much more rapidly as condensation can start immediately. Assembly will be limited by the number of nucleating sites available. That elongation can not occur without a prior nucleation event ensures that functionally-sound MTs are constructed. Unrestricted condensation would lead to haphazard polymerization, resulting in aberrant structures that are incapable of normal behaviour.

The relative activities of nucleation and condensation determine an important parameter of MT populations: the ratio of MT number to polymer length. With subunit concentration relatively constant, increased incidence of nucleation would increase the total number of MTs but average MT length would decline. Alternatively, an increase in condensation reactions under similar conditions would result in fewer MTs of increased average length.

1.4.2 *In Vitro* Assembly

The discovery that tubulin, extracted from various sources, is capable of re-assembly *in vitro* (Weisenberg 1972) has greatly improved our understanding of many aspects of the MT assembly process. Because the simulated physiological conditions can be easily controlled, it is possible to determine how various factors that are important in MT assembly operate. Moreover, the structural aspects of the assembly process can be followed with microscopy, turbidimetry and X-ray diffraction to provide a detailed description of the structural events that take place.

Assembly of MTs *in vitro* is characterized by three phases: an initial lag phase involving nucleation, followed by a period of elongation in which MT length undergoes rapid increases and finally an equilibrium phase or steady-state in which MTs undergo both elongation and shrinkage. In addition to tubulin dimers and MT polymers, intermediate assembly products have been identified. These include closed rings (Pantaloni *et al.* 1981) composed of tubulin and MAPs (Kirschner *et al.* 1974; Weingarten *et al.* 1975; Vallee & Borisy 1978) and short, protofilament-like fragments (Mandelkow *et al.* 1980) or oligomers. From X-ray diffraction analysis, it has been established that the ring structures are not the basic MT template from which elongation can proceed. Instead, rings appear to break down into oligomers that subsequently form MT seeds (Mandelkow *et al.* 1980), presumably by lateral bonding and the attachment of associated proteins.

1.4.3 *In Vitro* Assembly Conditions

In vitro experiments have established that MT assembly is only possible within a very narrow range of conditions. The essential requirements include an adequate tubulin concentration, the presence of MAPs or non-physiological stabilizers, sufficient GTP and Mg^{2+} and a low concentration of Ca^{2+}. Temperature, pH and ionic strength are also important factors for *in vitro* MT assembly. Assembly occurs optimally around pH 6.9 and deviation from this

condition leads to disassembly (Regula *et al.* 1981) or unusual MT structure (Matsumura & Hayashi 1976; Burton & Himes 1978). Temperature affects both kinetic (Barton *et al.* 1987) and structural aspects of MT assembly (Pierson *et al.* 1979; Mandelkow *et al.* 1980). At low temperatures, abnormal assembly products are usually produced but by increasing the temperature, MT nucleation and 'normal' assembly can proceed (Bordas *et al.* 1983; Mandelkow *et al.* 1988). Conversely, sudden temperature drops cause rapid disassembly. Similar temperature-mediated effects would be expected to occur *in vivo* yet there are many organisms that maintain normal MT behaviour in a wide range of temperatures. It is presumed in these cases that factors such as glycerol enable MT arrays to assemble and operate under extreme conditions.

Ionic strength must be carefully regulated. Monovalent salts at high concentrations reduce electrostatic interactions between MAPs and oligomeric and polymeric tubulin. This alters the stability (Marcum & Borisy 1978; Vallee 1982) and the assembly kinetics (Barton *et al.* 1987) of MTs. Calcium ions can destabilize MTs (see section 1.4.8) so ethylene glycol bis (β-amino ethyl ether) N, N, N^1, N^1-tetraacetic acid (EGTA) is included in assembly buffers to chelate most of the Ca^{2+}.

Other agents that affect MT assembly include glycerol, dimethyl sulphoxide (DMSO) and taxol which can all be used to promote polymerization in the absence of MAPs. Glycerol occurs naturally in some cold- and salt-tolerant algae where it is believed to impart MT stability at very low temperatures by decreasing the rate of assembly and disassembly (Keates 1980). Its action is thought to be mediated through changes in thermodynamic interactions by the displacement of H_2O molecules (Lee & Timasheff 1977; Na & Timasheff 1981). *In vitro*, glycerol allows assembly to proceed in MAP-free extracts (Na & Timasheff 1981) but may also produce abnormal assembly products such as double rings and tubulin sheets (Matsumura & Hayashi 1976). Similar aberrant assembly is elicited with DMSO

(Himes *et al.* 1976, 1977; Burton & Himes 1978; Mandelkow & Mandelkow 1979); this property has been exploited for determining the polarity of MTs through the attachment of C-shaped tubulin sheets to MT walls (Heidemann & McIntosh 1980; Euteneuer & McIntosh 1980). Taxol stimulates assembly and imparts stability by lowering the critical concentration of tubulin that is necessary for nucleation (Schiff *et al.* 1979). It too affects MT morphology; MTs with reduced protofilament number (Böhm et al 1984) or with C- and S-shaped tubulin sheets (Schiff *et al.* 1979; Vater *et al.* 1983) are usually formed.

1.4.4 Tubulin Concentration

Tubulin concentration is an important factor in MT assembly whose rate is proportional to the concentration of tubulin dimers in solution. Promotion of MT assembly *in vitro* requires a critical tubulin concentration of about 1 mg/ml under otherwise favorable conditions (Olmsted *et al.* 1984). *In vivo*, there is a constant balance between MTs and unpolymerized subunits. Thus, a cell can control the assembly status of its MTs by regulating the amount of unpolymerized tubulin. If there is a limited number of nucleating centers, MT length will be proportional to the number of tubulin dimers available for assembly. Tubulin concentration, however, is not wholly dependent on its rate of synthesis and denaturation but can be modulated by a variety of mechanisms which can operate very rapidly to alter the assembly competence of the tubulin subunits. Specialized sites known as MT organizing centers (MTOCs) may also exist that can promote localized MT assembly perhaps by reducing the critical tubulin concentration (see section 1.6).

1.4.5 Magnesium

Magnesium is an important cofactor in the promotion of MT nucleation (Martin *et al.* 1987) and assembly. There is at least one Mg^{2+}-binding site per tubulin dimer (Olmsted & Borisy 1975; Monasterio 1987), but extra (up to 48)

magnesium ions may be required for tubulin polymerization (Olmsted & Borisy 1975; Lee & Timasheff 1975; Himes et al 1977; Luduena 1979). Mg^{2+} is involved in the guanine nucleotide cycle (see section 1.4.6) and thus plays a role in regulating the MT assembly/disassembly process. Magnesium is also important for controlling MT morphology (Carlier & Pantaloni 1978; Heusele *et al.* 1987). Other divalent cations (Mn^{2+}, Co^{2+} and Zn^{2+}) can substitute for Mg^{2+} (Buttlaire *et al.* 1980; Himes *et al.* 1982) but in the case of Zn^{2+} and Co^{2+}, the assembly products may be abnormal. Changes in interprotofilament bonding in the presence of Zn^{2+} (Larsson *et al.* 1976; Gaskin & Kress 1977; Eagle *et al.* 1983) and the formation of broad sheets in Zn^{2+} or Co^{2+} (Wallin *et al.* 1977; Haskins *et al.* 1980) suggest that Mg^{2+} may play a role in the lateral bonding of protofilaments.

1.4.6 The Guanine Nucleotide Cycle

MT assembly is closely coupled to the guanine nucleotide cycle. *In vitro* studies have shown that guanosine tri-phosphate (GTP) is required for assembly and that GDP has an inhibitory effect (Jameson & Caplow 1980; Martin & Bayley 1987), causing disassembly in a manner similar to that induced by colchicine (Carlier & Pantaloni 1982). The hydrolysis of GTP is therefore implicated in the regulation of MT assembly and disassembly.

Tubulin dimers contain two guanine nucleotide binding sites (Weisenberg *et al.* 1968). One site is non-exchangeable and does not appear to be involved in the assembly process (Kobayashi 1975; Jacobs 1979; Weisenberg 1981); GTP remains unhydrolyzed throughout repeated cycles of assembly and disassembly (Kobayashi 1975; Penningroth *et al.* 1976). The second site, located on the β-tubulin molecule (Geahlen & Haley 1979; Hesse *et al.* 1987), can bind and readily exchange either GTP or GDP (Levi *et al.* 1974; Jacobs & Caplow 1976). This latter site, known as the exchangeable GTP-binding site (or E-site), plays an important role in the MT assembly process. Other nucleotides such as ATP, UTP and CTP show almost no

affinity for this site. The Mg^{2+} binding site is very close to the E-site (Jemiolo and Grisham 1982), and Mg^{2+} forms a metal-nucleotide complex with GTP (Monasterio 1987) that activates GTPase (David-Pfeuty & Huitorel 1980), thereby promoting hydrolysis. The Mg^{2+} concentration can affect the relative affinity of tubulin for GTP or GDP (Correia *et al.* 1987) so theoretically Mg^{2+} can control the rephosphorylation process as well.

Changes in the assembly state of tubulin may be correlated with the cyclical process of GTP hydrolysis and rephosphorylation. Tubulin-GTP is hydrolyzable only after it has been polymerized (Hamel *et al.* 1982) whereas tubulin-GDP can be rephosphorylated (by exchange with GTP) only when in its soluble, dimeric form (Jacobs *et al.* 1974; Zeeberg *et al.* 1980; Caplow *et al.* 1982; Carlier *et al.* 1987; Monasterio & Timasheff 1987). The active unit for nucleation and polymerization is tubulin-GTP (Maccioni & Seeds 1983; Karr *et al.* 1979b) and although GTP hydrolysis accompanies polymerization (Weisenberg *et al.* 1976; Carlier & Pantaloni 1978), hydrolysis is not a requirement for polymerization. Assembly of MTs is not prevented when GTP is replaced with nonhydrolyzable analogues (Gaskin *et al.* 1974; Olmsted & Borisy 1975; Weisenberg *et al.* 1976; Arai & Kaziro 1977; MacNeal & Purich 1978; Penningroth & Kirschner 1977; Sandoval *et al.* 1978; Terry & Purich 1980; Cote & Borisy 1981; Margolis 1981; Maccioni & Seeds 1982; Monasterio & Timasheff 1987), although it does proceed at a much slower rate. If hydrolysis of tubulin-GTP is not necessary for the assembly process, why does it accompany polymerization? It appears that GTP hydrolysis is necessary for subsequent disassembly (Weisenberg and Deery 1976; Purich *et al.* 1982; Kirsch & Yarlbrough 1981). When hydrolysis is prevented with the incorporation of nonhydrolyzable analogues, disassembly of MTs is greatly inhibited (Arai & Kaziro 1977; MacNeal & Purich 1978; Sandoval *et al.* 1978; Sandoval & Weber 1979). Thus, while hydrolysis of tubulin-GTP is not necessary

for polymerization, it may release the subunit from its assembly-competent configuration (Maccioni & Seeds 1983) so that dissociation is possible.

Since tubulin-GDP subunits depolymerize two to three orders of magnitude faster than tubulin-GTP subunits (Carlier 1988), it is likely that the presence of unhydrolyzed GTP-tubulin forming a cap at the end of a MT would stabilize against MT disassembly. The prediction from a mathematical model for kinetic parameters of GTP capping (Hill & Carlier 1983) that the rate of MT elongation should not increase linearly with increasing monomer concentration (Oosawa & Kasai 1962) but instead should show a phase transition at critical concentration, has been confirmed experimentally (Carlier *et al.* 1984). GTP capping may thus provide the control for phase transitions between growing and shrinking MTs that is central to current ideas of MT dynamics (Mitchison & Kirschner 1984b). Under steady state conditions, the presence of terminal GTP subunits would prevent MT disassembly but below a critical tubulin-GTP concentration, the unstable GDP core would be exposed, resulting in catastrophic disassembly (McIntosh 1984). *In vivo* behavior of MTs would of course be more complex than the above scenario because MAPs are present.

The timing of GTP hydrolysis in relation to tubulin polymerization is critical to the mechanism of GTP capping. If GTP is hydrolyzed slowly and at random throughout the tubulin-GTP domain of the MT as proposed by Hill and Carlier (1983), hydrolysis will be uncoupled from elongation at all tubulin concentrations. This is because the rate of GTP hydrolysis should increase according to the number of tubulin-GTP subunits being added so that at any given tubulin concentration that permits elongation, a GTP cap will have a constant size. Some early studies supported this concept (Pollard & Weeds 1984; Carlier *et al.* 1984) but more recent work has favored an alternate model whereby hydrolysis occurs only at the interface between the GTP cap and the GDP core (Caplow *et al.* 1985). This model predicts that hydrolysis should occur at a rate independent to that of

elongation so that apparent coupling of hydrolysis and elongation should be expected at low tubulin concentrations (*i.e.*, when elongation is slower than GTP hydrolysis). At higher tubulin concentrations, uncoupling of the two reactions should become increasingly apparent. This model also predicts a small GTP cap at low tubulin concentrations and an increasingly larger cap as the rate of elongation increases. The results of Carlier and co-worker's attempts to measure the rates of MT elongation and accompanying GTP hydrolysis simultaneously (Carlier & Pantaloni 1985; Carlier *et al.* 1987) favor this model and suggest that MT stability is linked to the relatively strong interaction between tubulin-GDP and tubulin-GTP subunits at the elongating site (Carlier *et al.* 1987). In apparent contrast, other researchers have detected no lag at any tubulin concentration and suggest that if uncoupling of polymerization and hydrolysis does exist, it would be too small to measure either during elongation or at steady state (Obrien *et al.* 1987; Schilstra *et al.* 1987). Thus, GTP capping might be limited to the outermost layer of tubulin subunits (Obrien *et al.* 1987). If GTP hydrolysis is more closely coupled to tubulin polymerization than Carlier *et al.* estimated, other mechanisms might be involved in phase transitions between MT assembly and disassembly. In this context, the possible uncoupling of the release of P_i from GTP hydrolysis and the resultant formation of transient tubulin-GDP-P_i complexes with altered structural and thermodynamic characteristics (Carlier 1988) could be significant.

1.4.7 Cyclic AMP

The effects of adenosine triphosphate (ATP) on MT assembly *in vitro* include MT destabilization (Olmsted & Borisy 1975; Jameson & Caplow 1980) promotion of MT polymerization (Olmsted & Borisy 1973; Penningroth & Kirschner 1977; Jacobs & Huitorel 1979), an increase in the rate of treadmilling[1] (Penningroth &

---

1. Treadmilling is a model whereby tubulin subunits are incorporated at one end of the MT and eventually dislodged at the other end. See section 1.5.2.

Kirschner 1977; Margolis & Wilson 1979) and the formation of tubulin rings (Zabrecky & Cole 1980). ATP can favor MT assembly despite not having a binding site (Jacobs *et al.* 1974; Jacobs & Caplow 1976). One action of ATP that would favor assembly is its role as a substrate for a MAP-based transphosphorylase enzyme to increase the rate of GDP rephosphorylation (Jacobs & Huitorel 1979). The activation of ATP-dependent protein kinase can phosphorylate MAPs (Terry & Purich 1979) and weaken tubulin-MAP interactions. This could destabilize MTs (Jameson *et al.* 1980; Vallee 1980; Murthy & Flavin 1983), leading to MT disassembly or - given the appropriate conditions - an increase in tubulin turnover and hence, the rate of treadmilling (Margolis & Wilson 1979). In some cases, ATP reacts with tubulin in a site-specific manner (White *et al.* 1980) that does not imply competition for the GTP binding sites (Zabrecky & Cole 1982). Such binding could explain the formation of tubulin rings and other unusual *in vitro* assembly products.

1.4.8 Calcium and Calmodulin

The sensitivity of MT assembly to Ca^{2+} apparently involves the calcium regulatory protein calmodulin. Calmodulin's association with MTs, which is apparent *in vivo* (DeMey *et al.* 1980), has been suggested to be due to a specificity for tubulin (Kumagai & Nishida 1979; Nishida *et al.* 1979) or for the Tau fraction proteins (Kakiuchi & Sobue 1981; Sobue *et al.* 1981). Ca^{2+} on its own inhibits MT assembly *in vitro* and has several tubulin-binding sites including one that appears to be competitively inhibited by Mg^{2+} (Hayashi & Matsumura 1975). Ca^{2+} is thus a powerful regulator of MT assembly and could effectively control MT assembly at a subcellular level by mechanisms such as localized Ca^{2+} currents as suggested by Gunning & Hardham (1982).

1.4.9 Microtubule-Associated Proteins

The inability of MAP-free tubulin to polymerize *in vitro* without glycerol, DMSO or other non-physiological agents implies that MAPs are required for the MT assembly process. The function of various MAPs has been explored mainly by *in vitro* assembly experiments. Isolated MAPs are incorporated into solutions of purified tubulin to observe their effects on tubulin polymerization and MT structure. The recent development of monoclonal antibodies against various brain MAPs (Asai *et al.* 1985; Huber *et al.* 1986; Matus *et al.* 1987) offers a novel approach for studying MAP function. Antibodies may be used *in vitro* or injected into living cells. The role of a particular MAP can be interpreted from the effects of an antibody specific for that MAP on MT function.

MAPs appear to have the ability to control the morphology of MTs. Given appropriate conditions, tubulin can polymerize *in vitro* without MAPs but the assembly products are unlikely to resemble normal MTs (Waxman *et al.* 1981). Inter-tubulin and inter-protofilament bonding does not seem to be controlled by MAPs (Gaskin & Kress 1977) but MAPs do appear to be able to control the lattice structure of MTs. This has been inferred from the observation that during tubulin purification procedures, as MAPs are degraded or lost through successive cycles of disassembly and reassembly, an increasing proportion of MTs with less than 13 protofilaments are assembled (Pierson *et al.* 1978). Just as MAPs induce the ring-like closure of oligomers and MTs (Weingarten *et al.* 1975; Vallee & Borisy 1978), they could control the protofilament number by affecting the curvature of MT walls (Amos 1979; Böhm *et al.* 1984).

It is still not clear how the various MAPs contribute to MT assembly but it seems plausible that they may enhance the stability of MTs by reducing the rate of subunit dissociation. *In vitro* experiments have indicated that MAPs can quantitatively suppress both dynamic instability and treadmilling (see section 1.5.2) behaviours (Farrell *et al.* 1987). Job *et al.* (1985) have suggested that a

steady state population of MTs that is partially depleted of MAPs consists of MAP-free MTs which are unstable and MTs associated with MAPs that are relatively stable. Early experiments with MAPs suggested that the Tau proteins were responsible for promoting MT assembly (Weingarten *et al.* 1975; Murphy & Borisy 1975; Fellous *et al.* 1977) but that HMW MAPs had no such effect (Fellous *et al.* 1977). More recent evidence suggests that in addition to the Tau proteins, MAP-2 can also be an important mediator of MT assembly.

Both the Tau proteins and MAP-2 have been shown to favor MT assembly (Stearns & Brown 1979) and to stabilize brain MTs against Ca^{2+}-destabilization (Schliwa *et al.* 1981). Tau proteins seem to be specifically involved in stabilizing the longitudinal bonds between tubulin dimers in protofilaments (Nagle *et al.* 1977; Luduena *et al.* 1981). The specific action of MAP-2 is unclear but treatment of living cells with anti-MAP-2 by microinjection caused inhibition of tubulin polymerization as well as MT bundling and the formation of irregular, shortened filaments (Matus *et al.* 1987). The inhibitory action on MT assembly of phosphatidylinositol may be due to this phospholipid's strong binding affinity to MAP-2 (Murthy *et al.* 1985). Weakening of interactions between MTs and MAP-2 (Yamauchi & Purich 1987) would account for resultant increases in the apparent critical concentration for assembly. Interestingly, phosphatidylinositol appears to have no effect on the cross-linking properties of Tau proteins (Yamauchi & Purich 1987).

The role of MAP-1 in MT assembly remains unclear. Whereas Villasante *et al.* (1980) demonstrated that removal of MAP-1 from tubulin preparations had no effect on polymerization, others have claimed that it does promote MT assembly (Kuzetsov *et al.* 1981; Vallee 1982). It has been suggested that LMW MAPs are associated with the function of MAP-1 since their removal from tubulin preparations in the presence of MAP-1 leads to an increase in the rate of tubulin polymerization (Vallee 1982). Thus LMW MAPs could modulate the ability of

MAP-1 to promote MT assembly. The difficulty assessing the activity of MAP-1 could be because, as a very large molecule, it is easily degraded - and possibly inactivated - during purification procedures. This problem can be overcome with antibody microinjection experiments in living cells. Treatment with one antibody for MAP-1 revealed no change in MT assembly activity (Matus *et al.* 1987), supporting the opinion that MAP-1 does not play a role in MT assembly. The same technique has recently been applied to examine the function of some novel HMW brain MAPs. Consequently, both MAP-3 (Huber *et al.* 1986) and MAP-5 (Riederer *et al.* 1986; Matus *et al.* 1987) have been implicated in tubulin polymerization.

1.4.10 Tubulin Heterogeneity

(i) Multi-Gene Families

Tubulins of diverse species are remarkably conserved. Heteropolymers can be formed *in vitro* and heterologous antibodies have a high degree of cross-reactivity with tubulins from a wide range of organisms. On the other hand, heterogeneity of tubulin within single organisms has been demonstrated using several criteria including electrophoretic mobility, amino acid sequence, proteolytic cleavage patterns, drug-binding affinity and antibody specificity (Cleveland & Sullivan 1985). Fulton and Simpson's multi-tubulin hypothesis (1976) proposed that differences in properties of tubulin could be reflected in the MTs that they assemble. There are now many examples of multiple tubulin genes encoding unique tubulin isotypes (for review see Cleveland 1983) but only limited evidence that such isotypes are functionally distinguishable (Gard & Kirschner 1985; Edde *et al.* 1981). In some systems, it has even been demonstrated that all classes of MTs can be assembled from every available tubulin isotype (Kemphues *et al.* 1982; Joshi *et al.* 1987). Thus, Raff (1984) has proposed that multiple isotypes are functionally equivalent but represent the products of duplicated genes which have

evolved to possess different regulatory sequences for activation of transcription during alternative programs of differentiation. Although some of the more recent evidence favors the latter hypothesis, the idea that subtle differences in polypeptides could manifest functional distinctiveness to MTs can not be ruled out.

(ii) Posttranslational Modification

Posttranslational modification has been suggested to be another way of changing the properties of tubulin and ultimately, of MTs. Phosphorylation, tyrosinolation (hereafter referred to as tyrosination) and acetylation have all been implicated as examples of post-translational changes that could affect MT properties. The best documented of these is tyrosination. Tyrosination and detyrosination occur by the cyclical addition and removal of a tyrosine residue at the carboxy terminal position of the α-tubulin molecule. The observation that detyrosinated tubulin is relatively abundant in MTs that are stable has led to speculation that tyrosination and detyrosination may be involved in the assembly properties of tubulin. The research has been facilitated by the identification of two enzymes involved in the cycle (Arce *et al.* 1978; Argaraña *et al.* 1980; Kumar & Flavin 1981) and the development of antibodies with specificity for tyrosinated (Kilmartin *et al.* 1982) and detyrosinated α-tubulin (Gundersen *et al.* 1984; Wehland & Weber 1987; Kreis 1987).

When α-tubulin is initially synthesized, it is tyrosinated in all but a few cases (*e.g.*, Monteiro & Cox 1987). Subsequently, repeated cycles of detyrosination and retyrosination can take place. Tubulin dimers that are in the detyrosinated form (Glu-tubulin) undergo rapid tyrosination, a reaction that requires ATP hydrolysis and is catalyzed by the enzyme tubulinyl-tyrosine ligase (TTL). TTL acts principally on unassembled tubulin dimers (Arce *et al.* 1978). In contrast, the enzyme responsible for detyrosination, tubulinyl-tyrosine carboxypeptidase (TTC), shows preference for MT-bound subunits (Kumar & Flavin 1981). It has been

proposed that if only Tyr-tubulin can undergo polymerization, the rate of tyrosination, regulated by TTL, could determine the size of the assembly-competent tubulin pool and thereby regulate MT assembly. Evidence has shown, however, that Glu- and Tyr-tubulins have equal propensity to polymerize into MTs both *in vitro* (Raybin & Flavin 1977; Arce *et al.* 1978; Kumar & Flavin 1982) and recently, *in vivo* (Webster *et al.* 1987a). By default, Tyr-tubulin is the major assembly-competent isotype because TTL appears to retyrosinate unassembled tubulin very rapidly. Detyrosination, in contrast, is a relatively slow reaction (Wehland & Weber 1987) and is therefore more likely to be the rate limiting step in the tyrosination-detyrosination cycle.

Although tyrosination does not by itself regulate MT assembly, there is evidence that other mechanisms exist that can affect the assembly competence of tubulin. A Ca^{2+}/calmodulin-activated protein kinase phosphorylates the carboxy-terminal region of both α- and β-tubulin and subsequently prevents polymerization (Wandosell *et al.* 1986). Insulin receptor kinase can also phosphorylate tubulin (Kadowaki *et al.* 1985). Wandosell and co-workers have shown that this enzyme specifically phosphorylates the terminal tyrosine residue of α-tubulin and that when this occurs, the tubulin is rendered non-polymerizable. When Glu-tubulin is treated with insulin receptor kinase, other tyrosine residues are apparently phosphorylated and assembly is not prevented; clearly tubulin must be tyrosinated so that this enzyme can be effective. Although tubulin tyrosination may not on its own determine assembly competency, it may be an important feature of complex mechanisms that regulate MT assembly for specific functions throughout the cell cycle.

Glu-tubulin is found predominantly in older, more stable MTs whereas MTs that are newly assembled or exhibiting rapid turnover contain mainly Tyr-tubulin (Gundersen *et al.* 1984; Gundersen & Bulinski 1986a, 1986b; Schulze & Kirschner 1986; Webster *et al.* 1986; Gundersen *et al.* 1987; Webster *et al.* 1987b; Kreis

1987; Sherwin *et al.* 1987). Stabilization of MTs with the drug taxol has been shown to cause elevated levels of Glu-tubulin (Wehland & Weber 1987) suggesting that detyrosination could be a consequence of stable MTs. It has also been suggested that detyrosination could be part of the mechanism that imparts stability to selected MTs. For example, the removal of tyrosine from tubulin could allow the binding of a MAP that would inhibit disassembly (Burns 1987). This proposal is particularly attractive because it involves a modification of the acidic region of the tubulin molecule - a putative location of tubulin- MAP interaction.

The idea that detyrosination can affect the stability of MTs is less credible in light of recent evidence that although MTs containing Glu-tubulin are more resistant to drug-induced disassembly, they show no difference in susceptibility to cold treatments (Khawaja *et al.* 1988). Khawaja and co-workers (1988) also demonstrated that treatment of cells with an exogenous supply of carboxypeptidase (to induce detyrosination) did not alter the resistance of the MTs toward dilution-induced disassembly. Finally, there are examples of cells lacking Glu-tubulin in which sub-populations of stable MTs have been detected (Gundersen & Bulinski 1986b; Khawaja *et al.* 1988). The possibility thus emerges that stable MTs could be enriched with glu-tubulin simply because there is more time for detyrosination to take place and that their resistance to disassembly is mediated by some other property.

Acetylated α-tubulin (Ac-tubulin) was first recognized in axonemal MTs of *Chlamydomonas* flagella (L'Hernault & Rosenbaum 1983) and has subsequently - with the use of a monoclonal antibody specific for acetylated α-tubulin (Piperno & Fuller 1985) - been detected in a number of other organisms (Piperno & Fuller 1985; Diggins & Dove 1987; Piperno *et al.* 1987; Sasse *et al.* 1987; Sale *et al.* 1988). Acetylation, thought to involve the ε-amino group of a lysine residue (L'Hernault & Rosenbaum 1985a), is a reversible reaction (L'Hernault &

Rosenbaum 1985b) like detyrosination that arises primarily in polymerized tubulin (Piperno *et al.* 1987; Bulinski *et al.* 1988).

In *Chlamydomonas*, Ac-tubulin is found in axonemes, basal bodies and a subset of sub plasma membrane MTs radiating from the basal bodies (LeDizet & Piperno 1986). In Physarum, Ac-tubulin is present in the flagellate and myxamoebal stages (in flagella and MTOCs respectively) but has not been detected (with immunofluorescence or immunoblotting) in the short-lived MTs of the plasmodial stage (Diggins & Dove 1987; Sasse *et al.* 1987). Similarly, Ac-tubulin of certain (but not all - see Piperno *et al.* 1987) mammalian tissue culture cells has been identified in the relatively stable MTs of cilia and centrioles, and in a sub-population of MTs in the mitotic spindle and mid-bodies (Piperno *et al.* 1987). Thus, acetylation is a property that - like detyrosination - is often associated with MTs that are relatively stable. High levels of Ac-tubulin can be induced by treating cells with taxol (Piperno *et al.* 1987) and like detyrosinated MTs, acetylated MTs display resistance to nocodazole and colchicine (Piperno *et al.* 1987; Sale *et al.* 1988). Interestingly, acetylated MTs are not resistant to cold-induced disassembly (Piperno *et al.* 1987).

Since acetylation and detyrosination are both reversible postpolymerization reactions and are associated with increased MT stability it is not surprising that co-distribution of Ac-tubulin and Glu-tubulin has been detected in some cell types (Geuens *et al.* 1986; Cambray-Deakin & Burgoyne 1987; Schulze *et al.* 1987; Bulinski *et al.* 1988). It must be noted, however, that there are many examples of cells with stable MTs that have only one or other type of posttranslational modification (Bulinski *et al.* 1988; Khawaja *et al.* 1988) and in cells that have both types, differences in their patterns of accumulation after mitosis or disassembly suggest the two forms of modifications are controlled by independent mechanisms (Bulinski *et al.* 1988). Therefore, the suggestion that co-ordinated detyrosination

and acetylation plays a role in the maintenance of stability (Cambray-Deakin & Burgoyne 1987), seems unjustified.

1.5 MICROTUBULE DYNAMICS

1.5.1 Microtubule Polarity

The alternation of α- and β-tubulins along protofilaments and the uniform alignment of protofilaments within MTs implies an intrinsic structural polarity. This polarity has functional implications. Motile process, including mitosis (Heidemann & McIntosh 1980; Euteneuer & McIntosh 1980; Telzer & Haimo 1981), inter-MT sliding (Haimo *et al.* 1979; Satir *et al.* 1981; Euteneuer & McIntosh 1981a), organelle translocation (McNiven *et al.* 1984; McNiven & Porter 1986) and pigment transport (Euteneuer & McIntosh 1981a) exhibit polarity. The orientation of the uniformly-spaced dynein arms that extend flagellar and ciliar MTs is a precise indicator of MT polarity (Haimo *et al.* 1979; Satir *et al.* 1981); decorating the MTs of lysed cells with purified dynein can thus be used for determining their polarity (Telzer & Haimo 1981). Similarly, MT polarity can be determined by decorating MTs with curved sheets of tubulin protofilaments (Heidemann & McIntosh 1980; Euteneuer & McIntosh 1981 a, b; McNiven *et al.* 1984; McNiven & Porter 1986).

The intrinsic structural polarity of MTs is also reflected in MT growth. Whilst the rate of polymerization is proportional to tubulin concentration, the rate of dissociation is proportional to MT number (Johnson & Borisy 1977; Karr *et al.* 1980a, b). This implies that association and dissociation of tubulin subunits are end-mediated processes. End-wise addition was first observed by labelling fragments of brain MTs with DEAE-dextran so that they could be distinguished with electron microscopy from tubulin subunits that polymerized onto the MT fragment ends (Olmsted *et al.* 1974). It has more recently been demonstrated by observing the addition of fluorescently-labelled tubulin to the ends of pre-existing

MTs both *in vitro* (Kristofferson *et al.* 1986) and *in vivo* (Soltys & Borisy 1985; Sammak *et al.* 1987). Furthermore, polymerization reactions are different at opposite MT ends (Allen & Borisy 1974; Olmsted *et al.* 1974; Summers & Kirschner 1977; Farrell & Jordan 1982). One end (the + end) exhibits much faster rates of growth (Cote *et al.* 1980) but will also disassemble more quickly than the (-) end (Karr & Purich 1979; Bergen & Borisy 1980; Bergen *et al.* 1980). Thus, the net change in MT length is the sum of the association and dissociation events at both ends of the MT.

Biased polar growth is also apparent in MTs that are associated with nucleating sites or MTOCs (see section 1.6). Flagellar and ciliar MTs show preferential growth at the end distal to the basal bodies. This was first observed *in vivo* (Rosenbaum & Child 1967) and later confirmed by following the assembly of purified brain tubulin subunits on flagellar MTs of *Chlamydomonas* (Allen & Borisy 1974; Borisy *et al.* 1975; Binder *et al.* 1975) and sea urchin sperm tails (Kuriyama 1975; Kuriyama & Miki-Nomura 1975). Similarly, centrosomal (Bergen *et al.* 1980) and spindle pole MTs (Heidemann & McIntosh 1980; Telzer & Haimo 1981) have (+) ends distal to the nucleating center. Kinetochores are unlike other MTOCs in that the (+) end of the MT is proximal to the site of attachment (Euteneuer & McIntosh 1981b; Mitchison & Kirschner 1985b). Thus, the ability of MTOCs to regulate the temporal and spatial aspects of MT assembly depends on their ability to recognize the structural polarity of MTs.

1.5.2 Models of Microtubule Dynamics: Treadmilling and Dynamic Instability

Apart from some relatively stable MTs found, for example in cilia and flagella, the behaviour of most MTs is quite often dynamic. Exchange of tubulin subunits results in continuous fluctuations in MT length, even in conditions of "steady state" where there is no net change in total polymer length. It has been

obvious for some time that the behaviour of MTs could not be governed by a simple equilibrium between polymer and monomer (cf. Oosawa & Kasai 1962). Apart from the coupling of GTP hydrolysis to MT assembly, MT growth was recognized as being an end-mediated process. Margolis & Wilson (1978) proposed a treadmilling model for MT dynamics whereby tubulin subunits are incorporated at one end of the MT (+ end) and eventually dislodged at the other (- end). Although some reports suggest that treadmilling can be induced *in vitro* (Farrell *et al.* 1987), *in vivo* testing has demonstrated that poleward treadmilling of subunits does not occur (Wadsworth and Salmon 1986).

Mitchison & Kirschner (1984b) followed the assembly behaviour of MTs assembled *in vitro* and observed that the MT population at steady state in fact contains a majority of MTs that are elongating at a steady rate and a small number of MTs that are undergoing rapid disassembly. This "dynamic instability" model has subsequently been verified with real time observations (Horio & Hotani 1986; Walker *et al.* 1986; Sammak & Borisy 1988). Under dynamic instability, MT length, even in the steady state, becomes a mere statistic since individual MTs are either elongating or rapidly shortening. Regulation of MT assembly by GTP capping (section 1.4.6) fits well with the model; the transition between elongation and rapid, catastrophic shortening can be explained by the loss of the GTP cap. MT assembly behaviour is therefore dependent on the relative frequencies of nucleation, catastrophic shortening (if the GTP cap is lost) and rescue (if the GTP cap is restored). Any factor that can alter the frequency of one of these events should thereby modify dynamic instability. MAPs, for example, might suppress the frequency of phase transitions which could account for treadmilling behaviour (Farrell *et al.* 1987) or increased MT stability.

1.6 MICROTUBULE ORGANIZING CENTERS

1.6.1 Function of Microtubule Organizing Centers

An essential feature of eukaryotic cells is the existence of sites that are capable of regulating the behaviour of MTs. MTs may associate with conspicuous cell structures such as centrosomes, basal bodies, spindle poles and kinetochores or with less readily discernible sites (see Brinkley 1985). The description of such sites as MT organizing centers (MTOCs) by Pickett-Heaps (1969) was appropriate because "organization" encompasses their many functions which include, in addition to initiation of assembly, the "capture" of MTs (Pickett-Heaps *et al.* 1982).

By promoting the nucleation of MTs, MTOCs overcome the lag phase that would otherwise be necessary for assembly. Consequently, MTs assembled at MTOCs have a kinetic advantage over freely-assembled MTs (Mitchison & Kirschner 1984a). Another interpretation is that MTOCs favor assembly by creating an unusual microenvironment that lowers the critical tubulin concentration necessary for MT initiation (De Brabander *et al.* 1980). MTs may be stabilized against depolymerization through the capping of a thermodynamically unstable end (Kirschner 1980; Hill & Kirschner 1982) by a MTOC. Capping of the slow growing end, for example, has been demonstrated for centrosomal MTs (Euteneuer & McIntosh 1981a). Thus, MTOCs can promote MT assembly, through nucleation and/or stabilization, under conditions that are unfavorable for the existence of "free" MTs.

MTOCs can exert spatial and temporal control over MTs throughout the cell cycle by initiating the assembly of distinct sets of MTs at various times. In the transition between interphase and mitosis for example, the centrosome, from which interphase MTs radiate, undergoes duplication to form the two spindle pole bodies. In the process, interphase MTs disassemble and are replaced by the highly oriented spindle and aster MTs (Brinkley *et al.* 1976). The two arrays are distinct both in their function and in their spatial distribution. It seems possible that a MTOC

should also possess the ability to recognize different tubulin isotypes or to associate with specific MAPs and in so doing, promote the assembly of MTs with specific properties.

The extent to which MTOCs organize MTs can vary. It has been suggested that MTOCs can act as MT-nucleating templates (Pearson & Tucker 1977) that not only initiate assembly but also impose specific patterns on MTs. Since many MTOCs associate with a precisely defined number of MTs, it has been suggested that MTOCs have a finite number of 'nucleating elements' (Tucker 1977). A precise configuration of MTs may also be associated with MTOCs. For example, flagellar axonemes have a characteristic '9 + 2' (9 outer doublet MTs surrounding two central MTs) arrangement. Many unicellular organisms including *Ochromonas* (Brown & Bouck 1974), *Polytomella* (Brown *et al.* 1976), *Nassula* (Pearson & Tucker 1977) and *Chlamydomonas* (Goodenough & Weiss 1978) possess MT arrays that show precise spatial organization. Stearns and Brown (1981) examined the nature of MT assembly from the basal body rootlets of *Polytomella* by applying purified brain tubulin to permeabilized cells. They demonstrated that the rootlet MTOCs not only initiate MT assembly but also specify MT orientation.

MTOCs can also regulate the lattice structure of MTs they nucleate whereas MTs that assemble spontaneously are less likely to have a strictly controlled protofilament number (Scheele *et al.* 1982; Evans *et al.* 1985). Conversely, certain MTOCs may nucleate a functionally distinct set of MTs with a protofilament number other than 13 (Chalfie & Thomson 1982; Saito & Hama 1982; Davis & Gull 1983; Eichenlaub-Ritter & Tucker 1984) just as they are responsible for the incomplete B & C tubules of centrioles, basal bodies, cilia and flagella (Fujiwara & Linck 1982).

1.6.2 Diagnosis of Microtubule Organizing Centers

MTOCs can be identified in various cells by observing MT assembly patterns at the transition between interphase and mitosis (*e.g.*, spindle poles) and after cytokinesis (*e.g.*, centrosomes). Following MT recovery from drug-induced disassembly is another way of determining the preferred sites of MT assembly (DeBrabander et al. 1981). The development of techniques for studying assembly of MTs from isolated MTOCs (Allen & Borisy 1974; Binder *et al.* 1975; Weisenberg & Rosenfeld 1975; Mitchison & Kirschner 1984a) and in lysed cells (McGill & Brinkley 1975; Pepper & Brinkley 1979; Brinkley *et al.* 1981a; Stearns & Brown 1981; Deery & Brinkley 1983) supplied with an exogenous source of tubulin has been of great benefit. These assays can be useful, not only for demonstrating the nucleating capacity of MTOCs, but also for studying structural and biochemical aspects of MTOC-mediated assembly (see Brinkley 1985).

In many cases, MTs display considerable order but do not appear to be associated with a conspicuous nucleating site. Elongating axons, for example, contain a very large number of MTs that are not directly associated with the centrosome of the cell body. Instead, axonal MTs show frequent breaks, (Bray & Bunge 1981; Sasaki *et al.* 1983) suggesting either that MTs could be assembled at the centrosome and later moved into the axons or alternatively, that the axon contains MT-nucleating material that is distributed along its length. Similarly, the epidermal cells of the developing leg tarsomere of the blowfly have two distinct MT populations including a layer of cortical MTs in addition to a typical array of centrosomal MTs (Tucker 1979). The cortical MTs do not appear to be associated with the centrosome or any other structure yet they are obviously well organized.

Evidence that MT nucleation and assembly can be organized in the absence of conventional nucleating structures has recently been put forward. McNiven and co-workers showed that centrosome-free fragments of teleost melanophores can reorganize a centralized MT array after surgical isolation from the main cell body

(McNiven *et al.* 1984). By following the recovery process, it was also demonstrated that MTs radiate from a general region rather than any specific site or structure (McNiven & Porter 1988). The authors have proposed that reorganization of the MT array "involves the action of a dynamic structural continuum or gel". In *Drosophila* wing epidermal cells, where centrosomes are absent, Mogensen and Tucker (1987) have implicated plasma membrane associated plaques as possible MT nucleating sites.

In consideration of the possibility that MTs may be initiated from dispersed nucleating material, it should be remembered that MT assembly around centrosomes is initiated from the amorphous pericentriolar material rather than from the well defined centrioles (Gould & Borisy 1977; Berns & Richardson 1977; Schulze & Kirschner 1986). It has even been suggested that the electron dense material detected by electron microscopy for various MTOCs is merely the material that anchors nucleating elements (Tucker 1984). Therefore, MTOCs may show considerable structural variations or be indiscernible altogether but still maintain the capacity to nucleate and organize MT assembly.

1.6.3 Microtubule Organizing Centers in Plant Cells

Plant cells display various arrangements of MTs throughout the cell cycle including interphase cortical arrays, preprophase bands, mitotic spindles and phragmoplast arrays (see Tiwari *et al.* 1984). The phragmoplast, is the only array that is distinctly focussed (Euteneuer *et al.* 1982), suggesting that there may be a common nucleating site for its MTs. Otherwise, plant cells do not show any evidence for structurally well defined MTOCs. Their MTOCs, are probably more numerous and more widely dispersed than those of animal cells (Jackson & Doyle 1982).

The nuclear envelope appears to be the site of MT nucleating activity in many plant cells. The chlorophytes *Boergesenia* and *Ernodesmis* (La Claire II 1987),

Lilium microspores (Dickinson & Sheldon 1984; Sheldon & Dickinson 1986), *Haemanthus* endosperm cells (Lambert 1980; De Mey *et al.* 1982; Schmit *et al.* 1983; Bajer & Molè-Bajer 1986b) and meristematic onion root tip cells (Wick & Duniec 1983) all feature MTs that radiate from the periphery of the nucleus. The structural basis for this nucleating activity is uncertain. The suggestion that the surface of the nuclear envelope can behave like an expanded centrosome to permit nucleation at several sites (Mazia 1984) seems reasonable. Perhaps the nuclear envelope of plant cells is structurally specialized to allow the attachment of MT nucleating material as appears to be the case for the heliozoan *Actinophrys sol* (Ockleford & Tucker 1973) whose MTOC is located on the outer surface of the nuclear envelope (Jones & Tucker 1981).

MTs organized at perinuclear sites could be involved in some endoplasmic process such as motility or nuclear positioning (Van Lammeren *et al.* 1985; Hogan 1987). In addition, the nuclear envelope could nucleate the assembly of MTs but not act as a template for their spatial organization. Preprophase band MTs, for example, appear to be physically connected to the nucleus (Wick *et al.* 1981; Wick & Duniec 1983, 1984) and spindle MTs have been shown to originate at foci on the nuclear surface (Wick & Duniec 1984). Some researchers also regard it as the site of initiation for MTs of the interphase cortical array (De Mey *et al.* 1982; Wick & Duniec 1983; Dickinson & Sheldon 1984; Bakhuizen *et al.* 1985; Clayton *et al.* 1985; Wick 1985). The existence of nucleating sites for cortical MTs that are not located on the nuclear surface, however, is also highly likely.

In many plant cells, MTs appear to radiate from discrete, cytoplasmic foci. Such foci have been observed along the edges between cell faces in *Azolla* root cells (Gunning *et al.* 1978; Gunning 1980) and in stomatal cells of *Azolla* (Busby & Gunning 1984), *Cyperus* and *Phleum* (Gunning 1981), *Zea* (Galatis 1982) and *Adiantum* (Galatis *et al.* 1983). Cortical MT foci have also be detected in several

types of plant cells during recovery from MT disassembly (Hoffmann 1986; Hogetsu 1986; Cleary & Hardham 1988; Falconer *et al.* 1988).

Further characterization of plant MTOCs has so far been largely unsuccessful. A human autoimmune serum that recognizes pericentriolar material of animal centrosomes (Calarco-Gillam *et al.* 1983) has been applied to meristematic onion root tip cells (Lloyd *et al.* 1985; Clayton *et al.* 1985; Wick 1985). These researchers reported some cross-reactivity with the nucleus and the broad spindle poles (Wick 1985) but no reactivity with cortical sites. The lack of adequate controls in these experiments and the recent finding that normal human serum gives just as strong a reaction pattern in *Allium* root tip cells as 5051 but does not label the pericentriolar material of *Chlamydomonas*, HeLa or SP2/O cells (Harper *et al.*, manuscript in preparation) suggests that this assay may not be appropriate for plant MTOCs. Until such a probe is available, and the structural aspects elucidated, plant MTOCs will remain poorly understood.

1.7 CORTICAL MICROTUBULES IN PLANT CELLS

The preceding discussion has outlined structural and biochemical properties of MTs as well as various aspects of their assembly behaviour. This very general description, which has relied heavily on evidence from *in vitro* work, has summarized in some detail the mechanisms responsible for co-ordinating these ubiquitous but functionally-diverse organelles. The focus of the remaining discussion will be narrowed to concentrate on the specific assemblage of MTs that forms the subject of this thesis, the cortical array of plant cells.

1.7.1 Evidence for Microtubule Involvement in Wall Deposition

Cortical MTs are now widely recognized as agents of morphogenesis in plant cells through their role in cellulose microfibril (mf) alignment (see Robinson & Quader 1982) They are generally located very close or attached to the plasma

membrane (Brower & Hepler 1976; Hardham & Gunning 1978, 1980; Lloyd *et al.* 1980b) where they can participate in the ordered deposition of cellulose mfs which in turn impose directionality to wall yielding under the isotropic turgor pressure (for reviews on the organization of cell walls and cell expansion see Wardrop 1962; Preston 1974; Hepler & Palevitz 1974; Taiz 1984; Preston 1988). The orientation of cortical MTs is therefore of relevance to their presumed function in morphogenesis.

Evidence that MTs are involved in mf alignment includes observations of parallel alignment of subplasmalemmal MTs and the innermost cellulose mfs. This has been reported in electron microscopical studies (Ledbetter & Porter 1963; Pickett-Heaps 1967a & b; Newcomb 1969; Hepler & Palevitz 1974; Palevitz & Hepler 1976; Seagull & Heath 1980; Mueller & Brown 1982; Seagull 1983) and more recently in the double-labelling of MTs and cellulose mfs for fluorescence microscopy (Falconer & Seagull 1985a; Galway & Hardham 1986; Seagull 1986). Further support for the idea that MTs control cellulose mf orientation has come from the effects of depolymerizing MTs on wall texture and cell shape (reviewed by Gunning & Hardham 1982; Lloyd 1984). There have been numerous reports of the growth of plant cells becoming impaired or altered when treated with colchicine (Gorter 1945; Green 1962; Grimm *et al.* 1976; Hogetsu & Shibaoka 1978; Okamura 1979; Mita & Shibaoka 1983) or various dinitroaniline herbicides (Quader et al 1978; Richmond 1983; Cleary & Hardham 1988; Wacker *et al.* 1988) and these effects on growth can be correlated with changes in mf deposition (Green 1963; Pickett-Heaps 1967b; Palevitz & Hepler 1976; Hogetsu & Shibaoka 1978; Richmond 1983).

1.7.2 Developmentally-Dependent Orientation of Cortical Microtubules

MTs have an approximately transverse orientation in cells expected to be elongating (Itoh & Shimaji 1976; Hardham & Gunning 1978; Hardham *et al.* 1980;

Lloyd *et al.* 1980a; Wick *et al.* 1981; Busby & Gunning 1983; Mita & Shibaoka 1983; Simmonds *et al.* 1983; Traas 1984; Falconer & Seagull 1985a; Hogetsu & Oshima 1985; Roberts *et al.* 1985; Galway & Hardham 1986) and shifts in MT orientation are detected at the time of growth cessation. Elongating cells of *Raphanus* root tips, for example, have transversely-oriented MTs, but in regions where elongation is complete, the cells have highly variable MT orientations (Traas 1984). In tip-growing protenema of the fern *Adiantum*, cortical MTs are arranged circumferentially in the elongating subapical zone but are parallel to the cell's long axis in the non-growing region of the cell (Murata *et al.* 1987).

The ability of a plant cell to not only maintain but also to alter the orientation of its cortical MTs is an important feature of morphogenesis. Many plant cells undergo shifts in their direction of expansion at some stage of their growth history and co-ordinated shifts in MT orientation have been documented in a few cases. For example, during bulb development, onion leaf sheath cells undergo swelling that has been attributed to a shift in the orientation of cortical MTs from transverse to random (Mita and Shibaoka 1983). Application of the naturally occurring plant hormone ethylene to elongating cells can induce lateral expansion in pea epicotyl (Apelbaum & Burg 1971) and mung bean hypocotyl (Roberts *et al.* 1985) cells. Following such treatments, the normally transverse MTs become obliquely and longitudinally oriented. Conversely, gibberellin promotes elongation in epidermal cells of dwarf pea internodes and at the same time, increases the proportion of cells with transverse MT arrays (Akashi & Shibaoka 1987).

In multicellular tissues, the complex task of co-ordinating the expansion of different cell faces may also involve MTs. In cortical cells of the root primordia of *Azolla*, MTs are perpendicular to the major axis of expansion of the particular cell surface they underlie (Gunning 1981). Thus, it appears that individual cells can "deploy their MTs in specific, and different, orientations on different cell faces" (Busby & Gunning 1983). A similar relationship has been described for

differentiating root cells of *Raphanus sativus* (Derksen *et al.* 1986) in which MTs are transversely oriented along elongating surfaces but randomly oriented at the non-expanding ends.

1.7.3 Microtubule-Guided Microfibril Deposition Hypotheses

Several models have been proposed to explain the nature of MT involvement in cellulose mf deposition. These models all consider various features such as how close MTs are to each other and to the plasma membrane, the existence of cross-bridging elements and mechanisms of force generation for mf deposition and MT movement.

Two of these models propose that MTs are directly linked to the cellulose synthesizing complexes of the plasma membrane whereas others propose an indirect relationship. Heath (1974) proposed that movement of the synthetase complexes could be mediated by mechano-chemical cross-bridging elements like dynein. Although MT-plasma membrane cross-links have been identified (Hardham & Gunning 1978; Marchant 1979), there is no evidence that these elements associate with the synthetase complexes. This model came under early criticism because it proposed that MT and mf lengths should be similar and most evidence disagrees with this prediction (see review by Heath & Seagull 1982). With the recent evidence that MTs can undergo rapid changes in length (Schulze & Kirschner 1986), the need for similar MT and mf lengths does not, in retrospect, seem valid.

A modification of Heath's model (Seagull & Heath 1980) suggested that synthetase complexes could be statically-linked to MTs and their movement generated by sliding interactions with interconnecting actin microfilaments. This latter idea is interesting in light of recent evidence favoring the existence of a transverse array of fine filaments, possibly actin, in the cortex of higher plant cells (Seagull *et al.* 1987; Traas *et al.* 1987) that possibly co-distribute with MTs. The

function of such associations, however, seems dubious since cytochalasin treatments that inhibit actin-dependent cytoplasmic streaming do not seem to affect morphogenesis (Bradley 1973).

The existence of cross-bridges between MTs and cellulose synthetase complexes is refuted because there is no observational evidence that such connections exist and some further indirect evidence against the idea. Seagull (1983) compared the paths of MTs and mfs around plasmodesmata and pit-fields and in observing that the two paths were not congruent, concluded that the idea that synthetase complexes are attached to MTs via short cross-bridging elements is untenable. Continued parallel mf deposition in *Oocystis* after colchicine treatment (Robinson *et al.* 1976) suggested that MTs, although necessary for mediating periodic shifts in the orientation of the array, do not directly control mf deposition.

Several models have been proposed that do not rely on direct links between MTs and synthetase complexes. One such model argues that stick-like projections from MTs to the plasma membrane could generate flow in which cellulose synthetase complexes could become aligned (Hepler & Fosket 1971). The flow could be generated by a beat cycle with, for example, dynein arms or alternatively, could be caused by inter-MT sliding. Evidence for either mechanism is not compelling; MT-plasma membrane cross-bridges have not been characterized in plant cells (Hardham & Gunning 1978; Marchant 1979) and the distance between adjacent MTs (Seagull & Heath 1980) seems too great to permit intertubule sliding.

Schnepf (1974) proposed that co-ordinated sliding between MTs that are statically-linked to the plasma membrane and other MTs could create an extracytoplasmic channel that would constrain the movement of cellulose synthetase complexes. How active sliding could generate enough force to pull the plasma membrane away from the inner cell wall against substantial turgor pressures is uncertain.

A much simpler model considers a passive role for MTs (Herth 1980). It suggests that MTs might form static linkages with the plasma membrane and thereby act in a fence-like manner to control the movement of synthetase complexes. Such a mechanism would account for the imperfect co-alignment between MTs and mfs that is observed (Seagull 1983). Herth also proposed, by analogy with mf-generated movement of *Acetobacter xylinum* cells, that the motive force for movement of the synthetase complexes could be provided by the crystallization of cellulose. Such a mechanism is attractive because it would allow for the exceptional case of continued parallel deposition of cellulose that has been reported in *Oocystis* in the absence of MTs (Robinson *et al.* 1976). It is also supported by the observation that ordered mf deposition is prevented in *Poterioochromonas* when crystallization is suppressed with congo red or calcafluor white treatments (Herth 1980). Finally, recent electron microscope images (Herth 1985; Schneider & Herth 1986; Giddings & Staehelin 1988) are consistent with the model, and clearly show synthetase complexes within "channels" delineated by MTs that are closely appressed to the plasma membrane.

Recent uncertainty over the role of MTs in wall deposition (see Preston 1988) is largely due to the observation that many cells frequently retain a large number of cortical MTs whose orientation patterns are unlike those of the innermost wall mfs. Such exceptions include tip-growing cells whose non-expanding sub-apical zones have axially-aligned MTs but helicoidally or apparently randomly distributed mfs (Emons & Wolters-Arts 1983; Derksen *et al.* 1985; Lloyd & Wells 1985; Lancelle *et al.* 1987; Murata *et al.* 1987) and cells that are no longer expanding (Parameswaran & Liese 1981; Roland 1981; Roland *et al.* 1982; Roland & Mosiniak 1983; Neville & Levy 1984). Helicoidal walls may arise by self-assembly of mfs at precise angles to previously deposited fibres so do not require mediation by MTs (Neville *et al.* 1976). Evidently, cortical MTs are required for

functions other than transverse wall deposition; otherwise their presence in such cells would not be justified.

1.7.4 Organization of Cortical Microtubule Arrays

To understand how MTs are organized into cortical arrays that are able to regulate morphogenesis requires structural evidence and a complete understanding of the assembly behaviour of the MTs in question. Structural evidence includes such features as MT length and density, proximity to other cell structures and the existence of cross-bridges that might help orient and stabilize the MTs. Other potentially significant features include the expression of associated proteins, enzymes, cofactors and different tubulin isoforms which might influence the assembly behaviour.

The techniques required for such work include electron microscopy which is indispensable for examining the precise structure of the MTs, sites of initiation, approximate orientation (with respect to cellulose mfs), the existence of cross-bridging elements and length measurements (reviewed by Gunning & Hardham 1982) The development of immunofluorescence microscopy has enabled researchers to observe the patterns of MT arrays in whole cells so that the overall spatial organization of MTs in cells of various stages of differentiation can be interpreted (for a recent review see Lloyd 1987). The rapid progress in the understanding of MT assembly and dynamics (reviewed above) has dramatically changed our concept of MTs in general; determining the dynamic properties of plant MTs will undoubtedly be helpful in understanding their behaviour.

When Ledbetter and Porter (1963) first identified cortical MTs in plant cells from electron micrographs, they described their arrangement as "hundreds of unbroken hoops around the cell". Similar impressions were subsequently expounded (Hepler & Newcomb 1964; Newcomb 1969; Green *et al.* 1970; Hepler & Palevitz 1974; Pickett-Heaps 1974; Schnepf *et al.* 1976; cf. Ledbetter 1967)

until serial sectioning revealed that MTs arrays were "composed of overlapping, component MTs, which are short relative to the dimensions of the cell" (Hardham & Gunning 1978). Other MT length analyses in plant cells by various techniques (Robinson & Quader 1980; Traas 1984; Lloyd *et al.* 1980b; Van der Valk *et al.* 1980) have also concluded that individual MTs are not long enough to circumscribe cells. To account for this evidence, Green (1980) refined an earlier model (Green & King 1966) for control of MT orientation whereby short MTs could be oriented transversely by maximizing their overlap with adjacent MTs, thereby forming a self-cinching loop whose most stable position of minimum circumference would be transverse. The existence of putative cross-linking elements that could account for connections between adjacent MTs has been reported (Hardham & Gunning 1978).

The introduction of immunofluorescence microscopy to the study of cortical MT arrays (Lloyd *et al.* 1979; 1980a, 1980b; Van der Valk *et al.* 1980; Wick *et al.* 1981; Simmonds *et al.* 1983) has provided a better picture of how MTs are spatially arranged within cells. Recently, the self-cinching loop model has been modified to account for the variety of orientations from transverse through oblique to longitudinal that are observed in certain higher plant cells when the technique of whole cell immunofluorecence is applied. Lloyd & Seagull's dynamic spring model (1985) proposes that MTs are organized as a helix that can change direction as an integral rather than fragmentary array through inter-tubule sliding. This model relies on the occurrence of cross-bridging between MTs and the ability of MTs to undergo changes in direction by a mechanism that has not been clearly specified but presumably involving minimal assembly or disassembly of component MTs.

An alternate strategy for MT reorientation would involve depolymerization followed by repolymerization in a new direction. The manner in which the MT array undergoes shifts in orientation about the cell's axis of expansion (*i.e.*,

whether it occurs by realignment or by disassembly/reassembly) would, if known, be of great value for understanding how MTs are organized. To date, real time observations of plant cell MTs have not been carried out so any ideas about how MT arrays shift direction have been inferred from observing fixed cells at different stages of development. In the differentiation of *Zinnia* tracheary elements, for example, it has been observed that before lateral association occurs, MTs reorient from an axial to transverse direction (Falconer & Seagull 1985a). Taxol treatments prevent this reorientation from taking place (Falconer & Seagull 1985b) but this observation does not favor one particular mechanism for reorientation. Ethylene treatments cause MTs to become oriented predominantly in an axial direction (Lang *et al.* 1982; Mita & Shibaoka 1983; Roberts *et al.* 1985) whereas gibberellin generally favors transverse orientation (Takeda & Shibaoka 1981; Mita & Shibaoka 1984; Akashi & Shibaoka 1987). Such experimentally amenable systems should be ideal for determining whether MTs 'move' into new orientations or simply depolymerize and reassemble.

1.8 SELECTION OF A MODEL FOR STUDYING CORTICAL MICROTUBULE ORGANIZATION

Investigation of any process is best conducted using the simplest available model. In the case of directed expansion of plant cells, this involves the uniform elongation of a single cell as a cylinder. Such a shape results from the formation and maintenance of a parallel array of MTs, which through guidance of mf deposition, cause uniform expansion predominantly in one direction. In this thesis, I have tackled the problem of how MTs are organized by using a suitably uncomplicated cell model, the giant internodal cells of the characean algae. These cells, situated between the multicellular nodal regions, expand uniformly (Green 1954) along their length under many conditions (Taiz 1984) to produce nearly perfect cylinders. Apart from some species, whose internodal cells may be surrounded by a layer of smaller cortical cells, most have internodal cells that only share common walls with the nodal cells situated at either end.

Since their characteristic, rotational streaming was documented by Corti in 1774, characean internodal cells have been recognized as exceptional specimens for biological research. In addition to their value in studies of cytoplasmic streaming (recently reviewed by Kamiya 1986), they have also been excellent models for membrane physiology (Hope & Walker 1975) and cell wall research (Taiz 1984).

To gain a better understanding of cortical MT organization, I have investigated various properties of MTs in the internodal cells of *Nitella tasmanica* and *Chara corallina*. The work that is described in the following chapters details a large proportion of this research including: (1) a description of the distribution and general arrangement of MTs in internodal cells using immunofluorescence techniques, (2) a detailed analysis of the orientation patterns of cortical MTs throughout development and (3) an investigation of MT assembly behaviour.

CHAPTER 2

MICROTUBULE LOCALIZATION IN CHARACEAN INTERNODAL CELLS WITH IMMUNOFLUORESCENCE MICROSCOPY

It is assumed that *Charophyta* are one of the most useless plants in Japan, just as in other parts of the world.

Kozo Imahori (From Ecology, Phytogeography and Taxonomy of the Japanese Charophyta, 1954)

2.1 INTRODUCTION

Characean internodal cells have been profitably used in cell morphogenesis studies because they are unusually large and have a predictable pattern of growth. For the same reasons they should be ideal specimens to study cortical MTs, which are implicated in directing the shaping of cells. Nagai and Rebhun (1966), Pickett-Heaps (1967a) and Hotchkiss & Brown (1987) have verified the presence of MTs in these cells by electron microscopy, but this method is unsuitable for extensive analysis because it can only be used to examine a small part of a cell at one time. Immunofluorescence microscopy has contributed to the understanding of MT organization in many other plant cells (for a recent review see Lloyd 1987) so should also be useful for overcoming the limitations of electron microscopy for studying the overall distribution and orientation patterns of MTs in giant internodal cells. Immunofluorescence labelling by vacuolar perfusion has already been successfully developed for the study of cytoskeletal elements involved in cytoplasmic streaming in these cells (Williamson *et al.* 1984) so it was felt that a similar method might be applied to examine their MTs.

The little that is known about the distribution and function of MTs in characean internodal cells has been determined through a few electron microscopical observations and work with MT inhibitors. Evidence from electron microscopy (Nagai & Rebhun 1966) suggests that MTs in *Nitella* internodal cells are confined to the cortical cytoplasm. Pickett-Heaps (1967a) observed non-cortical MTs - most frequently located around nuclei - in young cells of *Chara fibrosa* but whether these non-cortical MTs persist in older, multinucleate internodal cells was unclear. Drugs that induce MT disassembly cause normally cylindrical internodal cells to grow as spheres (Fig. 1.1; Green 1962; Richmond 1983) without affecting cytoplasmic streaming (Bradley 1973). Cell expansion patterns but not cytoplasmic streaming are therefore attributed to the presence of

MTs, consistent with their apparent confinement to the stationary cytoplasm in the cortex.

The orientation of cortical MTs is of relevance to their presumed function in morphogenesis. Internodal cells form nearly perfect cylinders but have cytoplasmic features that are characteristically helical. These features include files of chloroplasts - along which run actin bundles causing cytoplasmic streaming - and the chloroplast-free neutral line which separates zones of oppositely streaming cytoplasm (Williamson, 1975). Such distinctive patterns might be reflected in MT orientation but the MTs that have been described by electron microscopy (Nagai and Rebhun 1966; Pickett-Heaps 1967a; Hotchkiss & Brown 1987) are not aligned parallel to the helical cytoplasmic features. They have, however, been seen to lie parallel to wall mfs (Pickett-Heaps 1967a; Hotchkiss & Brown 1987), which are mainly perpendicular to the long axis in growing cells (Green 1958; Probine & Preston 1961; Richmond 1983) and of varied orientation in older, non-expanding cells (Green 1958; Probine & Barber 1966; Richmond 1983). The neutral line is also marked at the cell wall level by a local specialization known as the "wall striation" (Green 1954). In this region, mf orientation apparently differs from surrounding areas (Green and Chapman 1955; D. Flanders, personal communication). This observed anomaly in the wall structure suggests that the MTs in this region may also show altered configuration, a possibility that has not been explored by electron microscopy.

In this chapter, the application of vacuolar perfusion for examining the MTs of characean internodal cells by immunofluorescence is described. MT distribution and orientation patterns visualized with this technique are presented and possible functions are discussed.

2.2 MATERIALS AND METHODS

The standard culturing, immunofluorescence and microscopical methods described below (sections 2.2.1, 2.2.3 & 2.2.5) were used for all experiments described in later chapters unless otherwise stated. Internodal cells of both *Nitella tasmanica* and *Chara corallina* were used for the development of the immunofluorescence technique but the observations detailed in this chapter are based primarily on *Nitella*.

2.2.1 Cell Culture

Nitella tasmanica plant material was collected from the Murrumbidgee river at Old Yaouk homestead near Adaminaby, New South Wales. *Chara corallina* plant material was obtained from Googong Dam near Queanbeyan, New South Wales. Plants were maintained in a glasshouse in 75 l plastic bins containing a layer of soil and filled with tap water. After comparing growth in various media (Forsberg 1965; Andrews *et al.* 1984 ; Williamson & Hurley 1986) a modification of Forsberg's medium (1965) was found to be optimal. This medium contained (mM): NH_4Cl, 0.07; $CaCl_2$, 0.49; $MgSO_4$, 0.41; Na_2CO_3, 0.19; KCl, 0.4; morpholinepropane sulphonic acid, 0.5; together with (μM): K_2HPO_4, 3.23; $FeCl_3$, 1.48; nitrilotriacetic acid, 10.5; $ZnCl_2$, 0.73; $MnCl_2$, 0.01; $CoCl_2$, 8.4X 10^{-3}; H_3BO_3, 6.5; Na_2MoO_4, 0.49; $CuCl_2$, 2.99 X 10^{-2}; pH 7.0. For some early experiments, shoots containing several internodal cells were trimmed from plants and grown in 20 l glass aquaria as described by Williamson & Hurley, 1986. For experiments requiring unchanging growth conditions, cells were cultured in a controlled temperature room at 18-20^{o} under Grow-lux lighting with a 16/8 light/dark cycle. To simplify handling of plant material, shoots were attached with dental wax to short plastic cylinders (the non-tapered end of pipetman tips). These plastic cylinders were anchored to the bottom of the tank by sliding them over a glass rod (see Fig. 2.1). This culturing method enables the transfer of several

shoots linked together by the glass rod (for example in transfer to fresh medium or inhibitor treatments) or the removal of one shoot at a time (for growth measurement or harvesting). The culture solution was replaced hebdomadally to maintain rapid growth.

2.2.2 Immunocytochemistry

For immunoblotting, the contents of internodal cells were extracted and proteins - precipitated with trichloroacetic acid - electrophoresed as described (Grolig *et al.* 1988 in press). Proteins were transferred overnight to nitrocellulose for blotting (Williamson *et al.* 1986). Ponceau-staining was done in order to observe the banding pattern of the extracts and the molecular weight standards. After a 1h incubation with primary antibodies, blots were treated with anti-mouse IgG-biotin (Amersham, RPN1021) for 1h (diluted 1:300 in PBS/BSA) then with streptavidin-horseradish peroxidase complex (Amersham,RPN1051) for 45 min (diluted 1:400 with PBS/BSA) and developed in 4-chloro-1-naphthol substrate solution (Williamson *et al.* 1986).

2.2.3 Antibodies

Anti-tubulins screened included YL1/2, a rat monoclonal anti-α-tubulin of yeast (Kilmartin *et al.* 1982; Sera-Lab, MAS 077b; supernatant solution used undiluted); K2D7B8, a mouse monoclonal raised against SDS-purified mung bean α-tubulin (Mizuno *et al.* 1985; supernatant used undiluted); Amersham anti-α-tubulin, a mouse monoclonal raised against native chick brain MTs (Amersham N.356; ascites fluid diluted 1:1000 in phosphate buffered saline (PBS) with 1% BSA); Amersham anti-β-tubulin, a mouse monoclonal raised against native chick brain MTs (Amersham N.357; ascites fluid diluted 1:500 in PBS with 1% BSA); 6-11B-1, a monoclonal antibody specific for acetylated α-tubulin (generously provided by Dr. G. Piperno; supernatant used undiluted; Piperno and Fuller 1985)

and TU-1, a mouse monoclonal antibody raised against pig brain tubulin (Czechoslovak Academy of Sciences; ascites fluid diluted 1:500 in PBS with 1% BSA).

2.2.4 Immunofluorescence technique

Cells were prepared for immunofluorescence microscopy by a variant of the vacuolar perfusion method described by Williamson (1975) using the 10^{-7}M free Ca^{2+} ATP-free solution (PS) containing 10 mM piperazine-N,N'-bis(2-ethanesulfonic acid) (Pipes) buffer with 5 mM ethyleneglycol-bis-(β-amino-ethyl ether)N,N,N',N'-tetraacetic acid (EGTA), 4.49 mM $MgCl_2$, 70 mM KCl, 1.48 mM $CaCl_2$ and 200 mM sucrose at pH 7.0. In the standard method, cells were: given a two minute perfusion to remove vacuole, tonoplast and most of the endoplasm; fixed with 1% glutaraldehyde in PS for 20 min; washed in PBS for 15 min; labelled for 1 h with primary antibody diluted in PBS with 1% bovine serum albumin and 0.02% sodium azide; washed in PBS for 15 min; labelled for 1h with secondary antibody also diluted in PBS/BSA/azide; washed in PBS for 15 min and finally perfused with mounting medium. Cells were mounted in either modified mowiol (Wick & Duniec 1986) solution or 50% (v/v) glycerol in PBS containing 0.1% (w/v) p-phenylene diamine (Johnson *et al.* 1981), re-crystallized as described by Yocum (1980).

2.2.5 Immunofluorescence Screening of Tubulin Antibodies

The anti-tubulins used for immunoblotting were also screened for immunofluorescence microscopy. Supernatants were used undiluted and ascites fluids were diluted 1:500 for initial tests. FITC-conjugated secondary antibodies were diluted 1:30. Goat anti-rat IgG (Sigma, F-6258) was used with YL1/2 while a sheep anti-mouse IgG (Silenus, DDF) was used for all the other primary antibodies.

2.2.6 Standard Immunofluorescence Labelling Procedure

For standard anti-tubulin immunofluorescence and all comparative experiments, YL1/2 (Sera Lab, MAS 077b) was applied at 1:10 to 1:50 (depending on the lot used). For labelling actin, C4, a mouse monoclonal raised against chicken gizzard actin (Provided by Dr. J. Lessard; Otey *et al.* 1986) was used at a concentration of 30 µg/ml (diluted 1:33). To double label actin and tubulin, anti-actin was applied first, followed as usual with an anti-mouse IgG-FITC conjugate (either Sigma F-6258 or Silenus DAF/369). The rat monoclonal anti-tubulin, YL1/2 was subsequently applied and was followed with a species specific anti-rat IgG secondary antibody (preabsorbed with mouse IgG) that was conjugated to phycoerythrin (PE) (Biomeda, P76).

2.2.7 Microscopy

To observe visible cytoplasmic features and MTs, perfused cells were examined intact as described (Williamson *et al.* 1984) using a Photomicroscope III (Zeiss, Oberkochen, FRG) equipped with Nomarski optics. For MTs, standard Zeiss fluorescein filters and an additional red-excluding barrier filter (Zeiss KP590) to reduce chloroplast autofluorescence were used. Cortical MTs of the upper hemicylinder were visible without interference from the light-absorbing chloroplast layer but those below the chloroplast layer and on the lower hemicylinder could not generally be seen. To observe MTs in the endoplasm, internodal cells that had been fixed and immunolabelled by perfusion were carefully cut open along the long axis and the cell opened to produce a flat slab with the cell wall surface against the slide.

For double label immunofluorescence a system of barrier filters was devised so that fluorescein (FITC) and phycoerythrin (PE), which use the same excitor filter and fluoresce at similar wavelengths, could be used in the same preparation. Using an SP555 (Becton-Dickinson) and KP560 (Zeiss) filter combination

effectively eliminated the PE emissions from the FITC signal while a KP590 (Zeiss) and LP570 (Becton-Dickinson) filter combination greatly reduced the FITC from the PE signal.[1] Both barrier filter combinations eliminated chloroplast autofluorescence.

To label nuclei, the DNA-specific fluorochrome Hoechst 33258 (a gift from J. Oliver; Laloue *et al.* 1980) was applied by perfusion. A 4 µg/ml solution in PBS was applied for 10 minutes after antibody treatments. For Hoechst fluorescence, the ultra violet (BG12) excitor filter and standard Zeiss barrier filters for UV excitation were used. Nuclei were also visible by Nomarski differential interference contrast microscopy.

Photomicrographs were taken with Kodak Tri-X film, asa 400 with the automatic exposure meter set at 1600 asa and processed with Diafine developer. For work requiring finer detail, Kodak T-Max film (asa 400), "pushed" to 800 asa, was used.

2.2.8 Fixation/ Microtubule Stabilization Experiments

To compare preservation of MT structure, antigenicity and fluorescence quality, formaldehyde (1 to 3.7% w/v paraformaldehyde in PS) and glutaraldehyde (0.2 to 2% v/v in PS) were used alone and in combination. For studying the effect of perfusion on MT stability, cells were perfused for varying lengths of time prior to glutaraldehyde fixation. Alternative MT stabilizing methods included use of the glycerol-based MT-stabilization buffer of Bershadsky et al. (1978) instead of perfusion solution and the inclusion of dimethyl sulphoxide (DMSO) (Schroeder *et al.* 1985) at 1 to 20% (v/v) in PS.

---

1. KP and SP signify short pass whereas LP refers to long pass. Short pass filters attenuate light of longer wavelength than the indicated number while long pass filters attenuate light that is of shorter wavelength. Thus, the KP590/LP570 combination works as a band pass (BP) filter passing light between 570 nm and 590 nm.

2.2.9 Inner Wall Replicas and Electron Microscopy

For replica production, cells were prepared by a method similar to that used by Green (1958). Replicas could be produced from perfused and fixed internodal cells and from freshly harvested cells using the same method, with equal ease. In both cases the protoplasm was easily removed by placing the cell - with both ends removed - in a small amount of water and gently stroking with an eyelash attached to a wooden applicator stick. Cells were then air-dried, cut along one side, re-wetted and unfolded as described (Green 1958) being careful to make the cut parallel to the long axis for future reference. Sections of the wall were then placed inner side upward onto gelatin-coated coverslips and allowed to dry. Sections were placed in the shadow-casting device (Balzers; IKR010) with the long axis perpendicular to the platinum (Pt) gun and shadowed with C-Pt at an angle of 45^{o} then shadowed with carbon normally. Excess coating was scraped away as close as possible to the coated specimen using a razor blade and chromic acid applied at half strength. When the specimen floated off the coverslip (the gelatin coating facilitated this) the strength of the chromic acid was increased to 5%. Specimens were left overnight to complete the removal of the wall material from the replica. The solution of chromic acid was gradually replaced with distilled water followed by sodium hypochlorite (half-strength at first, gradually increased to full-strength) and finally distilled water. Replicas were placed on coated grids and examined with a Hitachi-500 electron microscope.

2.3 RESULTS

2.3.1 Immunofluorescence Technique

For all comparative studies in this chapter, young cells shown in preliminary studies to have transverse MT arrays were selected.

(i) Fixatives

Glutaraldehyde fixation was selected for all immunofluorescence work. It preserves the *in vivo* appearance of the visible cortical structures (Fig. 2.2) and gives qualitatively and quantitatively (see chapter 3) uniform preservation of MTs and excellent antigenicity. Background fluorescence was minimal when a 1% solution of glutaraldehyde was used (Fig. 2.3a). Formaldehyde, used alone or in combination with glutaraldehyde resulted in MTs aggregated in places and absent in others and weak MT fluorescence (Fig. 2.3b).

(ii) Pre-fixation Perfusion Time

Pre-fixation perfusion time was found to be critical for the accurate preservation of cortical MTs (Fig. 2.4). Initial perfusion without fixative is necessary for removal of the tonoplast membrane to ensure rapid fixation, even penetration of antibodies into the cortex and reduction of background fluorescence (Fig 2.4 a-c). If fixative is introduced later than 2 minutes after the start of perfusion, gradual disassembly of MTs occurs (Figs. 2.4 d-l) presumably because of a decrease in the free tubulin concentration. Depolymerization does not, however, appear to occur uniformly throughout the population of MTs. For example, some very short MTs are seen at intermediate stages of disassembly (Figs. 2.4 f & g) while others remain relatively long.

Similar patterns of disassembly can often be seen near the cut ends of a perfused cell, possibly due to larger or longer acting (ie. tonoplast is first lost at the

cell ends) concentration gradients of free tubulin in these regions or mechanical damage during cutting. That this is not a normal pattern at the ends of cells was confirmed by starting the perfusions from positions distant to the nodal regions; MT depletion was now present in regions that formerly had many MTs. Clearly it is very important to keep disassembly to a minimum by using short perfusion and to avoid the cut ends of cells for qualitative and quantitative analysis.

(iii) Microtubule Stabilizers

The ATP-free perfusion solution provides optimal MT preservation without the need for commonly-used MT-stabilizers such as glycerol or DMSO. The glycerol-based MT-stabilization buffer of Bershadsky *et al.* (1978) preserves MTs but disrupts the alignment of visible cytoplasmic features such as chloroplast files and hence may locally disorient MTs (results not shown). DMSO at low concentrations (1%) has no obvious effects while higher concentrations (2-10%) cause massive disruption of chloroplast files and MTs (Figs. 2.5 to 2.9). Regulation of pre-fixation perfusion time was found to be the most reliable means of consistent MT preservation.

2.3.2 Antibody Screening by Immunoblotting

To identify monoclonal antibodies specific for *Nitella* tubulin, total protein extracts of internodal cells were electrophoresed (Fig. 2.10) and immunoblotted (Fig. 2.11). Four antibodies that tested positively were: YL1/2, a rat anti-yeast tubulin monoclonal specific for the tyrosinated carboxyl terminus of the α-tubulin subunit (Kilmartin *et al.* 1982; Wehland *et al.* 1983); K2D7B8, a mouse monoclonal raised against SDS-purified mung bean α-tubulin (Mizuno *et al.* 1985) and both Amersham anti-α-tubulin and anti-β-tubulin, mouse monoclonals raised against native chick brain microtubules (Blose *et al.* 1982). Two antibodies were negative on blots: 6-11B-1, a monoclonal specific for acetylated α-tubulin (Piperno

& Fuller 1985) and TU-1, a monoclonal raised against pig brain tubulin (Viklicky *et al.* 1982).

2.3.3 Immunofluorescence Screening of Tubulin Antibodies

The antibodies tested by immunoblotting were also screened for MT recognition by immunofluorescence microscopy. Cells of similar age and fixed according to the same protocol were used to compare the various anti-tubulins. Of 6 antibodies tested, YL1/2, the antibody specific for tyrosinated α-tubulin, (Fig. 2.12) gave the best results. By comparison, Amersham β-tubulin (Fig. 2.15) labelled the MTs relatively weakly and non-specific fluorescence was quite high. K2D7B8 was very weak and labelled MTs of highly variable orientation (Fig. 2.13) which appeared to be arranged in branched clusters of 2 or more elements. On close examination similar MT clusters can be seen in cells labelled with YL1/2 (Fig. 2.12). Amersham anti-α-tubulin (Fig. 2.14), anti-acetylated tubulin (Fig. 2.16) and TU-1 (not shown) did not label any filamentous MT structures. However both Amersham α-tubulin and 6-11B-1 caused bright fluorescence in vesicles of the chloroplast layer.

2.3.4 Cortical Microtubules

(i) Location and General Description

Immunofluorescence microscopy using anti-tubulin confirmed earlier electron microscopy (Nagai & Rebhun 1966) in showing MTs in the cortical cytoplasm between the plasma membrane and chloroplast files. Following the standard glutaraldehyde fixation, the MT array looks uniform throughout the length of the cell (with the exception of some disassembly and mechanical damage near the cut ends). The individual structures are short in relation to cell circumference and of variable length within an array. Most of the MTs lie in a thin layer of the outer

cortex; apart from MTs moving out of focus with the curvature of the cell (see Figs. 2.3a & 2.18a) they lie in one plane of focus.

(ii) Orientation of Cortical Microtubules

Orientation patterns were quite variable in different cells with young cells having MTs mostly perpendicular to the cell's long axis (Fig. 2.18) while the MTs of older cells appeared to lack any preferred orientation (Fig. 2.19). MTs are not strictly parallel to one another in the arrays of young cells but instead are scattered about the transverse axis. In addition, a few MTs are generally seen at angles quite removed from the transverse (see Fig. 2.12 & 2.13). Some MTs are occasionally seen running parallel to the chloroplast files (Fig. 2.22b) but this seems to be an exception and in general the non-transverse MTs are oriented in highly variable directions (see Fig. 2.13) and frequently in forked clusters (see Fig. 2.13 and discussion in section 2.4.2).

(iii) Microtubules at the Neutral Line:

Above the neutral line (the region between the two opposing flows of streaming cytoplasm) the MT array frequently shows an altered configuration. This is partly because chloroplasts, which lie beneath the MT array and contribute to background fluorescence are absent from this zone as shown in Figure 2.22. In addition, MTs above the neutral line tend to be unevenly dispersed and frequently are reduced in number or completely absent (Fig. 2.24) after the standard perfusion/fixation procedure. This tendency is less noticeable when cells are fixed immediately after perfusing (Fig 2.23, 2.25) so it is likely that the lack of MTs above the neutral line is caused by depolymerization during perfusion. Unfortunately cells that are fixed immediately upon perfusion are also very poorly permeabilized causing inconsistent labelling and high background fluorescence. In cases where permeabilization is incomplete, MTs on one or both sides of the

neutral line often remain unlabelled (Figs. 2.25 & 2.26) indicating differential accessibility of antibodies to this region. Although the initial perfusion step appears to cause MT depolymerization above the neutral line it was necessary for good immunolabelling of the remaining MTs. Thus, cortical MTs above the neutral line appear to be less stable than those of adjacent regions.

In summary, the cortical MT array, observed with immunofluorescence appears to consist of a continuous planar array of relatively short, discrete linear elements. This array lies subjacent to the plasma membrane and is separated from the streaming cytoplasm by a layer of chloroplasts. The orientation of the cortical MTs is variable within an array but seems to be perpendicular to the long axis in younger internodal cells and highly variable in older non-expanding cells. The orientation of such features as the chloroplast files and the direction of cytoplasmic streaming is not obviously related to the organization of cortical MTs.

2.3.5 Cell Wall Texture

The organization of cell wall mfs was determined by examining replicas of the inner cell wall with an electron microscope. Microfibrils were found to be oriented in similar directions as cortical MTs in cells of similar age; in young cells they are aligned perpendicular to the cell's long axis (Fig. 2.20) while in older, non-expanding cells they appear to be randomly-oriented (Fig. 2.21). Comparing the distribution of MTs and mfs (Compare Figs. 2.18 and 2.19 with Figs. 2.20 and 2.21 respectively), microfibrils, however, appear to be much more tightly packed than MTs. The pattern of mf deposition is uniform throughout the length of a cell except outside the neutral line, where mf alignment is distinct from adjacent regions (Fig. 2.27) possibly reflecting the altered MT patterns seen in the outer cortex.

2.3.6 Endoplasmic Microtubules

(i) Visualization

Using immunofluorescence, MTs were detected not only in the cortex but also in the endoplasm. Conventional viewing of the intact perfused cell from the outer surface generally does not reveal endoplasmic MTs except occasionally at the neutral line region. This is due to light absorption from the chloroplast layer which also prevents detection of cortical MTs on the far side of the cell (*i.e.*, the lower hemicylinder). Extracting chlorophyll with acetone permitted endoplasmic MTs (and cortical MTs on the far side of the cell) to be seen but background fluorescence was also increased (results not shown). However, by cutting open internodal cells to produce single layer preparations and viewing these preparations from the inner side, endoplasmic MTs were easily observed (Figs. 2.28 & 2.29).

(ii) Distribution and Orientation of Endoplasmic Microtubules

Endoplasmic MTs are seen in two configurations. Some are of highly variable orientation and are located in the streaming cytoplasm (Figs. 2.34, 2.35 & 2.36). Others are aligned in approximately the same orientation as the chloroplast files (Figs. 2.29 & 2.30). These are generally short in length, sparsely distributed and positioned at the same level as the subcortical actin cables (Fig. 2.37b). Both sets of MTs showed disassembly behaviour similar to cortical MTs when perfusion was extended beyond the standard 2 minutes (data not shown).

(iii) Nuclei and Microtubules

The DNA-specific fluorescent dye Hoechst 33258 was used to identify the nuclei of internodal cells. These nuclei are spherical to ovoid in shape and elongated nuclei occasionally show constricted mid-regions (Fig. 2.35a). In size they are highly variable and range from about 5 μm to over 20 μm in length. Located in the streaming endoplasm close to the chloroplast layer, they are often

very numerous in internodal cells and can occur singly (Figs. 2.31 & 2.34) or in large clusters (Figs. 2.35 & 2.40).

Anti-tubulin immunofluorescence using the antibody YL1/2 showed that MTs were frequently associated with nuclei. In some cases MTs appeared to be appressed to the outer surface of nuclei (Figs. 2.34b & 2.36c) while in other cases they were dispersed throughout the region surrounding clusters of nuclei (Fig. 2.35). Whereas MTs near the actin cables are generally straight, those associated with nuclei are frequently curved (Figs. 2.34 & 2.36) or oriented at a variety of different angles (Fig. 2.35).

(iv) Perinuclear Fluorescence

In addition to the labelling of MTs a diffuse signal associated with nuclei was also detected with anti-tubulin immunofluorescence. This fluorescence was mostly restricted to the nucleus itself but occasionally labelled surrounding material (Fig. 2.31b); in the case of large clusters of nuclei (Fig. 2.35) this is particularly evident. Control experiments with only the FITC-conjugated secondary antibody showed no such fluorescence (Figs. 2.32 & 2.33) demonstrating that this perinuclear labelling is the result of binding of the tubulin antibody. Perinuclear fluorescence was not as bright as the signal from labelled MTs (Fig. 2.34) but much greater than the usual weak autofluorescence of the nuclei. Whether this fluorescence is due to specific or non-specific binding remains to be determined. It is of interest however that the intensity of the fluorescence is variable among nuclei. For example, nuclei that appear to be in the process of division are more intensely fluorescent than otherwise (Fig. 2.36).

2.3.7 Anti-Actin Immunofluorescence:

To compare the distribution of MTs with actin filaments, a survey of actin in *Nitella* internodal cells was carried out using glutaraldehyde fixation and an

antibody raised against chicken gizzard actin (Otey *et al.* 1986). Most conspicuous were the subcortical arrays of actin cables aligned beneath and parallel to the chloroplasts (Fig. 2.30). The cortical cytoplasm was devoid of actin staining apart from occasional actin cables that were seen to cross the chloroplast layer into the cortex (Fig. 2.39). Accidental mechanical removal of the actin cables and the chloroplasts (Fig. 2.30) does not affect the sub-plasmalemmal MTs and furthermore, the orientation of the cortical MT array appears to be unrelated to the orientation of the actin cables (see also Ch. 3). It therefore seems unlikely that there is a direct connection between the two arrays. It seems plausible however that the MTs of the endoplasm that are aligned parallel to the chloroplasts are in some way associated with the actin cables. Attempts to double label the cells with tubulin and actin antibodies (Fig. 2.30) have so far been unable to determine the nature of this association.

Following anti-actin immunofluorescence, virtually every nucleus had actin filaments associated with it. These generally formed hoops of variable diameter that often encircled the nuclei. Orbital patterns are variable and frequently more than one such hoop was found attached to a nucleus (Figs. 2.38-43). In some cases, filaments also projected from the nuclei (Fig. 2.43) and appeared to be associated with the actin cables. Examination of nuclei that appeared to be undergoing division did not show unusual actin filament conformations.

2.4 DISCUSSION

2.4.1 Immunofluorescence Technique

Immunofluorescence microscopy has many advantages over electron microscopy for studying the cytoskeleton of characean internodal cells. Many more cells can be processed with relative ease and the difficulties of fixation and embedding for E.M. (e.g., plasmolysis, distortion of chloroplasts) are avoided. Of particular value, the whole cell can be observed essentially intact so that the overall distribution of various elements can be observed in three dimensions. Thus, with immunofluorescence MTs are seen in the cortex as previously reported (Nagai & Rebhun 1966) and for the first time, aligned with and near to the subcortical actin cables and surrounding and associated with nuclei of the streaming cytoplasm.

Instead of the standard methods for plant immunofluorescence microscopy involving wall digestion and detergent permeabilization, intracellular perfusion was used to permeabilize (by tonoplast removal), fix and treat *Nitella* cells with antibodies. Vacuolar perfusion was developed to support cytoplasmic streaming after tonoplast removal with minimal distortion to the components of the cortical cytoplasm visible *in vivo* (chloroplasts, sub-plasmalemmal organelles and actin bundles [Williamson 1975, 1985]). The method has attractive features for immunocytological applications. Proteases (Moriasu & Tazawa 1986) are quickly removed so that proteolytic inhibitors need not be included in the MT stabilizing buffer. By eliminating the tonoplast (Smith & Walker 1981; Williamson 1975) the contents of the endoplasm can be quickly exchanged such that fixative can be rapidly introduced to the cell and antibodies can penetrate relatively easily into the cortex. Likewise, washing the cell after fixation and between antibody treatments is very efficient. Vacuolar perfusion should also leave the plasma membrane in a functional condition (Smith & Walker 1981) with its associated MTs (Nagai & Rebhun 1966) minimally perturbed.

Extended perfusion stimulated MT disassembly, presumably by depleting unpolymerized tubulin. Comparison of cells fixed after various perfusion times and those exposed immediately to glutaraldehyde (Fig. 2.4), however, showed no obvious disassembly (apart from above the neutral line) unless the start of fixation was delayed more than two minutes after the cell was cut. This amount of time is sufficient for removal of the tonoplast and contents of the central vacuole.

After comparing glutaraldehyde with formaldehyde and investigating DMSO (Schroeder *et al.* 1985) and glycerol (Bershadsky *et al.* 1978) as MT stabilizers, glutaraldehyde in PS is clearly superior: MTs were uniformly preserved along the cell and the visible features of the cortical cytoplasm were undistorted. There are no conspicuous signs of finer components merging into substantially thicker structures separated by MT-depleted regions whereas MTs of formaldehyde-fixed *Nitella* (Fig. 2.3b) and other plant cells (Wick *et al.* 1981; Roberts *et al.* 1985) show such configurations commonly interpreted as lateral aggregation. Formaldehyde fixation is adequate for preservation of the MT array but does not provide the quality of detail provided by glutaraldehyde fixation. Glutaraldehyde is conventionally considered the best fixative for plant material (Mersey & McCully 1978) but is generally not used for immunofluorescence because nonspecific staining is frequently induced (Simmonds *et al.* 1985). High background fluorescence was clearly not a problem with the vacuolar perfusion method of immunolabelling presumably because extraction of soluble proteins was complete before the fixative was introduced.

The value of agents that promote MT stability in immunofluorescence is dubious. It is possible that agents such as DMSO and glycerol may promote MT assembly (see chapter 6) such that the normal configuration is altered. Furthermore glycerol and DMSO clearly have deleterious effects on cell structures and the organization of the MT array in *Nitella* (Figs. 2.5 to 2.9).

2.4.2 Immunocytochemistry

The results of the immunoblotting experiment show that *Nitella* tubulin is recognized by monoclonal antibodies raised against a diverse selection of tubulins including yeast α-tubulin, mung bean α-tubulin and chick brain α- and β- tubulins. Immunofluorescence labelling with these antibodies can therefore be attributed to tubulin specificity. The best fluorescent image (Fig. 2.12) was obtained with YL1/2, the antibody specific for tyrosinated α-tubulin (Wehland *et al.* 1983) which also cross-reacts with α-tubulin of mammals (Kilmartin *et al.* 1982) and detects all types of MT arrays known in higher plant cells (Wehland *et al.* 1984). Labelling with the other anti-tubulins was either very weak or negative.

K2D7B8, an antibody specific for plant α-tubulin labelled what appeared to be a subpopulation of MTs in the cortical MT array. Since these generally non-transverse, branched clusters of MTs are also seen amidst the predominantly transverse MTs labelled with YL1/2, they do not merely represent a random sample of the total set of MTs. The antibody could be recognizing a separate tubulin isoform that assembles to branched clusters but a more plausible explanation is that it cannot recognize the transversely-oriented MTs because the antigenic site is modified or obscured [the binding site for YL1/2 is known to be accessible in assembled MTs (Wehland *et al.* 1983)]. K2D7B8 was raised against highly purified tubulin (Mizuno, *et al.* 1985) which may differ antigenically from intact MTs. Attachment of a MT-associated protein could, for example, account for such a change in antigenicity (and perhaps a change in orientation as well).

Posttranslational modification is one way the cell can produce different tubulin isoforms that possibly contribute to varied MT behaviour and function. Both detyrosination and acetylation of α-tubulin appear to correlate with MT stability (Kumar & Flavin 1982; Piperno & Fuller 1985; LeDizet & Piperno 1986; Gundersen and Bulinski 1986b; Piperno *et al.* 1987; Gundersen *et al.* 1987; Sasse *et al.* 1987; Wehland & Weber 1987; Webster *et al.* 1987b; Kreis 1987; Bulinski *et*

al. 1988; Cambray-Deakin & Burgoyne 1987; Khawaja *et al.* 1988) suggesting that these processes may be involved in the process of MT stabilization. Microtubules containing acetylated α-tubulin have been found in a wide range of cells including mammalian culture cells (Piperno *et al.* 1987), Physarum (Sasse *et al.* 1987; Diggins & Dove 1987) and the green alga *Chlamydomonas* (L'Hernault & Rosenbaum 1983). A monoclonal antibody specific for acetylated α-tubulin (Piperno & Fuller 1985) was negative in immunoblotting and immunofluorescence trials suggesting that this type of posttranslational modification does not occur in *Nitella* internodal cells (the antibody used was shown to have retained activity against *Chlamydomonas* flagellar and sheep brain tubulins (personal communication, P.P. Jablonsky & R.E. Williamson). That detyrosinated tubulin is present has not yet been determined; however, the similar staining observed with YL1/2 which is specific for tyrosinated α-tubulin (Wehland *et al.* 1983) and with an anti β-tubulin suggests that the vast majority of MTs are rich in tyrosinated α-tubulin. These preliminary findings suggest that posttranslational modification is not a feature of MT assembly in *Nitella* internodal cells. It could mean that the MTs are relatively dynamic, *i.e.* short lived (Schulze *et al.* 1987) or alternatively that stability is imposed by other means, for example by GTP-capping or the binding of MAPs.

2.4.3 Patterns of Microtubule Disassembly

The gradual loss of MTs observed after prolonged perfusion is likely caused by a steady drop in the concentration of free tubulin. Comparing immunofluorescence patterns after different perfusion times suggests that disassembly is non-uniform; MT numbers are reduced while mean length of the remaining MTs appears to remain relatively constant and some very long MTs are present even when disassembly is nearly complete. These observations are in line with the behaviour of MTs *in vitro* subjected to lowered free tubulin concentration

and referred to as dynamic instability (Kirschner & Mitchison 1986). According to this model, some MTs rapidly shorten while others continue to slowly elongate even when the free tubulin concentration is decreased. It would clearly be interesting to follow such disassembly patterns in a single cell and to compare MT disassembly and orientation.

2.4.4 Cortical Microtubules

Although immunofluorescence microscopy cannot determine the precise location of the cortical MT array, removal of the chloroplast layer and actin cables leaves MTs unaltered (Fig. 2.30) suggesting that they are not linked to these structures. Furthermore, MTs appear to form a relatively planar rather than 3-dimensional network. These observations and the results of E.M. studies (Nagai & Rebhun 1966; Pickett-Heaps 1967a; Hotchkiss & Brown 1987) support the idea that the cortical MT array is very close or attached to the plasma membrane (Brower & Hepler 1976; Hardham & Gunning 1978, 1980; Lloyd *et al.* 1980b) where it can participate in the ordered deposition of cellulose microfibrils. *Nitella* MTs do not occur in large bundles nor do they form helices - configurations that sometimes are seen in other plant cells prepared for anti-tubulin immunofluorescence (see Lloyd 1984; Lloyd & Seagull 1985). Instead they appear as relatively short, discrete elements (possibly individual MTs) oriented at various angles but contributing to the overall pattern of the array. Thus MTs in young cells are distributed about the transverse axis whereas those in older, non-growing cells appear to be distributed with no preferred orientation (compare Figs. 2.18 and 2.19).

2.4.5 Cell Wall Microfibril Organization

The observed similarity in wall mf and cortical MT orientation patterns in cells of similar age supports the idea that MTs are involved in controlling wall

deposition (Green & King 1966). The appearance of the inner cell wall replicas suggests that mfs are much more densely packed than MTs. This impression probably results from the fact that replicas show the accumulation of mfs over a relatively long period whereas anti-tubulin immunofluorescence reveals the MTs that are present at only one moment in time.

2.4.6 Microtubules at the Neutral Line

Above the neutral line - the chloroplast-free region separating opposing streams of cytoplasm - the array of cortical MTs often contains fewer elements than adjacent areas. This change in MT concentration appears to be largely a result of MT depolymerization during pre-fixation perfusion, since cells that are not perfused prior to fixation show little sign of MT loss in this region (Fig. 2.23). Why are the cortical MTs above the neutral line less stable than those of adjacent regions? It may be that the neutral line exposes the cortex directly to the endoplasm (which during perfusion may become relatively free of unpolymerized tubulin) or to the perfusion solution itself whereas the cortical chloroplasts and associated organelles may "shield" adjacent regions. The existence of a membrane - the chlorolemma - between the streaming endoplasm and the stationary cortex of *Nitella* has been proposed (Gyenes & Saxena 1985) but there is very little direct evidence that such a membrane exists. Alternatively MTs above the neutral line, unlike those outside the neutral line, may not be stabilized through, for example, attachment to the plasma membrane. Although MT orientation does not appear to change at the neutral line, perhaps MTs in this region do not regulate mf deposition as they are evidently able to do in the rest of the cell wall (Green 1962; Richmond 1983; Chapter 5) resulting in a change observed in the cell wall structure of this zone (Fig. 2.27) - the wall striation of Green (1954).

2.4.7 Endoplasmic Cytoskeleton

The present immunofluorescence study has confirmed that MTs are present in the endoplasm of *Nitella* internodal cells contrary to Nagai and Rebhun's (1966) contention that MTs in *Nitella* internodal cells are confined to the cortex. By cutting open cells prepared for immunofluorescence, a clear description of nuclei, MTs and actin-containing elements (preserved by glutaraldehyde) in the endoplasm has been made. MTs were detected below the chloroplast layer and in the vicinity of nuclei in the streaming endoplasm. For the first time, actin filaments associated with nuclei were observed. The possibility that extraction of some cytoskeletal elements from the endoplasm could occur during perfusion cannot be ruled out. The picture gained from this study may therefore be incomplete.

2.4.8 Subcortical Microtubules

A small number of MTs were found at about the same level as the subcortical actin bundles. These subcortical MTs are predominantly oriented in the same direction (see Figs. 2.29 & 2.30) and lie in the same plane of focus (Fig. 2.37b) as the actin cables so it is possible there is some association between the two elements. Whether this relationship involves motive force generation seems unlikely since cytoplasmic streaming and its recovery from cytochalasin inhibition are not affected by treatment with MT inhibitors (Bradley 1973). The function of these MTs is therefore uncertain but it is interesting in the light of many recent observations of MTs co-distributing with actin filaments in plant cells (Gunning & Wick 1985; Clayton & Lloyd 1985; Derksen *et al.* 1986; Seagull *et al.* 1987; Palevitz 1987; Traas *et al.* 1987; Kobayashi *et al.* 1987; Kakimoto & Shibaoka 1987a & b).

It would clearly be interesting to know how these sub-cortical MTs are aligned. If they are extremely long-lived they might be strain-aligned by wall-deformation along the major growth axis as are chloroplasts and actin cables

(Green 1954, 1963, 1964). However since they disassemble at about the same rate as cortical MTs during perfusion this seems unlikely. More plausibly they are indirectly strain aligned through connections to either the chloroplasts or actin cables. Alternatively, these MTs could themselves be motile: either flow-oriented by the direction of streaming cytoplasm (see Williamson *et al.* 1984) or linked to the actin cables through for example, myosin (Grolig *et al.* 1988 in press) or an analogue of MAP-2 known to link MTs and F-actin in mammalian cells (Pollard *et al.* 1984).

2.4.9. Perinuclear Microtubules

Hoechst staining allowed vast numbers of nuclei of various sizes and shapes to be observed. Presumably these included nuclei at different stages of division since larger nuclei were often elongated and displayed constricted mid- regions. Immunolabelling with anti-tubulin showed MTs close to and attached to some of the nuclei. Such MTs appeared to follow no regular pattern with MTs interspersed in groups of nuclei (Fig. 2.35) generally oriented at any angle. The full extent of endoplasmic MTs may be greater than seen in this study since some might be removed from the cell or rearranged by the flow of perfusion solution. Those MTs attached to nuclei appeared highly convoluted (Fig. 2.34b) or curved with the perimeter of the nucleus (Fig. 2.36c). What function these MTs might have is uncertain but the fact that they are only associated with some of the nuclei suggests that they may be involved in a transient process such as nuclear division which, according to Pickett-Heaps (1967a) occurs by amitosis. It may be significant that only young internodal cells were examined in this study for endoplasmic MTs since Pickett-Heaps (1967a) described MTs around nuclei of young vegetative cells of *Chara fibrosa.*

In addition to filamentous staining patterns, a diffuse fluorescence specific to anti-tubulin was usually observed around the periphery of nuclei. The intensity of

this fluorescence is variable with those nuclei that appear to be dividing fluorescing much more intensely than others. This suggests that the presence of tubulin may be related to the division process. Perinuclear fluorescence could be due to unpolymerized tubulin but it could also indicate the presence of MTs within the nucleus but not resolved because the nuclei are not permeabilized. Interestingly, Pickett-Heaps (1967a) and Bradley (1973) reported the presence of 28 nm tubular elements within the nuclei of *Chara* and *Nitella* internodal cells. These were arranged in groups and frequently were found near the nuclear envelope. They did not, however, closely resemble "normal" MTs. Diffuse perinuclear fluorescence has been observed in other plant cells using various anti-tubulins (Simmonds & Setterfield 1983; Wick & Duniec 1983; Schroeder *et al.* 1985; La Claire 1987) and appears to signal the onset of mitosis.

The relevance to other plant cells of perinuclear tubulin and MTs in *Nitella* internodal cells is questionable; the nuclei are motile and cytokinesis is no longer coupled with nuclear division which proceeds without disassembly of the cortical MT array. Whether such unusual MT arrays are the result of the multinucleate condition of these cells or whether it is a phylogenetic peculiarity is uncertain. It is, perhaps significant that similar arrays have been observed in the coenocytic chlorophytes *Ernodesmis* and *Boergesenia* (La Claire 1987). As in *Nitella* internodal cells, nuclei in *Ernodesmis* and *Boergesenia* undergo division without disassembly of the cortical MT array. La Claire speculates that this may occur because the perinuclear MTs provide a pool of tubulin needed for repeated nuclear division. Thus, both cell types appear to have cortical and endoplasmic MT arrays that are spatially and functionally distinct and therefore should require sufficiently large tubulin pools in order to operate at the same time. Consistent with this idea, perinuclear MTs are not observed in the chlorophytes *Aphanochaete* (Segaar & Lokhorst 1988) and *Mougeotia* (M. Galway, personal communication) in which mitosis and cytokinesis are coupled.

Pickett-Heaps' (1967a) observation that MTs of unknown function are frequently found around the nucleus of young, mononucleate, vegetative cells of *Chara* suggests that such arrays may not be unique to the giant internodal cells. Thus, perinuclear MTs of *Nitella* internodes might not be a manifestation of the specialized, multinucleate condition. Other functions such as the anchorage of nuclei (Lloyd *et al.* 1987) have been attributed to MTs. For example, in *Ernodesmis* and *Boergesenia*, the MT-laden nuclei are stationary whereas in *Bryopsis* - whose nuclei are motile - no perinuclear MTs have been described (Menzel & Schliwa 1986). Characean nuclei, however, normally move in the endoplasm.

2.4.10 Actin Filament Association with Nuclei

Nuclei were seen to have associated actin filaments in the form of rings or loops of various sizes. Unlike MTs, actin filament rings are found on virtually every nucleus suggesting that they are involved in a process that operates constantly. It seems unlikely that they are involved in the nuclear cycle because no obvious pattern changes occur with dividing nuclei [cf. the filamentous structures involved in plastid division (Tewinkel & Volkmann 1987)]. More likely, these filaments are involved in the movement of nuclei through the cytoplasm. The fact that actin filaments form rings or loops is of great interest. These could act as tracks along which myosin could move and this might explain the characteristic spinning of nuclei that is seen in some charophytes (Kamiya 1962; Kuroda 1964) as they move through the cytoplasm. Finally, actin filaments occasionally formed short projections from the nuclei (Fig. 2.43) by which in some cases the nuclei appeared to be connected with the actin cables (Fig. 2.39). [This was particularly evident when a scanning confocal microscope was used to examine these elements; data not shown.] The dissimilar arrangement of nuclear MTs and actin filaments

suggests that the 2 elements are not co-aligned. Whether they operate independently or in some co-ordinated fashion remains to be determined.

2.5 CONCLUSION

Immunofluorecence microscopy using the vacuolar perfusion method provides excellent preservation and visualization of MTs in characean internodal cells. Several anti-tubulins of diverse origin cross-reacted with *Nitella* tubulin on blots and at least three labelled glutaraldehyde-fixed MTs in immunofluorescence trials. Most prominent is the extensive array of cortical MTs located just below the plasma membrane. In growing cells these MTs are mostly oriented circumferentially, supporting the view that they are involved in the alignment of cell wall microfibrils. MTs show little sign of bundling or forming helices and the overall orientation does not appear to be directly related to the orientation of the helical cytoplasmic features. Specific configurations within the array and MT disassembly patterns suggest that MTs are dynamic structures with variable stabilities. The arrangement of MTs observed by immunofluorescence may therefore represent one moment in a system that is in a state of constant flux.

MTs were also found in the sub-cortical layer, aligned and possibly associated with the prominent actin cables. The abundant nuclei, located in the streaming endoplasm were also examined and a system of actin rings and peripheral MTs was discovered.

CHAPTER 2 - FIGURES

In all figures, except 2.32 to 2.35, photographs are presented so that their relative orientation with respect to the cell axis and to each other is preserved. Thus, all photographs are positioned so that the orientation with respect to the long axis of the cell corresponds to the vertical axis of the page.

Fig. 2.1. *Chara* shoots growing in controlled conditions. Shoots containing several internodal cells are attached with dental wax to plastic cylinders which are then slid over a glass rod. This system enables individual shoots to be removed one at a time for measurement or harvesting. Alternatively, all of the shoots attached to one rod can be removed at once as is necessary for reculturing in fresh medium or for inhibitor treatments.

Fig. 2.2. *In vivo* and fixed appearance of visible features of the cortical cytoplasm of a single *Nitella* internodal cell. Nomarski differential interference contrast micrographs of the same field of view (a), before perfusion and (b), after fixation with 1% glutaraldehyde. **Fig. 2.2a:** Parallel files of chloroplasts are the dominant visible features of the cortex and form a helix with respect to the cell's long axis. The rapidly streaming endoplasm lies at a lower focal plane. **Fig. 2.2b:** When fixed by perfusion with 1% glutaraldehyde in perfusion solution, files of chloroplasts retain their *in vivo* appearance and alignment.

Fig. 2.3. Comparison of glutaraldehyde and paraformaldehyde fixation for the preservation of microtubules. Both cells were processed for anti-tubulin immunofluorescence using the vacuolar perfusion technique. **Fig. 2.3a:** 1% glutaraldehyde fixation: MTs are clearly defined and brightly fluorescent. There is very little evidence of regions devoid of MTs or of the aggregation of MTs into bundles. The MTs of the upper left and lower right corners of the photograph are out of focus due to the curvature of the cell and the shallow depth of field of the objective lens. **Fig. 2.3b:** 3.7% paraformaldehyde fixation: MTs are weakly fluorescent and are unevenly distributed with numerous gaps (arrows) between what appear to be aggregated MTs.

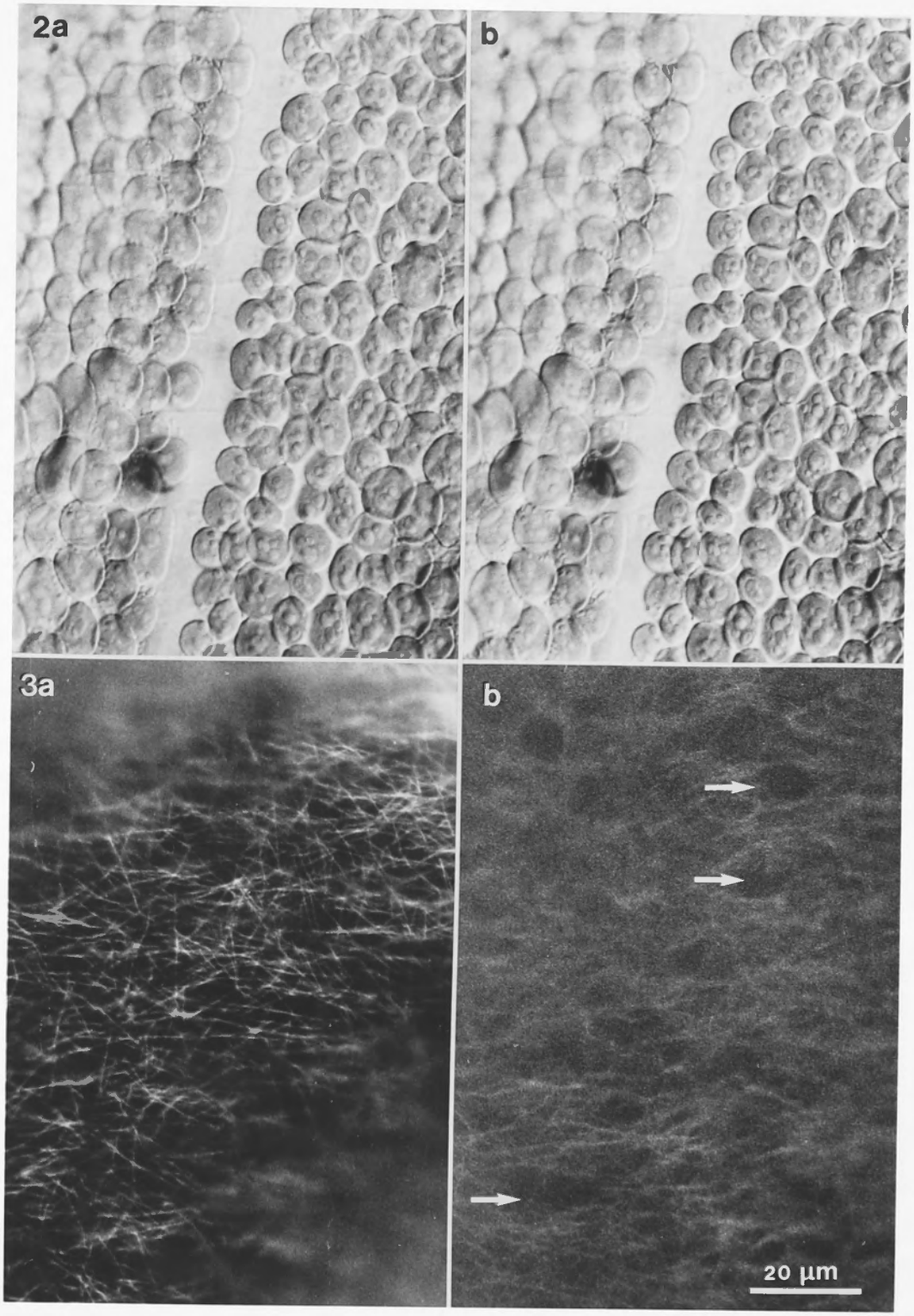
2a
b
3a
b
20 µm

Fig. 2.4. Effect of pre-fixation perfusion time on the preservation of the MT array. All micrographs are from cells of similar age processed for anti-tubulin immunofluorescence. **a & b:** Fixative included in initial perfusion solution. The cortical microtubules are preserved but incomplete removal of the tonoplast membrane and endoplasm results in inconsistent antibody penetration. In some regions, MTs are unlabelled (a) whereas in others (b), background fluorescence is very high. **c:** 2 minute perfusion prior to fixation. MTs are well preserved, brightly fluorescent and at least as numerous as in a. Note the predominantly transverse MT orientation. **d to l:** Progressively longer perfusion times: 4 min (d), 6 min (e), 8 min (f), 10 min (g), 12 min (h), 14 min (i), 16 min (j), 18 min (k), 20 min (l). Microtubules decrease in number (d & e) and eventually very short MTs are seen (g, h, i). The density of the array continues to decrease for about 20 minutes after which very few MTs are observed. In the later stages of MT depolymerization (h to l) relatively long MTs are still observed suggesting that disassembly is not uniform among all MTs. MTs are also maintained in their predominantly transverse orientation throughout disassembly.

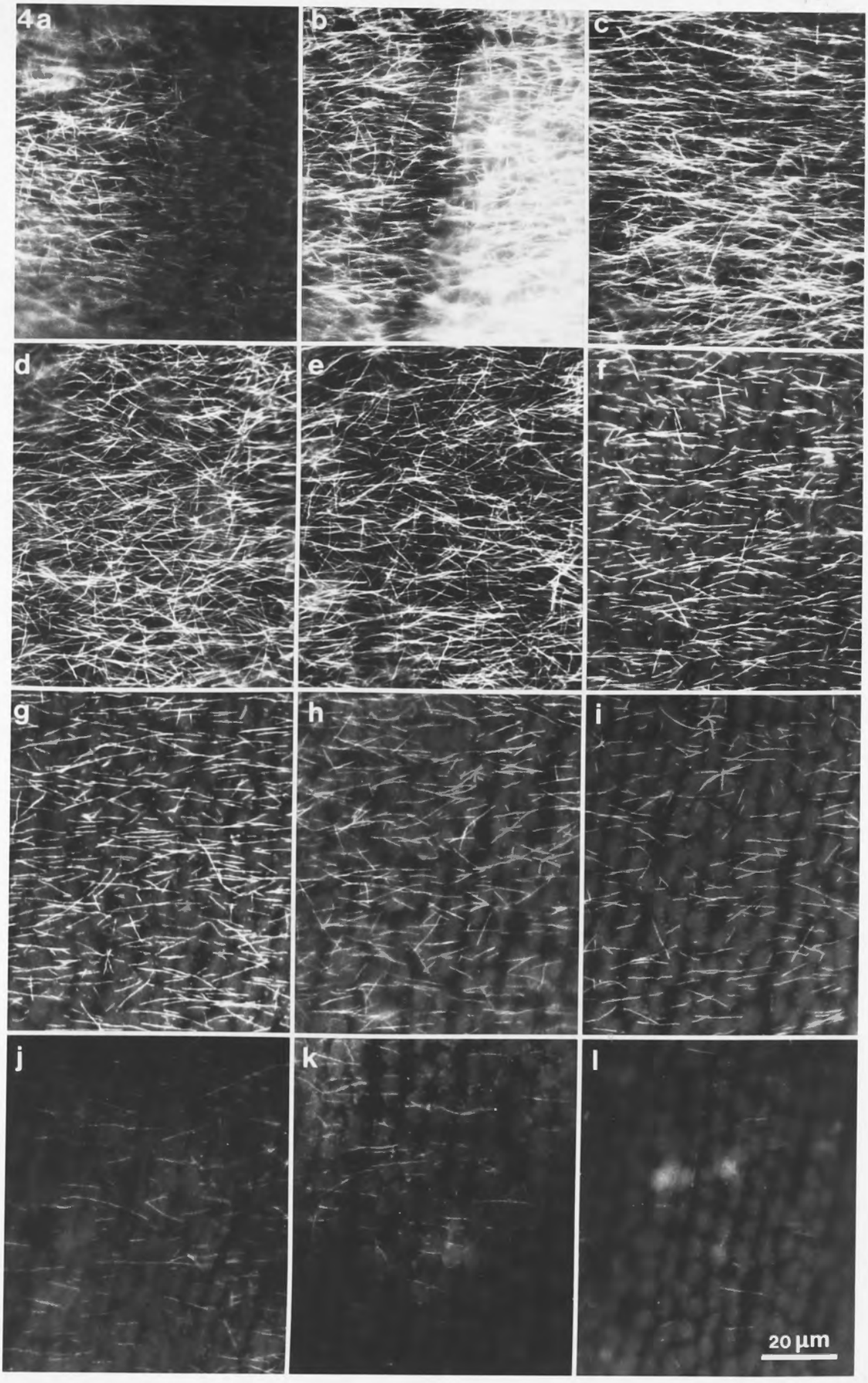
4a
b
c
d
e
f
g
h
i
j
k
l
20 µm

Figs. 2.5 to 2.9. Effect of Dimethyl Sulfoxide (DMSO) on Microtubule Stability.

Fig. 2.5. Fluorescence micrograph of MT array after 2 min perfusion with 2% DMSO in ATP-free perfusion solution and standard 1% glutaraldehyde fixation. DMSO has had very little effect on the preservation of the MT array which looks similar to standard perfusion (compare with Fig. 2.4c).

Fig. 2.6. 2% DMSO included in perfusion and fixation solutions. The orientation of the MT array is distorted and MTs frequently appear to be bundled or broken.

Fig. 2.7. 5% DMSO treatment during perfusion and fixation. **a:** No MTs are visible but there is high fluorescent labelling around the chloroplast files which have been massively distorted. **b:** Bright field photograph of same area as **a** confirms that chloroplast files are disrupted by the 5% DMSO treatment.

Figs. 2.8 & 2.9. 10% DMSO treatment during perfusion and fixation. Chloroplasts and MTs are disrupted.

Fig. 2.8. Some very short filamentous structures - possibly MTs - are seen around the chloroplast files and nuclei (N) are brightly fluorescent.

Fig 2.9. Nuclei clearly visible because of the disruption of the chloroplast layer.

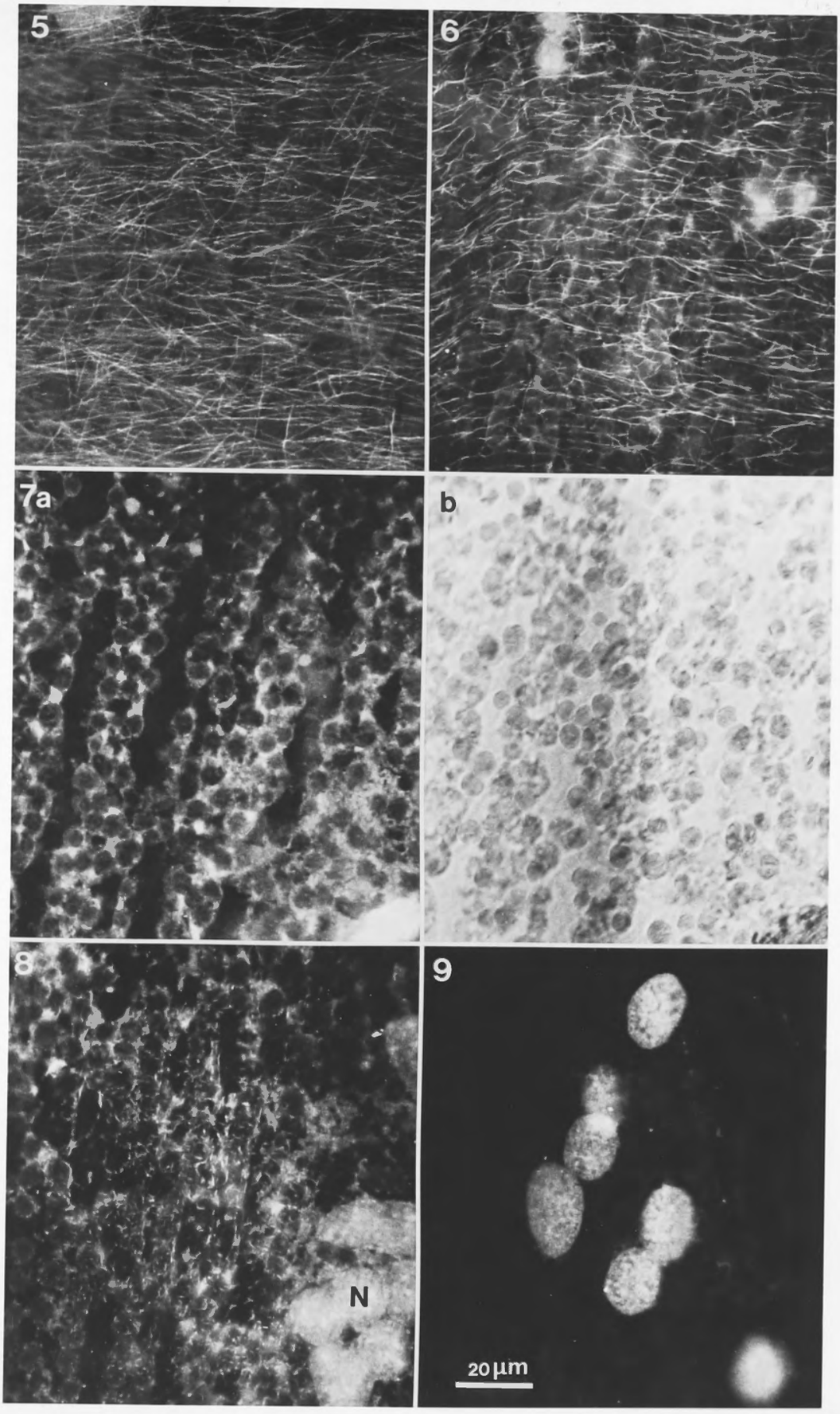
5
6
7a
b
8
N
9
20 µm

Fig. 2.10. Ponceau-stained nitrocellulose replica of electrophoresed *Nitella* extract showing banding pattern of major proteins. The left hand lane indicates the positions of molecular weight standards.

Fig. 2.11. Immunoblotting of *Nitella* protein extracts shown in Fig. 2.10 with various anti-tubulin antibodies after transfer to nitrocellulose. The antibodies that were positive for tubulin protein include: YL1/2 (lane I), a rat monoclonal anti-α-tubulin of yeast; K2D7B8 (lane II), a mouse monoclonal raised against SDS-purified mung bean α-tubulin; and Amersham anti-α (lane III) and anti-β (lane IV) tubulins, mouse monoclonals raised against native chick brain MTs. 6-11B-1 (lane V), a monoclonal specific for acetylated α-tubulin and TU-1 (lane VI), a mouse monoclonal raised against pig brain tubulin were both non-reactive. Blots were treated with anti-mouse IgG-biotin (which also recognized the rat IgG in lane I) then with streptavidin-horseradish peroxidase complex and developed in 4-chloro-1-naphthol substrate solution. Lane VII is a secondary antibody-complex control showing staining of a non-specific band at ca. 37000-M_r.

Fig.2.10

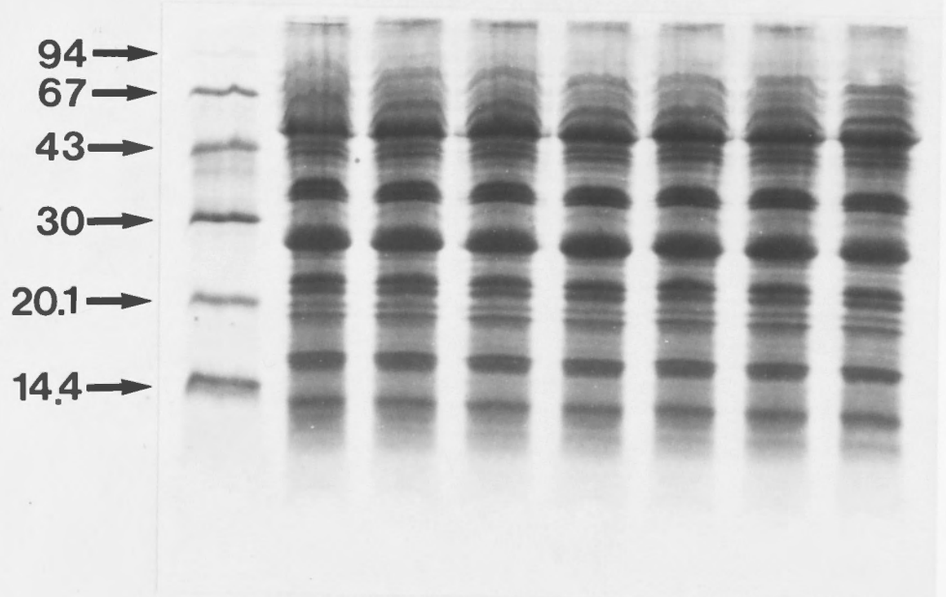

Fig. 2.11

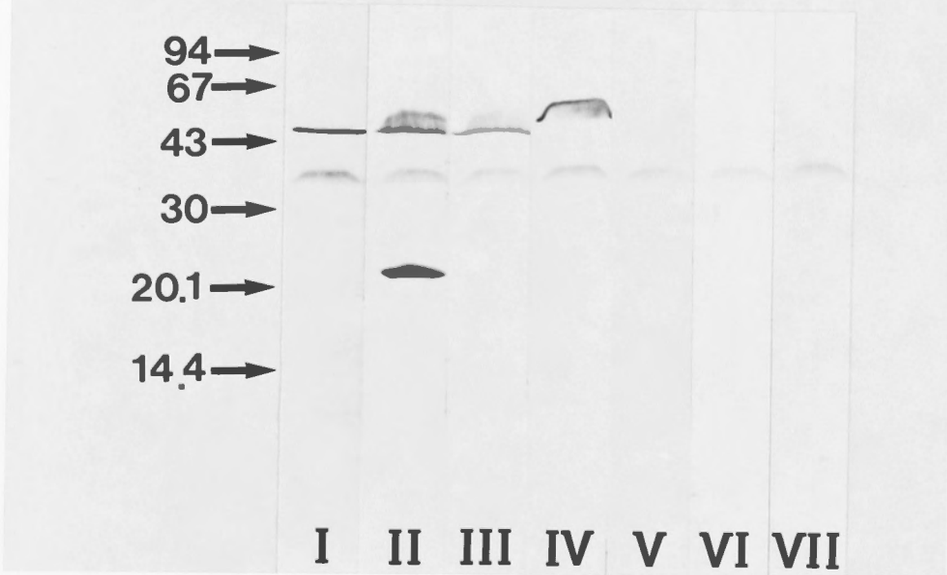

Figures 2.12 to 2.17. Screening of various anti-tubulin antibodies for indirect immunofluorescence microscopy. For accurate comparison only young, rapidly growing cells were used.

Fig. 2.12. YL1/2, a rat monoclonal anti-tubulin of yeast specific for tyrosinated α-tubulin. MTs are brightly-fluorescent and background is very low. MTs are predominantly transverse but some distinctly non-transverse MTs (arrow) are also seen.

Fig. 2.13. K2D7B8, a mouse monoclonal raised against SDS-purified mung bean α-tubulin. A very small number of MTs are labelled relatively weakly. These are generally non-transverse and often arranged in forked clusters (arrows) similar in appearance to the non- transverse MTs in Fig. 2.12.

Fig. 2.14. Amersham anti-α-tubulin, a mouse monoclonal raised against native chick brain MTs. Some brightly-stained vesicles are observed but no MTs were labelled with this antibody.

Fig. 2.15. Amersham anti-β-tubulin, a mouse monoclonal raised against native chick brain MTs. MTs are weakly labelled with this antibody. Like YL1/2, predominantly transverse MTs are observed.

Fig. 2.16. 6-11B-1, a monoclonal specific for acetylated α-tubulin. Vesicles are brightly-fluorescent but no MT structures are seen.

Fig. 2.17. FITC-conjugated secondary antibody control.

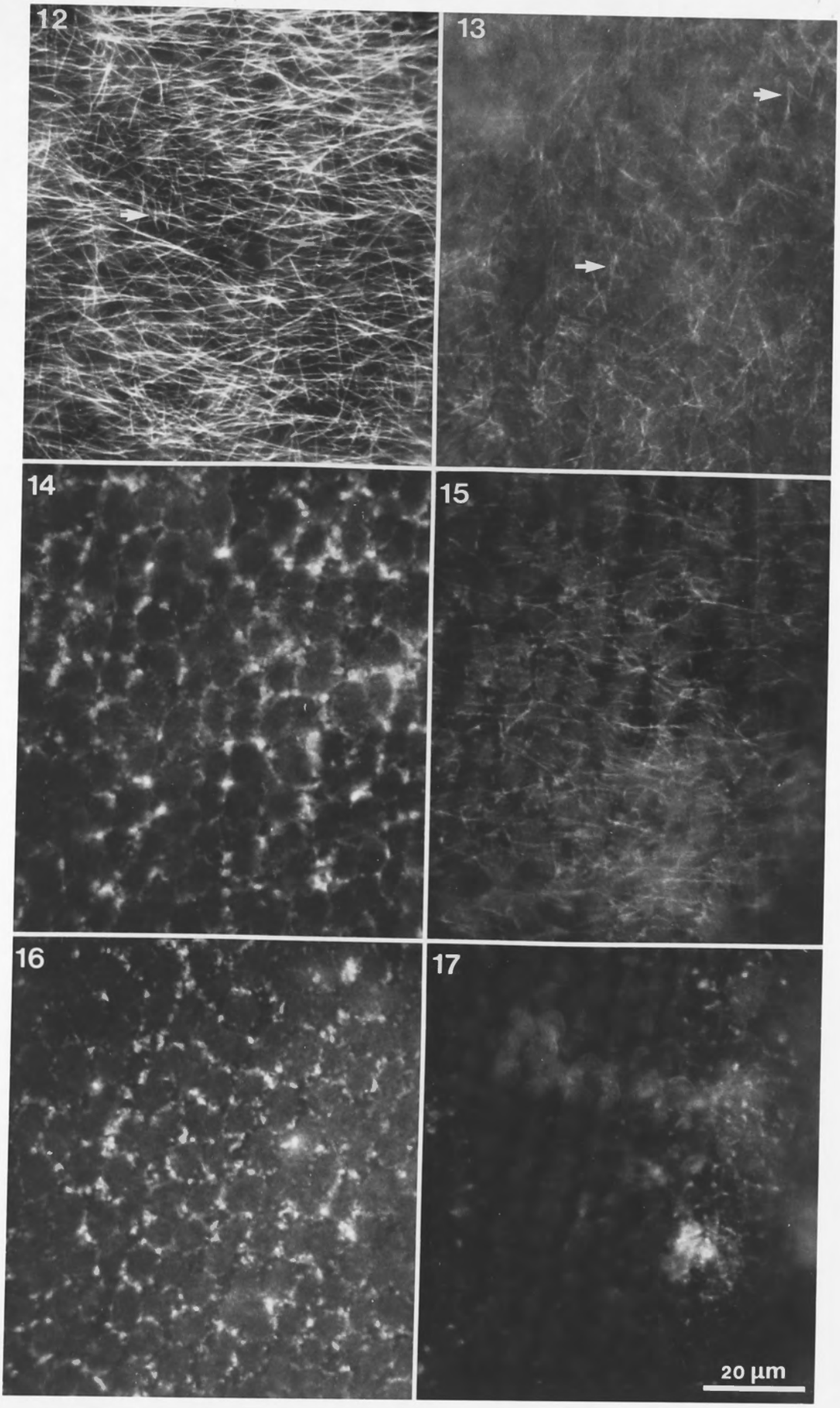
12
13
14
15
16
17
20 µm

Figs. 2.18 and 2.19. Comparison of cortical MT and chloroplast patterns in young, rapidly elongating and old, non-growing internodal cells of *Nitella*. Anti-tubulin immunofluorescence micrographs of MTs (a) and chloroplast files from the same field of view visualized by Nomarski differential interference contrast (b) are shown.

Fig. 2.18. MTs in Fig. 2.18a are oriented mainly perpendicular to the cell's long axis (the vertical axis of the photograph) while chloroplast files in Fig. 2.18b are aligned in a gradual spiral. The edges of the photograph appear out of focus because of the curvature of the cell; this is more prominent in young cells because of their smaller circumference.

Fig. 2.19. MTs show highly variable orientation in older cells that are no longer growing. The orientation of chloroplasts (b) remains essentially the same as in younger cells (Fig. 2.19b).

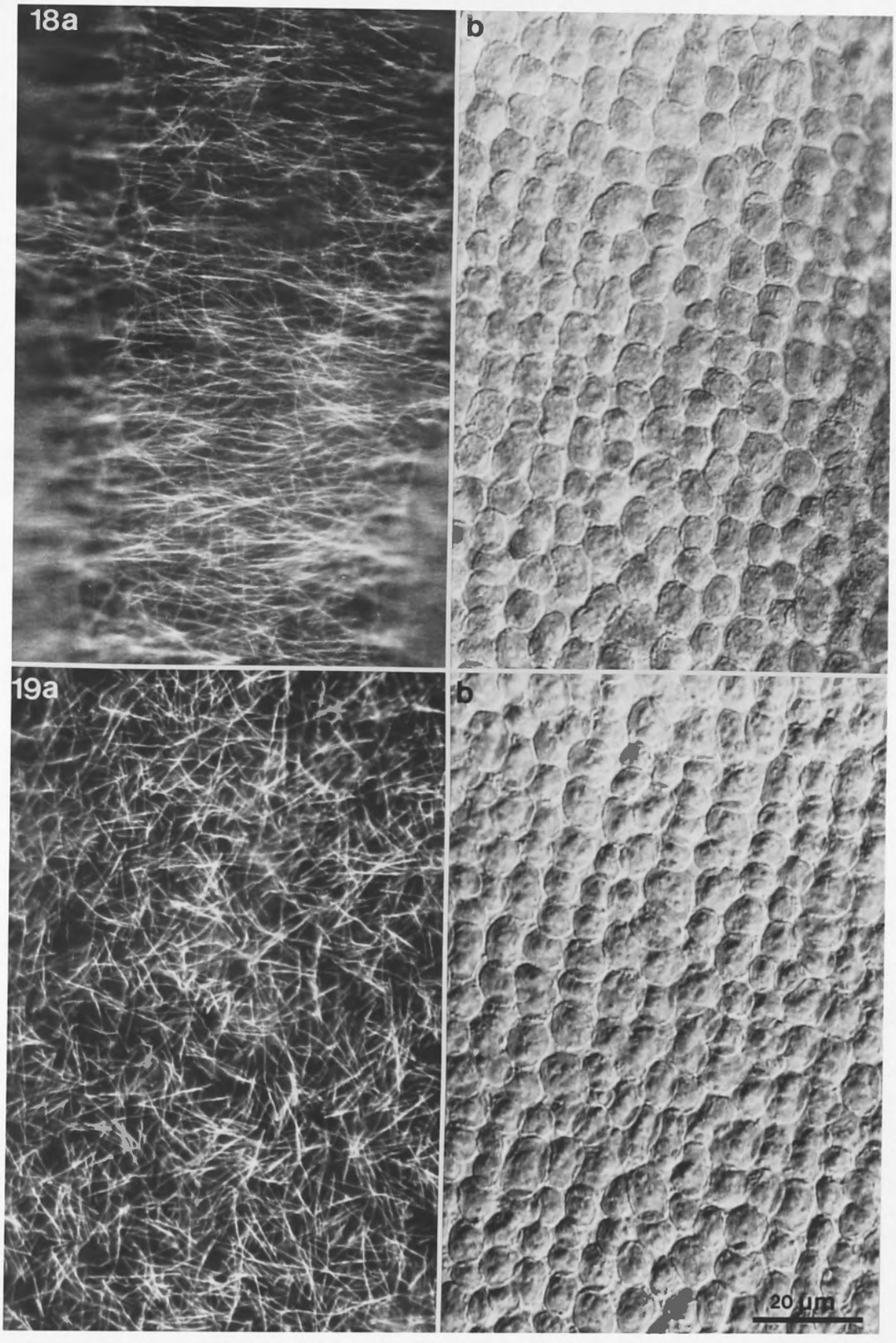
18a
b
19a
b
20 µm

Figs. 2.20 and 2.21. Electron micrographs of Pt/C replicas of the inner cell wall comparing the orientation of mfs in a young, rapidly growing cell (Fig. 2.20) and an older, non-growing internode (Fig. 2.21). In Fig. 2.20 the mfs are aligned mostly parallel to one another and approximately perpendicular to the cell's long axis. In older cells (Fig. 2.21) mfs are oriented in many directions and the wall appears to be more coarsely textured.

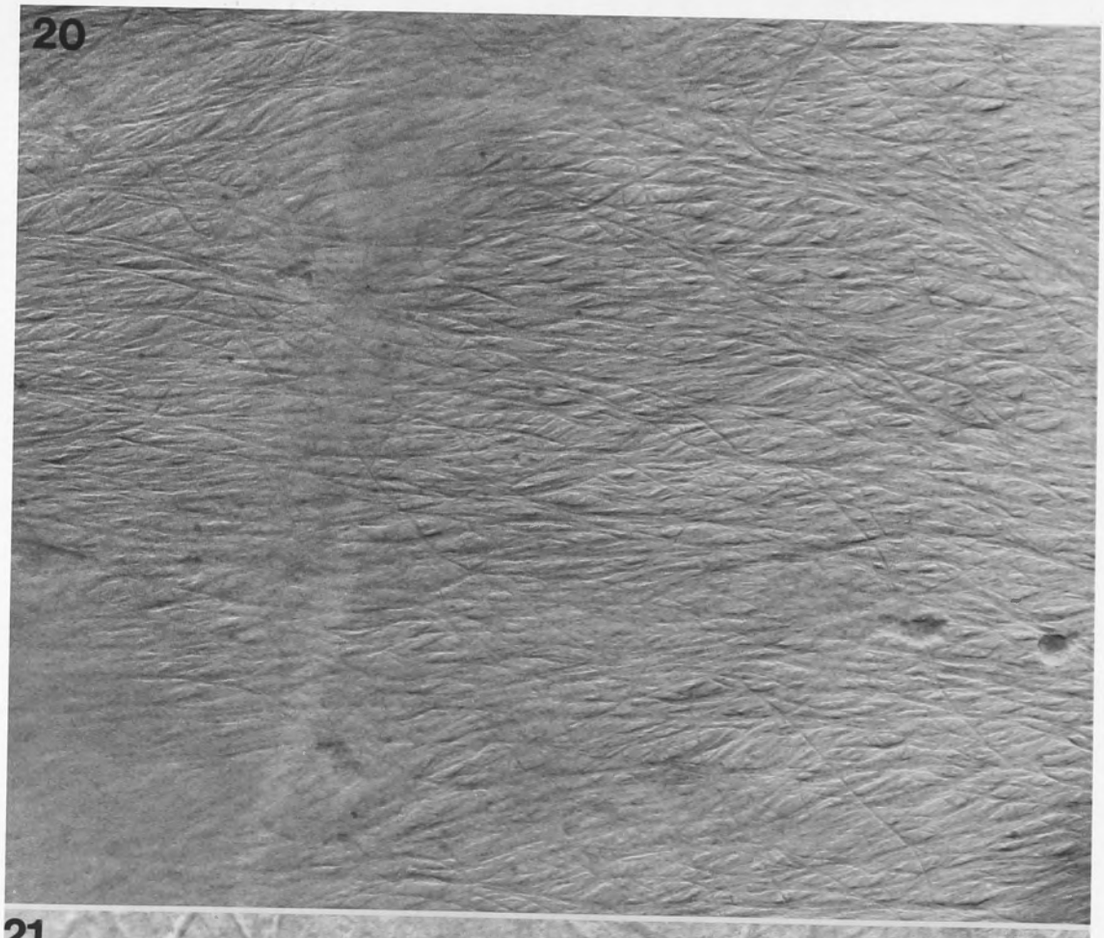
20

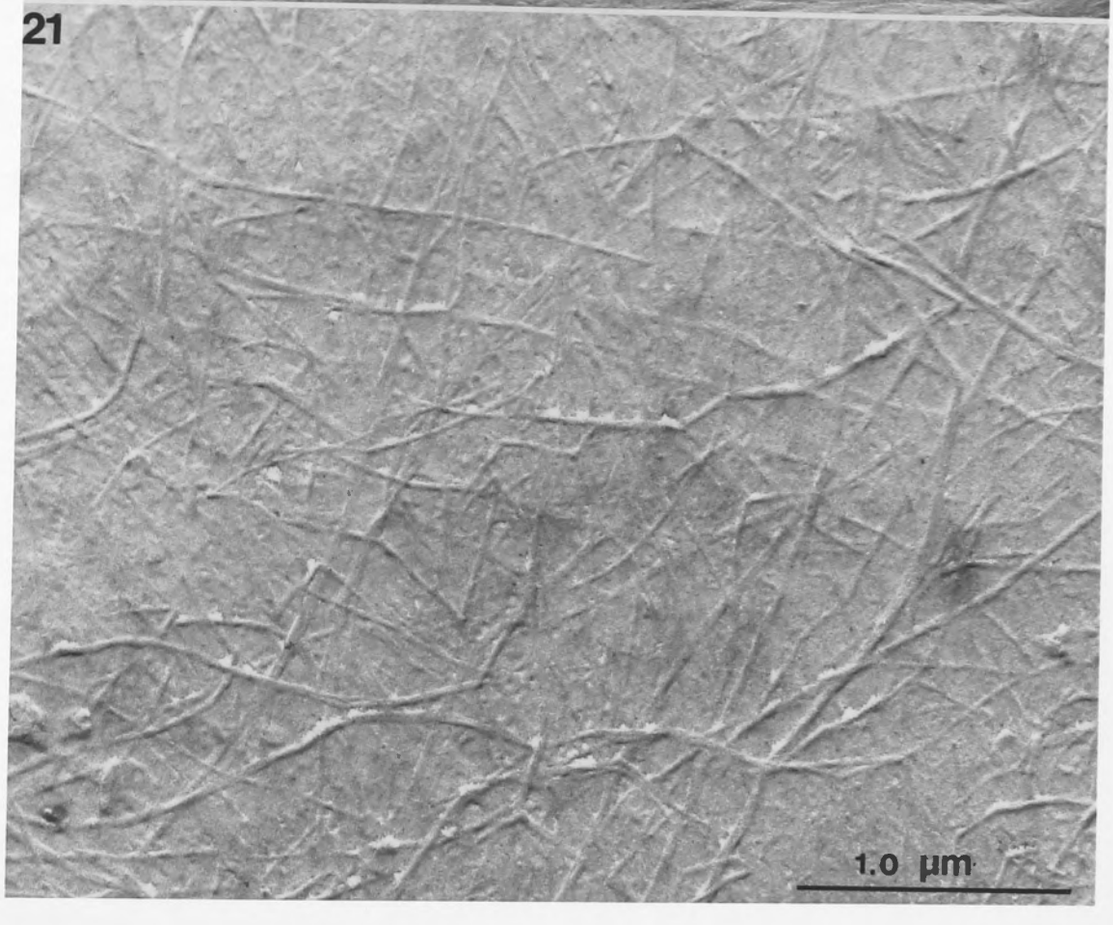
21
1.0 µm

Figs. 2.22 to 2.26. The appearance of the cortical MT array outside the neutral line.

Fig. 2.22a. The neutral line is identified by a rift between parallel files of chloroplasts and represents an endoplasm-free area separating opposite directions of flow.

Fig. 2.22b. Anti-tubulin immunofluorescence micrograph of the same field of view shows MTs crossing the neutral line but oriented perpendicular to the cell's long axis. A few MTs that lie parallel to the neutral line (arrows) are occasionally observed. The different appearance of the neutral line is partly due to the lack of background fluorescence of the chloroplast files which is present on each side.

Fig. 2.23. When pre-fixation perfusion is omitted, the cortical MT array displays little sign of MT reduction (*) at the neutral line.

Fig. 2.24. When the standard two minute perfusion is carried out MTs are considerably fewer above the neutral line than in surrounding areas.

Figs. 2.25 and 2.26. Incomplete permeabilization after omission of the standard two-minute perfusion step causes inconsistent labelling of MTs. In Fig. 2.25 only the MTs at the neutral line are labelled while in Fig. 2.26 only the MTs to one side are visible. Since the cortex above the neutral line is more accessible to antibodies than adjacent regions it may also be more closely connected to the underlying endoplasm.

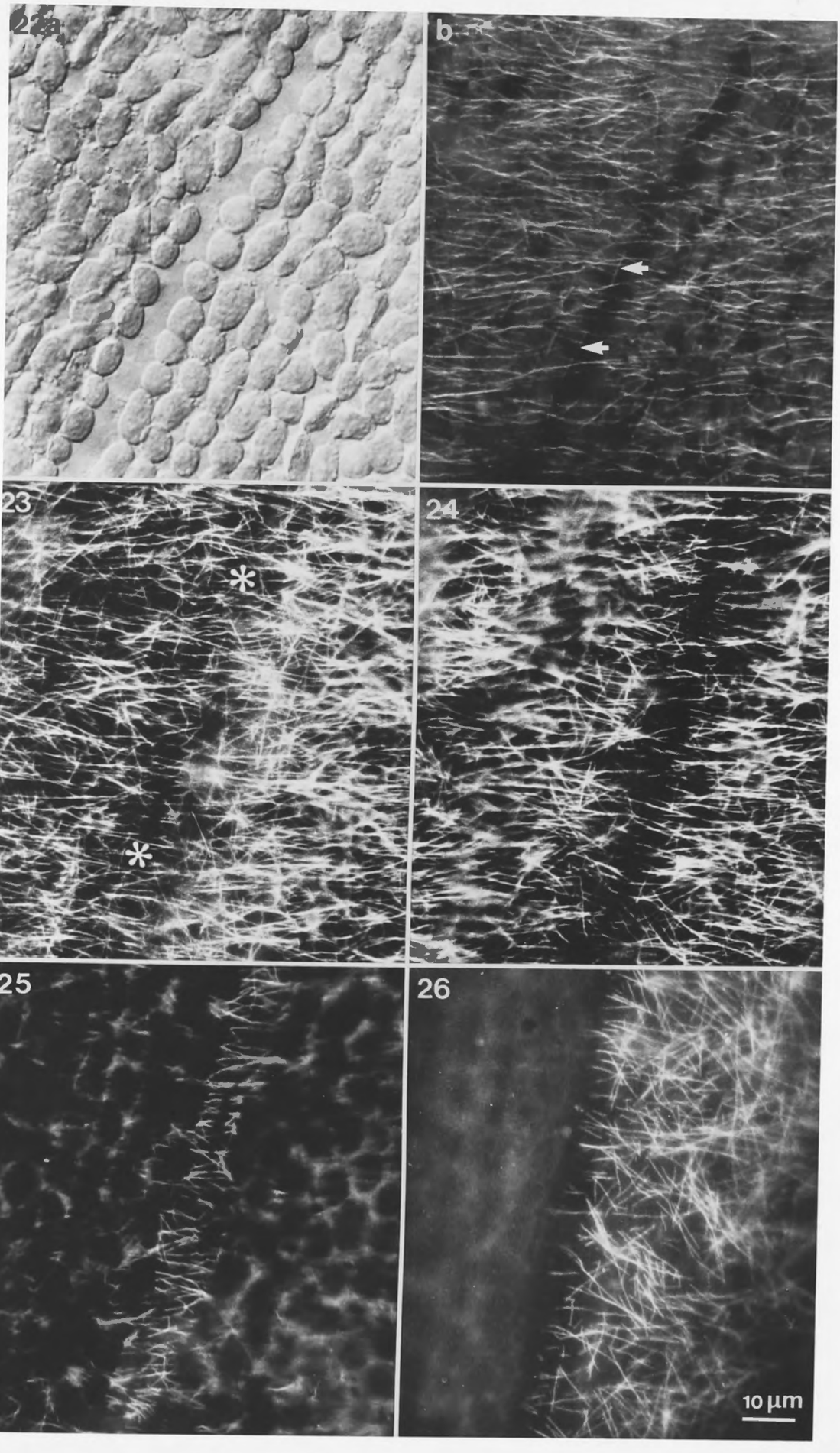
22a
b
23
24
25
26
10 µm

Fig. 2.27. Electron micrograph of an inner cell wall replica showing altered texture at the striation line, the zone outside the neutral line. Microfibrils appear to be of different orientation than mfs of adjacent areas. The handedness of the striation line appears opposite to that of the neutral line seen in the light microscope (Figs. 2.22 to 2.26) because the replica presents a view from inside the cell.

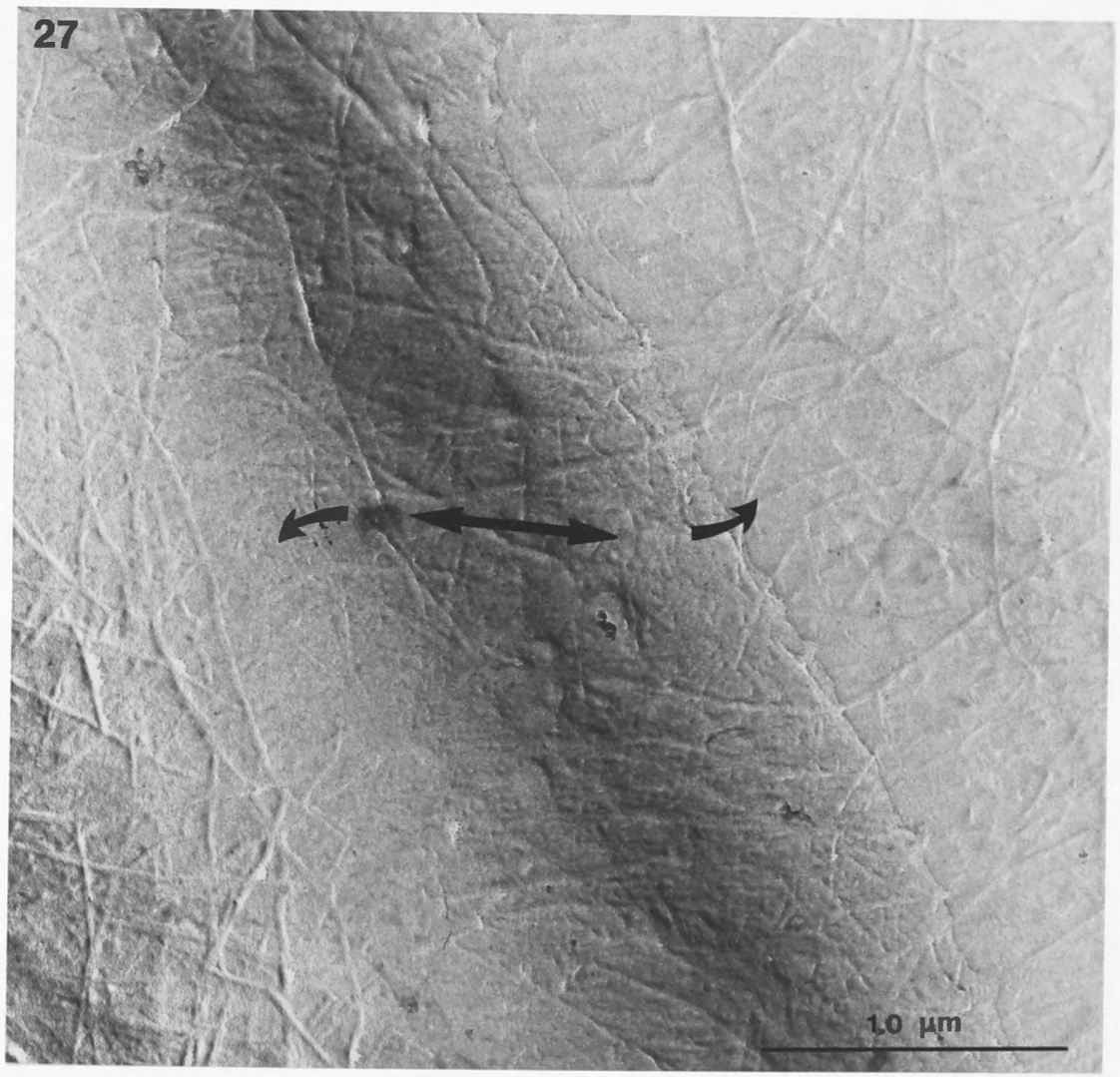
27
1.0 µm

Figs. 2.28 and 2.29. Single layer preparation of an internodal cell, viewed from the cortical (Fig. 2.28) and endoplasmic (Fig. 2.29) side of the chloroplast layer.

Fig. 2.28. (a) Cortical MTs visualized by immunofluorescence displaying predominantly transverse orientation. Endoplasmic MTs are not visible because they are at lower focal plane and because chloroplasts **(b)** absorb much of their fluorescence.

Fig. 2.29. The same preparation turned over and viewed from the endoplasmic (inner) side of the chloroplast layer (note that the handedness of the chloroplast files (b) is opposite to that in Fig. 2.28b). Most of the subcortical MTs are parallel to the chloroplast files. Cortical MTs are not in focus but some fluorescence is detected through gaps in the chloroplast layer.

Fig. 2.30. Endoplasmic view of a single layer preparation, double-labelled with anti-tubulin and anti-actin using phycoerythrin (PE) and FITC-conjugated secondary Abs respectively. Cortical MTs are visible where chloroplast layer is removed (c). The FITC labeling of the actin cables, parallel to the chloroplast files, is still visible when the PE filter combination is used (a) but the FITC filter combination (b) eliminates the PE signal. The actin cables are closely associated with chloroplasts; loss of chloroplasts removes actin cables (b) while cortical MTs remain intact (a).

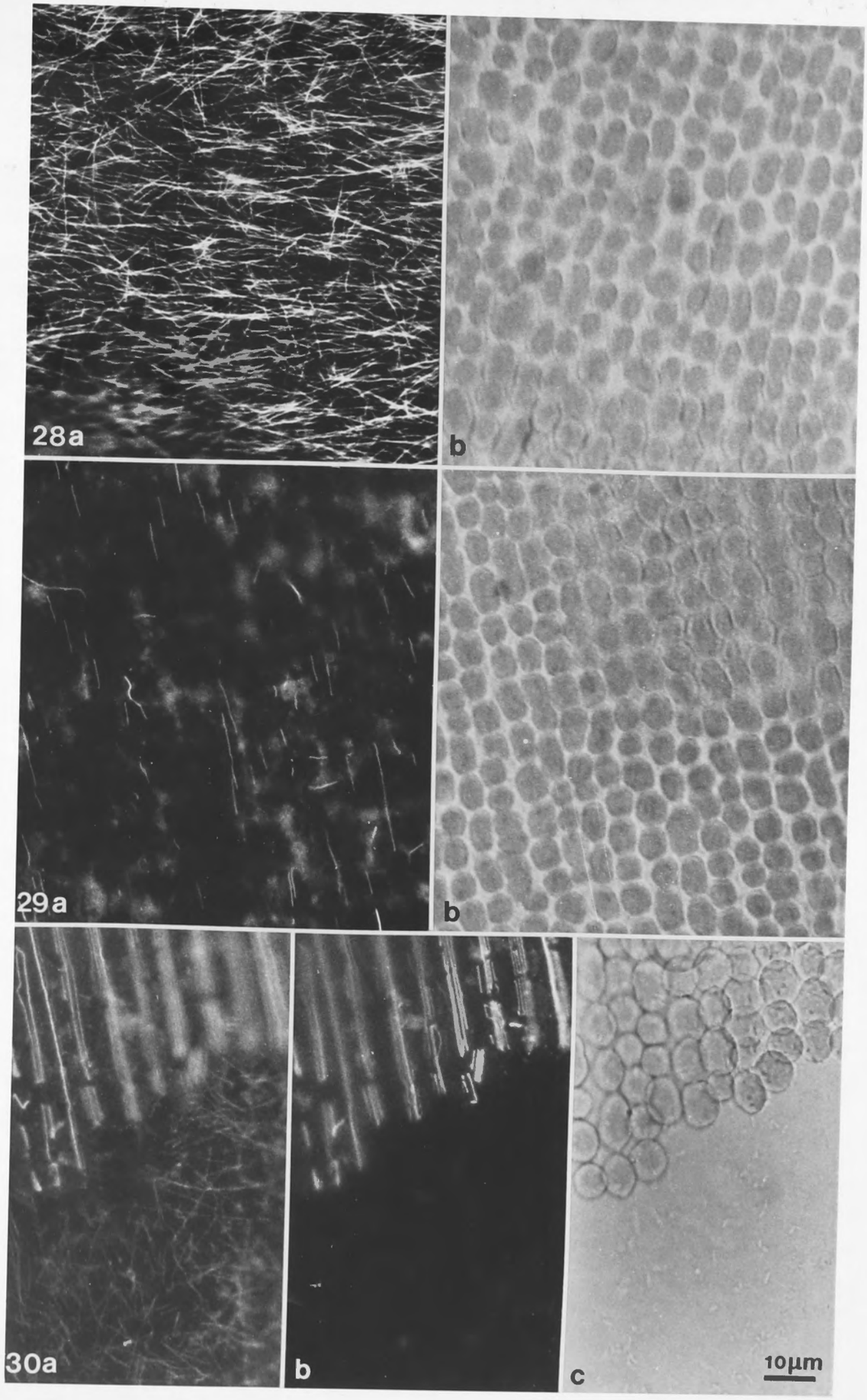
28a
b
29a
b
30a
b
c
10µm

Figs. 2.31a to 2.35a. Labelling of nuclei with the DNA-specific fluorescent dye Hoechst 33258.

Figs. 2.31b to 2.33b. Anti-tubulin based perinuclear fluorescence. All micrographs result from a 10s manual exposure and identical print parameters (f5.6 for 8s).

Fig. 2.31b. Diffuse peripheral fluorescence typical of labelling pattern with standard anti-tubulin immunofluorescence protocol using FITC-conjugated secondary antibody.

Fig. 2.32b and 2.33b. FITC-conjugated secondary antibody control. Fluorescence associated with nuclei is very low or non-existent.

Fig. 2.34. An S-shaped MT associated with the surface of a nucleus.

Fig. 2.35. A large cluster of nuclei (a) and associated MTs in different focal planes (b and c). In addition to MTs, the area surrounding the nuclei in this cluster is of high fluorescence suggesting that it contains material that differs from the adjacent cytoplasm. MTs are not organized in any obvious pattern. Diffuse perinuclear fluorescence is not apparent.

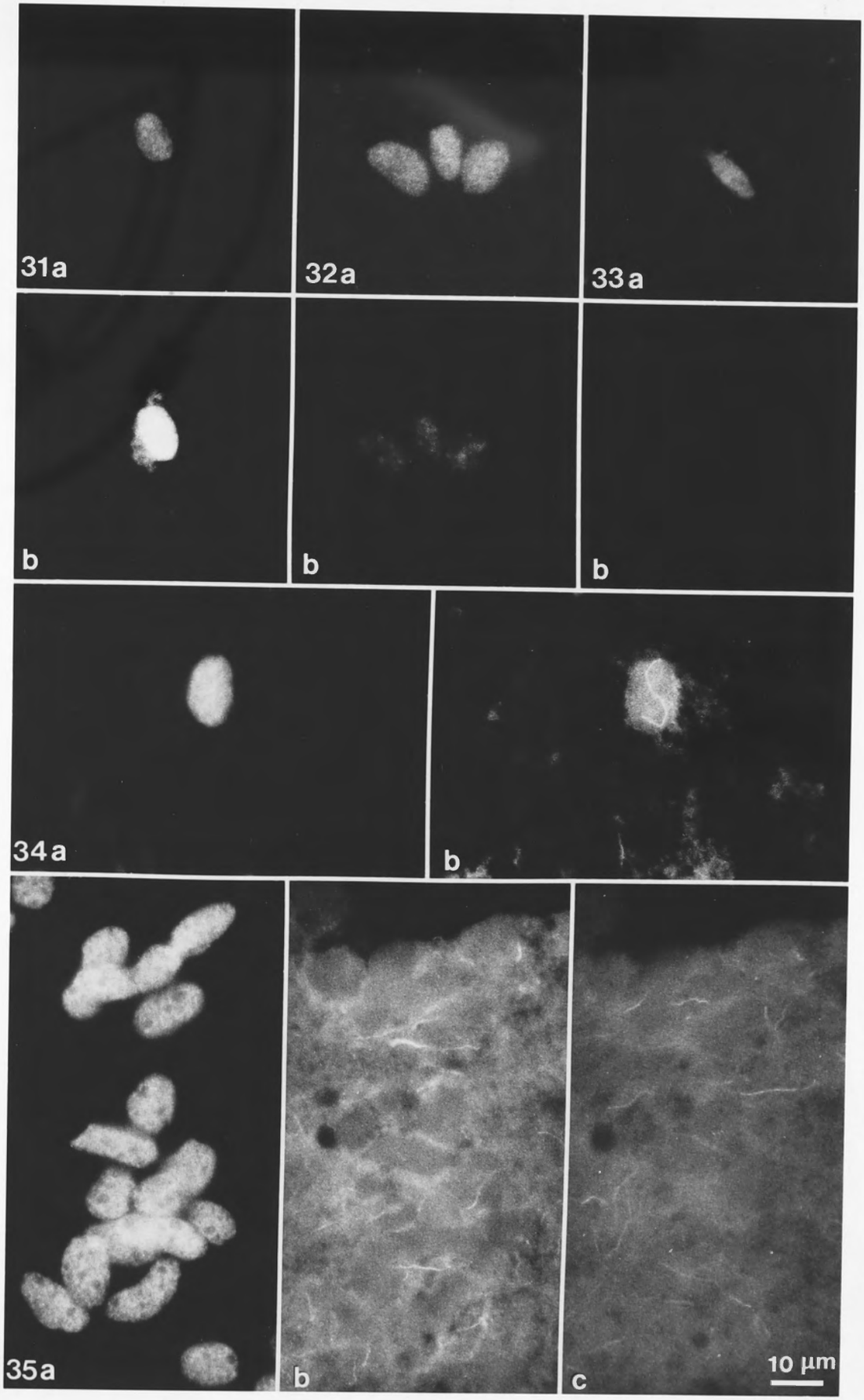
31a
32a
33a
b
b
b
34a
b
35a
b
c
10 µm

Fig. 2.36. Through focus series of MTs and nuclei in a single layer preparation viewed from the endoplasmic side. Micrographs are presented so that the long axis of the cell lies horizontally.

Figs. 2.36a to c. Anti-tubulin immunofluorescence.

Fig. 2.36a. Outer cortex. Predominantly transverse MTs are partially visible below the chloroplast layer as are some subcortical MTs.

Fig. 2.36b. Inner cortex / endoplasm interface. Subcortical MTs are predominantly oriented parallel to the helically-aligned chloroplast files. The pair of nuclei on the right are surrounded by an intense, diffuse fluorescence.

Fig. 2.36c. Endoplasm. MTs present around interphase nucleus include MTs in surrounding cytoplasm as well as a MT that appears to be appressed to the periphery (smaller arrow). The bright staining around what may be newly divided nuclei is diffuse but some filamentous structures can be resolved which may represent MTs (larger arrow).

Fig. 2.36d. Four nuclei - identified by Hoechst 33258 staining - are seen in this area. These include a pair that appear to have just undergone division (upper right corner of the micrograph), an unusual (possibly edge on) elongated nucleus (lower right) and a typical, ovoid nucleus (center).


36a
b
c
d
20 µm

Figs. 2.37 to 2.39. Anti-tubulin and anti-actin immunofluorescence of *Nitella* internodal cells. All micrographs include the neutral line region.

Fig. 2.37. Anti-tubulin immunofluorescence of a single layer preparation viewed from endoplasmic side. MT array of outer cortex (a) and a subcortical MT (arrow) lying parallel and in the same plane as actin cables (b).

Figs. 2.38 and 2.39. Anti-actin immunofluorescence seen in cortical views from intact internodal cells.

Fig. 2.38. Filaments associated with nuclei. The neutral line is devoid of chloroplasts (d) so that nuclei located in this area (c) are easily visualized when viewed from the outer side. Actin filaments are associated with each nucleus; by comparing different focal planes (a and b) it appears that they form peripheral loops. In addition to the abundant subcortical actin cables, faintly visible in the lower focal plane (b), a small number of actin filaments are also located on the upper side of the chloroplasts (a).

Fig. 2.39. Through focus series (a to d) of an actin filament loop around a nucleus (e). Due to the curvature of the cell the actin cables on either side of the neutral line are in different focal planes. As in Fig. 2.38, actin filaments that are not organized in the usual parallel cables subjacent to the chloroplast files are visible. In this case, one such filament appears to be associated with the nucleus (a & b).

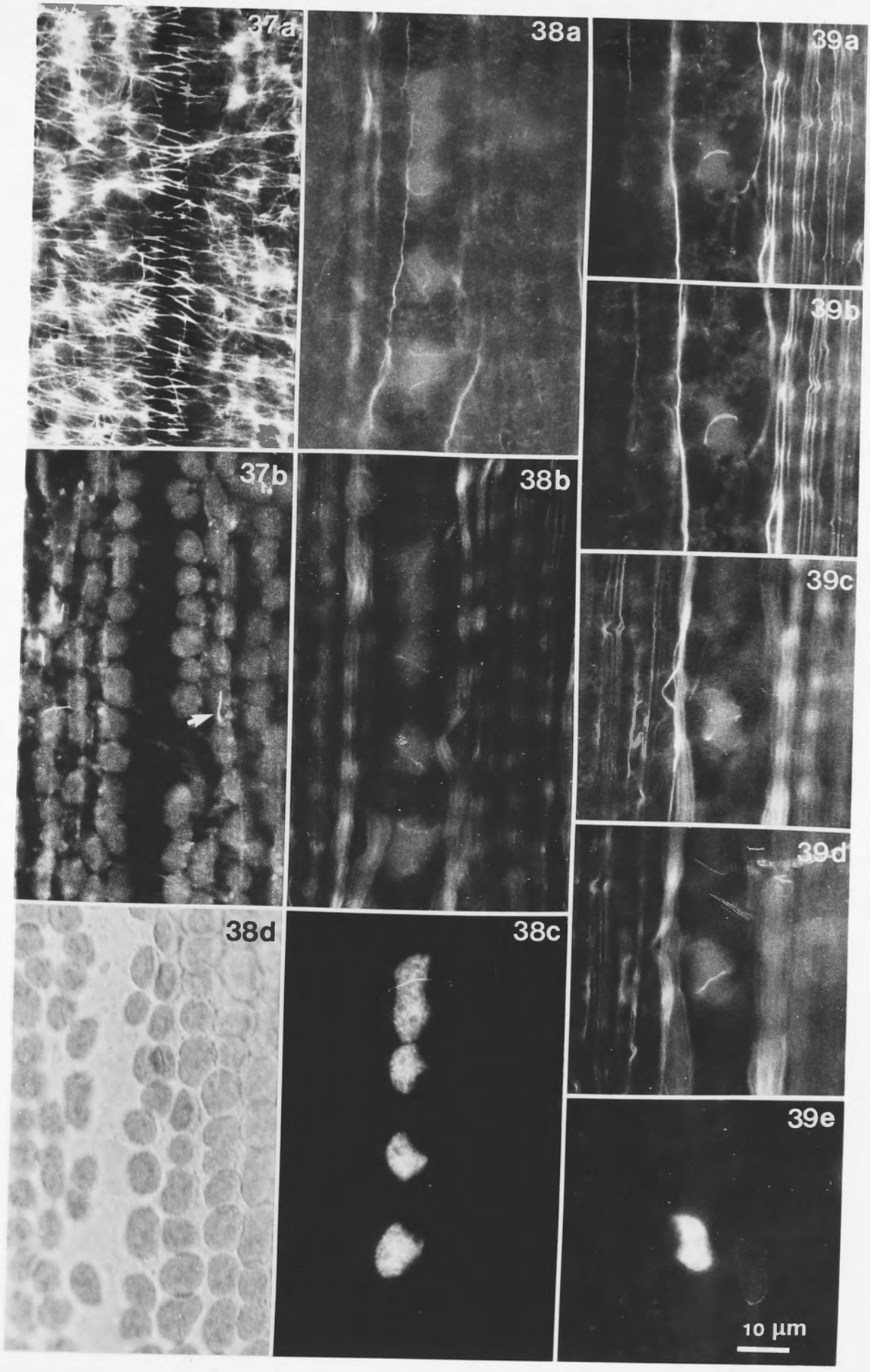
37a
38a
39a
39b
37b
38b
39c
39d
38d
38c
39e
10 µm

Figs. 2.40 to 2.43. Anti-actin immunofluorescence of *Nitella* internodal cells in regions containing nuclei; single layer preparations viewed from endoplasmic side.

Fig. 2.40. Actin filaments associated with a small cluster of nuclei. Viewed from the endoplasmic side, the subcortical actin cables are clearly visible without interference from light absorbing chloroplasts. Endoplasmic nuclei are encircled by loops of actin filaments. Here, most of the nuclei are positioned with their long axes perpendicular to the plane of focus so that entire loops are visible.

Figs. 2.41 and 2.42. Subcortical actin cables (a) and endoplasmic actin filament loops associated with nuclei (b). The actin loops do not appear to make direct contact with the actin cables.

Fig. 2.43. Endoplasmic nuclei lying well above the subcortical actin cables (not in focus) showing loops of actin filaments as well as short filaments projecting from the nuclear surface (arrows).

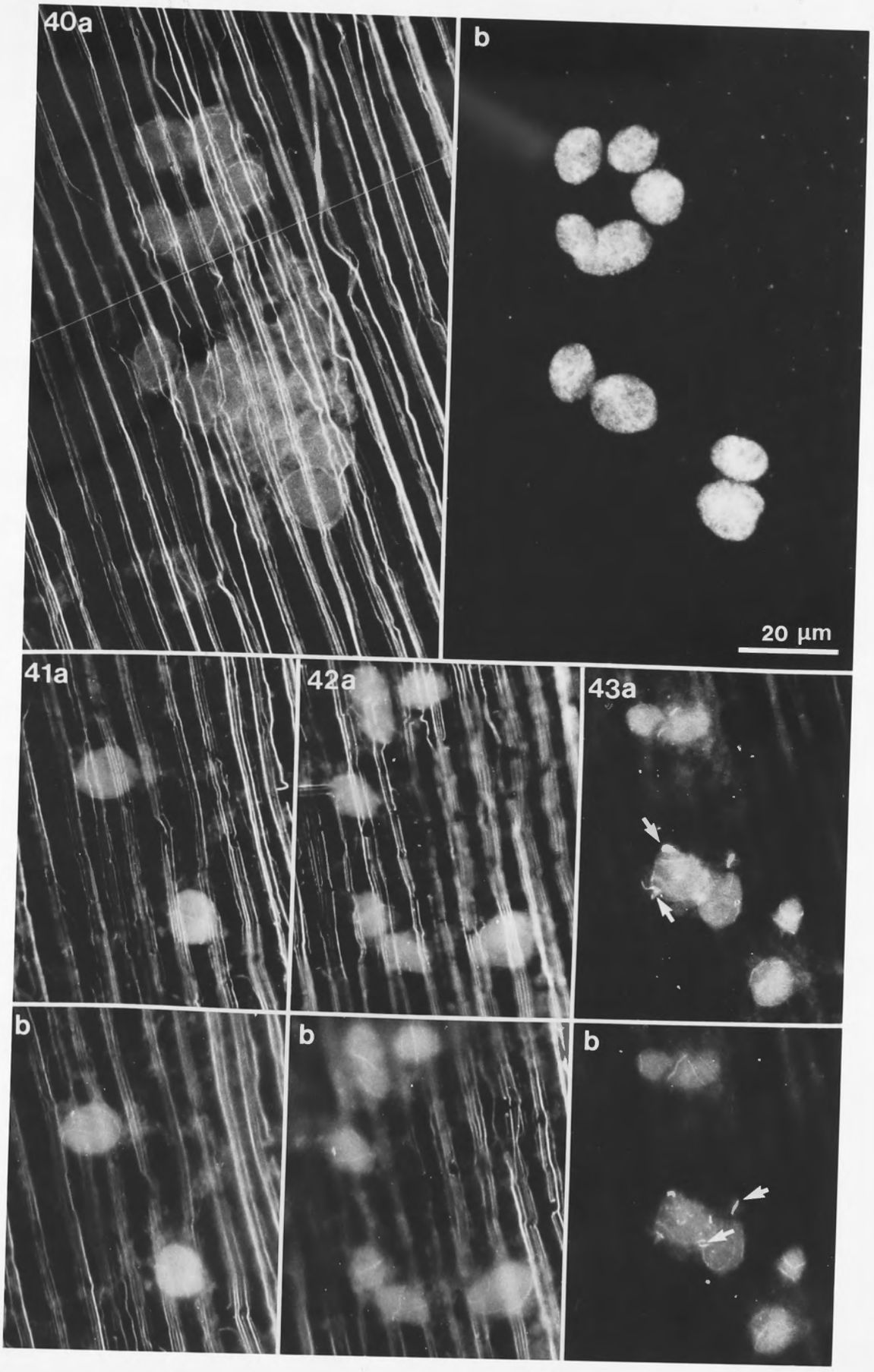
40a
b
20 µm
41a
42a
43a
b
b
b

CHAPTER 3

MICROTUBULE ORIENTATION IN DEVELOPING INTERNODAL CELLS OF *NITELLA*: A QUANTITATIVE ANALYSIS

Some of the work presented in this chapter has been published as:

Wasteneys, G. O., Williamson, R. E. (1987) Microtubule orientation in developing internodal cells of *Nitella*: a quantitative analysis. Eur. J. Cell Biol. 43: 14-22.

Williamson, R. E. and Wasteneys, G. O. (1987) Growth and orientation of the cytoskeleton in internodal cells of the characean algae. Fortschritte der Zoologie, 34: 17-23.

The results were also presented as a poster at the Eighth National Symposium of the Microscopical Society of Australia in Sydney, February 1986 and in a paper given at the Australian Society of Plant Physiologists annual meeting in Melbourne, May 1986.

3.1 INTRODUCTION

For the common situation of a plant cell uniformly expanding into an elongated cylinder, it is frequently (Green 1963, 1980; Simmonds *et al.* 1983) although not universally (Neville & Levy 1984; Roland *et al.* 1982) believed that the deposition of nearly transverse cellulose mfs favors the cell increasing in length rather than diameter. MTs underlying the plasma membrane are often parallel to the mfs being synthesized outside the membrane and disassembling MTs interferes with mf orientation and consequently, the directionality of expansion (for review see Robinson & Quader 1982). Studies of the giant internodal cells of characean algae have been influential in formulating some of these widely applicable ideas.

The internodal cells of *Nitella* and *Chara* are elongated cylinders (ca. 0.5 mm diameter, up to 100 mm long) that grow from flattened cylinders (ca. 50 μm diameter, 20 μm long; (Green 1954; Probine & Preston 1961). Growth can be uniformly distributed over the cell (Green, 1954) or confined to bands of net proton extrusion (Métraux et al, 1980). Migration of these zones along the cell leads to uniformly distributed growth when averaged over a 24 hour period (Métraux *et al.* 1980). Cell length, after a brief phase of exponential growth increases linearly so that relative growth rate (defined as $\ln L_2 - \ln L_1 / t_2 - t_1$; L=length, t=time) steadily declines towards zero (Green 1954). The cell twists as it grows and the major cytoplasmic features of the cell (the chloroplast files, actin cables and neutral line) describe a helix whose divergence from the long axis initially increases before gradually decreasing over the remainder of the growth period (Green 1954). Measurements of cells growing normally (Green, 1964) and under various perturbations (Green & Chen 1960; Green 1962) support Green's view that these cytoplasmic features follow the lines of maximum cumulative growth, *i.e.*, they are strain-aligned. Furthermore, measurements of the mechanical properties of *Nitella* cell walls imply that the predominantly transverse alignment of the recently deposited cellulose favors the predominantly longitudinal growth (Métraux & Taiz

1978; Probine & Preston 1962; Richmond 1983; Richmond *et al.* 1980) that shapes the cell into an elongated cylinder and strain aligns its cytoplasmic features. MT disruption allows the apparent deposition of randomly oriented cellulose mfs that permit transverse expansion to match longitudinal (Green 1962; Richmond *et al.* 1980) with far-reaching morphogenetic results.

The mechanisms controlling MT alignment therefore underlie the morphogenesis of internodal cells just as they underlie the morphogenesis of many other plant cells. In this chapter MT orientation is described quantitatively for *Nitella* cells fixed at known stages of growth.

3.2 MATERIALS AND METHODS

3.2.1 Plant Material

Nitella tasmanica shoots were cultured in modified Forsberg (1965) medium, pH 7.0 at room temperature with window and room lighting. Rapidly growing tips including two or three internodal cells were anchored in a layer of agar in the bottom of a 30 litre aquarium. Vertical growth was maintained throughout the culturing period with new internodal cells appearing about every 8 days. When harvested, shoots contained up to 9 internodes.

3.2.2 Growth Records

The length and diameter of each internodal cell was measured at two day intervals using an ocular micrometer or ruler (for the length of larger cells). Absolute and relative rates of growth were calculated from length, diameter and time records.

3.2.3 Immunofluorescence Technique

Cells were prepared for immunofluorescence microscopy as described in chapter 2 however some modifications of the standard procedure were used. To process successive internodes along a shoot, perspex wells with two diametrically opposed grooves on the bottom rim were used. These were positioned over each nodal region after removal of the branch cells so that the adjacent internodal cells emerged through the two grooves. To begin perfusion, a cut was made at either side of the node and levels of PS regulated carefully so that the contents of one cell did not flow into the adjacent one. The 10^{-7} M free Ca^{2+} PS was used throughout the procedure for perfusion, fixation, washing and antibody dilution. For indirect immunofluorescence labelling of the MTs, cells were incubated with a 1 in 10 dilution of a supernatant solution of YL1/2 (Sera-Lab, MAS 077b), followed by a 1 in 32 dilution of fluorescein-conjugated rabbit anti-rat IgG (Sigma). Cells were

mounted in modified Mowiol (Wick & Duniec 1986) solution containing 2% n-propyl gallate (Giloh & Sedat 1982) and examined as described in chapter 3.

3.2.4 Image Analysis

At least ten fluorescence micrographs were taken of the cortical MTs of each cell along with corresponding bright field images of underlying chloroplasts and parallel views of the cell edge. Photographs were printed at 1900X magnification for ease in tracing of microtubules. An image analyser (Kontron, FRG) recorded the orientation and length of each fluorescent linear structure within a given area. At least 3 micrographs, each covering an area of 90 x 130 μm and selected from different regions of the internode were included in the analysis of each cell. The size of the sample areas was chosen so that both ends of a large number of the MTs in the area could be seen. MTs that lay partially outside the designated area were not measured. In addition to avoiding areas of localized damage or areas crossed by the neutral line, micrographs were selected with minimal area out of focus due to the curvature of the cell (see Figs. 2.2a and 2.17). MT orientation was measured relative to the long axis of the cell, the long axis being indicated by the cell edge in parallel bright-field photographs (Fig. 3.1). In this way, angular distribution histograms can be produced in which an orientation of 90^{o} indicates an orientation transverse to the cell's long axis whereas 0^{o} and 180^{o} denote MTs parallel to the long axis. The 0 to 90^{o} and 90 to 180^{o} sectors were distinguishable because of the spiral features of the cell (Green 1954; Probine 1963) - the cell was always arranged so that the neutral lines and chloroplast files lay in the range of 160 to 180^{o}. The orientation of the chloroplast files and neutral line relative to the long axis of the cell was determined by measuring the distance between the apparent cross-over points of the neutral lines and applying Green's formula (1954):

$$\tan \alpha = 2 \text{ "inter-X" distance} / \pi \text{ Diameter}$$

These values agreed well with direct measurements of the angle between the chloroplast files and the cell edge measured from photographs that included these 2 features.

3.3 RESULTS

3.3.1 Image Analysis

In order to provide an accurate measurement of MT orientation, at least 3 micrographs - each from a different region of the same cell - were selected for image analysis. Frequency distribution histograms for all samples were compared before they were combined into a single data file for each cell. Statistical analysis of angle data confirmed qualitative observations that the cortical MT array is organized uniformly throughout internodal cells.

3.3.2 Pattern of Cell Growth

Relative growth rates for both longitudinal and circumferential expansion were recorded for several cells from the start of elongation (when length and diameter were approximately equal) until growth cessation. In Figure 3.2, relative growth rates, expressed as percentage increase per day are plotted against cell age. The relative elongation rate undergoes a rapid increase until about day 7, followed by a period of steady decline. After 20 days, the decrease in relative elongation is more gradual leading up to growth cessation at about 30 days. During the period of development that was followed, relative circumferential growth declined gradually and generally stopped a few days before longitudinal expansion.

3.3.3 Changes in Microtubule Length with Development

Microtubules were of non-uniform lengths within single cells. Of the cells included in this survey, considerable variation in mean length from 5.4 to 17.6 μm was recorded. Mean MT length was low in younger cells but increased with age until about the time of growth cessation after which time MTs became quite short (Fig. 3.3). When plotted against cell elongation rate (Fig. 3.4), the mean MT length is seen to be lower in cells that are undergoing rapid growth than in those

undergoing slow growth. Cell circumference appears to have little influence on MT length (Fig. 3.5) but cells of lesser circumference tend to have shorter MTs.

3.3.4 Microtubule Density

There was considerable variation in the number of MTs per unit area at all stages of development but in general, MT frequency appeared to decline with cell age (Fig. 3.6). Expressed as total MT length per unit area, MT density is also highly variable at all stages of development (Fig. 3.7). There was no clear change during the growth period but there is a general decline in MT density after elongation stops.

3.3.5 Microtubule Orientation and Helical Cell Structures

Plotting median MT angle for growing cells as a function of the angle of the neutral line in the same cell (Fig. 3.8) rules out a direct association between cortical MT and chloroplast (or neutral line or actin) orientation. The regression line shows that MT orientation does not follow a helical pattern but is centered about the cell's transverse axis. (The median MT angle was plotted in Fig. 3.8; using the mode or mean did not change the conclusion that there was no relation between MTs and the visible helical features of the cells.) Examples of cortical MTs running parallel to chloroplast files or the neutral line are observed but there is no consistent sign on the histograms for individual cells of even a minor peak of MTs at the neutral line angle or at 90^{o} to it. Endoplasmic MTs which often are oriented in the same direction as the neutral line do not interfere with the image of cortical MTs because they are located in a lower plane of focus and because they are usually obscured by the light absorbing chloroplasts.

3.3.6 Microtubule Orientation and Cell Age

Representative immunofluorescence micrographs from cells of increasing age are presented in Fig. 3.9a'-e'. Also included are the histograms showing relative abundance of MTs of different angles (a"-e"). These selected figures show that the predominance of near transverse MTs declines as cells age until non-extending cells have a nearly random distribution pattern. The continuous nature of this change is apparent when the data for a larger sample of cells over a similar range of ages are presented in a 3-dimensional plot (Fig. 3.10) relating the abundance of MTs of different angles to cell age. These figures also show that longitudinal MTs appear before elongation ceases and become transiently predominant shortly thereafter. This is also apparent when the relative number of transverse, oblique and longitudinal MTs are compared throughout development (Fig. 3.11). For the period of cell development covered in this study, relative elongation rate declines continuously with cell age (Fig. 3.2). The angular distribution of MTs in growing cells is therefore a complex function of relative growth rate (Fig. 3.12) with mainly transverse order giving way to mainly longitudinal before disorder prevails at the end of the growth period.

3.4 DISCUSSION

This study provides a quantitative picture of MT orientation in *Nitella* cells fixed at known times covering much of their development.

Printing of micrographs at high magnification made it possible to digitize the fluorescent images with a fair degree of accuracy. However, a small amount of error was undoubtedly introduced where fluorescent units merged or crossed at very slight angles. Because of this, length and number are less certain than angle measurements and may be reflected in a bigger scatter of points on graphs pertaining to MT length frequency and density.

3.4.1 Microtubule Organization

(i) Microtubule Length and Density Measurements

The cortical MT array of *Nitella* seen by immunofluorescence microscopy comprises relatively short, linear elements. The lengths of the fluorescent units measured in the internodal cells of *Nitella* are similar to the lengths of single MTs measured in other plant cells. Mean values ranging from 5.4 to 17.6 μm per cell have been recorded with an average length for all cells in this sample of 10.6 μm. By comparison, MTs ranging from 3.75 to 25 μm and on average 11 μm in length were recorded by immunofluorescence for carrot suspension cell disc preparations (Lloyd *et al.* 1980b) while protoplast ghosts of tobacco have yielded MTs up to 16 μm long (Van der Valk *et al.* 1980). Similar but somewhat shorter MT lengths have been measured using the electron microscopical methods of serial sectioning (Hardham & Gunning 1978; Robinson & Quader 1980) and dry cleavage (Traas 1984). Ultrastructural analysis of *Nitella* MTs must be applied to confirm whether the fluorescent structures in *Nitella* are, in fact, single MTs. Hotchkiss and Brown's (1987) freeze-fracture study of *Nitella* internodal cells indicated pairing of some MTs in expanding cells; however, their evidence does not suggest that all MTs are in fact paired.

Three interrelated parameters, mean MT length, MT frequency (number per area) and MT density (total MT length per area) are all generally greater in growing cells than in older cells that have finished expanding. This suggests that MT assembly may be depressed at growth cessation when strict regulation of mf deposition is perhaps no longer necessary.

MT length shows an obvious change during the growing phase with relatively short MTs measured in the youngest cells and very long MTs recorded in cells judged to be near completion of growth (neither frequency nor density shows any clear trend during the same period). The change in mean length is also related to the rate of elongation, with MTs much shorter in rapidly expanding cells (see Fig. 3.5). Mean length can be considered to be the product of two variables, tubulin concentration and MT number. If the number of MTs is constant but tubulin concentration drops, then MTs will become shorter on average. Cell expansion may have a diluting effect on the tubulin pool that must be repleted with synthesis of new tubulin. In rapidly expanding cells, the rate of tubulin synthesis might not keep pace with the rate of expansion so that a relatively low concentration of tubulin is maintained.

Alternatively, the variation in mean length could be related to a difference in MT lability between rapidly and slowly growing cells. MTs might be more dynamic in rapidly growing cells in order to retain their control over wall deposition in the presence of strong realigning forces imposed by extension. If MTs in young cells are more dynamic, artifactual shrinkage during pre-fixation perfusion (see Ch. 2, section 2.4.3) could account for the relatively short MTs that are observed.

A third possibility is that MT length is somehow determined by the dimensions of the cell. Hardham & Gunning (1978) reported that the cortical MTs of *Azolla* root cells were, on average, about one eighth of a cell circumference in length. This ratio was thought to relate to the possible existence of MTOCs at each

of the cell's four edges (Gunning *et al.* 1978). A length of one eighth a circumference and therefore one half a cell face, would allow MTs nucleated at opposite edges to interact (Gunning *et al.* 1978). *Nitella* internodal cells do not have edges (except at either end) but could conceivably have a finite set of nucleating sites per circumference. The comparison of mean MT length and circumference suggests no such relationship. Although there is a tendency for smaller cells to have shorter MTs, this may relate more strongly to the fact that these cells are young or rapidly growing. In many cases, cells with approximately the same circumference had vastly different mean MT lengths.

(ii) Microtubule Orientation

The data on orientation show continuous MT changes during and immediately after the linear phase of growth (Green 1954) that can be examined by perfusion. The population of transverse MTs in young, rapidly expanding cells gradually declines along with relative growth rate. Longitudinal MTs supplant the transverse ones and are predominant soon after growth ceases. A slight predominance of longitudinal MTs persists in the near random MT arrangement of older, non-growing cells.

A number of qualitative studies of other cells show that MTs have an approximately transverse orientation in cells expected to be elongating. These studies cover a diversity of cell types including unicellular (Hogetsu & Oshima 1985) and filamentous green algae (Galway & Hardham 1986), *Azolla* root tip cells (Hardham & Gunning 1978; Busby & Gunning 1983), higher plant suspension cultures (Lloyd *et al.* 1980a; Simmonds *et al.* 1983; Falconer & Seagull 1985a) and intact tissues (Traas 1984; Itoh & Shimaji 1976; Hardham *et al.* 1980; Roberts *et al.* 1985; Wick *et al.* 1981; Mita & Shibaoka 1983).

Developmentally-dependent shifts in MT orientation patterns have also been documented in some plant cells. Mita and Shibaoka (1983) observed a change in

the orientation of MT arrays from transverse to random associated with swelling of onion leaf sheath cells, during bulb development. The MTs of mung bean hypocotyl (Roberts *et al.* 1985) cells are usually predominantly transverse yet oblique and longitudinal arrays have also been observed. It is suggested that this change in pattern - induced experimentally by ethylene treatment - may occur in response to environmental cues as part of normal development. Differentiation of *Raphanus* root tip cells involves a change from consistently transverse MTs in meristematic cells to highly variable orientations in elongated cortical cells (Traas 1984). Takeda and Shibaoka (1981) observed a predominance of transverse wall mfs (presumably controlled by cortical MTs) in young *Vigna* epicotyl epidermal cells. At a later stage of development, transverse, longitudinal and oblique mfs were observed in similar frequencies, while older non-growing cells had predominantly longitudinal mfs. The establishment of an organized MT array appears to be necessary for directed cell expansion. Apparently, the ability of a cell to alter the orientation of such an array is also an important feature of differentiation.

3.4.2 Microtubules and Cell Wall Organization

Cortical MTs are now widely recognized as agents of morphogenesis in plant cells through their role in cell wall mf alignment. Support for this role has come from the observation that MTs frequently are positioned parallel to the innermost mfs of the cell wall and from the dramatic effect anti-MT drugs have on the shape of expanding cells (See Fig. 1.1). Because *Nitella* internodal cells have contributed heavily to the development of both the multinet growth hypothesis (Green 1960) and the self-assembly hypothesis (Neville *et al.* 1976; Neville & Levy 1984) of plant cell wall structure, they are ideal specimens for the study of mf alignment by MTs. Indeed, Green's proposal (1962) that "proteins of spindle fiber nature exist in the cortical cytoplasm and are active in the control of wall texture and cell form"

was based on experiments with *Nitella* internodal cells even before the 'discovery' of MTs in higher plant cells with the electron microscope (Ledbetter & Porter 1963). Subsequent electron micrographs of Nagai & Rebhun (1966) confirmed the presence of MTs in the cortical cytoplasm of *Nitella* and Pickett-Heaps (1967a) described co-alignment of MTs and mfs in *Chara* but further ultrastructural evidence has been very limited. On the other hand, work with MT inhibitors in *Nitella* (Green 1962, 1963; Richmond 1977; Chapter 5) has demonstrated that mf alignment is dependent on MT organization. Visualization of MT-mf parallelism in *Nitella* has been achieved recently by freeze-fracture techniques for both elongating and mature internodal cells (Hotchkiss & Brown 1987). However, this evidence is only qualitative. To analyse MT organization in characean internodal cells quantitatively, so that MT orientation can be compared with the detailed description of cell wall patterns that is available, it has been necessary to apply immunofluorescence microscopy.

If MT orientation controls wall mf alignment in *Nitella* as predicted by Green and King (1966), then the changing MT pattern reported here should be reflected in equivalent changes in mf patterns throughout development. Microfibrils should be deposited in a transverse orientation during elongation with increased deviation about the transverse axis as the relative growth rate declines. Longitudinal alignment should be detected about the time of growth cessation with a more random pattern of deposition in non-growing cells. The evidence from several detailed studies on *Nitella* internodal cell wall structure will be reviewed that strongly supports the view that MTs are responsible for the alignment of mfs in expanding cells. Whether this role persists in non-expanding cells is less certain.

When an internodal cell is first formed from the division of a segment cell, it has the shape of a flattened cylinder and a wall that is isotropic in polarized light (Green 1958) containing randomly oriented mfs (Green 1958; Fig. 2 of Hotchkiss & Brown 1987). Coincident with the change to predominantly axial expansion is

the establishment of an optically birefringent wall (Green 1958; Probine & Preston 1961; Richmond 1983) with mfs of the innermost wall in parallel arrays of transverse (see Fig. 4 of Green 1958; Fig. 3 of Hotchkiss & Brown 1987) or nearly transverse (Probine & Preston 1961) orientation. During expansion, mfs continue to be deposited within the plane of the inner wall in a dispersed but mostly transverse orientation. This has been demonstrated by the relatively constant birefringence index[1] maintained throughout growth (Richmond 1983) and from electron micrographs of inner wall replicas (Green 1958) and stripped wall lamellae (Probine & Preston 1961).

Changes in cell wall mf deposition occur with the cessation of growth. Birefringence declines (Fig. 3 of Richmond 1983) and an isotropic wall pattern is detected (Green 1958; Probine & Preston 1961). During this shift, mfs have been shown to be deposited in non-transverse orientations. Green (Fig. 6 of Green 1958) observed "groups of near parallel fibrils running in directions quite removed from the transverse" and Probine & Preston (1961) concluded that in maturing cells mfs were deposited at all angles from the transverse with the second preferred orientation after transverse being longitudinal. The emergence in older cells of longitudinal MTs may thus be significant and it is conceivable that they are contributing to the formation of a crossed-fibrillar wall pattern.

Based on evidence from X-ray diffraction studies (Probine & Barber 1966) and polarized light microscopy (Green 1958; Richmond 1983), the structure of

---

1. Birefringence index (BRI) is a measurement of the degree of mf alignment from which the mean angular dispersion of mfs can be derived. It is determined by placing an intact internodal cell between crossed polarizers and measuring the relative positions of the dark bands that result from the action of polarized light on cell wall texture. BRI is then calculated by dividing the distance of separation between the midpoints of the two lateral dark bands by the cell diameter. Thus, a BRI of 1.0 would indicate zero dispersal about the transverse axis whereas a BRI of 0 would correlate with maximal dispersal (a mean angular dispersion of 45^{o} about the transverse axis). Because BRI measurements rely on the curvature of the internodal cell, they can be utilized for documenting changes in the wall texture of living cells. For details, see Richmond 1983.

mature, non-expanding internodal cell walls has been described as "random" or "disorganized". Although such a pattern of deposition would be predicted from the results of the MT investigation presented in this chapter, examination of the walls of mature internodal cells using electron microscopy has revealed distinctly non-random patterns. Inner wall replicas show that mfs in *Nitella axillaris* are arranged in small fields of parallel fibrils (Green 1958). Adjacent fields are oriented at distinct angles to one another such that the overall pattern perceived by polarized light microscopy is isotropic. From the MT pattern observed in mature internodal cells (Fig. 3.4e') it seems unlikely that MTs can influence the deposition of such a pattern.

Oblique sectioning through an inner wall strip of *Nitella opaca* (Probine & Barber 1966) produced a "herring-bone" pattern suggestive of the arced patterns seen in oblique sections of helicoidal walls. By tilting a vertical section in opposite directions about an axis parallel to the plane of cell wall deposition (using a goniometric stage), Neville and Levy (1984) demonstrated a reversal in the direction of arcs showing that the pattern of wall deposition was helicoidal. That mfs are responsible for the arcing patterns has been more clearly demonstrated recently in oblique cell wall fractures (See Fig. 4 of Hotchkiss & Brown 1987) and after EDTA extraction, resin removal and Pt-shadowing of oblique sections (See Fig. 2 of Levy 1987). A helicoidal wall would be optically non-birefringent; interpretations from polarizing microscopy of "random" wall patterns could just as likely be helicoidal.

It has been suggested that the helicoidal pattern might arise through self-assembly of mfs (Neville *et al.* 1976) at a precise angle to previously deposited fibers. The description of inner wall replicas (Green 1958) showing locally ordered fields of mfs in non-growing cells is not inconsistent with the self-assembly concept. It is possible that each 'field' of mfs might be shifted through a given angle with respect to the previously deposited field.

The quantitative description of MT orientation provided by this study and the detailed descriptions of cell wall patterns are consistent with the idea that MTs play a role in cell wall deposition during expansion in internodal cells of *Nitella*. Early on in the development of the internodal cell there forms a parallel array of MTs which perhaps, through interactions with the plasma membrane or the cellulose synthesizing complexes located there (EF globules and PF rosettes; Hotchkiss & Brown 1987) resists what may be the natural tendency for a helicoidal wall to be assembled. Instead mfs are deposited transversely such that predominantly longitudinal expansion takes place and an elongated cylinder is formed. As relative growth rate declines, changes in MT and mf patterns are observed. The emergence of longitudinal MTs in cells at the end of the growth phase is reflected by similar changes observed in wall patterns; however, a one-to-one relationship between the randomly-arranged MTs and the helicoidally-arranged mfs of mature non-growing cells seems unnecessary. Furthermore, it has been demonstrated that cortical MTs are not involved in the deposition of helicoidal walls in other types of plant cells (Emons 1982) Thus, MTs may function in overriding the tendency for a helicoidal wall to be formed by self-assembly and the cue for such behaviour appears to be cell growth. Helicoidal walls that have been observed in other plants have only been found in non-growing cells (Roland 1981; Roland *et al.* 1982; Roland & Mosiniak 1983; Parameswaran & Liese 1981) or non-growing parts of tip-growing cells (Emons & Wolters-Arts 1983). The available evidence and the present understanding of directed cell expansion cannot substantiate Neville and Levy's claim (1984) that a helicoidal wall is produced at different stages of cell elongation. It seems more likely that as growth cessation approaches the MT array desists from regulating mf orientation and self-assembly begins.

3.4.3 Control of Microtubule Orientation

A complete theory of the mechanisms by which *Nitella* MTs are aligned should take account of their strictly transverse (not helical) alignment (Figs. 3.1 and 3.3), their progressive dispersion as relative growth rate declines (Figs. 3.4, 3.5 and 3.7) and the slight predominance of longitudinal MTs particularly just after growth stops.

The strain-aligned helical features of the cell (chloroplast files, neutral line, actin bundles and streaming) have all been considered as structures by which MTs and/or mfs could be oriented (Gertel & Green 1977; Green 1963; Green & King 1966; Probine 1963; Probine & Preston 1958). At no stage of development, however, were cortical MTs seen in a helical organization (cf. Lloyd & Seagull 1985); the median MT angle in growing cells remains close to 90^{o} irrespective of the orientation of the helical features (Fig. 3.3). The MTs in these cells therefore resemble the truly transverse template envisaged by Green and King (1966).

The gradually increasing dispersion of MTs about the median transverse orientation implies that orientation is regulated by some continuous variable(s) rather than by a switch between one MT array in growing cells and a second in non-growing cells. One possible regulator is strain, which decreases in proportion to relative growth rate.

Any relationship between strain and MT alignment could potentially operate in either direction; the rate of growth could affect MT organization or conversely, MTs, through alignment of wall mfs, might affect the rate of growth. Growth is subject to a variety of metabolic and physical controls (Green 1968; Green *et al.* 1971; Métraux & Taiz 1978; Métraux 1982; Probine & Preston 1962; Richmond *et al.* 1980; reviewed by Taiz 1984). It seems unlikely that the decreasing degree of transverse MT alignment causes wall changes that reduce relative growth rate (and hence strain) since correlated decreases in relative growth rate and transverse order of MTs occur with little change in the ratio of transverse to longitudinal

growth (Green & King 1966; Probine & Barber 1966). Furthermore, the 'randomization' of mfs following MT disassembly affects the directional aspects of growth but has little or no effect on the plasticity of the wall and consequently the overall growth rate (Richmond 1983).

Strain is required for the deposition of transverse mfs; when growth is mechanically prevented in parts of expanding *Nitella* cells (Green & Chen 1960; Gertel & Green 1977), mfs are deposited "randomly" in the non-growing regions while remaining transverse elsewhere in the same cell. If these mf arrangements correlate with a change in MT orientations similar to that seen in mature internodal cells, the idea that strain affects the degree to which MTs are transversely aligned would be supported. Strain could then be one factor in normal growth to which the MT array continuously adjusts to produce the gradual orientation changes observed.

It is held that strain is required for deposition of transverse mfs but that the direction of strain does not determine their orientation (Gertel & Green 1977). The same could hold for MT alignment since, while the degree of transverse alignment correlates with the magnitude of the strain, the median MT orientation is unresponsive to the changing direction of strain recorded cumulatively in the varying helical arrangement of cytoplasmic features (Fig. 3.3). A possible alignment mechanism that is independent of the direction of strain is that microtubules maximise their overlap to form "self-cinching loops" (Green 1962, 1963, 1980) whose stable position of minimum circumference is therefore transverse. The "loops" could take the form of an interconnected network of individual MTs. In dilute colchicine solutions mfs were aligned perpendicular to maximum strain, about 35 degrees off transverse, (Green 1963) suggesting that if MTs are partially disassembled and cannot therefore form connections with one another their transverse orientation is lost. It is noteworthy however that young *Nitella* cells have many transverse microtubular structures lacking the contact with

their neighbours that this hypothesis predicts (See Fig. 3.4a'). Thus, the source of the persistent transverse orientation remains unresolved.

How strain might act on MTs is unclear. There could be some direct realignment involving a comparable mechanism to that realigning wall mfs. The effect would be small, however, if there are forces resisting realignment (*e.g.*, self-cinching loops) or if individual MTs have a short life span as suggested by the dynamic instability model (Kirschner & Mitchison 1986).

MTs may be unstable when subjected to strain above a critical threshold level (B.C. Goodwin, personal communication). If so, MTs might depolymerize rapidly when aligned along the axis of maximum strain in a cell that is rapidly elongating but withstand the minor circumferential strain or the declining longitudinal strain at later stages of growth. This idea is supported by the fact that relatively few non-transverse MTs are seen in rapidly elongating cells (see Fig. 3.7) but become more numerous as the elongation rate declines. Similarly, circumferential strain is greater than longitudinal in the early stages of internodal cell development when the cells are shaped like flattened cylinders. It is plausible that circumferentially-aligned MTs would be unstable under these conditions and therefore be unable to regulate mf orientation which is apparently random at this stage (Green 1958; Hotchkiss & Brown 1987).

To explore the possibility that strain is involved in MT orientation, it will be necessary to examine the process of MT assembly to determine if MTs in rapidly expanding cells (subject to maximum strain) are preferentially assembled in transverse directions, whether they are moved into these positions by other elements or forces after they have assembled or are assembled randomly and differentially stabilized according to orientation relative to strain or some other factor.

3.5 CONCLUSION

At the start of the period of *Nitella* development studied, many MTs have a nearly transverse orientation. This is gradually lost in older cells as relative growth rate declines, but the median MT orientation remains transverse in growing cells as the helically arranged features in the cortical cytoplasm are reoriented by strain. The results are not wholly compatible with orientation mechanisms relating MT alignment to other cortical structures or with mechanisms depending on interactions between MTs. It seems possible however that MT alignment depends on differential MT stability in a changing physical environment.

CHAPTER 3 - FIGURES

Fig. 3.1. Cortical cytoplasmic features of the *Nitella* internodal cell. All photographs are from the same glutaraldehyde-fixed cell; are arranged so that their relative orientation with respect to the cell axis and to each other is preserved; and are optically tangential to the cell wall.

Fig. 3.1a. Fluorescence micrograph of cortical microtubule array subjacent to the plasma membrane. The median MT orientation is along the transverse axis indicated in c.

Fig. 3.1b to d. Nomarski micrographs.

Fig. 3.1b. Same field as in a but in lower focal plane.

Fig. 3.1c. Cell edge adjacent to field shown in a and b. Grid indicates the cell's longitudinal and transverse axes; arrow shows the orientation of the chloroplast files and other parallel spiral features.

Fig. 3.1d. Neutral line in same focal plane as b but another region of the cell. The neutral line separates opposing flows of the streaming cytoplasm and is recognized by a rift between parallel chloroplast files and by a wall striation. The orientation of the helix formed by the neutral line, wall striations, chloroplast files, sub-cortical actin bundles and streaming cytoplasm changes gradually during expansion but is of a uniform angle throughout the cell at any given time.

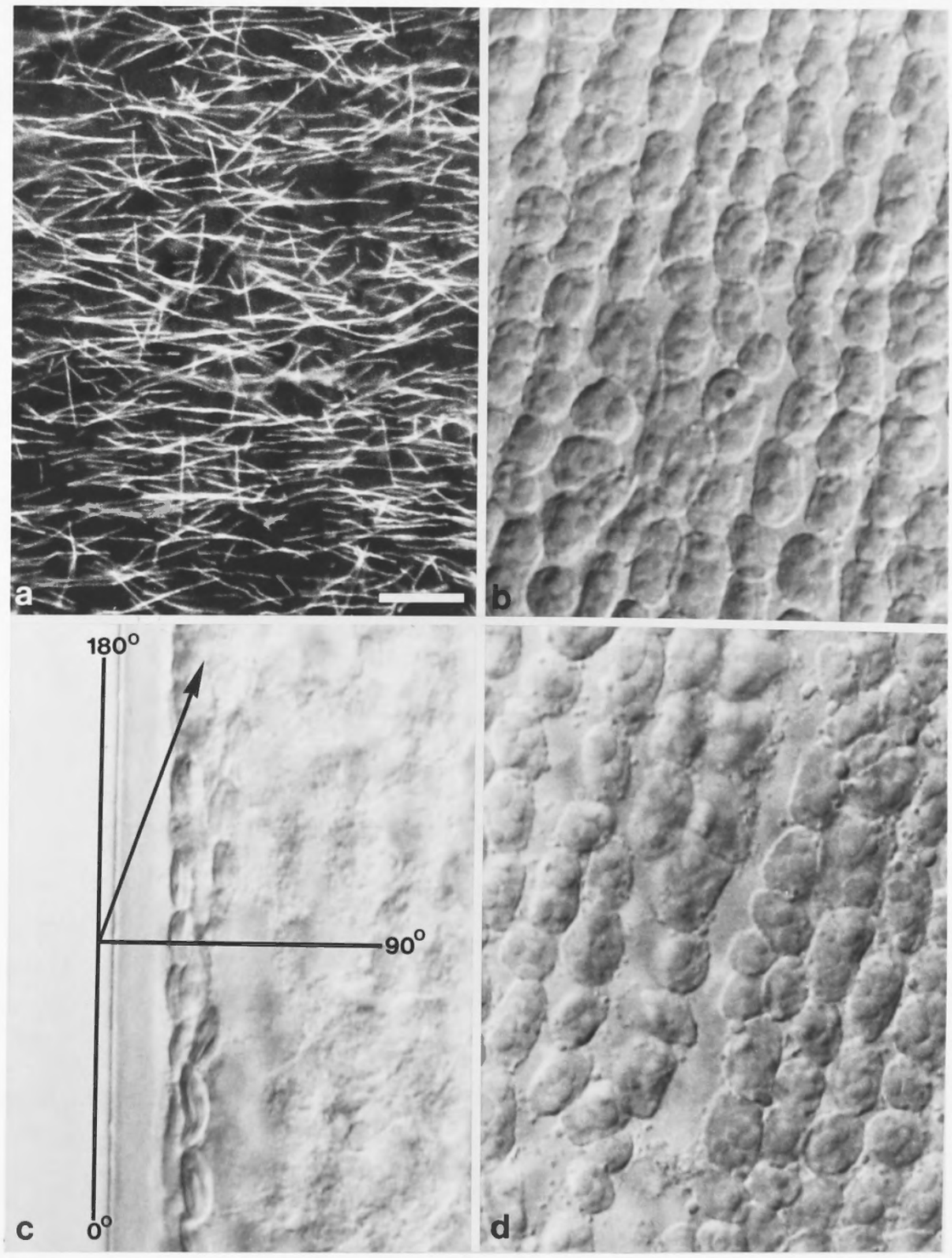
a
b
180°
90°
0°
c
d

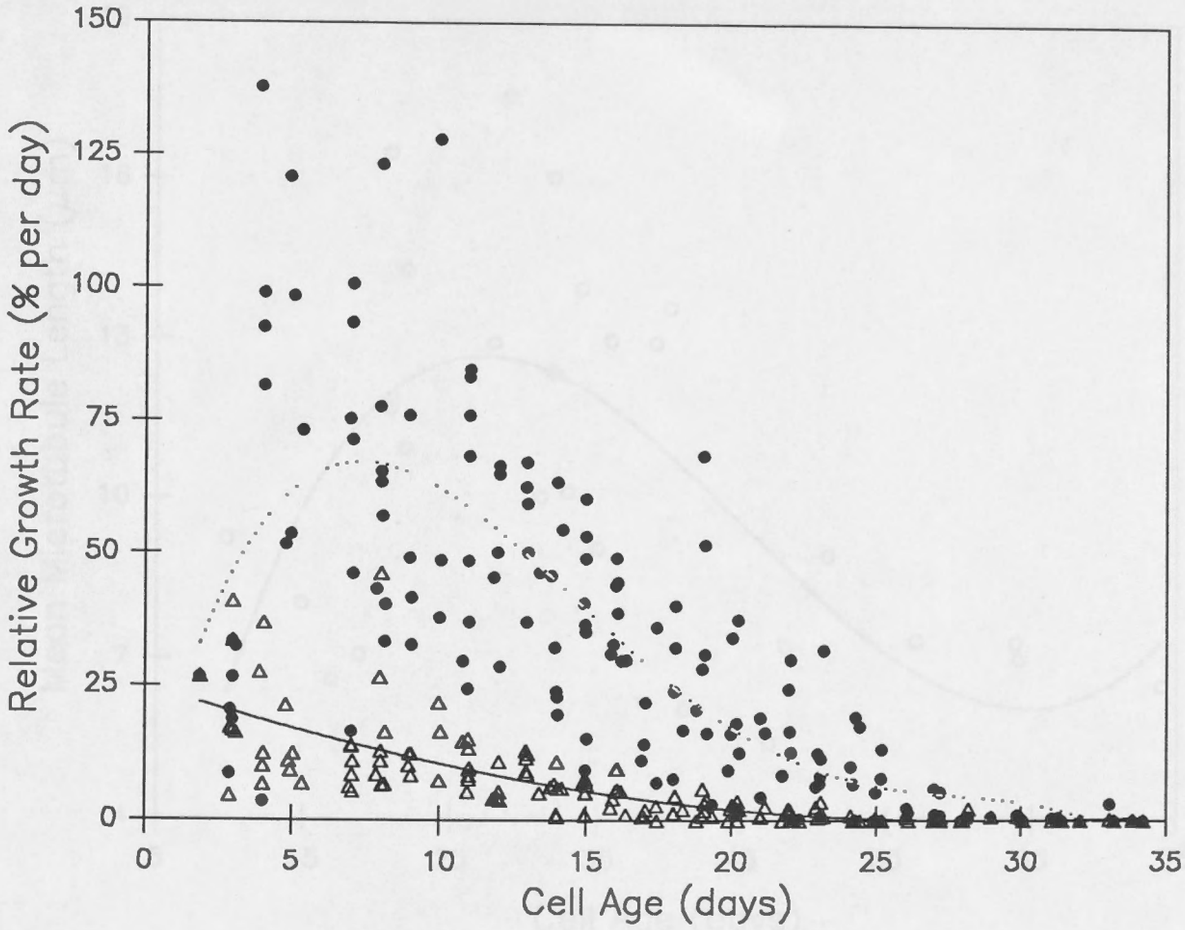

Fig. 3.2. Changes in the rate of expansion during the development of internodal cells. Relative longitudinal (•) and circumferential (Δ) growth rates (expressed as a percentage) were calculated at various stages in the development of 24 cells up to 35 days of age. There is an initial rapid increase in the relative longitudinal growth rate followed by a steady decline until about 20 days after which the decline is more gradual. Elongation stops at about 30 days. Relative circumferential growth declines gradually and generally stops a few days before elongation is complete.

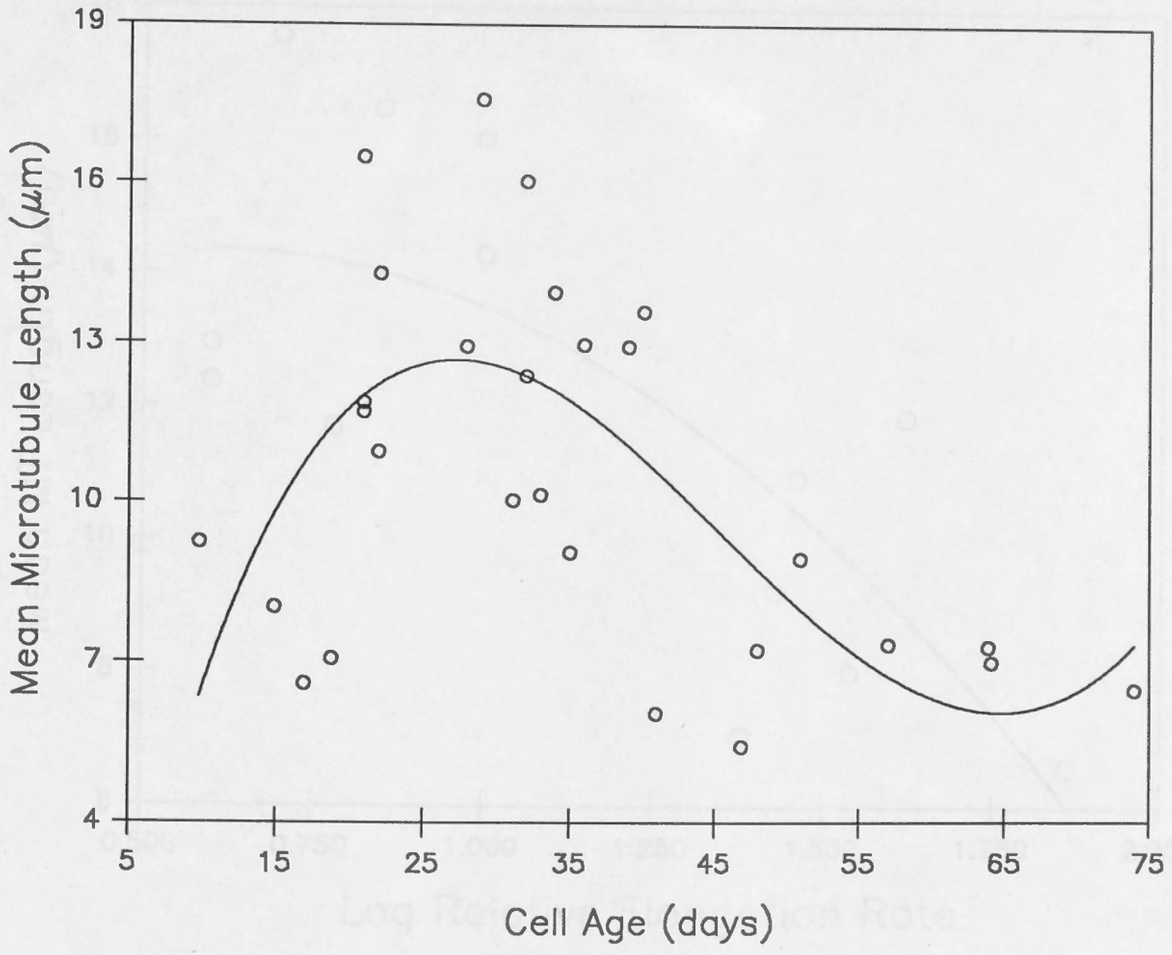

Fig. 3.3. Changes in MT length with cell age. Mean lengths of MTs were calculated for each cell and are plotted against cell age. The fourth order regression line indicates a tendency for mean length to increase with age up until about 30 days after which time there is a gradual decline.

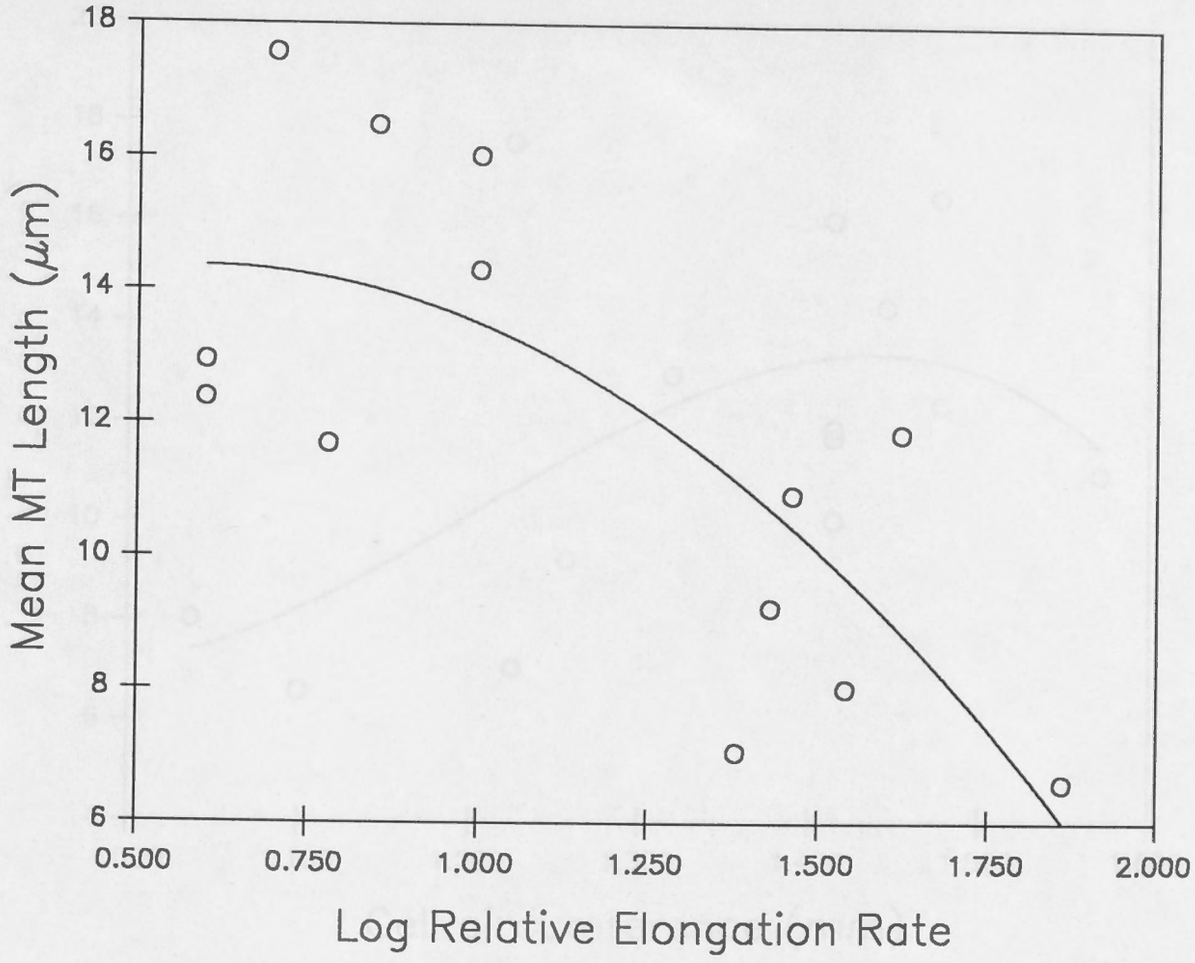

Fig. 3.4. Changes in MT length with relative elongation rate. Mean MT length for each cell is plotted against the relative elongation rate. There is a tendency for rapidly expanding cells to have shorter MTs than those cells which have slow growth rates.

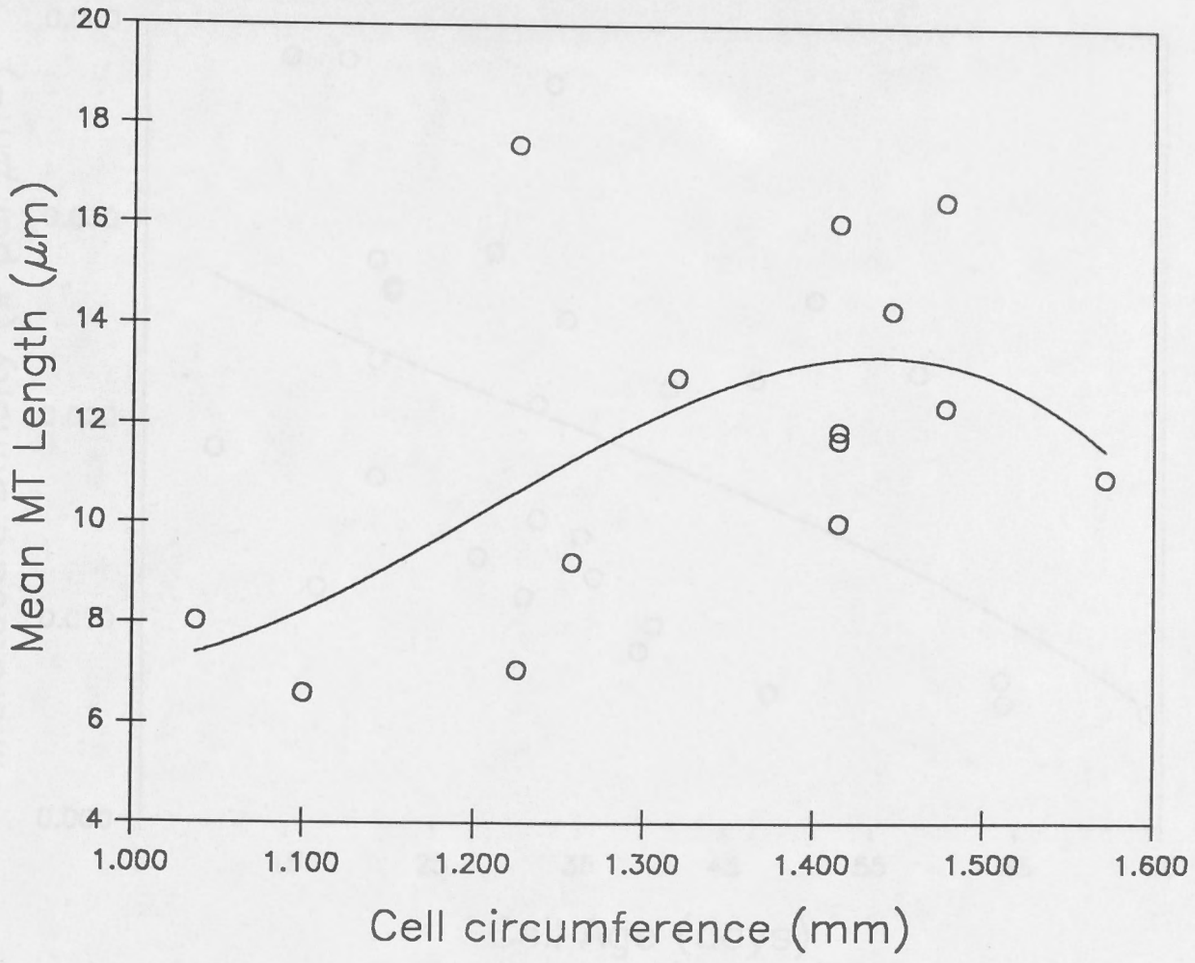

Fig. 3.5. Changes in mean MT length with cell circumference. Mean MT length is compared with the circumference of cells that contained predominantly transverse MT arrays.

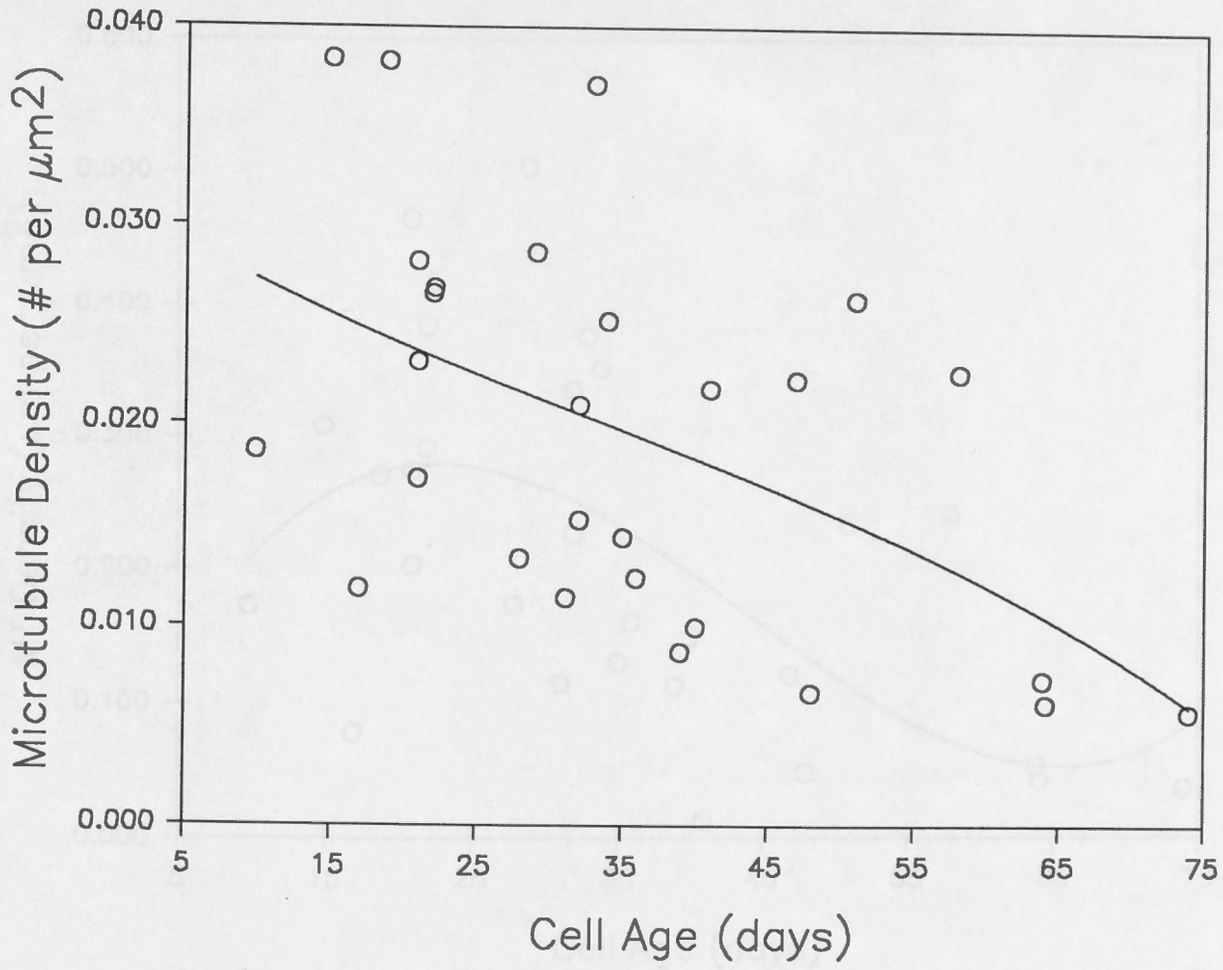

Fig. 3.6. Microtubule Density and Cell Age. The number of MTs per μm^2 is compared for cells of various ages. There appears to be much variation in MT density at all stages of development but there is a general reduction in older cells.

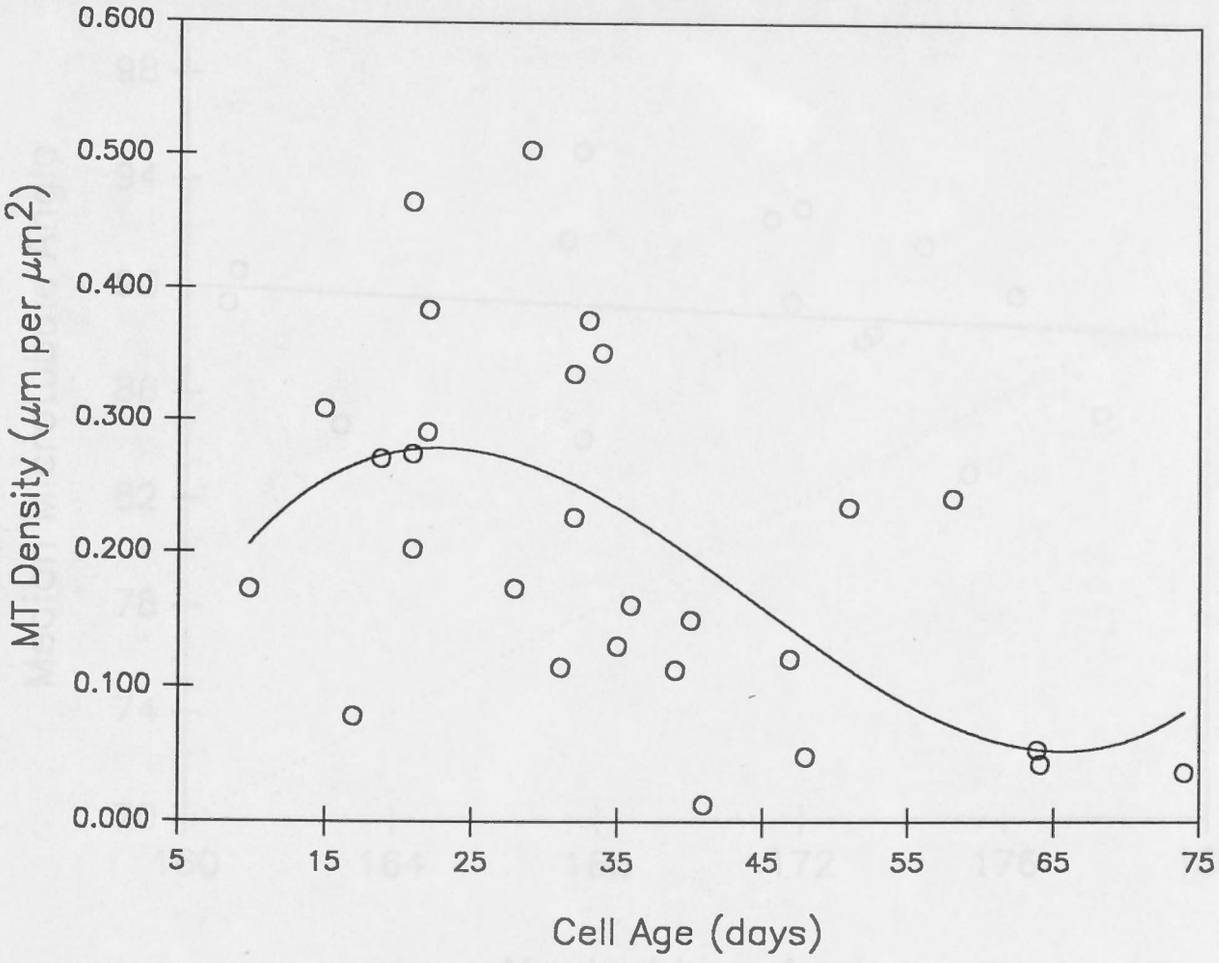

Fig. 3.7. Microtubule Density and Cell Age. MT density, expressed as total MT length per area (independent of the total number of MTs) undergoes an increase until about 20 days after which a gradual decline is observed.

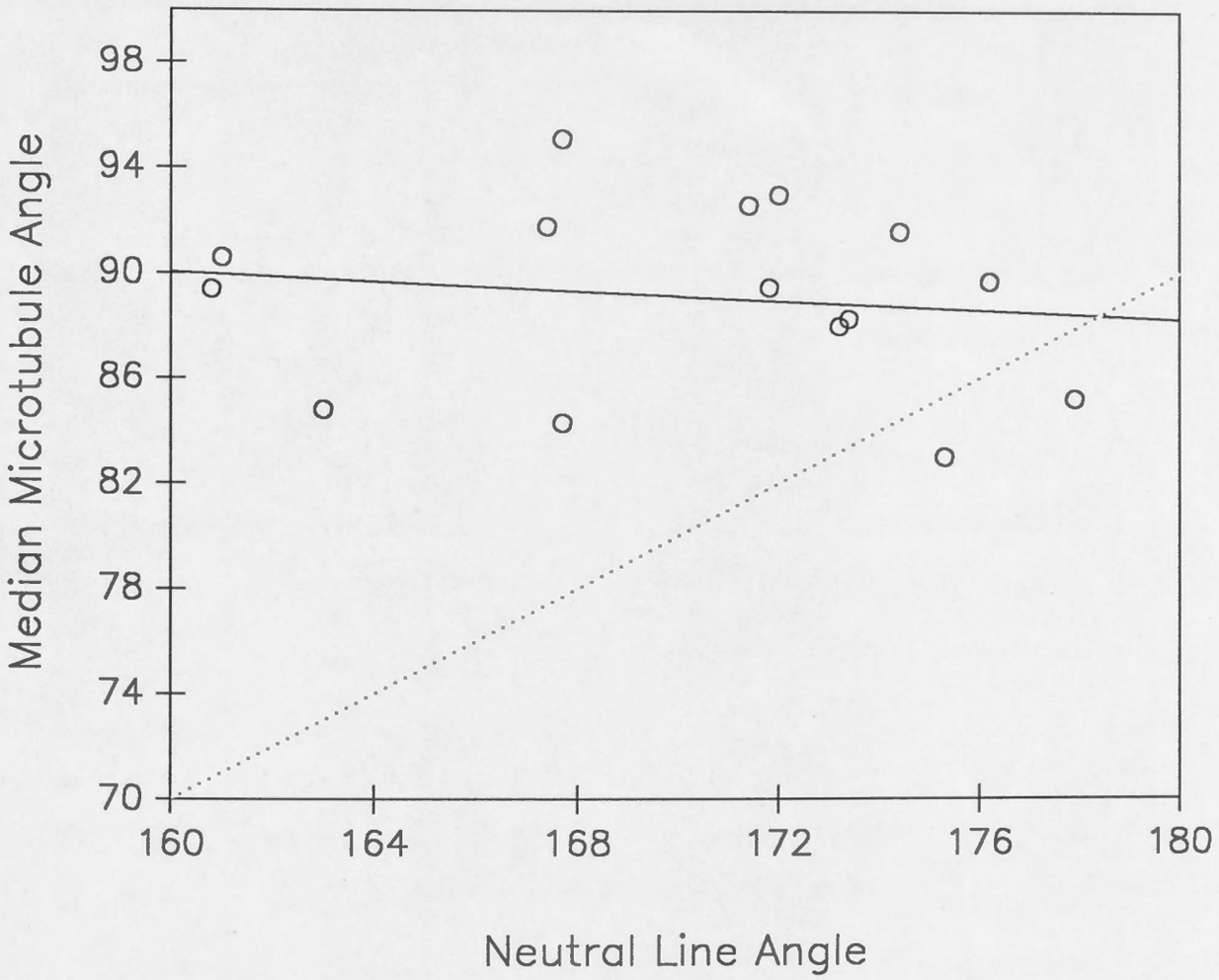

Fig. 3.8. Median MT orientation plotted against the orientation of the strain-aligned, helical features of the cell. The median MT angle is relatively stable and nearly transverse as indicated by linear regression analysis (solid line). The results do not support a direct relationship between MT orientation and the changing angle of the neutral line. The broken line shows the expected regression line if the median MT angle lay at 90^{o} to the neutral line and the other helical structures.

Fig. 3.9. Quantitative MT orientation analysis at representative stages of cell expansion.

a to e. Schematic representation of a *Nitella* shoot as grown under experimental conditions; approximately actual size.

a' to e'. Fluorescence micrographs of MT arrays for cells selected to approximately correspond with cells **a** to **e**. Photographs are positioned with vertical sides parallel to cells' long axes to compare orientation at different stages of development. - Bar 10 μm.

a" to e". MT angle frequency distribution histograms for the cell's shown in **a'** to **e'**. 0 and 180^{o} indicate long axis of cell; transverse orientation = 90^{o}. In young, rapidly expanding cells (**a**), MTs are tightly transverse (**a',a"**) but as relative growth rate decreases (**b**), MTs are increasingly dispersed (**b',b"**). During later stages of expansion (**c**), longitudinal orientation is more prominent (**c'**) with MTs grouped about both the transverse and long axes (**c"**). When expansion ceases (**d**), the preferred MT orientation is parallel to the long axis (**d'**) with a majority of MTs oriented close to 0 or 180Θ (**d"**). In older, non-growing cells (**e**), a random MT orientation pattern is approached (**e',e"**).

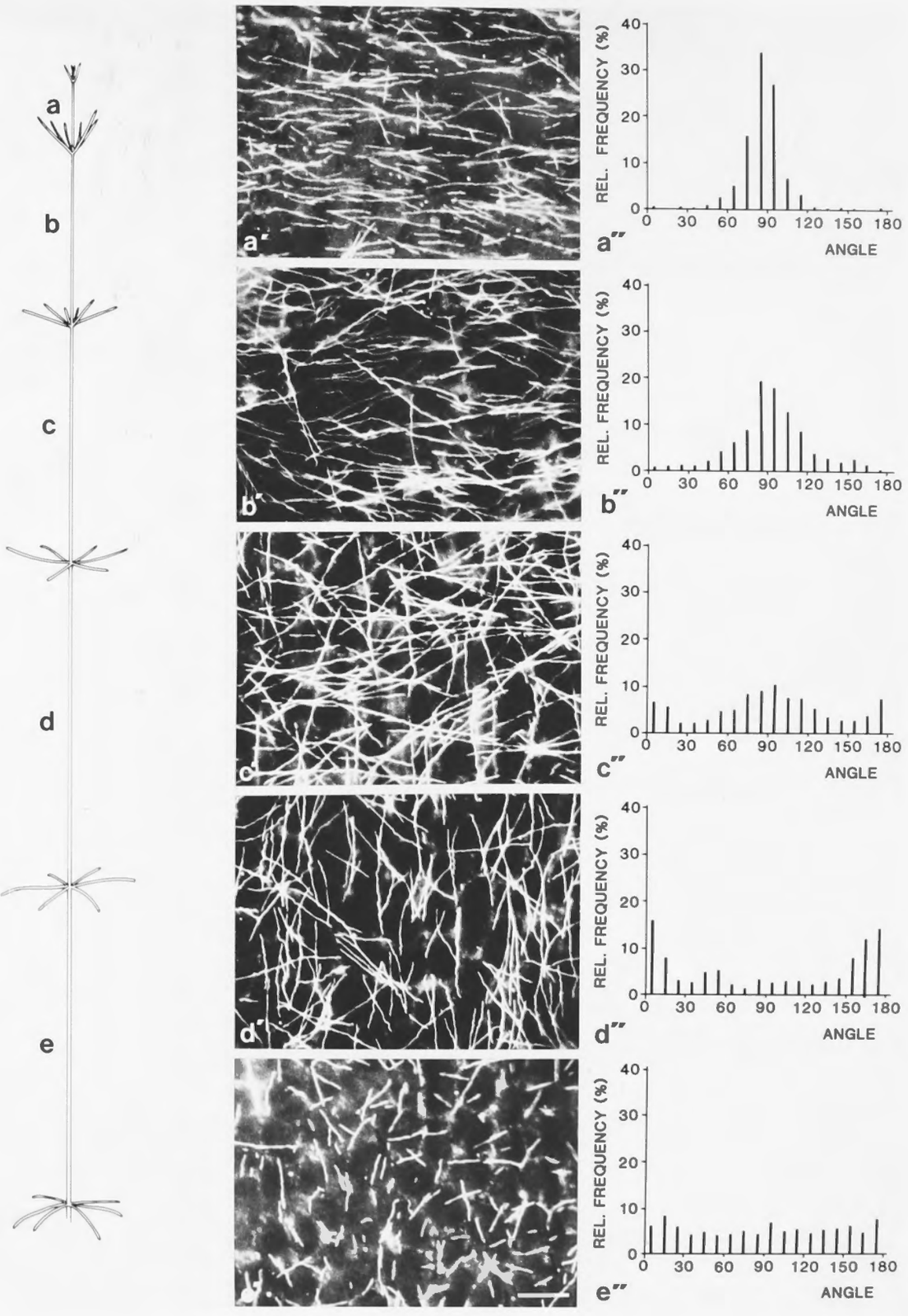
a
b
c
d
e
a'
b'
c'
d'
e'
REL. FREQUENCY (%)
ANGLE
0
10
20
30
40
0 30 60 90 120 150 180
a''
b''
c''
d''
e''

Fig. 3.10. Three dimensional plot relating MT orientation pattern to cell age. Microtubule image analysis was carried out as described in Materials and Methods for 26 cells between 10 and 74 days of age. Angular distribution was plotted against age using a contour map drawing routine. Although the plot is drawn through all of the input data points, interpolated values are included to produce a regular grid. These values were obtained using a double linear, quadratic and weighted average interpolation routine. The plot illustrates the gradual progression from a predominantly transverse to a longitudinal pattern and eventually to a near random distribution in older non-expanding cells.

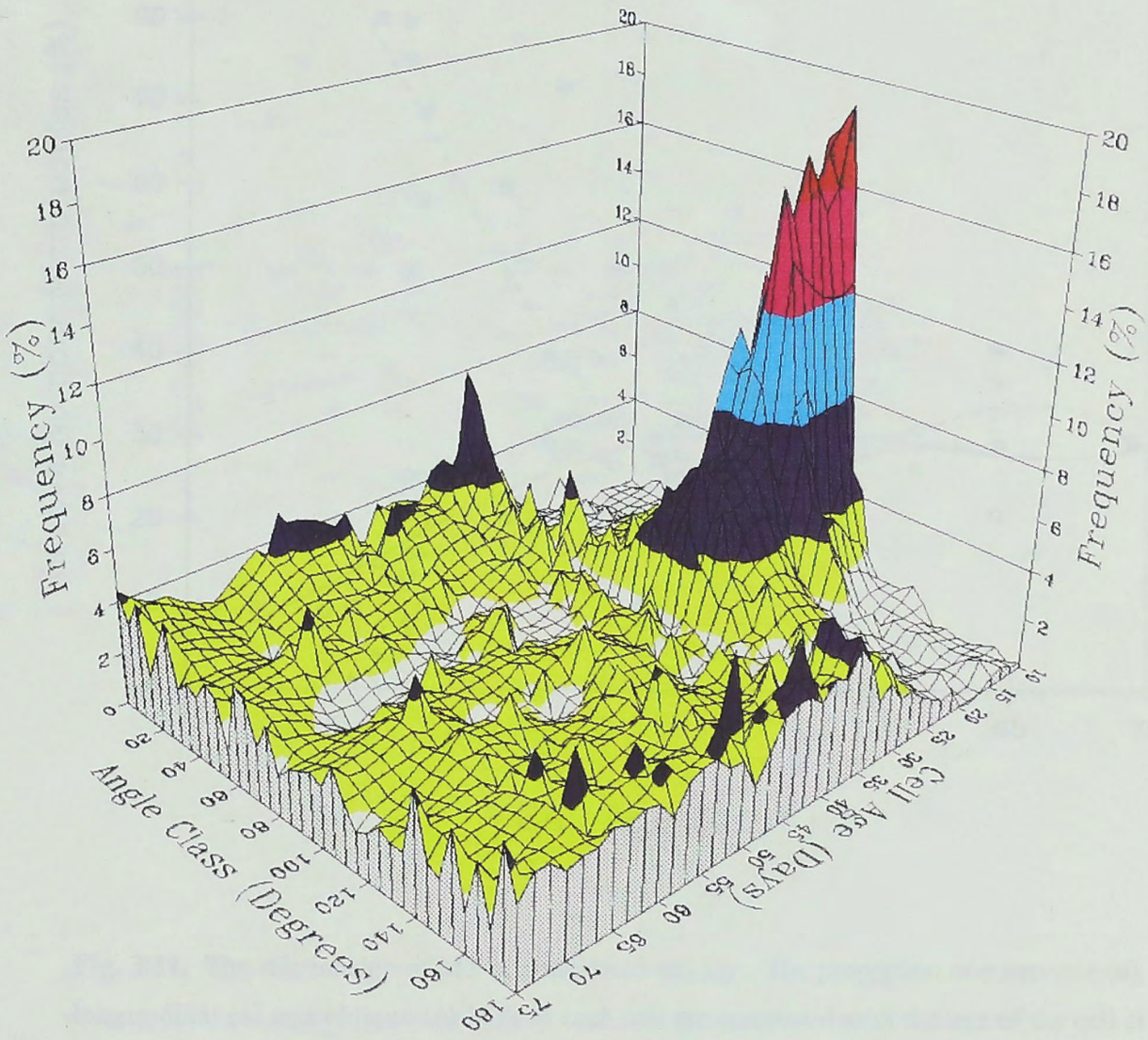
Frequency (%)
20
18
16
14
12
10
8
6
4
2
0
Angle Class (Degrees)
0
20
40
60
80
100
120
140
160
180
Cell Age (Days)
15
20
25
30
35
40
45
50
55
60
65
70
75
Frequency (%)
20
18
16
14
12
10
8
6
4
2

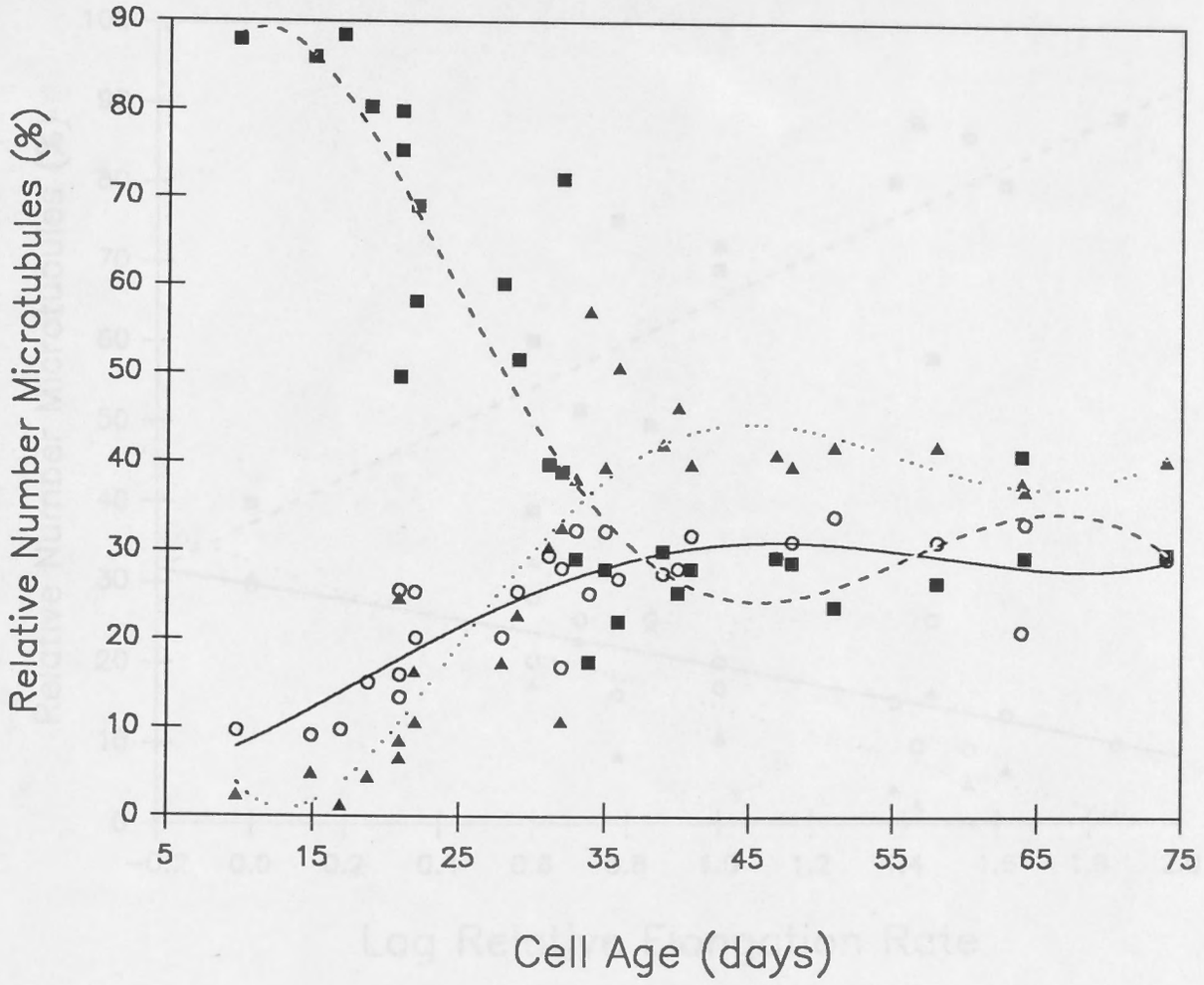

Fig. 3.11. The relationship of MT orientation to cell age. The proportion of transverse (■), longitudinal (▲) and oblique (o) MTs in each cell are compared with the age of the cell at time of fixation. Transverse MTs (MTs between 60 and 120° to the long axis) are predominant in young cells whereas longitudinal MTs (MTs between 0 and 30°; 150 and 180°) are very uncommon. This relationship gradually changes as cells become older until about 30 days of age (about the time of growth cessation) after which time longitudinal MTs predominate. The proportion of oblique MTs (30-60°; 120-150°) undergoes a gradual increase with time but is never predominant.

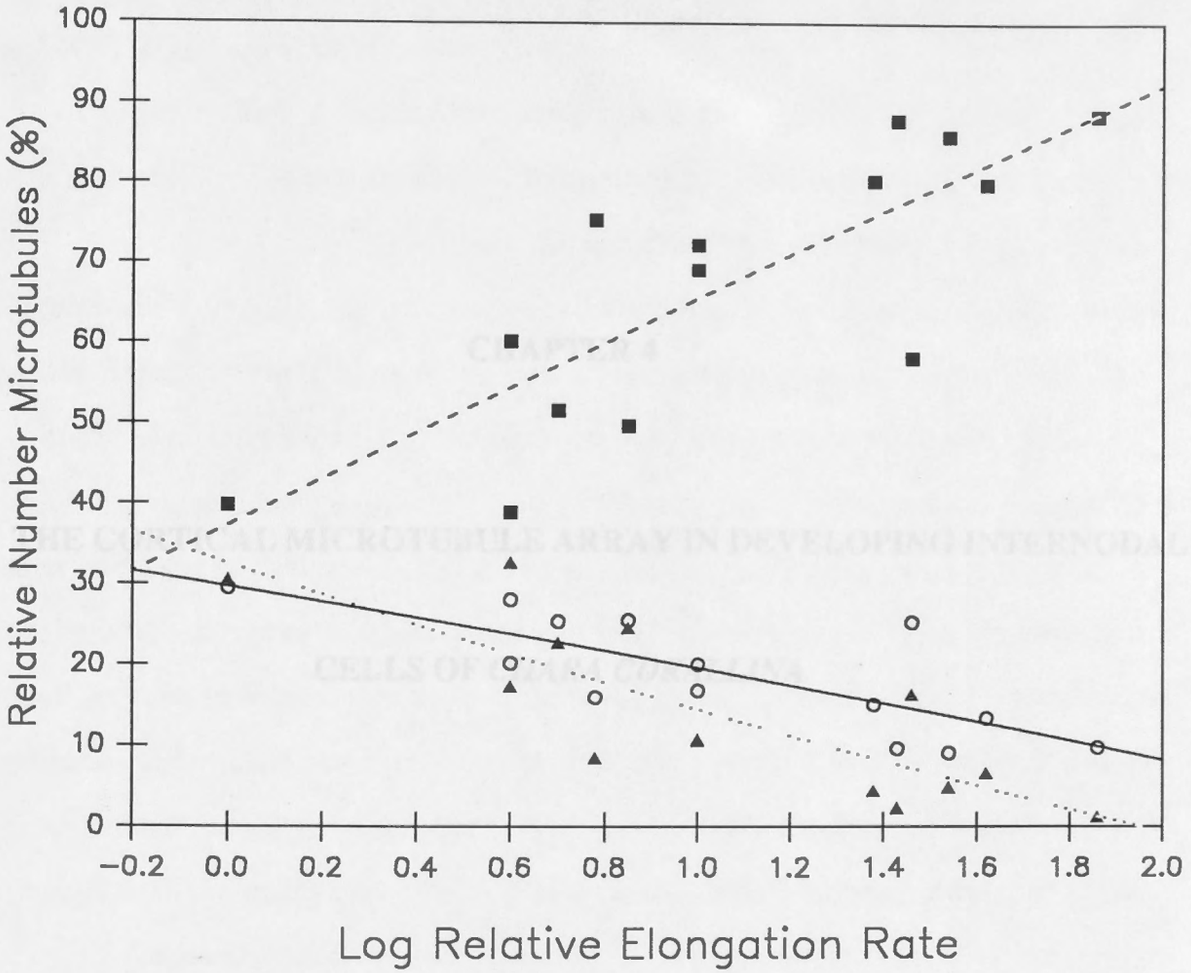

Fig. 3.12. The relationship of MT orientation to log relative elongation rate. The proportion of transverse (■), longitudinal (▲) and oblique (o) MTs in each cell are compared with the relative elongation rate at time of fixation. The high percentage of transverse MTs (MTs between 60 and 120° to the long axis) in rapidly expanding cells declines as relative elongation rate decreases. A reciprocal relationship is evident for longitudinal orientation (MTs between 0 and 30°; 150 and 180°) while the proportion of oblique MTs (30-60°; 120-150°) undergoes a somewhat smaller change.

CHAPTER 4

THE CORTICAL MICROTUBULE ARRAY IN DEVELOPING INTERNODAL CELLS OF *CHARA CORALLINA*

There is not so contemptible a plant or animal that does not confound the most enlarged understanding.

John Locke (From An Essay Concerning Human Understanding, 1690)

4.1 INTRODUCTION

The Characeae is divided taxonomically into two tribes on the basis of the number and arrangement of cells located in the coronula at the apex of the oogonium (Khan & Sarma 1984). In the tribe Nitelleae, which includes the genera *Nitella* and *Tolypella*, the coronula is two-tiered with each tier containing 5 cells while in the Chareae (*Chara, Nitellopsis, Lychnothamnus*) it has only one tier. The soundness of this separation is supported by karyotypic evidence; the basic chromosome number (polyploidy is very common) of the Nitelleae is 3 whereas in the Chareae it is 7 (Khan & Sarma 1984). Clearly this fundamental separation of the two tribes represents a very ancient evolutionary event. The Chareae and Nitelleae can in some cases be distinguished on the basis of cortication (*i.e.*, the presence of cortical cells overlying the internode); cortical cells are never found in the Nitelleae but are present in some members of the Chareae. The branchlets that emerge from the nodes may also be useful for the identification of characean algae; they are frequently divided in the Nitelleae but always simple in the Chareae.

Giant internodal cells from a diverse selection of charophytes have been utilized in several areas of investigation (cytoplasmic streaming, ion transport, cell morphogenesis) with equal success. This is not surprising since the basic organization of cells is remarkably preserved throughout the group. The ecorticated charophytes are particularly attractive for morphogenesis, cytoskeletal and ion transport studies because the growth of single cells can be followed without consideration for the influence of adjoining cells. Ecorticate internodal cells are also more suitable for immunofluorescence work because they can be examined without interference from overlying cortical cells.

Nitella tasmanica and *Chara corallina* are charophytes from diverse tribes but both have internodal cells that are devoid of cortical cells. A preliminary survey (Chapter 2) showed that the two cell types were equally amenable to the immunofluorescence technique and that MT distribution patterns were generally

very similar. Strikingly different patterns of MT organization were observed, however, in some older cells of *Chara*. In this chapter, the nature of such differences in MT organization is investigated.

4.2 MATERIALS AND METHODS

Cell culture, growth measurements, immunofluorescence and microscopy protocols are described in chapter 2, sections 2.2.1, 2.2.3 and 2.2.5. To compare growth patterns of *Chara* and *Nitella*, shoots of both species were cultured under standard conditions. Cells were measured from the time in early development when the cylindrical internodes were equal in length and diameter (day 1), through elongation phase until several days after growth had stopped. For assessment of MT organization, only cells of known size and growth rate were utilized.

4.3 RESULTS

4.3.1 Growth Analysis

When cultured under the standard growth conditions, shoots of *Chara corallina* and *Nitella tasmanica* have nearly identical appearance. In both species, the same sequence of cell divisions and differentiation results in the formation of ecorticate internodal cells separated by multicellular nodes from which arise simple lateral cells and shoots (see Fig. 4.1). The giant internodal cells show no obvious structural or behavioural differences apart from the greater size in *Chara*. Under the standard culturing conditions used for this study, the maximum internodal cell length recorded was 36.33 mm for *Nitella* and 58.22 mm for *Chara* and the largest diameter recorded was 0.526 mm for *Nitella* compared with 0.798 mm for *Chara*.

The pattern of internodal cell growth in *Chara* and *Nitella* was compared by plotting relative longitudinal and circumferential growth rates for cells of both species cultured under the same conditions (Figs. 4.2 & 4.3). Both cells start out as flattened cylinders with diameter greater than length and circumferential growth greater than longitudinal but cells quickly assume the shape of elongated cylinders when the transition to predominantly longitudinal growth takes place. From the onset of elongation, relative longitudinal growth rate was always considerably greater (generally about 3 to 10 X) than relative circumferential growth rate but the two directions of expansion show parallel changes throughout the growth period. Elongation growth can be arbitrarily divided into three phases: an initial short period of rapidly increasing relative growth rate, a second period of steadily declining growth rate during which time most of the increase in size occurs and a final period of very slow and more gradually declining growth rate. In both cases, relative growth rates peaked at about 10 days followed by the phase of steady decline until 25 days after which the gradual drop off in growth rate occurred. Circumferential growth generally stopped a few days before longitudinal and was very slight towards the end of the growth period.

In *Chara*, growth cessation occurs several days later than in *Nitella* and may account, in part, for the larger size achieved by *Chara* cells. Comparing the dimensions of internodal cells of *Chara corallina* and *Nitella tasmanica* throughout their development (Fig. 4.4) suggests that the longer growing period for *Chara* contributes mainly to the difference in final length. In contrast, this extended growth has very little effect on the circumference of *Chara* cells; the major difference in final circumference of the two cell types arises because *Chara* internodal cells have a larger circumference at the start of elongation. Thus, the most significant difference in the growth pattern of these cell types occurs before the elongation phase begins. Since the pattern of circumferential growth is very similar in *Chara* and *Nitella* throughout the elongation phase (Fig. 4.4b), the disparity in size is maintained and only slightly increased by *Chara*'s prolonged, slow growth phase.

4.3.2 MT Orientation Patterns

Internodal cells of known growth rates were selected for anti-tubulin immunofluorescence. Microtubule orientation patterns of *Chara* and *Nitella* internodal cells at similar stages of development are compared in Figs. 4.5 to 4.12. The two species show similar MT organization throughout the major growth phase when the array is predominantly transverse (Figs. 4.5 & 4.6) and in older, non-expanding cells where MTs are of highly variable orientation (Figs. 4.11 & 4.12). However, during the final few days of elongation when growth rate is very slow and for several days after growth cessation, the MT orientation patterns of *Chara* and *Nitella* show considerable differences. In *Nitella*, the shift in orientation of the MT array from transverse to longitudinal involves what appears to be (see Chapter 3) a reduction in the proportion of transverse MTs as longitudinally-oriented MTs become more prevalent (Fig. 4.7) until a predominantly longitudinal array is established (Fig. 4.9). This clearly does not occur in *Chara*. Instead, MTs remain

in parallel arrays that are aligned in oblique (Fig. 4.8) to longitudinal orientations (Fig. 4.10). Another difference at this stage of development is the organization of the MT array throughout the length of the cell; in *Nitella* it is uniform whereas in *Chara* it can be variable. It is of interest that the MTs of longitudinal arrays in both *Nitella* and *Chara* tend to have a wavy appearance (Figs. 4.9 & 4.10).

The organization of the cortical MT array in *Chara* throughout development is followed in closer detail in Figures 4.13 to 4.33 and is summarized for a sample of cells in Table 4.1.

The youngest internodal cells examined were rapidly growing cells between about 10 and 25 days of age with relative elongation rates greater than 0.07 (the phase of steadily declining relative growth rate shown in Figure 4.2). In these cells, the cortical MTs are tightly packed and oriented predominantly perpendicular to the cell's long axis (Figs. 4.13 & 4.14). As with *Nitella* (Figs. 2.12, 2.13, 3.11 & 4.5) such arrays are always interspersed with a small number of non-transverse MTs.

Changes in the organization of the MT array were observed during the period of gradually declining growth rate (cells over 25 days old and with relative elongation rates less than 0.07). Microtubules remain very numerous in such cells but the scatter of MTs about the transverse axis is often very large (Figs. 4.15 & 4.16). Near the completion of elongation and frequently coincident with cessation of circumferential growth, the MTs begin to be less numerous but generally more uniformly parallel within the array (Fig. 4. 17). It is also about this time that obliquely-aligned arrays become apparent (Fig. 4.18). At first, the MTs remain predominantly transverse with localized shifts of the array in slightly oblique directions. When a relative growth rate indicates that growth will soon end and for several days thereafter, the MT arrays are of highly variable orientation so that the orientation gradually changes through transverse, oblique and longitudinal directions (Figs. 4.19 & 4.20; 4.21 to 4.23) within single cells. Sometimes abrupt

shifts in direction are observed. Such shifts generally occur at the neutral line (Fig. 4.26).

In older non-growing cells, the MTs in a given area are often aligned in highly variable orientations. The establishment of such arrays seems to result from the gradual loss of parallel order as MTs tend to be increasingly dispersed (Fig. 4.28 to 4.30). This loss of order does not appear to occur uniformly throughout the cell. In many cases, pockets of randomly oriented MTs were seen amidst predominantly oblique arrays (Fig. 4.30) while in other cells there are signs of 'residual' local order amidst a predominantly random array (Figs. 4.31 to 4.33). In the oldest cells, MTs were randomly oriented throughout.

TABLE 4.1

Organization of Cortical MTs in *Chara* Internodal Cells and Cell Growth

Cell No.	R_L[1]	R_C[2]	MT Arrangement
IX	.215	.058	TT[3]
IY	.156	.044	TT
IC3	.156	.046	TT
IV2	.144	.026	TT
IV1	.132	.021	TT
ID3	.110	.036	TT
IQ	.107	.012	TT
IT	.099	.015	TT
IO	.094	.005	TT
IP	.081	.013	TT
IY2	.066	.038	ST[4]
IIE1	.072	.004	TT
IM2	.048	.008	ST
IIA1	.043	.013	ST
IIC1	.036	.012	ST
IIB1	.041	.006	T[5]
IM1	.039	.004	ST
IO2	.034	0	ST
IL3	.022	.011	ST
IQ2	.026	.006	T
IIC4	.032	0	T/O[6]
IID3	.021	.003	T
IID1	.024	0	ST
IIE3	.021	.002	T
IIA4	.018	0	ST
IIA2	.015	.002	ST
IM3	.011	0	O
IL4	.011	0	O/T
IM4	.007	.004	T
IID2	.009	0	T/O/L[7]
IC1	.010	0	T/O/L
ID1	.004	.002	O
IL1	.003	0	T/O/L
IIE2	.002	0	O/T/L
IIC2	0	0	T/O/R[8]
IIC3	0	0	O
IIC5	0	0	T/O/L
IIE4	0	0	T/O/L
IIA5	0	0	O/R
IIG2	0	0	O/R
IIF1	0	0	O/L/T
IIF3	0	0	O/R

1. relative elongation rate
2. relative rate of circumferential growth
3. tightly transverse, dense array
4. predominantly transverse with considerable scatter; very dense
5. uniformly transverse but with low density
6. uniformly oblique; low density
7. uniformly longitudinal; low density
8. randomly distributed

4.4 DISCUSSION

4.4.1 Comparison of Microtubule Orientation Patterns in *Chara* and *Nitella*

The internodal cells of *Chara* and *Nitella* both develop as elongated cylinders so it is not surprising that they show equivalent MT organization throughout the major phase of cell growth. Remarkable differences in MT organization in *Nitella* and *Chara*, however, are observed from just before growth cessation until several days afterwards. That this difference might reflect dissimilar growth behaviour is disproven by comparing relative growth rates of the two cell types; parallel changes in relative growth rates occur in both cells throughout development. Furthermore, the larger size of *Chara* internodal cells is mainly due to greater original circumference rather than any difference in growth at later stages of development when differences in MT organization are detected. It is therefore doubtful that the disparate MT orientation patterns reflect different growth strategies for the two cells.

There are many examples of elongated cells of higher plants where cortical MTs display shifts in orientation about the cell's axis of expansion, usually from transverse to oblique and axial directions. In some cases, such developmentally-dependent changes in MT organization involve a uniform shift in direction of the MT array throughout the length of the cell as, for example, in cotton fiber development (Seagull 1986) where transverse MTs become obliquely oriented.

More often, MTs are aligned in variable directions within single cells. Such arrays typically resemble those seen in mature *Chara* internodal cells with MTs locally parallel but with varied orientation throughout the length of the cell. Some examples include the outer cortical and epidermal cells of pea epicotyls and mung bean hypocotyls (Roberts *et al.* 1985), the outer tangential wall of epidermal cells of pea internodes (Akashi & Shibaoka 1987), cortical cells of *Raphanus* root tips (Traas *et al.* 1984) and epidermal cells from *Zea mays* mesocotyls (Mita & Katsumi 1986).

Clearly, the manner in which MT arrays shift to alternate orientations can vary. Nevertheless, the reason *N. tasmanica* and *C. corallina* internodal cells have adopted such diverse strategies is a mystery. Although the two species are very much alike, they are from distinct tribes and thus are evolutionarily divergent. *C. corallina* and *N. tasmanica* are both ecorticate species yet there are many examples of cortication in the Chareae and none in the Nitelleae. The different patterns of MT organization could therefore represent the trend toward a corticated condition in the Chareae. A tendency buried within multicellular tissues for cells to have shifting MT patterns that more closely resemble those in *Chara* than *Nitella* would support this idea but for the cells that have been examined, this does not appear to hold true. Scattered MT arrays like those in *N. tasmanica* are seen in outer epidermal cells from *Zea mays* coleoptiles (Bergfeld *et al.* 1987) and onion leaf sheath cells (Mita & Shibaoka 1983). Furthermore, single-walled cylindrical cells including cotton fibers (Seagull 1986) and the non-growing region of onion root hairs (Lloyd *et al.* 1985) often show MT patterns akin to *C. corallina.*

The different patterns of MT organization in *C. corallina* and *N. tasmanica* may be due to other factors. The presence in *Chara* of a different tubulin isoform that is present only at certain stages of development could, for example, give rise to MTs of different behaviour from those in *Nitella.* Alternatively, diverse microtubule-associated proteins or differences in the properties of the plasma membrane of the two species might explain their dissimilar MT patterns. Whether the different MT patterns have any taxonomic basis cannot be established unless screening of many more species from both the Nitelleae and the Chareae is carried out.

4.4.2. Cell Growth and Microtubule Orientation

Changing MT orientation in elongating higher plant cells from transverse to longitudinal is sometimes associated with a shift in the direction of cell expansion

from axial to circumferential. This is particularly evident in the case of ethylene-mediated lateral expansion (Mita & Shibaoka 1983; Roberts *et al.* 1985). From the growth data, it is clear that the realignment of MTs from transverse to oblique and longitudinal in *Chara* does not promote circumferential growth.

Alternatively, such shifts in MT orientation could coincide with growth cessation. This possibility more closely describes the pattern in *Chara* where the shift in MT orientation from transverse to longitudinal is first detected shortly before the cell stops elongating. It is interesting in this light that the MTs of many cylindrical plant cells are oriented longitudinally or obliquely where elongation is not occurring (Emons & Wolters-Arts 1983; Derksen *et al.* 1985; Seagull 1986; Lloyd & Wells 1985; Lancelle *et al.* 1987; Murata *et al.* 1987; Lin & Jernstedt 1987). If MTs maintain their control over mf deposition during the transition period, it is conceivable that the change occurs in order to alter the direction of mf deposition and subsequently bring about the cessation of longitudinal growth.

4.4.3 Microtubule Orientation and Cell Wall Deposition

Internodal cells of *Chara corallina* have been shown to have helicoidal walls (Neville & Levy 1984) so the shift in orientation of MTs before growth cessation could signal the change from transverse mf alignment to the deposition of a helicoidal wall in the mature internode. Whether MTs continue to control the alignment of mfs after growth cessation, as appears to be the case in cotton fibers (Seagull 1986), seems unlikely. It has been demonstrated that helicoidal wall deposition in *Equisetum*, for example, is not controlled by MTs (Emons & Wolters-Arts 1983) so it is just as likely that the described changes in MT organization in Chara at the time of growth cessation have no influence on mf alignment. Helicoidal walls are a common feature in the internodal cells of *Nitella opaca* (Neville & Levy 1984). If helicoidal walls also are found in *Nitella tasmanica*, it is difficult to imagine how such diverse MT patterns as are seen in

N. tasmanica and *C. corallina* could both be responsible for helicoidal wall formation. Thus, the argument against MTs playing a role in helicoidal wall deposition is strengthened.

If MTs are not involved in helicoidal wall deposition in *C. corallina*, the change in MT organization at the time of growth cessation might merely represent an uncoupling of MTs from their role in aligning transverse mfs. A trend towards longitudinal MT orientation in non-growing cells might represent a change to MT alignment based on the least energy equilibrium (Green 1984). Why cortical MTs should persist in non-expanding cells if they are not involved in wall deposition is uncertain. There are, however, many plant cells with axially or obliquely oriented cortical MTs that are not involved in mf alignment. These include the coenocytic green algae *Boergesenia* and *Ernodesmis* (La Claire 1987) and numerous tip growing cells (Emons & Wolters-Arts 1983; Derksen *et al.* 1985; Lloyd & Wells 1985; Lancelle *et al.* 1987; Murata *et al.* 1987; Raudakoski *et al.* 1987). The recent survey of cortical MTs in tip-growing fern protenema is especially interesting (Murata *et al.* 1987). Cortical MTs are arranged circumferentially in the elongating subapical zone but are parallel to the cell's long axis in the non-growing region. Evidently, cortical MTs are required for functions other than transverse wall deposition.

4.4.4. The control of Microtubule Orientation

In proposing a model to account for changing MT orientation it is important to consider how quickly the changes in orientation occur, how stable the MTs are, how the MTs are spatially organized within the array and finally, what function they have. Two fundamental uncertainties as to how the mechanism that aligns MTs operates include whether connections between nearby MTs exist and whether individual MTs undergo realignment or else depolymerize and reassemble in a new direction. The change in MT orientation that is observed in both *Chara* and *Nitella*

internodal cells around the time of growth cessation could occur either by direct realignment of stable MTs or by disassembly/reassembly. The available evidence does not favor one mechanism over the other.

It has been proposed that helical arrays of connected MTs can alter their pitch and thereby rapidly change orientation (Lloyd & Seagull 1985). This "dynamic spring" model relies on the existence of relatively long, overlapping MTs to form continuous helical arrays. In contrast, the MTs of *C. corallina* are clearly not bundled nor arranged in continuous helical arrays yet they can display dramatically different orientations from one region to another, frequently involving whole fields of parallel MTs. Contrary to the dynamic spring model, abrupt alterations in MT orientation occur within what might be considered one turn of the dynamic helix. This demonstrates that the dynamic spring model can not apply to MTs in *C. corallina.*

A second possibility is that transverse MT orientation is maintained throughout growth by the cross-linking of MTs and that loss of these cross-links at the time of growth cessation could cause MTs to no longer be constrained in the transverse direction. Transverse networks could be based on intertubule linkages as predicted by the self-cinching loop mechanism (Green 1962, 1963, 1980). The fact that MTs become less numerous in cells of *Chara corallina* when oblique and longitudinal arrays are first noticed supports this idea since a decrease in MT number should also minimize cross-linking.

Alternatively, MTs could be attached to some plasma membrane-borne template that somehow controls orientation. It seems unlikely, however, that even if MTs were released from bonds that previously held them in a tightly transverse direction, that they would display the uniform shifts in orientation that are observed. Instead, a scattered arrangement of MTs would be expected. If, for example, transverse MTs were to be realigned by the small amount of strain that is

still present at growth cessation, they would be just as likely to swing to the longitudinal in either direction.

One observation that favors the idea that MT connections are broken is that longitudinal MTs seen at the time of growth cessation in both *Chara* and *Nitella* (Figs. 4.9 & 4.10) have a wavy appearance. Such undulations could be artifacts of fixation but the fact that they are restricted to longitudinal MTs suggests in any case that these MTs have different properties from their transverse counterparts. The absence of connections that otherwise keep the MTs taut could account for the different appearance. It is perhaps of interest that post-translationally modified, stable MTs in cultured mammalian cells are curved whilst their dynamic counterparts are relatively straight (Piperno *et al.* 1987).

Since MTs are maintained in parallel arrays during the changes in MT organization, it seems probable that they are still being constrained by orienting mechanisms but that the orienting mechanisms no longer operate solely in the transverse direction. Thus, MTs may continue to be aligned in the same manner but in variable directions. The increasing randomness of MTs seen after expansion is complete could represent a decline in the influence of the orienting mechanism over MTs.

The disconnected network model is dependent on the existence of relatively stable MTs. While recent studies generally favor the view that MTs can be dynamically unstable (Sammak & Borisy 1988), there are many examples where relatively persistent MTs seem to exist. A particularly interesting system is described by Akashi and Shibaoka (1987) where the longitudinal MTs of gibberellin-sensitive cells have been demonstrated to be far more stable than their transverse counterparts. Perhaps in *Chara* and *Nitella*, the transverse arrays comprise relatively dynamic MTs while the longitudinal MTs are stable ones that have lasted long enough to become realigned.

4.5 CONCLUSION

The organization of MT arrays in the internodal cells of two charophytes, *Chara corallina* and *Nitella tasmanica* has been compared through much of their development by means of immunofluorescence microscopy. MT patterns appear to be virtually identical except around the time of growth cessation. In *Nitella*, the predominantly transverse array gradually incorporates more and more longitudinally-oriented MTs until the array becomes predominantly longitudinal. In contrast, the MTs of *Chara* remain locally organized in parallel arrays but show considerable variation throughout the length of the cell including oblique and longitudinally aligned arrays. The elongation phase of growth in both species follows an identical pattern so cannot account for the different arrangement of MTs observed. It seems more likely that the two patterns of MT behaviour make no difference to morphogenesis. The changing MT pattern in *Chara corallina* has been discussed in terms of mechanisms that might be responsible for controlling and altering MT orientation.

CHAPTER 4 - FIGURES

All micrographs are fluorescent images from cells processed with the same tubulin-specific monoclonal antibody. All are arranged so that their long axis or the long axis of the page corresponds to the long axis of the cell.

Fig. 4.1. *Chara corallina* (two shoots on left) and *Nitella tasmanica* (three shoots on right) growing under standard culture conditions. The two species are very similar in appearance except that the cells of *C. corallina* are larger in size to those of *N. tasmanica*.

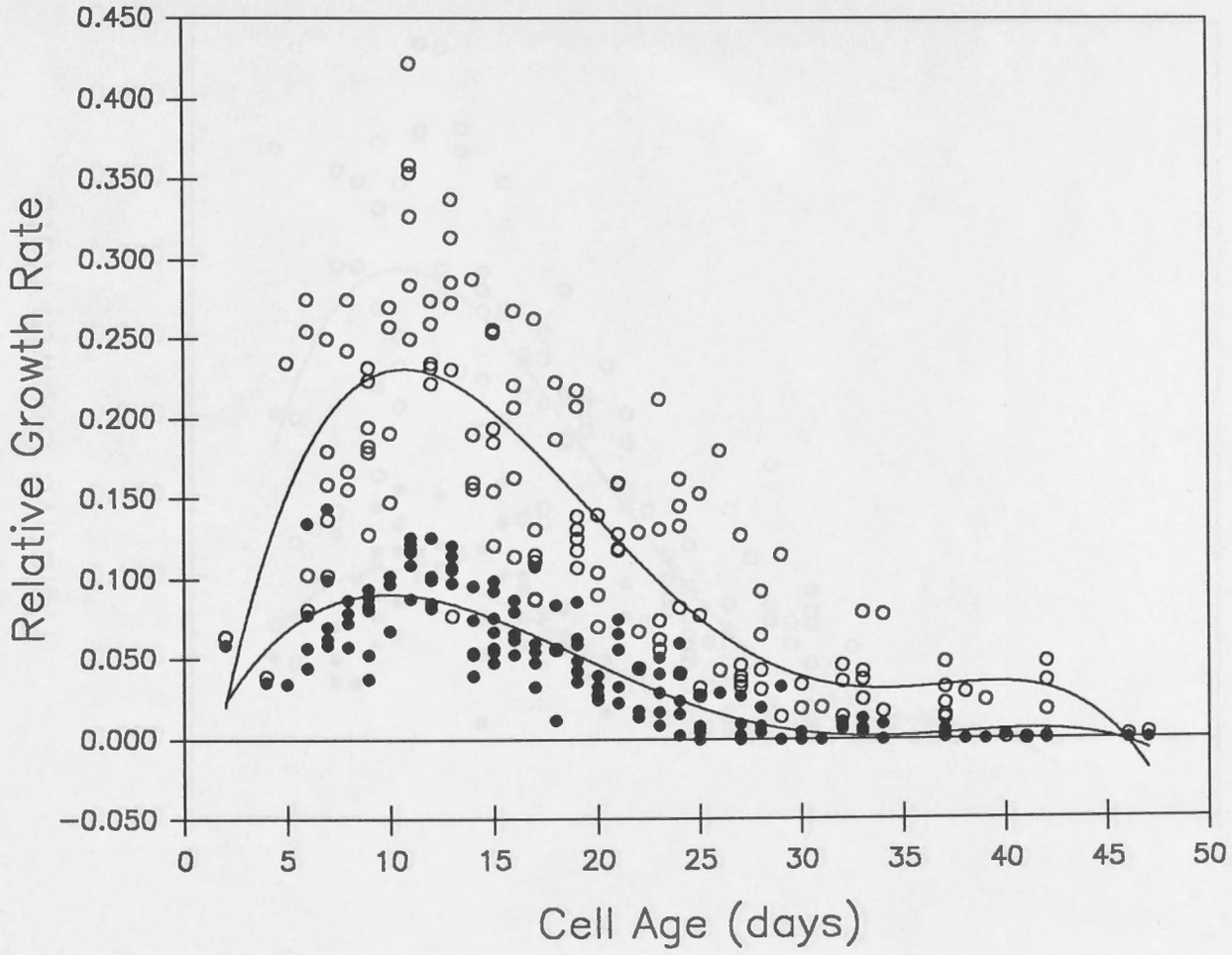

Fig. 4.2. Growth patterns of *Chara corallina* internodal cells from the onset of elongation growth. Relative longitudinal (o) and circumferential (•) growth rates recorded at various times during elongation for 6 cells are pooled and plotted along with fourth order regression lines.

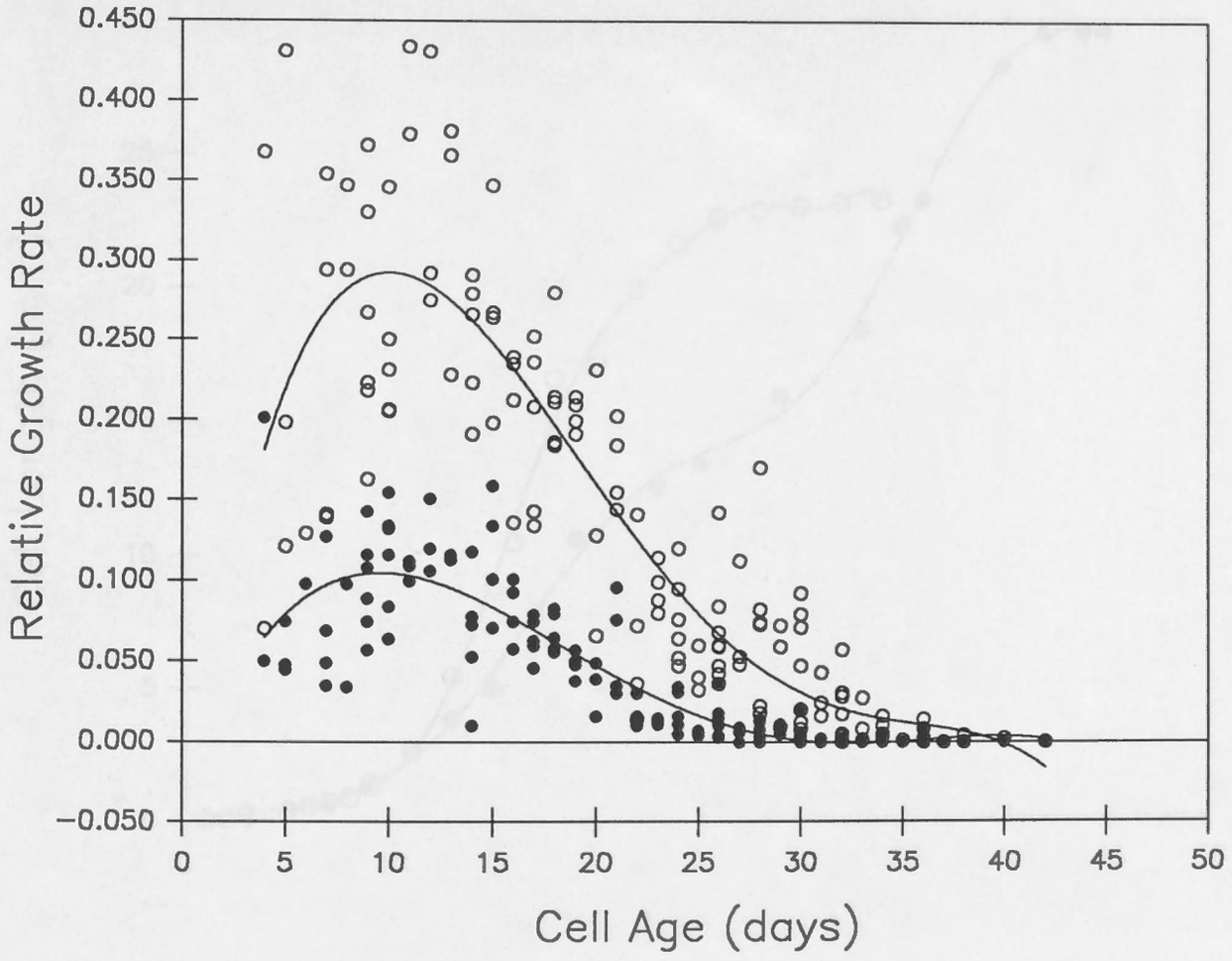

Fig. 4.3. Growth patterns of *Nitella tasmanica* internodal cells from the onset of elongation growth. Relative longitudinal (o) and circumferential (•) growth rates recorded at various times during elongation for 6 cells are pooled and plotted along with fourth order regression lines.

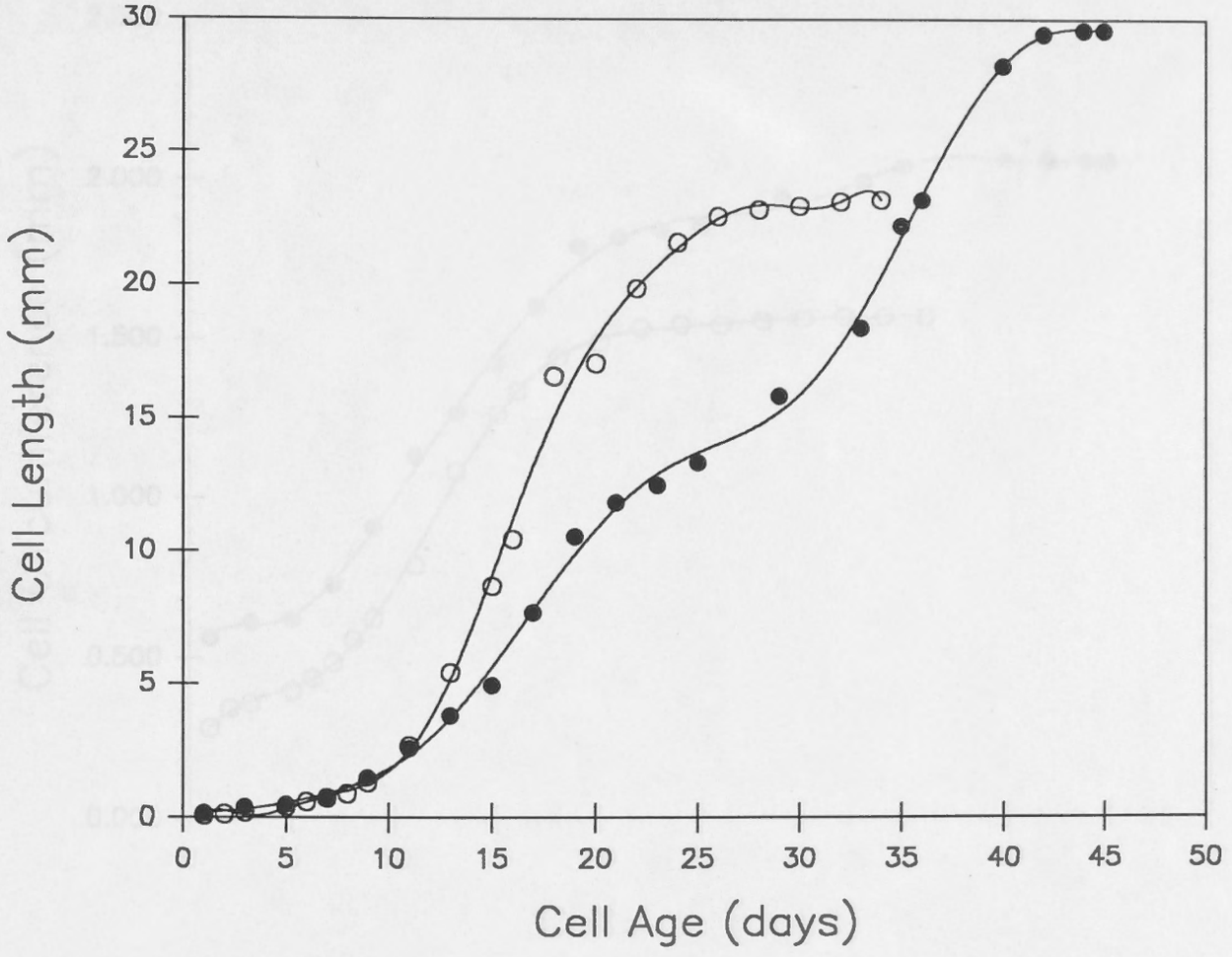

Fig. 4.4a. Elongation growth patterns in *Chara corallina* (•) and *Nitella tasmanica* (o).

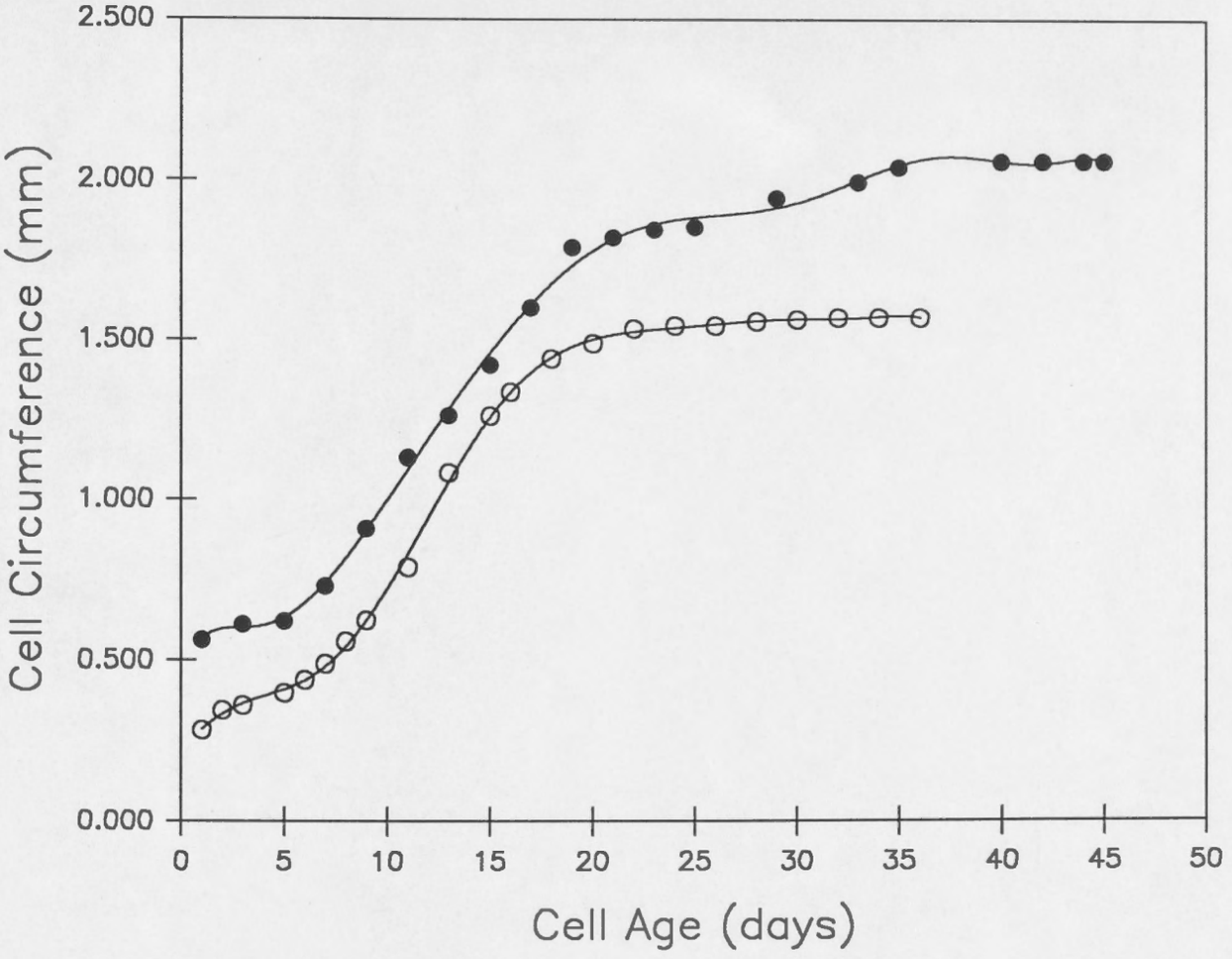

Fig. 4.4b. Circumferential growth patterns in *Chara corallina* (•) and *Nitella tasmanica* (o).

Figs. 4.5 to 4.12. Comparison of MT orientation patterns in *Nitella tasmanica* (Figs. 4.5, 4.7, 4.9 & 4.11) and *Chara corallina* (Figs. 4.6, 4.8, 4.10 & 4.12) at various stages of development.

Figs. 4.5 & 4.6. Young, rapidly elongating cells. In both cases MTs are predominantly transverse.

Figs. 4.7 & 4.8. Cells approaching the end of their growth period. In *Nitella* (Fig. 4.7) MTs are oriented both transversely and longitudinally whereas in *Chara* (Fig. 4.8) MT arrays are obliquely aligned.

Figs. 4.9 & 4.10. Cells just after growth cessation. In both cases MTs are oriented predominantly in a longitudinal direction and are of wavy appearance.

Figs. 4.11 & 4.12. Short, randomly oriented MTs of non-expanding internodal cells.

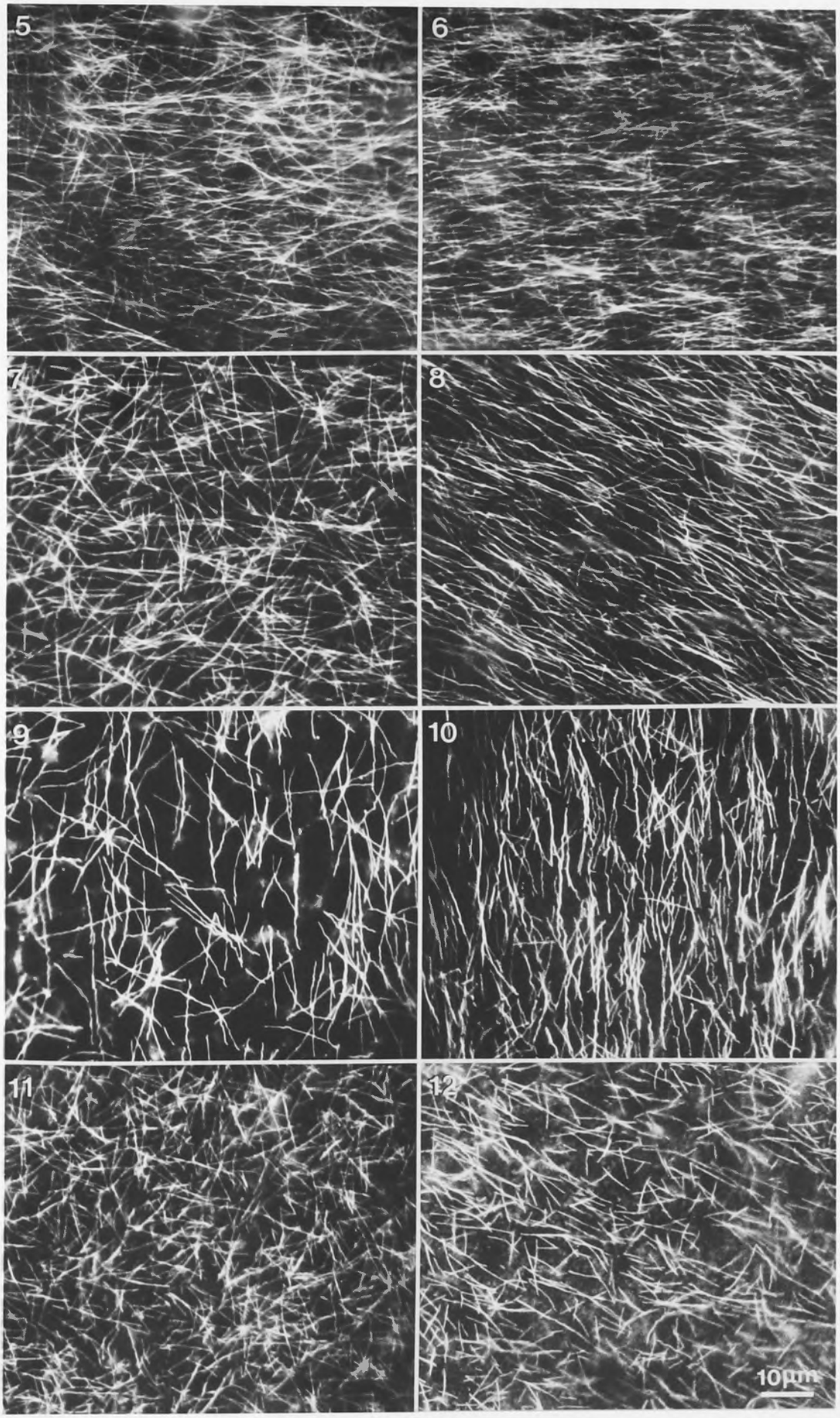
5
6
7
8
9
10
11
12
10μm

Figs. 4.13 to 4.18. Microtubule orientation patterns in *Chara corallina* internodal cells during elongation growth

Fig. 4.13. A rapidly elongating cell with relative longitudinal (r_L) and circumferential (r_C) growth rates of 0.132 and 0.021 respectively. MTs are predominantly transverse with a small number of MTs running at other angles.

Fig. 4.14. A rapidly elongating cell (r_L= 0.107 and r_C= 0.012) with predominantly transverse MTs.

Fig. 4.15. An internodal cell in the period of gradually-declining growth (r_L= 0.015, r_C= 0.002) showing predominantly transverse orientation of MTs with considerable numbers of non-transverse MTs.

Fig. 4.16. Slowly elongating cell in which circumferential growth has just stopped (r_L= 0.018, r_C= 0). MTs are still predominantly transverse but the total number of MTs appears to be declining.

Figs. 4.17 & 4.18. Slowly elongating cell in which circumferential growth is not occurring (r_L= 0.011, r_C= 0). MTs are predominantly transverse (Fig. 4.17) but in some regions of the cell (Fig. 4.18) the array is oriented at a slightly oblique angle.

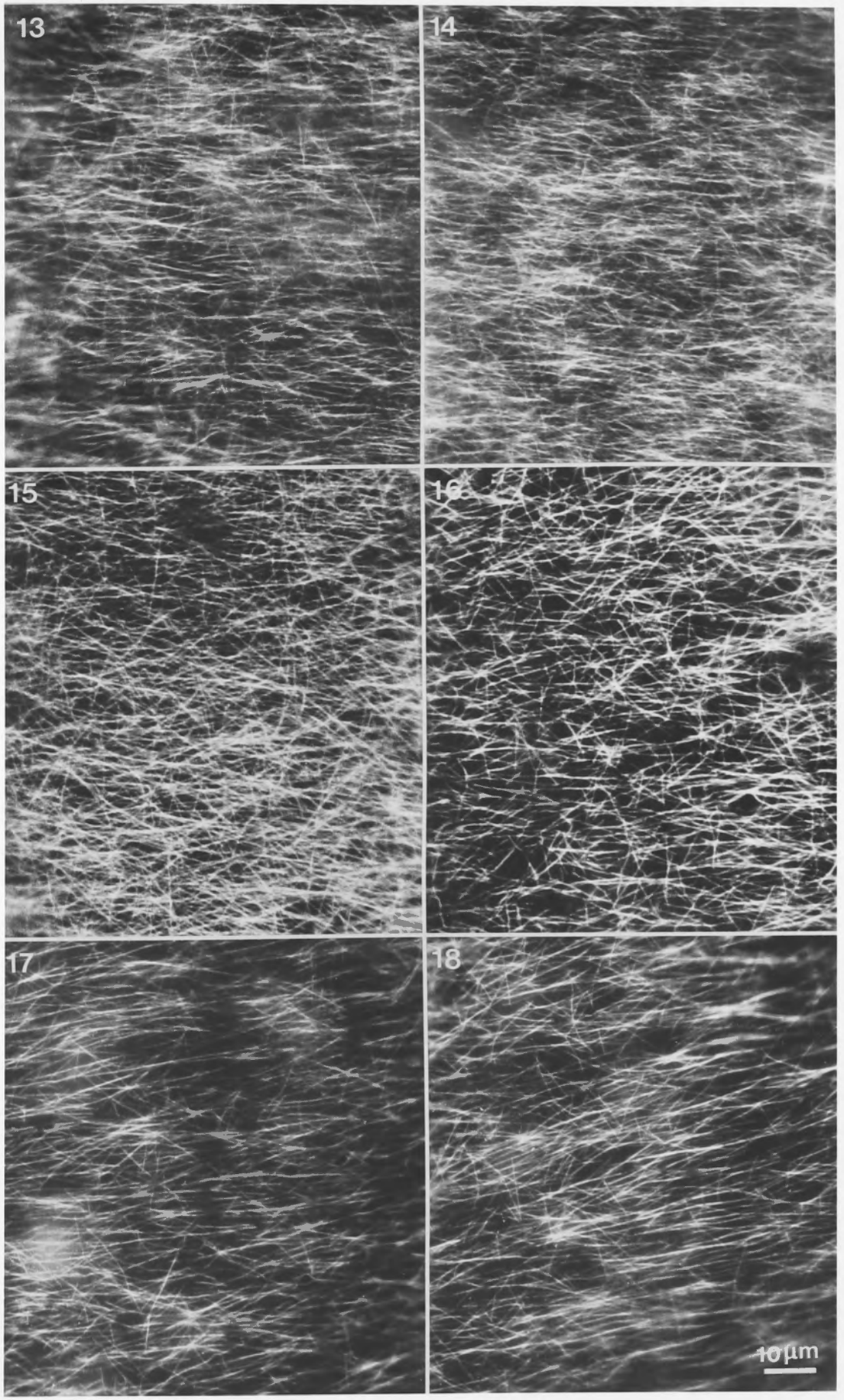
13
14
15
16
17
18
10 µm

Figs. 4.19 to 4.33. Microtubule orientation patterns in non-expanding internodal cells of *Chara corallina*

Figs. 4.19 & 4.20. MTs in adjacent regions of the same cell showing oblique (Fig. 4.19) and near-longitudinal (Fig. 4.20) orientation. In this case the cell had finished growing three days prior to fixation.

Figs. 4.21 to 4.23. Near-transverse (Fig. 4.21), oblique (Fig. 4.22) and near-longitudinal (Fig. 4.23) MT arrays in different regions of the same cell.

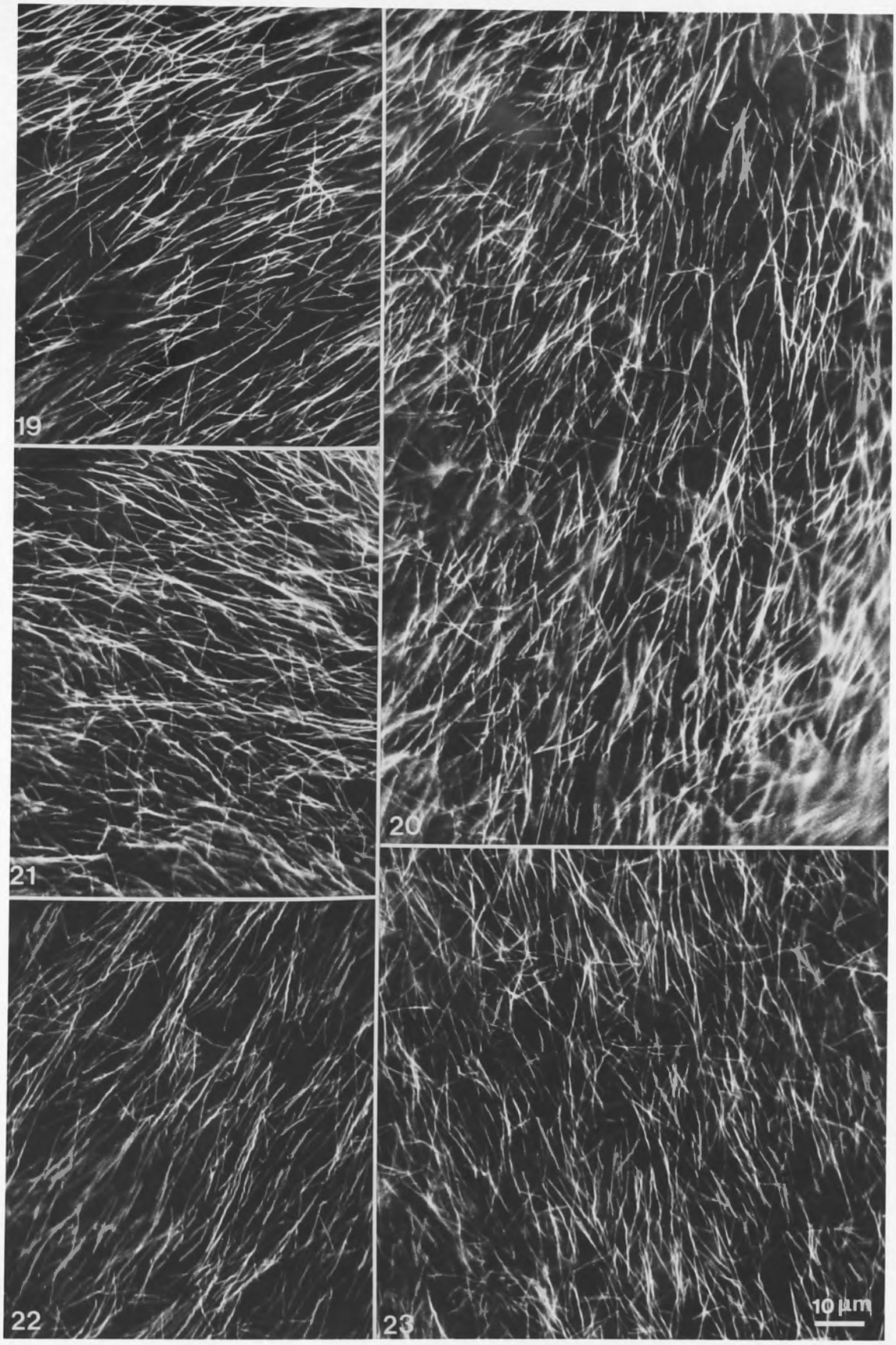
19
20
21
22
23
10 µm

Figs. 4.24 to 4.26. MT orientation patterns in a cell that had finished growing two days prior to fixation. In Figure 4.24, the MT array is only slightly oblique whereas in Figure 4.25 the 'pitch' is much greater. Figure 26a and b is a through focus series showing a dramatic shift in MT orientation that is occurring above the neutral line.

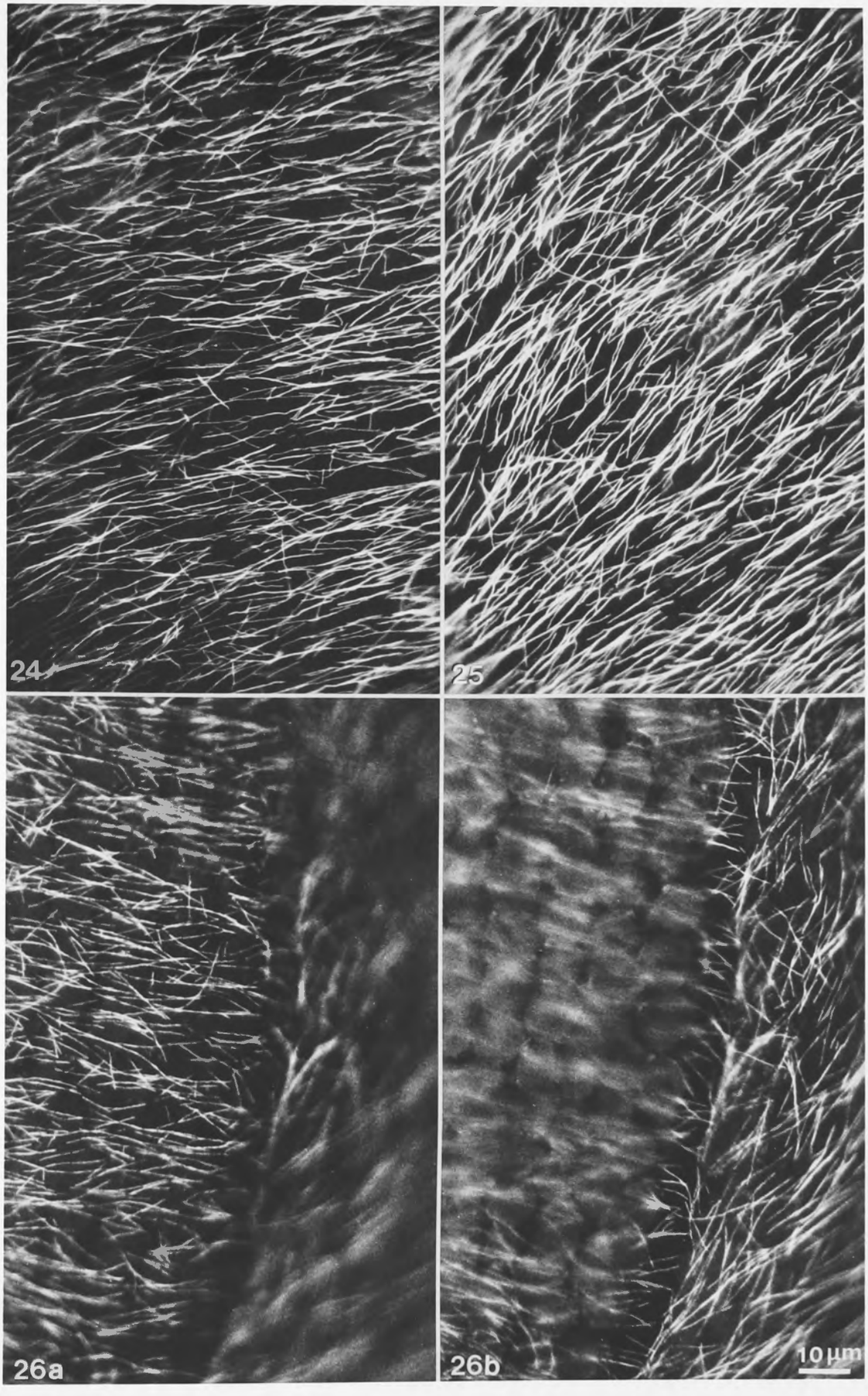
24
25
26a
26b
10 µm

Figs. 4.27 to 4.30. Various MT orientation patterns in a cell 8 days after growth has ended. In Figs. 4.27 to 4.29 the array still maintains a generally oblique orientation but there is a great deal of scatter. In Fig. 4.29 a gradual shift in MT orientation from near transverse (left side of photograph) to near longitudinal (right side) is observed. In Fig. 4.30, MTs appear to be randomly oriented.

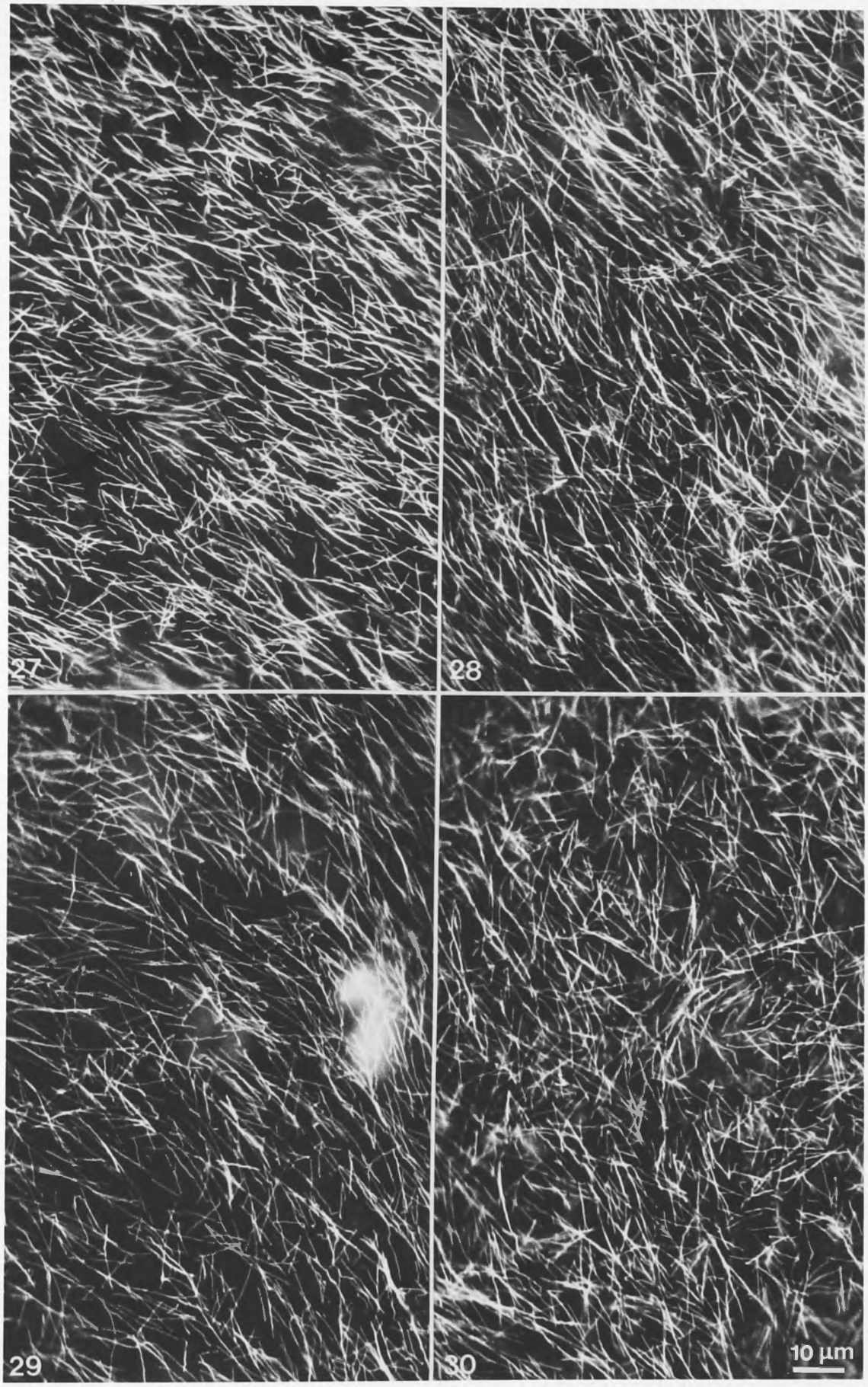
27
28
29
30
10 µm

Figs. 4.31 to 4.33. MT orientation patterns in a cell that had finished growing 6 days prior to fixation. Fig. 31 is a through focus series of one area of the curving cell showing predominantly longitudinal MTs in one region (4.31a) and oblique-transverse MTs in another (4.31b). In Figs. 4.32 and 4.33, (which are typical of the majority of the cell) the MTs are randomly distributed.

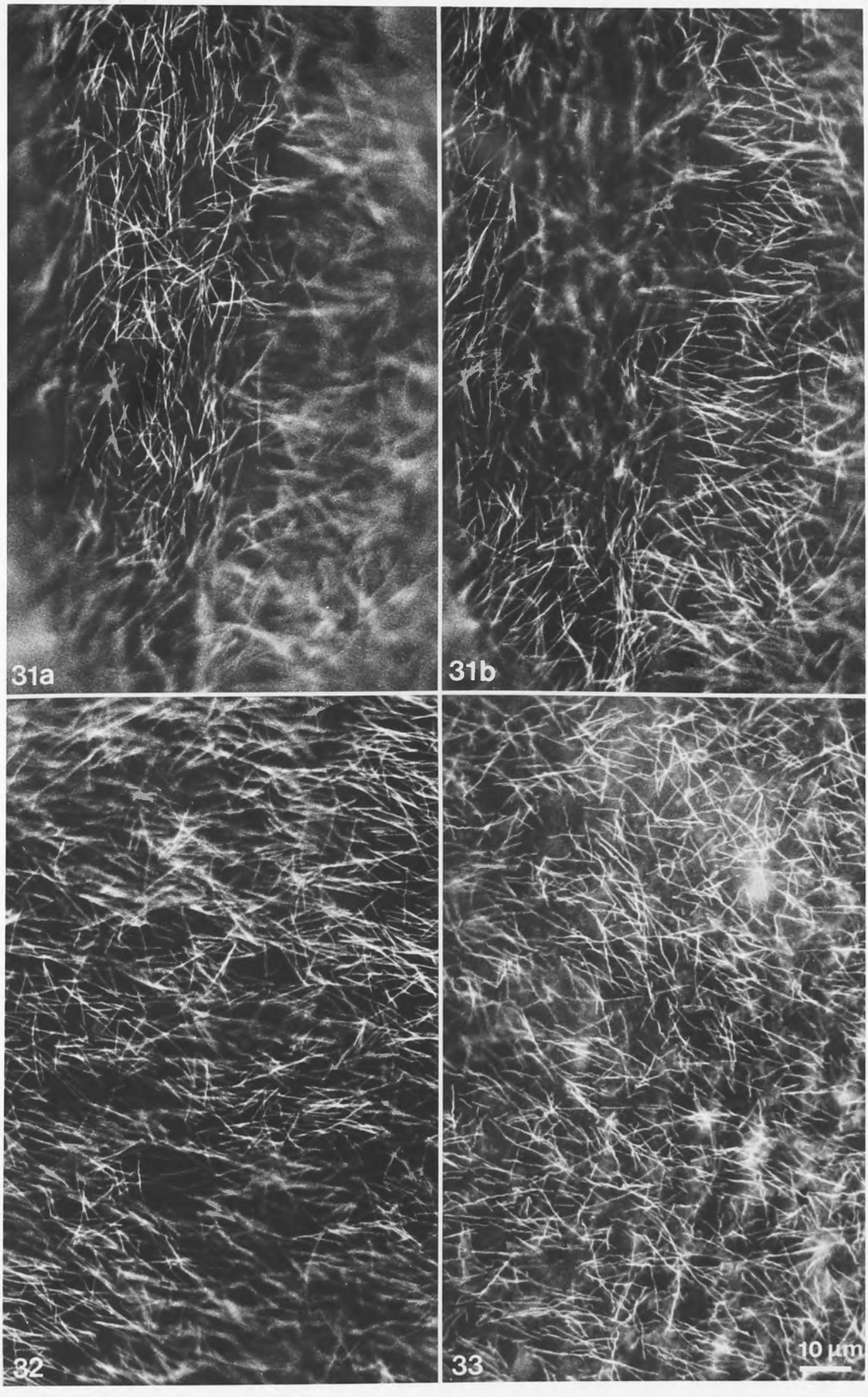
31a
31b
32
33
10 µm

CHAPTER 5

MICROTUBULE ASSEMBLY AND ORIENTATION

IN *NITELLA* INTERNODAL CELLS FOLLOWING DEPOLYMERIZATION

BY THE DINITROANILINE HERBICIDE ORYZALIN

Some of the results described in this chapter have been previously presented in a paper given at the joint meeting of the Australian and New Zealand Cell Biological Societies in Auckland, N.Z., in May 1987 and also in a poster at the 4th International Congress of Cell Biology in Montreal, in August 1988.

5.1 INTRODUCTION

The orientation of cortical MTs underlying expanding wall surfaces of plant cells is usually perpendicular to the direction in which that particular wall will expand. Cellulose microfibrils (mfs) deposited outside the plasma membrane of growing cells determine the yield properties of the wall (see Ch. 3) and have been observed to have the same orientation as subplasmalemmal MTs (Ledbetter & Porter 1963; Hepler & Newcomb 1964; Pickett-Heaps 1967a & b; Newcomb 1969; Palevitz & Hepler 1976; Seagull & Heath 1980; Mueller & Brown 1982; Seagull 1983; Falconer & Seagull 1985a; Galway & Hardham 1986; Seagull 1986). That MTs are responsible for the alignment of these mfs has been supported by disrupting MTs with tubulin-specific drugs (Grimm *et al.* 1976; Mita & Shibaoka 1983; reviewed by Gunning & Hardham 1982; Lloyd 1984) and following the effect on both mf orientation and cell shape. Knowing how MTs are aligned into these cortical arrays is therefore of great interest, not only for the implications on cell morphogenesis but in a broader sense, the understanding of the mechanisms that organize MTs in plant cells.

Organization of MTs into their functional arrays involves two aspects: assembly of MTs through polymerization of free tubulin and alignment of MTs in specific orientations and locations within an array. Assembly of subplasmalemmal MTs has been suggested to occur at various sites in plant cells including cell edges (Gunning *et al.* 1978), the nuclear envelope (De Mey *et al.* 1982, Clayton *et al.* 1985, Wick 1985a) and foci distributed in the cortical cytoplasm (Gunning 1980; Galatis *et al.* 1983; Falconer & Seagull 1986, 1987; Falconer *et al.* 1988; Hoffmann 1986; Hogetsu 1986; Cleary & Hardham 1988). MTs could either be assembled in their "appropriate" orientations at these sites or assembled but not oriented. In the latter case, MTs could either be moved into the "appropriate" orientation or be selectively depolymerized if they are in "inappropriate" positions.

Compounds that specifically inhibit one component of a biochemical pathway or molecular structure can be useful for determining functional relationships. In the case of MTs, the alkaloid colchicine has been especially useful not only for determining the role MTs play in mitosis, motility and morphogenesis but also for characterizing MT assembly sites and patterns of organization after MTs have been disassembled (see Dustin 1984). Colchicine's anti-MT effect results from its affinity for tubulin; in binding to tubulin dimers, it prevents further assembly, effectively lowering the free-tubulin concentration and leading to net disassembly of existing labile MTs through a shift in the equilibrium of free to polymerized tubulin. Whilst colchicine has anti-MT effects in most eukaryotic cells, its affinity for different tubulins is variable. Colchicine has a relatively low affinity for plant tubulin (Morejohn & Fosket 1984; Morejohn *et al.* 1987a) so that concentrations of up to 1000X those needed with mammalian cells are necessary. The increased chance of side effects such as wall loosening (Okuda & Mizuta 1987), abnormal wall thickening (Pickett-Heaps 1967b; Roberts & Baba 1968; Itoh 1976) and changes to the plasmalemma (Srivastava *et al.* 1977) make colchicine less suitable for specifically inhibiting MT function in plant cells than some other compounds. The dinitroaniline herbicide oryzalin (3,5-dinitro-N^4,N^4-dipropylsulfanilamide), for example, has a high affinity for plant tubulin (Strachan & Hess 1983) and inhibits its polymerization *in vitro* (Morejohn *et al.* 1983) in what appears to be a similar fashion to colchicine. Oryzalin can therefore be used at very low concentrations in plant cells (Upadhyaya & Nooden 1977; Bajer & Molè-Bajer 1986a; Morejohn *et al.* 1987b; Cleary & Hardham 1988) to inhibit MT assembly with fewer risks of non-specific effects.

The giant internodal cells of the green alga *Nitella tasmanica* have extensive arrays of cortical MTs that lie just inside the plasma membrane. In a previous study (Chapter 3; Wasteneys & Williamson 1987), orientation patterns of cortical MTs were described quantitatively throughout most of their development. The

change from transverse MTs in rapidly elongating cells to a nearly random distribution in non-expanding cells suggests that the mechanisms responsible for transverse orientation of MTs are active only in growing cells. A similar conclusion was reached for alignment of cellulose mfs in *Nitella* internodal cells (Gertel & Green 1977). In order to describe the pattern of MT assembly and alignment, MTs were depolymerized with oryzalin and events leading to recovery of the cortical array were followed. MT assembly sites and alignment patterns for growing and non-growing cells were compared.

Young internodal cells have, in addition to subplasmalemmal MTs, a small number of subcortical and endoplasmic MTs (Chapter 2). Subcortical MTs are aligned parallel to the subcortical actin cables and endoplasmic MTs are located close to nuclei in the streaming endoplasm. These MTs could either represent a separate MT array that is organized independently from the cortical array or be part of an interconnected MT network. Nucleating sites could exist in both the cortex and the endoplasm, for example, at discrete sites near the plasma membrane and at the nuclear surface; alternatively, MT nucleation might only occur in one region. To explore this question, cortical and endoplasmic MT assembly patterns were compared during the re-establishment of a transverse cortical MT array.

5.2 MATERIALS AND METHODS

5.2.1 Plant Material and Growth Analysis

Shoots of *Nitella tasmanica* were cultured under controlled conditions as described (Chapter 2). For all experiments, only cells of known size and growth rate were used.

5.2.2 Oryzalin Treatments

All treatments were carried out under standard growth conditions at constant temperature. Intact shoots containing a cell whose growth had previously been determined were removed from the aquarium in which they had been growing and placed in a glass petri dish along with oryzalin-containing culture medium. For the standard treatment, cells were incubated for 20 min in 10 μM oryzalin (Lilly Research Laboratories, Greenfield, Indiana) prepared by diluting a 1 mM stock solution in acetone into the standard culture solution (Chapter 2). For experiments requiring higher or lower oryzalin concentrations and for oryzalin-free controls, the final solution was always adjusted to contain 1 % acetone in order to match the standard protocol. After treatment, shoots were removed from the petri dish and passed through three washes of medium then anchored in a second aquarium (also containing fresh culture medium) for the duration of recovery.

5.2.3 Immunofluorescence Microscopy

After the specified recovery time, shoots were removed from the recovery aquarium and the selected internodal cell isolated from the rest of the shoot. Cells were processed for anti-tubulin immunofluorescence as described in Chapter 2. At least three cells were processed for each recovery time.

5.2.4 Image Analysis

Three sample areas were selected from different regions of each cell and photographed. For image analysis, micrographs were printed at 2000X magnification. MT angle and length measurements were recorded using a Kontron Image Analyser as described in Chapter 3 while area was measured using the area

measurement package on SigmaScan Image Analysis Software (Jandel Scientific) and a Numonics Corporation Graphic Digitizer (Model # 2210-0.30C). MT sample sizes, which varied according to MT density, were between 223 (for the earliest recovery time) and 3514 counts. Angle and length frequency distribution histograms were produced by combining all samples for each cell. Mean lengths for each sample were computed from their logarithms (since the length distributions were not normal) and a weighted average from all samples then calculated.

5.3 RESULTS

5.3.1 Oryzalin Treatments with Young, Rapidly Elongating Internodal Cells

(i) Microtubule Disassembly

Young, rapidly elongating internodal cells with predominantly transverse MTs (Fig. 5.1) were treated with oryzalin at various concentrations ranging from 2.5 to 40 μM and fixed after 5, 10, 15 and 20 minutes. The results (summarized in Table 5.1) show that complete disassembly is extremely rapid. In all treatments, MT shortening had occurred after 5 minutes (Figs. 5.2 & 5.3) and in oryzalin concentrations of 5 μM and greater no MTs were detected after 10 minutes (Fig. 5.4). The standard dose of 10 μM ensured complete and rapid MT depolymerization but after removal it had no detectable effects on subsequent cell viability or growth.

TABLE 5.1

Oryzalin Treatment Responses

Concentration Oryzalin (μM)	Treatment Time (min)	Description of MTs
2.5	5	Short
2.5	10	Short
2.5	15	Very Short
2.5	20	-
5	5	Short
5	10	-
10	5	Very Short
10	10	-
20	5	Very Short
20	10	-
40	5	-

The pattern of MT disassembly was impossible to assess quantitatively due to its rapidity (preparing a cell for perfusion took almost as long as disassembly). It was therefore difficult to determine if there was any selective depolymerization based on MT orientation but the few remaining MTs in partially disassembled arrays (Fig. 5.3) were almost exclusively transverse. In some cases, brightly-fluorescent vesicles are seen (Fig. 5.3) but there is no sign of these in cells whose MT array is completely disassembled (Fig. 5.4).

(ii) Microtubule Recovery Under Standard Growth Conditions

When young, rapidly elongating internodal cells were incubated in oryzalin and then returned to standard growth conditions, complete recovery (shown in Figures 5.5 to 5.16) of the predominantly transverse array took less than 140 minutes. MTs were first detected 20 minutes after removal of cells from the oryzalin solution at discrete sites in the cortex (Fig. 5.5). These assembly sites appeared to be fairly evenly dispersed throughout the cortical cytoplasm. MTs were frequently organized in V- and Y-shaped pairs (Figs. 5.5 & 5.6) or in groups of several MTs that formed branched assemblies (Figs. 5.7 to 5.9). Almost invariably, short MTs appeared to emerge from longer MTs, suggesting that newly formed MTs were assembled along existing MTs. As recovery progressed, MTs in the branching assemblies became both longer and more numerous (Figs. 5.7 to 5.10) and since MTs abutted one another at acute angles, fan-shaped patterns resulted. After about 70 minutes recovery (Fig. 5.10), branching assemblies of MTs began to overlap, filling in the areas that had previously been devoid of MTs. At about the same time, isolated MTs were apparent. From this time MT alignment became progressively more transverse until an array that was indistinguishable from an untreated cell was achieved. A small number of branching assemblies were seen amidst the fully recovered array (Fig. 5.16) just as they normally are found in untreated cells.

(iii) Interpretation of Microtubule Recovery Based on Quantitative Data

MT lengths and angles of orientation were recorded using an image analysis computer in order to compare MT organization at different recovery times. Frequency distribution histograms of MT angle (Fig. 5.17) show that the first MTs assembled were mostly transversely oriented. As branching assemblies became more extensive, MT orientation became increasingly variable until a nearly random distribution was observed at 60 minutes (Fig. 5.17; cf. Fig. 5.9). When branching assemblies had grown sufficiently to cause extensive overlap and MTs became evenly dispersed (60 min., Fig. 5.17; cf. Fig. 5.9), the proportion of transverse MTs began to increase (70 to 140 min. of Fig. 5.17; cf. Figs. 5.10 to 5.16). Eventually the angular distribution resembled that of untreated cells with only a small number of MTs oriented in oblique and longitudinal directions (compare control and 140 min. of Fig. 5.17).

Plotting mean MT length against recovery time (Fig. 5.18) shows that much of the original MT length is regained long before the array is fully reorganized in terms of orientation (70 min. vs. 140 min.). There was a steady increase in mean MT length until about 70 min; after this time it increases only slightly. Like MT length, the MT frequency (number of MTs per unit area; Fig. 5.18) and density (total MT length per area) (Fig. 5.19) increased very rapidly during early recovery and subsequently underwent very little change. In both cases, maximum values were achieved long before complete reorganization of the array (80 min. vs. 150 min.).

(iv) Microtubule Recovery After Prolonged Disassembly

Extending the period in which cells were incubated in oryzalin to 24 hours did not prevent the recovery of a transverse array. After oryzalin was removed, the first MTs assembled appeared randomly oriented, but the recovery pattern was otherwise normal; MTs reappeared shortly after removal of oryzalin and a

transverse MT array was reformed within a few hours. Increasing the concentration of oryzalin caused a delayed recovery (Figs. 5.21 to 5.24) and the earliest MTs detected were less precisely transverse as those in cells treated with 10 μM oryzalin. For example, the first MTs to assemble after a 30 minute treatment with 20 μM oryzalin were not observed until after 60 minutes (not shown) yet the recovery that followed (Figs. 5.23 & 5.24) was not unlike that induced by an inhibitor treatment of shorter duration and lower concentration.

(v) Microtubule Recovery at Increased Temperature

Allowing rapidly growing cells to recover at a higher temperature than used in the standard culturing conditions resulted in an accelerated recovery. When the temperature of recovery was raised from 18 to 25° C, MTs were detected as early as 13 minutes after removal of the cells from oryzalin (Fig. 5.25) and reformed a full complement of predominantly transverse MTs within 70 minutes (Fig. 5.33). Some V- and Y-shaped clusters were present in early stages of recovery (Figs. 5.26 to 5.30) but at no stage were extensive branching assemblies like those seen during recovery at 17°C observed. Instead, MTs increased in length and number while maintaining predominantly transverse orientation (Figs. 5.25 to 5.33).

5.3.2 Oryzalin Treatments with Mature Internodal Cells

(i) Microtubule Disassembly

Microtubule depolymerization/recovery was followed in older cells that were either approaching completion of elongation or no longer growing. When treated with oryzalin, the rate of MT disassembly was slower than in rapidly expanding cells. Even after 20 minutes in 10 μM oryzalin, some traces of MTs were still present (Fig. 5.38). The pattern of MT disassembly (Figs. 5.35 to 5.39) shows a progressive reduction in both length and number. The residual MTs seen in later stages of disassembly did not show any preferred orientation but lay in a variety of

angles similar to the MTs of the untreated array. For MT disassembly/recovery experiments on older cells, 10 μM oryzalin treatments of 30 minute duration were necessary to ensure complete removal of all MTs.

(ii) Microtubule Recovery in Mature Cells in the Final Stage of Elongation

The recovery pattern after MT depolymerization in older internodal cells approaching growth cessation is shown in Figures 5.40 to 5.48. MTs were first observed 60 minutes after removal of the cells from oryzalin (Fig. 5.40) and although they were less numerous and clearly not transversely oriented, they were arranged in branching assemblies similar to those seen in younger cells during early stages of recovery with short MTs projecting from longer MTs. At 80 minutes, MTs were arranged in less extensive but more abundant branching assemblies that formed circular fringes around areas that were now mostly devoid of MTs (Figs. 5.41 & 5.42). These patterns gave the impression that MTs were no longer present in what had previously been a site or sites of nucleation - as if depolymerization of the earlier formed trunks left only the branches intact. The existence of MT-free areas, fringed with branching clusters of MTs was still detectable after 120 minutes (Fig. 5.43) but by this time the number of MTs had greatly increased. In areas between the radiating clusters, MTs were frequently seen to be oriented in distinct and often parallel directions (Fig. 5.42). Eventually, MTs became very numerous and evenly dispersed throughout the cortex (Fig. 5.44). Subsequently, the proportion of transverse MTs increased until an array similar in appearance to that of much younger cells was observed after 180 minutes (Fig. 5.46). This highly organized, transverse array appears to be only temporary since cells sampled at slightly longer recovery times (Figs. 5.47 & 5.48) showed both a decrease in the number of MTs and an increasing variability in orientation. Thus, a transient period of relative organization precedes the gradual

return to the highly variable MT orientation typical of cells at this stage of development.

(iii) Microtubule Recovery in Older, Non-Growing Cells

In older, non-growing internodal cells, MT recovery was relatively slow and appeared to involve reassembly of the MT array without any detectable realignment. The rate of recovery also varied considerably between different cells and in some cases, was not uniform along the length of individual cells (see Figs. 5.69 & 5.70) The recovery pattern is represented in Figures 5.49 to 5.77. The first MTs - observed after 90 minutes recovery (Figs. 5.49 to 5.51) - were very short and arranged in clusters in which the component MTs radiated from a common focal point. These assemblies were similar to the V-shaped MT clusters seen in younger cells during recovery except that they generally contained several MTs. These putative nucleating sites were also relatively sparse, unevenly distributed and lacked a preferred orientation.

After the initiation of MT assembly at these discrete sites in the cortex, continued MT assembly occurred along the existing MTs, resulting in spectacular herringbone- (Figs. 5.55 & 5.56) and star burst-shaped (Figs. 5.57 to 5.63) assemblies. At first, MT nucleation appeared to prevail over MT elongation, resulting in the formation fairly dense assemblies of many very short MTs (Figs. 5.57 to 5.62). Most commonly, MTs of single assemblies were oriented through no more than 180^{o} but occasionally, double clusters were observed (Figs. 5.56, 5.58 & 5.59) with MTs spreading out in opposite directions from a single focus. Adjacent MT assemblies frequently branched in quite different directions (Figs. 5.52, 5.57 & 5.60) suggesting that there were no overriding forces of alignment. In later stages of recovery (Figs. 5.64 to 5.68), assemblies appeared to break up into progressively smaller groups of longer MTs (again as if depolymerization of the earlier formed trunks left only the branches intact). MTs

became increasingly dispersed but showed no sign of being oriented in any preferred direction (Figs. 5.70 to 5.76) so that eventually, a randomly organized array (Fig. 5.77) was established.

5.3.3 Microtubule Assembly Patterns in the Endoplasm During Recovery of Elongating Cells from Oryzalin Treatment

In an attempt to compare the organization of endoplasmic MTs with those in the cortex, MT patterns in both regions of the cell were followed throughout recovery after oryzalin-induced MT depolymerization. The results of this investigation are summarized in Figures 5.78 to 5.92. Endoplasmic MTs were rapidly depolymerized in the presence of oryzalin and were not observed during the early phase of cortical MT recovery (Fig. 5.78). Brightly fluorescing spots, however, were observed on the surface of nuclei after about 50 minutes (Fig. 5.79). Shortly after this time - at the stage when the recovering cortical MTs had reached maximum density (see Figs. 5.19 & 5.20) - endoplasmic MTs were very abundant (Figs. 5.80 to 5.85). MTs were arranged in extensive networks around nuclei as well as being aligned in the same direction as the actin cables. In many cases, the MT assemblies seen in the endoplasmic regions of recovering cells were more extensive than those of untreated cells. Bright spots on the surface of nuclei were no longer detected and generally, nuclei displayed very little or no fluorescence, especially when surrounded by a network of MTs (See Fig. 5.85).

As cortical MTs became increasingly oriented in a transverse direction, the number of MTs in the endoplasm appeared to decline (Figs. 5.86 to 5.89). Those aligned with actin cables appeared shorter (Fig. 5.88) and MT assemblies around nuclei (Fig. 5.89) became far less extensive. In some cells whose cortical MT reorganization was almost complete, no endoplasmic MTs were seen (Figs. 5.90 to 5.92). In these cases, bright spots on the surface of nuclei were generally observed.

Beyond this stage of recovery, endoplasmic MTs appeared to be organized as they had been prior to oryzalin treatment.

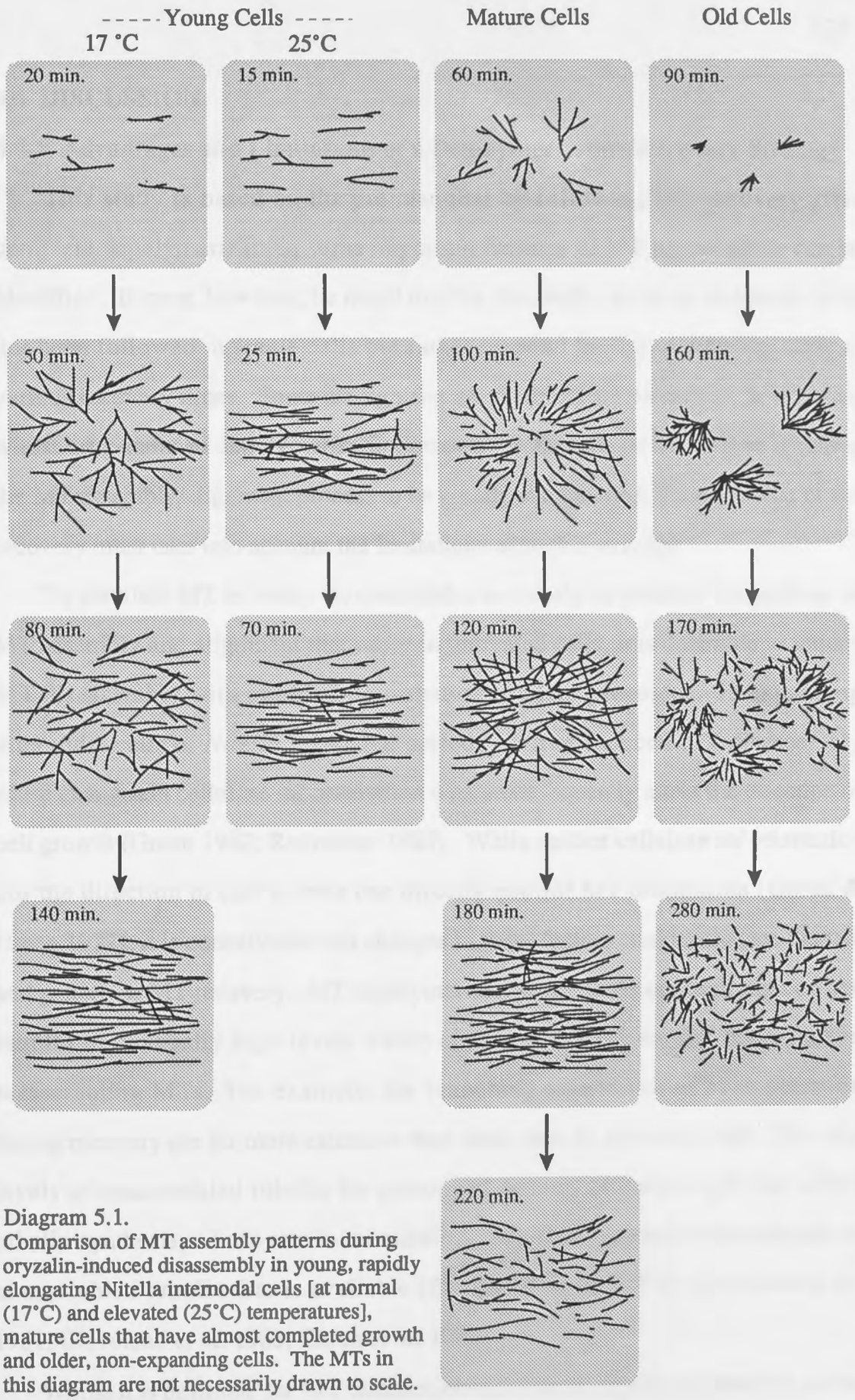

Diagram 5.1.
Comparison of MT assembly patterns during oryzalin-induced disassembly in young, rapidly elongating Nitella internodal cells [at normal (17°C) and elevated (25°C) temperatures], mature cells that have almost completed growth and older, non-expanding cells. The MTs in this diagram are not necessarily drawn to scale.

5.4 DISCUSSION

5.4.1 Advantages and Limitations of a Depolymerization/Recovery Strategy

This study is based on the premise that by following MT recovery after complete depolymerization, some important features of MT organization can be identified. It must, however, be noted that for this study, dynamic processes have not been followed in single cells but rather inferred by fixing different cells at various recovery times. Some ambiguities are therefore unavoidable. In addition, whilst drug-induced depolymerization/recovery is advantageous because it causes the MT assembly/alignment process to be greatly exaggerated, interpretation of the recovery must take into account the limitations of such a strategy.

To simulate MT recovery that resembles as closely as possible the patterns of MT assembly and alignment that occur in untreated cells, it is desirable to induce MT disassembly with minimal perturbation to other processes. In expanding internodal cells of *Nitella*, extended periods of drug-induced MT disassembly cause changes in cellulose mf orientation which consequently alters the direction of cell growth (Green 1962; Richmond 1983). While neither cellulose mf orientation nor the direction of cell growth can directly control MT orientation (Gertel & Green 1977), it is conceivable that changes in these factors could influence the rate and pattern of MT recovery. MT depolymerization raises the concentration of free tubulin to unusually high levels which could result in abnormal behaviour in reassembling MTs. For example, the branching assemblies of MTs observed during recovery are far more extensive than those seen in untreated cells. Elevated levels of unassembled tubulin for prolonged periods of time might also affect tubulin synthesis, whose rate in mammalian cells is modulated by the amount of unassembled tubulin that is available (Ben-Ze'ev *et al.* 1979; Cleveland *et al.* 1981; Cleveland *et al.* 1983; Caron *et al.* 1985).

Whilst it is desirable for MT disassembly to occur as rapidly as possible, at the same time it is necessary to avoid non-specific effects of inhibitors used at very

high concentrations. Dinitroaniline herbicides have, for example, been implicated in the inhibition of photosynthesis and respiration (Moreland *et al.* 1972), the inhibition of Ca^{2+} uptake by mitochondria (Hertel & Marme 1983) and other metabolic processes (Ashton *et al.* 1977). Moreover, inhibitor treatments must be fully reversible. It is therefore desirable to use a protocol that involves a minimal concentration of inhibitor as well as minimal exposure time.

The protocol for MT disassembly/recovery in *Nitella* internodal cells was designed with consideration for the aforementioned limitations. Oryzalin was chosen as an agent of MT disassembly because of its high affinity for plant tubulin (Strachan & Hess 1983). To avoid non-specific effects, a mild treatment of short duration was used. This induced rapid and complete disassembly which was followed by full recovery of the MT array. The effect of oryzalin on the MTs of *Nitella* internodal cells are therefore fully reversible at the concentrations used in this study. As a result, some clear pointers to various facets of MT behaviour can be inferred from the observed patterns of recovery.

5.4.2 Sensitivity of *Nitella* Microtubules to Oryzalin

Using a 10 μM solution of oryzalin, disassembly of all MTs in *Nitella* internodal cells occurred in less than 10 minutes in younger, rapidly elongating cells and in about 20 minutes in older, slowly- and non-growing cells. Compared with MTs of other plant cells that have been treated with oryzalin (Bajer and Molè-Bajer 1986b; Morejohn *et al.* 1987b; Cleary & Hardham 1988; Wacker *et al.* 1988), the MTs of *Nitella* internodal cells have an intermediate sensitivity to oryzalin. In multicellular root tips of *Zinnia*, Cleary and Hardham (1988) found that a 40 hour treatment with 10 μM oryzalin was required to remove all detectable MTs from 98% of the cells. In contrast, Morejohn *et al.* (1987b) reported the loss of virtually all MTs from single, wall-less *Haemanthus* endosperm cells, treated with 0.1 μM oryzalin, in less than two minutes. Such variations in sensitivity may

reflect different affinities of oryzalin for different plant tubulins or the relative lability of MTs. More likely, they reflect the facility of uptake of oryzalin into different cells. Since uptake appears to occur by diffusion (Upadhyaya and Nooden 1980), it is logical that single cells should be more accessible to oryzalin than cells of multicellular tissues. Moreover, since adsorption of dinitroaniline herbicides to cell walls can occur (Bayer *et al.* 1967), wall-less cells should be the most sensitive.

5.4.3 Microtubule Nucleating Sites in the Cortex

MTs first reappear at discrete, randomly distributed sites in the cortex, a phenomenon that has been observed in several other studies on MT recovery in plant cells (Gunning 1980; Galatis 1983; Hogetsu 1986; Falconer *et al.* 1988; Cleary & Hardham 1988). Peripheral nucleating sites have been described in other cell types, for example, the plasma membrane associated plaques in *Drosophila* wing epidermal cells lacking centrosomal MTOCs (Mogensen & Tucker 1987). It is conceivable then that the sites of MT assembly in the cortex of plant cells also represent structurally specialized nucleating centers. The sites of MT assembly in *Nitella*, however, do not have any obvious association with features that are visible with light microscopy. Electron microscopy could be used to explore the possibility that structurally specialized MT nucleating centers exist, and to identify the structures that may be involved in recovering cells.

Subsequent MT initiation appears to occur in close association with existing MTs throughout most of recovery, an event which results in the formation of branching assemblies of MTs. Although extensive, fan-shaped configurations like those seen during intermediate recovery (see Fig. 5.8) are not found in the cortical arrays of untreated cells, some less extensive branching arrangements of MTs are always present (see, for example, Figs. 2.12 & 2.13). One possible explanation for preferential MT assembly at sites along existing MTs is that the binding of one or more MAPs to the perimeter of existing MTs provides an initiation site from which

new MTs can assemble. Such sites would provide a cap for the slow growing end of MTs as occurs in other situations (Soltys & Borisy 1985; Mitchison *et al.* 1986) thus permitting assembly in conditions that would not normally favor MT growth.

That "branching assemblies" of cortical MTs have not been previously documented in plant cells is not surprising. If they represent a very minor part of the total array, they could miss detection with the electron microscope and the resolution of immunofluorescently labelled MTs in formaldehyde-fixed cells (the most common method of fixation of plant cells for anti-tubulin immunofluorescence) would be insufficient to discern such an arrangement. Thus, MT "branching" may not be unique to *Nitella* internodal cells. The "fir-tree" patterns of kinetochore fibres observed in *Haemanthus* endosperm (Inoué *et al.* 1985; Bajer & Molè-Bajer 1986b), and onion root cells (Palevitz 1988) and in the alga *Oedogonium* (Schibler & Pickett-Heaps 1987) may be arranged in a similar manner. The polarity of MTs could be the same in both types of arrays, that is, with the plus ends distal to the initiating site. Polarity of MTs is probably an important factor in the assembly and distribution of MTs in the cortex of plant cells just as it is in mitotic spindles (McIntosh 1981). In order to determine the polarity of cortical MTs of *Nitella*, the tubulin decoration technique of Euteneuer and McIntosh (1980) will be applied in future work.

The fact that MTs branch at what appear to be very consistent angles to the existing MTs suggests that if specialized assembly sites do exist, they also impart orientation to the MTs they nucleate. How this would operate is uncertain but in the case of isolated centrosomes from the rootlets of *Polytomella*, for example, MTOCs have been demonstrated to have prepatterned initiation sites which not only initiate MT assembly but also specify MT orientation (Stearns & Brown 1981).

Finally, MTOCs have the ability to control the lattice structure of MTs they nucleate whereas MTs that assemble spontaneously are less likely to have a strictly

controlled protofilament number (Evans *et al.* 1985). It seems logical then that structurally specialized sites for MT assembly - be they discrete plasma membrane associated sites or sites along existing MTs - should exist in the cortical cytoplasm of plant cells where MT assembly evidently takes place.

5.4.4 Microtubule Nucleating Sites in the Endoplasm

Recovery of endoplasmic MTs is also observed following oryzalin treatments of elongating internodal cells. During early reassembly of MTs in the cortex, there was no sign of MTs in the endoplasm. However, patches of intense fluorescence on the surface of nuclei became increasingly apparent and later, endoplasmic MTs were observed. These MTs - like those seen in the endoplasm of untreated cells though more abundant - were located around nuclei and along chloroplast files. Some researchers have suggested that MTs in plant cells are nucleated at the surface of the nuclear envelope (Lambert 1980; Schmit *et al.* 1983; Sheldon & Dickinson 1986; Hogan 1987) and may extend into the cortical regions (De Mey *et al.* 1982; Wick & Duniec 1983; Dickinson & Sheldon 1984; Bakhuizen *et al.* 1985; Clayton *et al.* 1985; Wick 1985). The patches of intense fluorescence observed on the surface of nuclei in *Nitella* could represent MT organizing sites such as those described for the nuclear surfaces of higher plant cells, thought to represent expanded centrosomes that permit MT organization at several sites on the nucleus (Mazia 1984) and MTs assembled at these sites could be involved in some endoplasmic process such as nuclear division, motility or nuclear positioning (Van Lammeren *et al.* 1985; Hogan 1987). Alternatively, these MTs might be synthesized in the endoplasm to be transported (possibly along branches of the actin cables which lead into the cortex- Williamson *et al.* 1985) to the cortical cytoplasm. Even if the nuclear surface is a site for MT assembly, however, it seems unlikely that it could be a major source of cortical MTs since considerable MT assembly had already taken place in the cortex before endoplasmic MTs were

detected. From this evidence, it is, if anything, more likely that the cortex is the source of endoplasmic MTs.

5.4.5 Microtubule Nucleation Patterns in Non-Growing Cells

The basic pattern of MT nucleation and assembly is perhaps most easily interpreted in mature, non-growing cells where the pattern does not appear to be complicated by MT alignment mechanisms. Re-establishment of an essentially randomly organized MT array appears to result from continued assembly of MTs, initially from discrete assembly sites in the cortex and later along existing MTs. The geometry of MT nucleation is very consistent; MTs are never dispersed symmetrically about early assembly sites and generally radiate through less than 90^{o}. They are also arranged at acute angles to each other in the subsequent formation of branching assemblies. Even when more than one MT cluster emerges from a single location in the cortex, the asymmetric form of the individual MT branching assemblies is maintained. Continued MT assembly from sites along existing MTs allows the extension of the fan-shaped clusters into heavily subdivided branching assemblies.

The breakdown of MT networks into smaller and smaller clusters and the apparent movement of MTs away from the original nucleation sites appears to result from the disassembly of the earliest formed MTs. This selective disassembly could occur because of the localized depletion of unpolymerized tubulin. If the MT assemblies are considered to be organized like a tree, it is as if the removal of the trunk and major limbs has occurred, leaving the outer branches intact from which new branches can be added. Continued MT assembly causes spreading MT "branches" of adjacent assemblies to encroach upon each other until MTs are evenly dispersed. Attainment of the original total MT length and concentration of unpolymerized tubulin should result in a much lower incidence of new MT

assembly which would account for the limited branching of MTs seen in fully recovered cells.

5.4.6 Microtubule Nucleation Patterns in Elongating Cells

When MT alignment is not considered, the pattern of MT nucleation and assembly in elongating internodal cells resembles the pattern observed in mature, non-growing cells; assembly initially occurs at discrete sites in the cortex and later along existing MTs. The branching assemblies in growing cells, however, do not become as extensive (in terms of MT number) as those in non-growing cells. This difference in assembly behaviour could be due to the transverse orienting mechanism that is active in growing cells which might "pull apart" the branching assemblies before they become too large.

Alternatively, the drop in concentration of free tubulin caused by MT polymerization could result in the disassembly of "trunk" MTs before the MT branching assemblies become too large. The observation that the 'break up' of MT assemblies in growing cells coincides with the attainment of maximum total MT length per area supports this idea. Branching assemblies in growing cells might not become as extensive because the growth of MTs may be more rapid, resulting in longer MTs with relatively few branches. Conversely, the MTs of older cells might grow more slowly so that more branches (of shorter lengths) form before the concentration of unpolymerized tubulin declines.

When the temperature of recovery was raised from 17^{o}C to 25^{o}C, both the reassembly of MTs and the recovery of transverse orientation occurred more rapidly. MT orientation remained relatively transverse throughout recovery in contrast to recovery at 17^{o}C where considerable randomization occurs. In addition, branching assemblies were never very extensive. The manner in which the recovery pattern is altered suggests how temperature might affect specific aspects of MT assembly and alignment. Perhaps the simplest explanation is that

since increasing temperature should increase most metabolic processes, the orienting mechanism itself might be more efficient at 25°C than at the lower temperature and therefore can more readily 'pull' assembled MTs into transverse orientation. The altered pattern of MT recovery could equally be the result of changes in MT assembly dynamics at a higher temperature (discussed in section 5.4.10). By raising the temperature, the rate of MT assembly should be increased in the same manner as it is in *in vitro* MT polymerization experiments (Weisenberg 1972). MT nucleation may also be an important factor. If temperature does not affect the rate of MT nucleation (along existing MTs) to the same degree as it affects MT extension, branching of MTs will be reduced, resulting in decreased randomization of MT alignment prior to the 'break up' of branching assemblies. Alternatively, branching assemblies might 'break up' more rapidly because the trunk MTs are shorter lived at higher temperatures.

5.4.6 The Nature of Microtubule Alignment Mechanisms

This study has demonstrated that the MT array of *Nitella* internodal cells can be depolymerized until no MTs are detected by fluorescence microscopy and subsequently recover - in relatively little time - a transverse array that is indistinguishable from the original one (compare angular frequency distribution histograms for control and 140 minutes recovery in Fig. 5.17). The survival of some transversely oriented fragments of MTs to guide reassembling MTs is therefore unnecessary. Thus, any mechanism dependent on alignment being imparted to MTs at an early stage of development, (for example, by strain alignment during the early phases of cell growth when circumferential expansion exceeds longitudinal - Green & King 1966) such that those MTs somehow impart orientation to further MTs as they assemble can not account for recovery. Rather, the orienting mechanisms must operate throughout elongation and be capable of functioning in the absence of cues from existing MTs. The observation that

recovery of a transverse array can occur even after 24 hours of MT disassembly, when less than 10 hours of MT disassembly can alter the major axis of expansion from longitudinal to circumferential (Richmond 1983), also rules out the possibility that MTs are aligned perpendicular to the major strain axis (Green & King 1966). A similar conclusion was reached for cellulose mfs by Gertel and Green (1977). It also implies that MT orienting mechanisms do not depend on cues from transversely aligned cellulose mfs abutting the outer face of the plasma membrane since Richmond (1983) showed that mf orientation "randomized" without a noticeable time lag upon MT disassembly.

5.4.7 Microtubule Alignment Mechanisms and Rate of Growth

In an earlier study, it was suggested that the degree to which MTs are transversely oriented depends on the rate of cell expansion (Ch 3; Wasteneys & Williamson 1987). Comparing recovery patterns in slowly and rapidly elongating cells shows that although it is not as rigorously maintained in slowly elongating cells, transverse order is transiently established. Thus, the mechanism that orients MTs transversely can operate equally well in both situations. A spurt of growth in the mature cells induced by inhibitor treatment is conceivable but seems unlikely.

5.4.8 Mechanisms of Alignment Based on Microtubule-Microtubule Interaction

The self-cinching loop hypothesis (Green & King 1966) is based on the idea that consolidation of the transverse array depends on interactions between nearby or overlapping MTs. Similarly the dynamic helix model (Lloyd & Seagull 1985) suggests that changes in MT orientation rely on sliding between overlapping MTs. Two observations made in this study could be interpreted to support these models. Firstly, during recovery of MTs in rapidly elongating cells, transverse order starts to increase at the time (*i.e.*, 70 min.) maximum MT density is reached. Secondly,

in older, slowly elongating cells, the decline in transverse order that occurs after the establishment of a tightly transverse array appears to coincide with a decrease in the number of MTs.

The idea that alignment depends on interaction between MTs, however, is not supported by other observations. Data from image analysis of MT recovery in rapidly elongating cells clearly show that the first MTs assembled after short (20 min.) disassembly periods have a high degree of transverse orientation. Cross-linking between such short and widely dispersed MTs therefore seems unlikely. After prolonged (24 hour) disassembly treatment, the first MTs to assemble are not transversely oriented. This suggests that the cell can 'remember' what transverse is but only for short periods of time. Transverse lines of MT-binding proteins in the membrane could, for example, survive short (*e.g.*, 20 min.) disassembly periods. In the prolonged absence of MTs, diffusion, a change in the major growth axis or a change in some membrane property would gradually dissipate these proteins so that the first MTs would be randomly oriented.

If MT orientation is dependent on MT-MT interaction, then the degree to which the MT array is transversely oriented should depend on the density of MTs and partial disassembly of the array should lead to randomization of the remaining MTs. It is therefore confusing that the youngest cells of *Nitella* have a much higher proportion of transverse MTs than older cells yet the MTs of younger cells appear to be less frequent and relatively short (see Ch. 3). MT depolymerization by oryzalin treatment (this study) or extended perfusion (Ch. 2) did not result in any detectable 're-orientation' of MTs during disassembly but neither of these treatments would have been long enough for "relaxation" to take place. It would be desirable to apply a very low concentration of inhibitor that would hold cells in a state of partial MT disassembly for long periods of time.

Although interaction between MTs may be involved in the orientation process, it is certainly not the only factor. MT reorganization during recovery appears to

involve a more complex sequence of events including a 'memory' that enables some newly assembled MTs to assume transverse orientation, a second assembly process that causes MTs to become oriented at a variety of angles and a third mechanism that consolidates fully assembled MTs in a transverse array.

5.4.9 Microtubule Stability and Transverse Orientation

Control of orientation could operate on the basis of selective depolymerization of unstable non-transverse MTs that are either assembled in inappropriate directions or have become misaligned. Conversely, MTs could be selectively stabilized in the transverse direction so that they are longer-lived than MTs oriented in other directions. Depolymerization of MTs in oryzalin-treated cells occurred too rapidly to assess the pattern of disassembly quantitatively but partially-disassembled arrays retained a preponderance of transverse MTs. Evidence recently presented by Richmond and co-workers (1988) suggests that transverse MTs of *Nitella* internodal cells are more resistant to disassembly than their longitudinal counterparts in the presence of 10 μM amiprophos-methyl. Thus, transverse MTs may be expected to have lower rates of tubulin association and dissociation than their non-transverse counterparts. MAPs are obvious candidates for mediation of such a property.

5.4.10 Dynamic Instability and Orientation

During recovery from oryzalin-induced disassembly, the observation that transverse order starts to increase when maximum MT density is reached could reflect the rate of MT assembly/disassembly. During the period when MTs are maximally-randomized (*i.e.*, between 40 and 70 min. recovery), MTs are undergoing rapid elongation (see Fig. 5.20). At this time, the relatively high concentration of unassembled tubulin would strongly favor assembly and decrease the probability of catastrophic shortening of MTs (see discussion on dynamic

instability in Ch. 1, section 1.5.2). Under such conditions, selective stabilization of MTs oriented in one direction would be inconsequential. When the tubulin concentration returns to pretreatment steady-state levels, MT length - on average - does not change. Catastrophic shortening of MTs becomes increasingly likely so any mechanism that suppresses the frequency of phase transitions between elongation and shrinkage (*e.g.*, interaction with MAPs) would be advantageous for the MTs affected.

The fact that re-establishment of transverse orientation is considerably faster when temperature is increased suggests that the orienting mechanism may involve a metabolic process (see section 5.4.5). It is also possible, however, that since MT assembly is faster at the higher temperature, the cell is returned to its tubulin-limited, steady-state environment more rapidly so that stabilizing mechanisms can become effective regulators of MT orientation sooner.

An alternate explanation for the random orientation of MTs in the branching assemblies that are formed during early recovery is that stabilization of newly formed MTs by capping of 'slow' ends at the initiation sites promotes stability. Thus, MT clusters continue to incorporate new MTs that are oriented (because of the geometric constraints imposed by the initiation sites) in increasingly diverse directions. When the concentration of free tubulin reaches a critically low level, catastrophic shortening of some of the MTs could lead to 'disconnection' of the branching assemblies.

The V- and Y-shaped branching clusters that are normally found amidst a predominantly transverse array (see Figs. 2.12 & 2.13) could comprise newly assembled MTs since they closely resemble the MTs observed during recovery from oryzalin treatment. How new MTs become transversely aligned is uncertain. They could be assembled in a transverse direction or become oriented by realignment. The results of this study do not rule out either possibility but it is worthwhile noting that the pattern in which MTs are initiated at apparently precise

angles along existing MTs could provide a means by which the orientation of newly formed MTs is constantly varied. Thus, transverse alignment could be achieved in the absence of a mechanism to 'pull' MTs into appropriate orientation; continuous branching would periodically provide transversely oriented MTs that could become stabilized, perhaps through interactions with a membrane-based template.

CONCLUSION

By following MT recovery after oryzalin-induced depolymerization, several features of MT organization in *Nitella* internodal cells have been elucidated. Cells of three stages of development were selected for oryzalin treatment: (1) young, rapidly elongating cells with predominantly transverse MTs, (2) mature cells, close to growth cessation with scattered longitudinal and transverse MTs and (3) older, non-growing cells with randomly-oriented MTs. In all cases, recovery of an array that resembled the original pattern was achieved but in the second group, a transient period of transverse orientation was observed. Putative MT assembly sites were identified in the cortex as well as in the endoplasm. From quantitative analysis of cortical MT orientation patterns throughout recovery, three processes were identified: (1) a 'memory' that enables some newly assembled MTs to assume transverse orientation, (2) formation of branching assemblies that causes MTs to become oriented at a variety of angles and (3) a mechanism that consolidates fully assembled MTs in a transverse array. The merits of potential orienting mechanisms were discussed with consideration for the observed recovery patterns.

CHAPTER 5 - FIGURES

All micrographs represent fluorescent images from cells processed with a tubulin-specific monoclonal antibody or the DNA-specific fluorochrome Hoechst 33258. All except Figs. 5.84 and 5.85 are arranged so that their long axis or the long axis of the page corresponds to the long axis of the cell.

Figures 5.1 to 5.4. Disassembly of cortical MTs by treatment with 10 μM oryzalin in young, rapidly elongating internodal cells. Anti-tubulin immunofluorescence.

Fig. 5.1. Untreated cell showing abundant, predominantly transverse MTs.

Fig. 5.2. Five minute treatment with 10 μM oryzalin. Cortical MTs are relatively short and sparse. Transverse orientation still prevails.

Fig. 5.3. Five minute treatment with 10 μM oryzalin. In addition to a few residual, mostly transverse MTs, brightly fluorescent vesicles are observed.

Fig. 5.4. Ten minute treatment with 10 μM oryzalin. No MTs detected with anti-tubulin immunofluorescence.

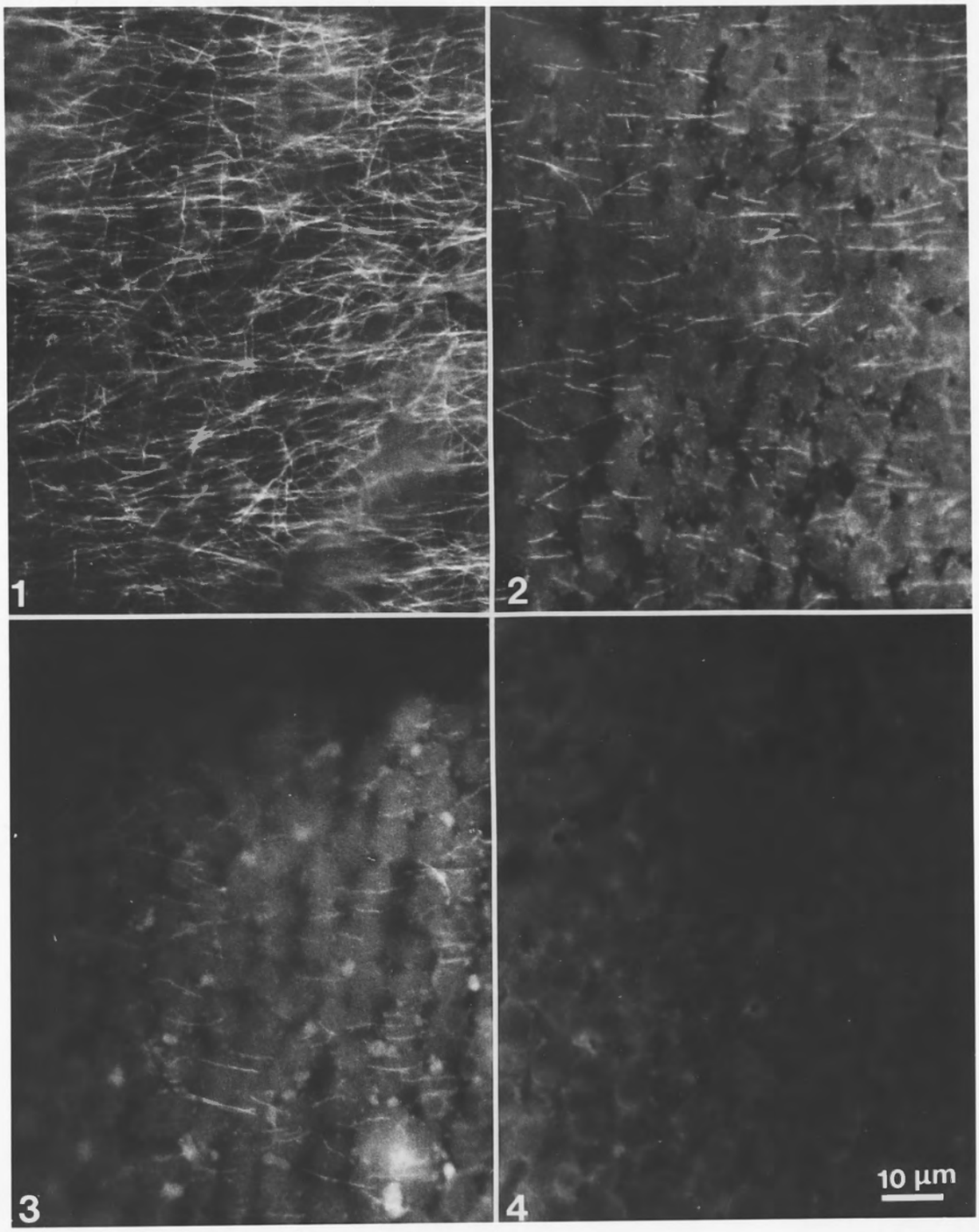
1
2
3
4
10 µm

Figs. 5.5 to 5.16. Recovery of transverse MT array after oryzalin induced disassembly. Cells were treated with 10 μM oryzalin for 20 minutes then allowed to recover under normal culturing conditions. Selected cells were fixed every ten minutes throughout recovery and MTs were visualized with anti-tubulin immunofluorescence.

Fig. 5.5. MTs were first observed about 20 minutes after removal from the oryzalin solution. At this time, they appeared mostly as single MTs with occasional groups of 2 or more MTs arranged in V- or Y-shaped patterns. MTs were mostly transversely oriented.

Fig. 5.6. 30 minutes recovery.

Fig. 5.7. At 40 minutes, MTs are longer, more abundant but orientation seems more scattered.

Fig. 5.8. 50 minutes; MTs are arranged in large, fan-shaped clusters of branching MTs with no preferred orientation.

Fig. 5.9. At 60 minutes, branching clusters show considerable overlap so that MTs are evenly distributed. There is no preferred orientation.

Fig. 5.10. By 70 minutes, MT branching assemblies are less apparent and a fair degree of transverse orientation is now observed.

Figs. 5.11 to 5.15. (80 to 120 min) MTs become evenly dispersed and increasingly oriented in a transverse direction.

Fig. 5.16. MT order is considered to be fully restored at 140 min. MTs are oriented predominantly transvesely just as in untreated cells (see Fig. 5.1).

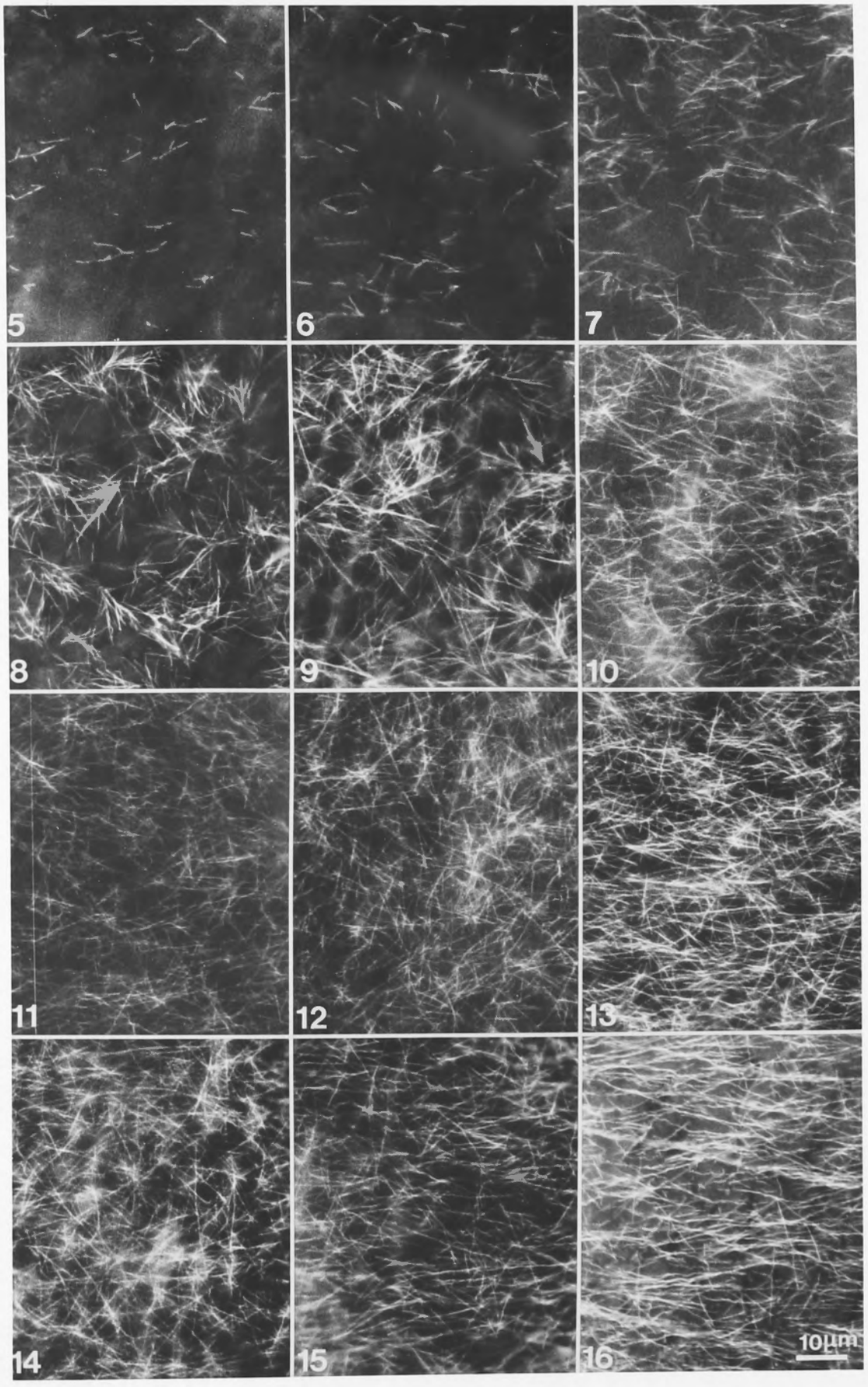
5
6
7
8
9
10
11
12
13
14
15
16
10µm

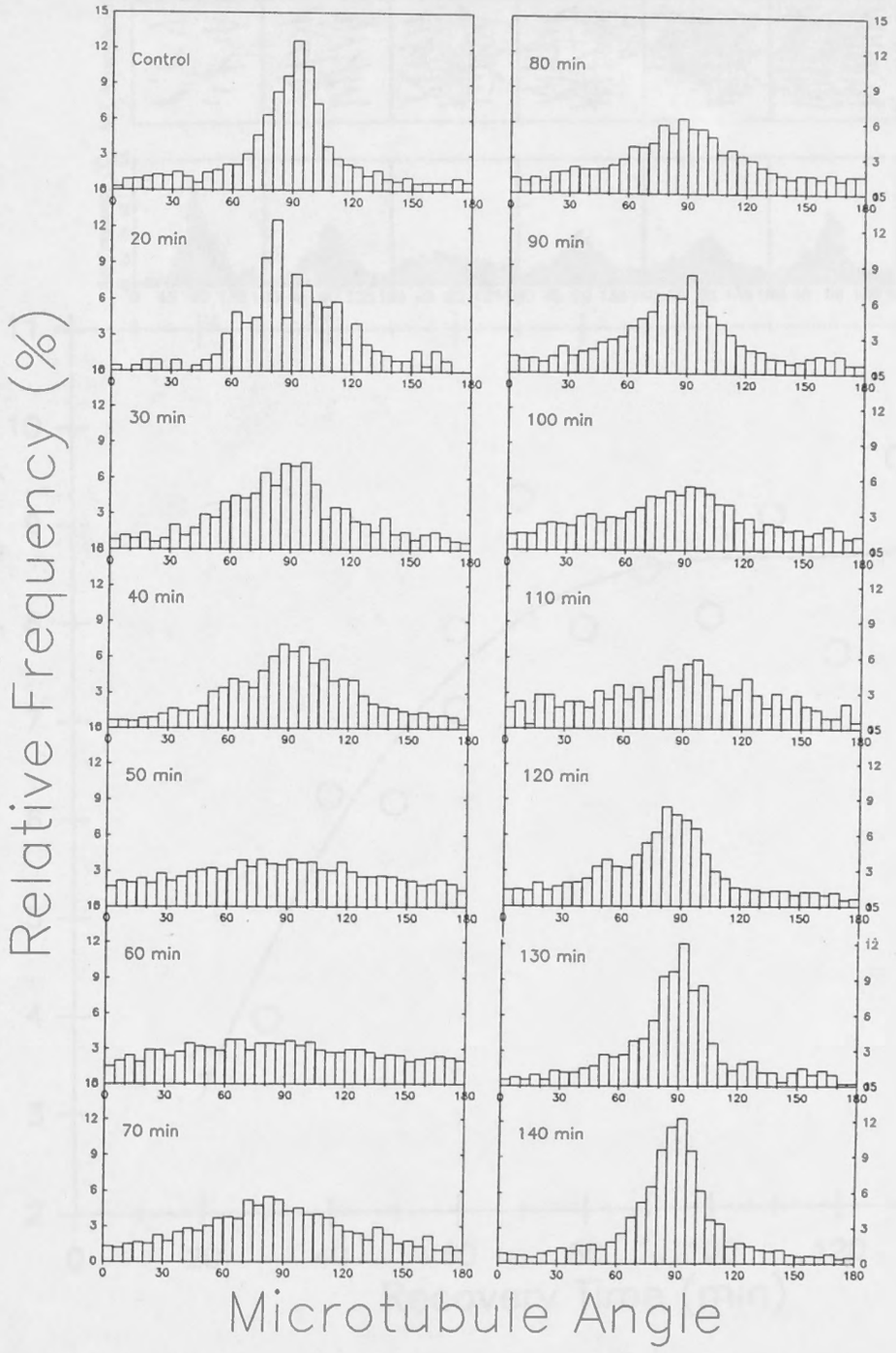

Fig. 5.17. Quantitative analysis of MT orientation throughout the recovery of a transverse MT array after oryzalin-induced disassembly. Frequency distribution histograms of MT angle plotted with an image analysis computer from digitized photographic images. 0^{o} and 180^{o} indicate the long axis of the cell; 90^{o} indicates transverse orientation. In early stages of recovery MTs are oriented predominantly transversely but later (40 to 60 min) they become increasingly dispersed about the transverse axis until a near random pattern is observed at 60 min. From this time, transverse orientation becomes increasingly apparent (70 to 140 min) until the angular dispersion pattern at 140 minutes closely resembles that of untreated cells.

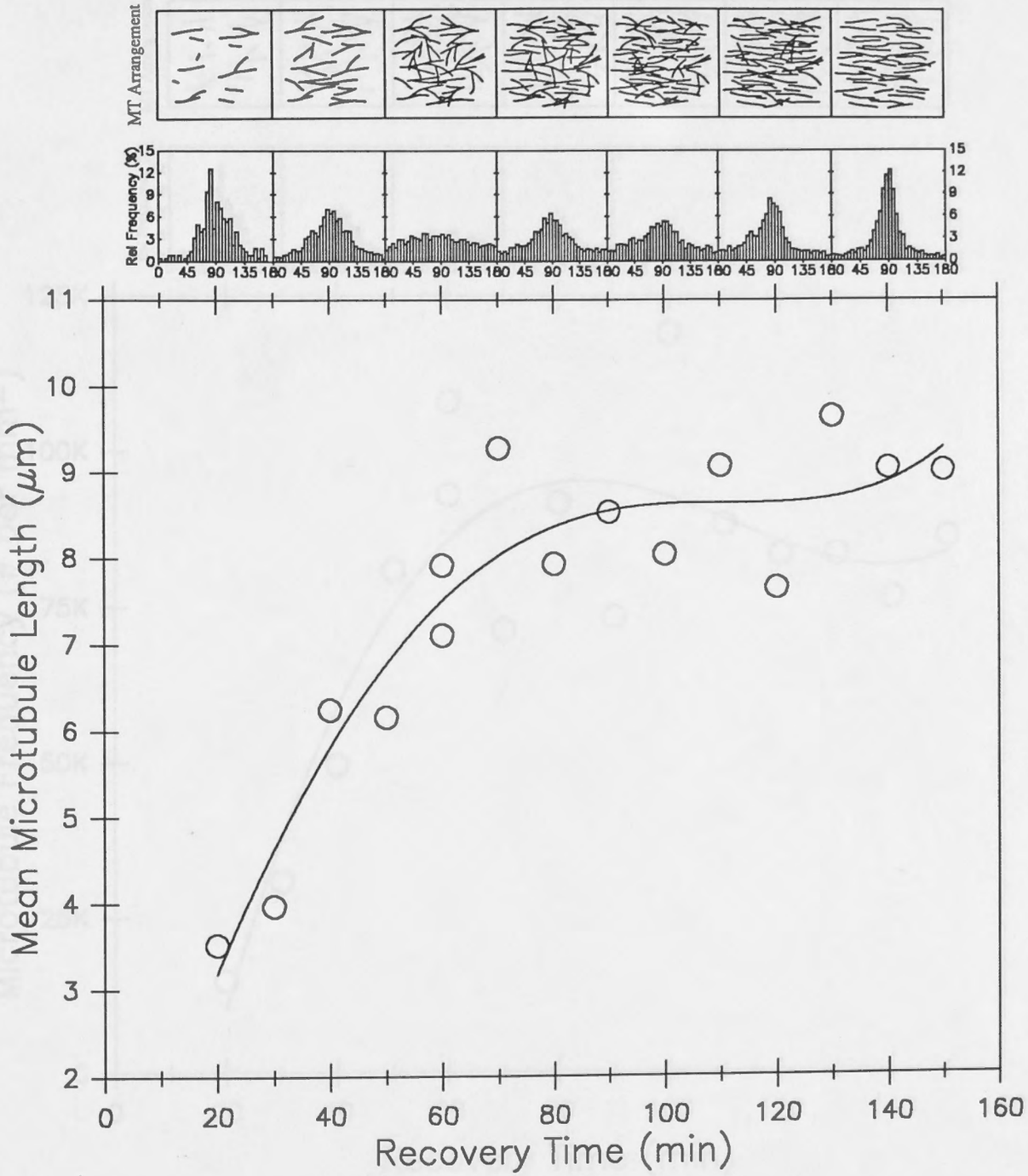

Fig. 5.18. Mean MT length compared with recovery time. Angular frequency distribution histograms from Fig. 5.17 are plotted on the upper axis along with schematic diagrams representing MT arrangement. There is a rapid increase in mean length from the first appearance of MTs (20 min) until 70 min, after which time mean length shows a more gradual increase. The period of rapidly increasing mean length coincides with the randomization of MT angle and the organization of MTs into branching assemblies. The more gradual period of increase in mean length occurs as branching assemblies become disconnected and MTs become increasingly transverse.

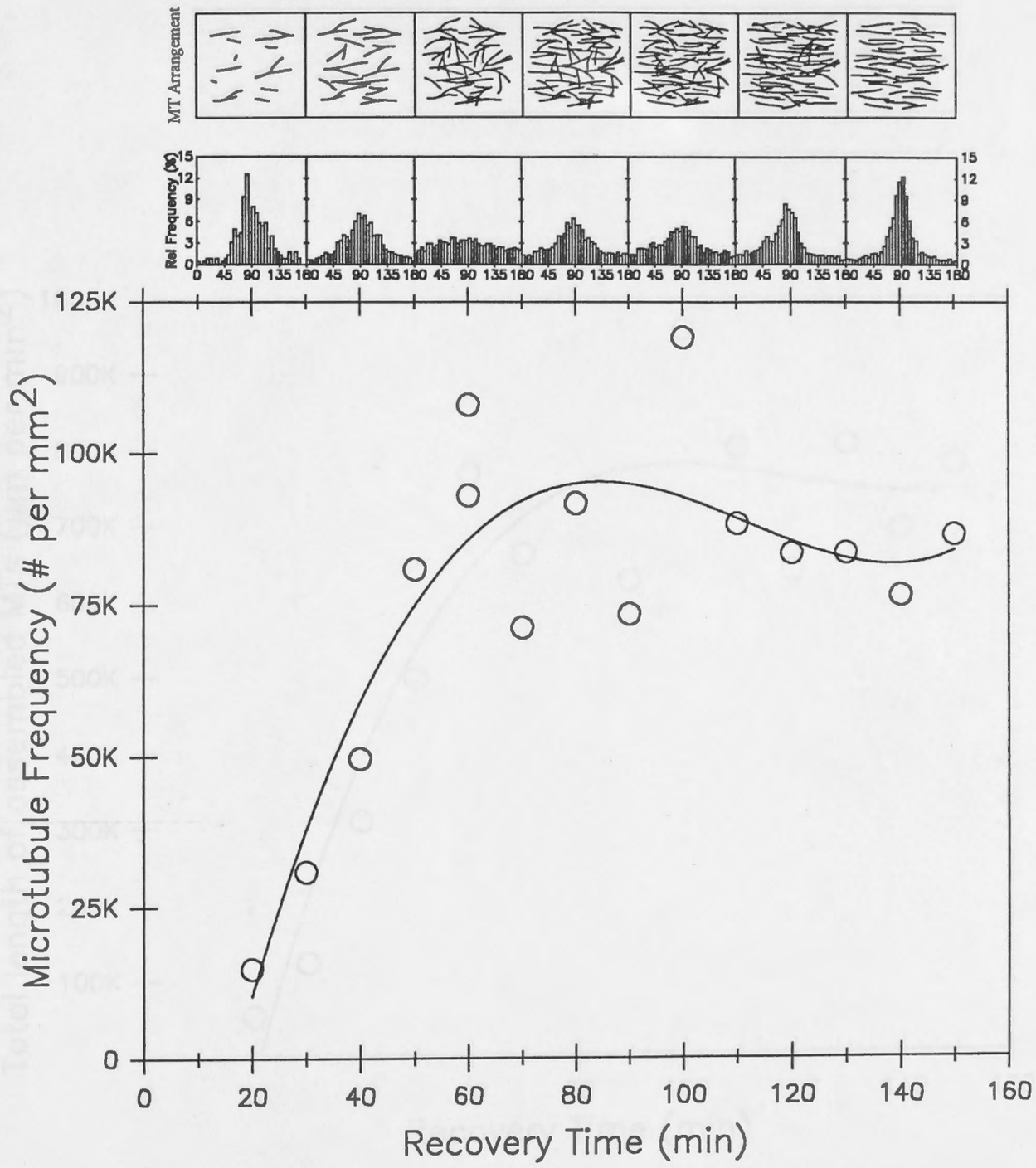

Fig. 5.19. MT frequency, expressed as the number of MTs per mm^2 compared with recovery time. Like mean MT length (Fig. 5.18), there is a rapid increase in the number of MTs between 20 minutes and 70 minutes during the randomization phase, followed by little or no change as MTs become transversely aligned. There is some suggestion that MT frequency becomes more precise in the final stages of recovery since there is a wide variation in this parameter between 60 and 100 min.

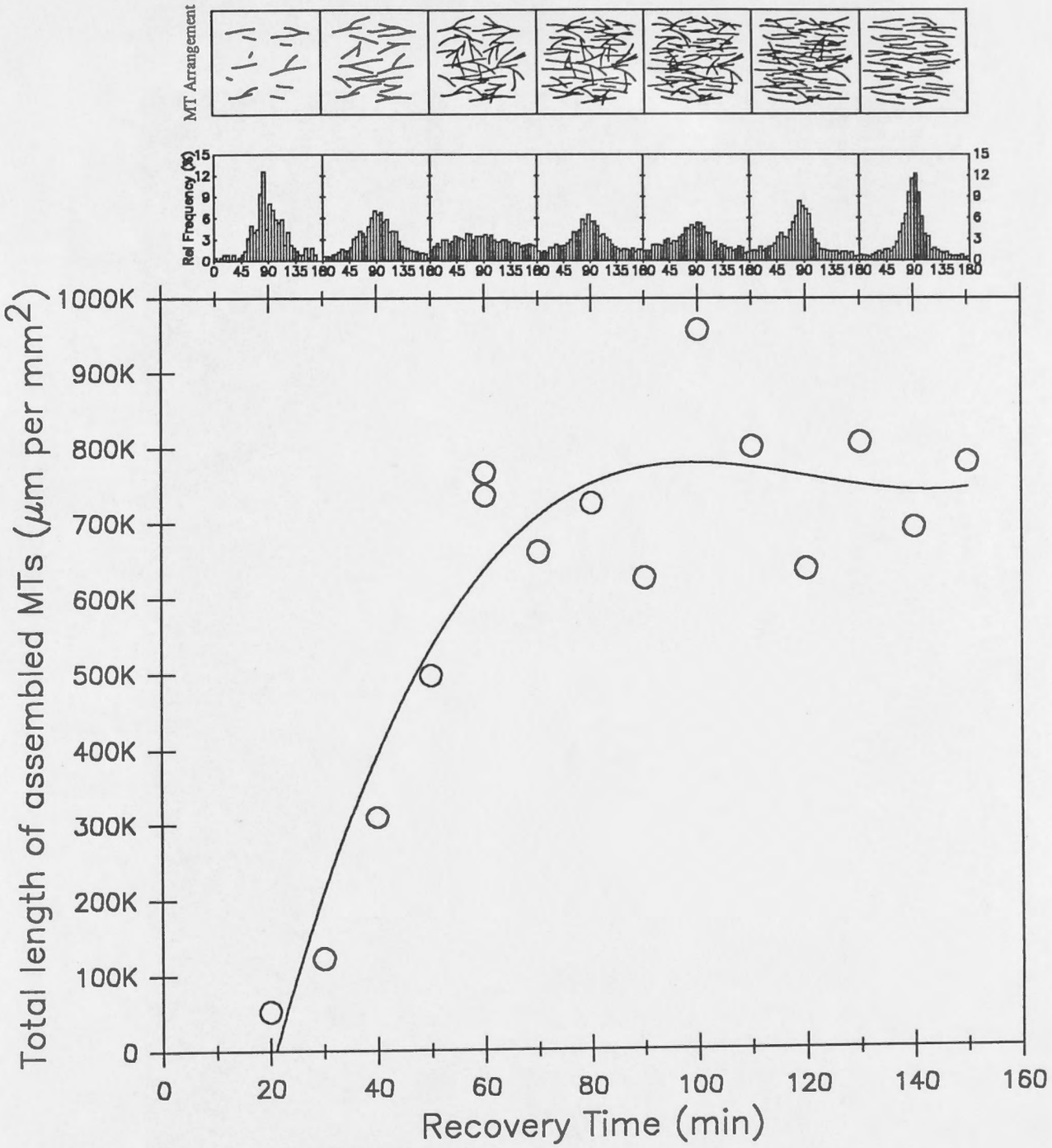

Fig. 5.20. MT density, expressed as total MT length per unit area (μm per mm^2) is plotted against recovery time. As in the case of mean MT length and MT frequency (Figs. 5.18 & 5.19), density increases rapidly during the initial period of recovery and changes very little after 80 minutes.

Figs. 5.21 to 5.24. Microtubule recovery after 30 minute treatment with high concentration (20 μM) of oryzalin.

Fig. 5.21. After 20 minutes recovery time, there is no sign of MT assembly (compare with Fig. 5.5).

Fig. 5.22. After 50 minutes recovery, there is little evidence of MT assembly (compare with Fig. 5.8).

Fig. 5.23. Partially reassembly of MT array after 80 minutes recovery. MTs are well dispersed but still show some sign of clustering.

Fig. 5.24. At 170 minutes recovery, the original transverse order is almost fully restored and MTs are very abundant.

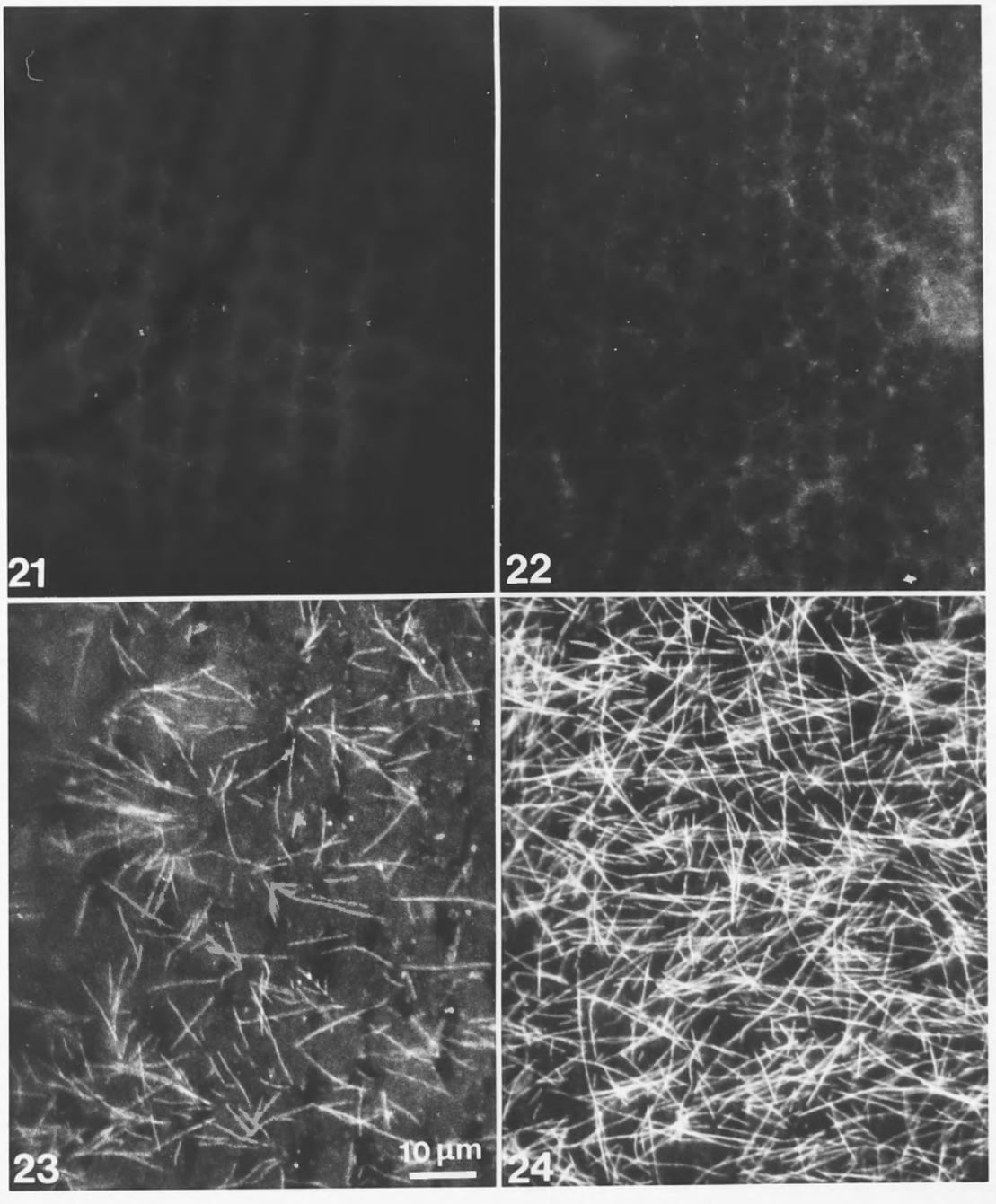
21
22
23
10 µm
24

Figs. 5.25 to 5.33. Microtubule recovery at elevated temperature. After normal inhibitor treatment (10 μM oryzalin for 20 min.), cells were placed in oryzalin-free culture medium at 25°C (compared with 18° C for normal recovery).

Fig. 5.25. MTs were detected as early as 13 minutes after removal from inhibitor solutions.

Figs. 5.26 & 5.27. 15 minutes recovery. MTs are short and predominantly transversely oriented.

Fig. 5.28. At 20 minutes recovery, MTs are still predominantly transverse and show little sign of becoming randomized or forming extensive branching assemblies. Some V-shaped arrangements are visible in this micrograph.

Figs. 5.29 to 5.32. Cells sampled at 25, 30, 50 and 60 minutes show continued assembly of MTs without significant randomization or formation of conpicuous branching assemblies that were seen at lower temperatures (compare with Figs. 5.7 to 5.9).

Fig. 5.33. Complete recovery of transverse array occurs after only 70 minutes in contrast to 140 minutes for lower temperature treatment (Fig. 5.16).

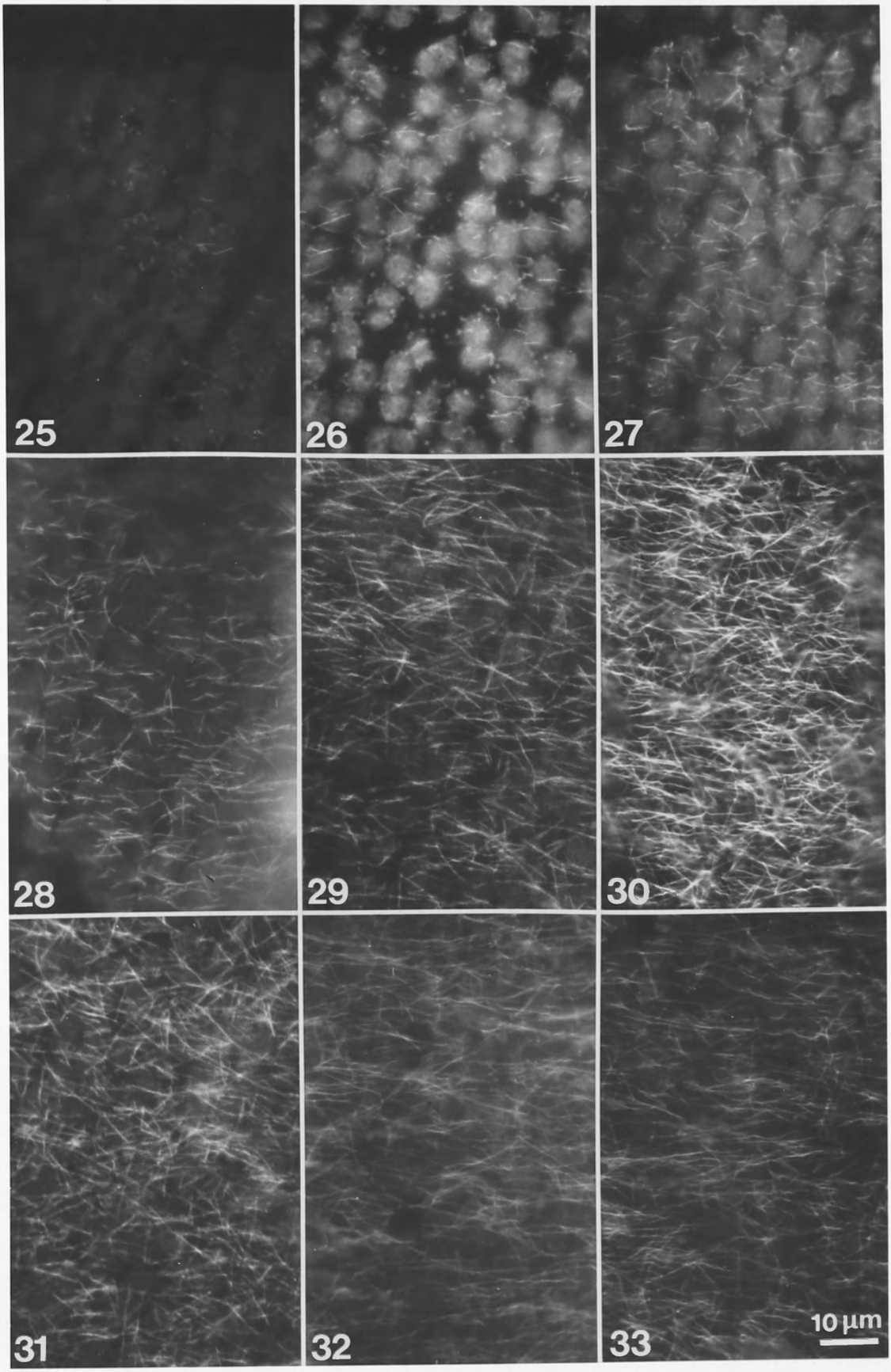
25
26
27
28
29
30
31
32
33
10 µm

Figs. 5.34 to 5.39. Pattern of MT disassembly in mature internodal cells treated with 10 μM oryzalin.

Fig. 5.34. Untreated cell showing near random arrangement of MTs.

Fig. 5.35. Partial disassembly of MTs after 5 minutes.

Fig. 5.36. 10 minute treatment. MTs are mostly disassembled but there are a few residual MTs (compare with Fig. 5.4).

Fig. 5.37. 15 minute treatment. A small number of apparently resistant MTs are still detected. These MTs are of reasonable length.

Figs. 5.38 & 5.39. 20 minute treatment. MTs are mostly disassembled but a few are occasionally detected (Fig. 5.38). In some cases, bright patches of fluorescence (Fig. 5.39) were observed.

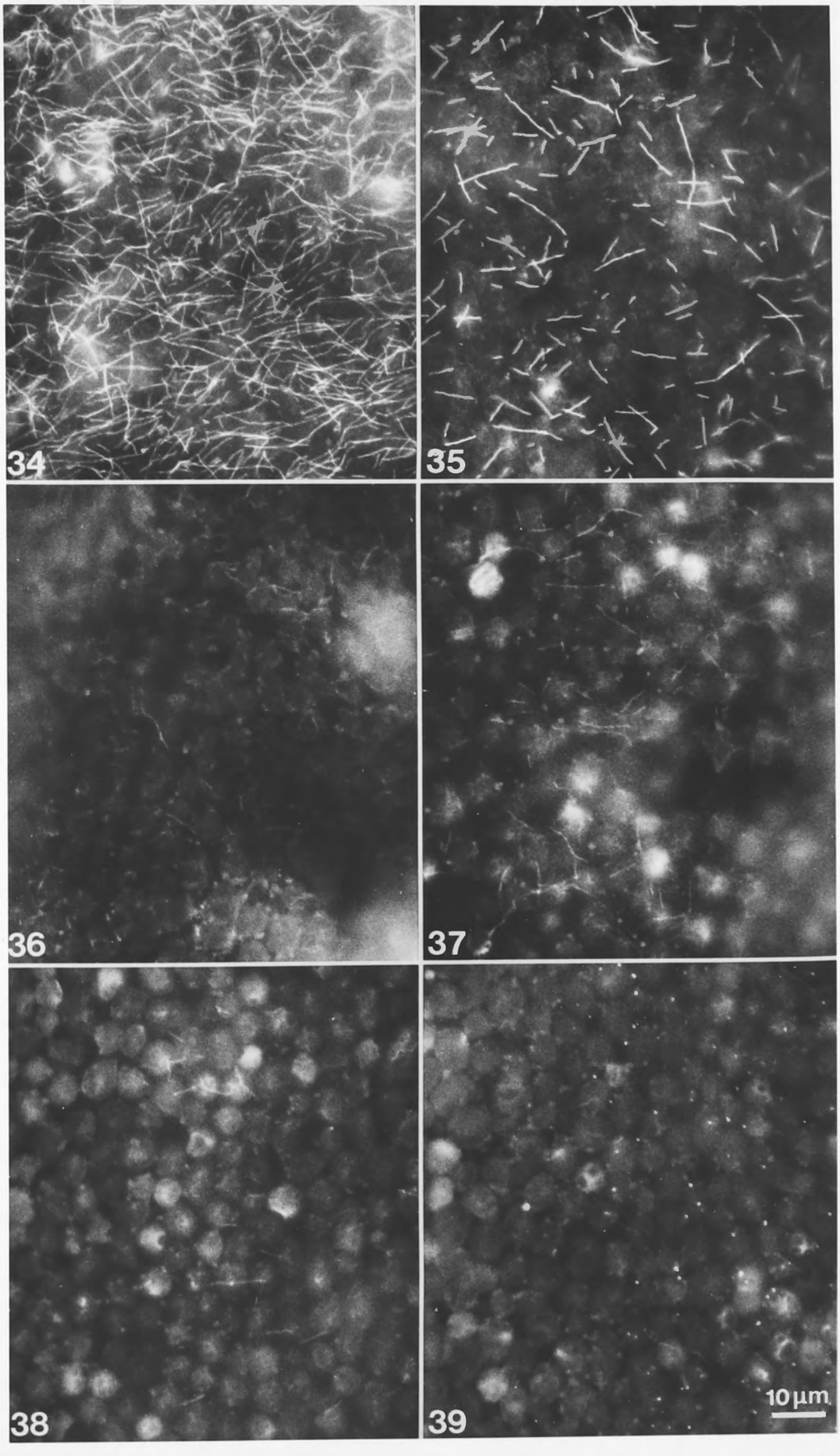
34
35
36
37
38
39
10 µm

Figs. 5.40 to 5.48. MT recovery in cells in the final stages of growth.

Fig. 5.40. After 60 minutes, MTs have assembled at discrete sites in the cortex from which they radiate. There is also some sign of branching assemblies which resemble those seen in younger cells during recovery (see Fig. 5.8).

Fig. 5.41. At 80 minutes, MTs are more dispersed and less likely to be organized in branching clusters. In this case, MTs appear to be oriented in a radial pattern around a central area that is mostly devoid of MTs.

Fig. 5.42. This photograph is from the same cell and adjacent to the area shown in Fig. 5.41. In the upper left corner, part of a radially-arranged group of MTs is shown whereas in the rest of the photograph, the MTs show no such 'focussed' arrangement. The cortical array at this stage of recovery therefore is organized in periodic radiating patterns with intervening regions of distinctly-oriented MTs.

Fig. 5.43. After 100 minutes recovery, MTs are still organized in radial patterns around periodic MT-depleted sites but are now far more numerous. There are many examples of MT branching (*i.e.*, short MTs contiguous with longer MTs) in this photograph.

Fig. 5.44. MTs are far more abundant after 120 minutes recovery than would be expected for cells at this stage of development (compare with Fig. 5.34) but like untreated cells show no preferred orientation.

Fig. 5.45. Cells fixed at later recovery times showed increasing degree of transverse orientation. This photograph, from a cell fixed after 140 minutes recovery shows an increasing tendency for MTs to be transversely oriented.

Fig. 5.46. 140 minutes recovery: the MTs in this cell are as consistently transverse and well ordered as would be expected for a rapidly elongating internode (compare with Figs. 5.1 & 5.16).

Figs. 5.47 & 5.48. 200 and 220 minutes recovery: continued sampling of mature internodal cells at longer recovery times showed an increased dispersal of MTs about the transverse axis along with a decline in the number of MTs.

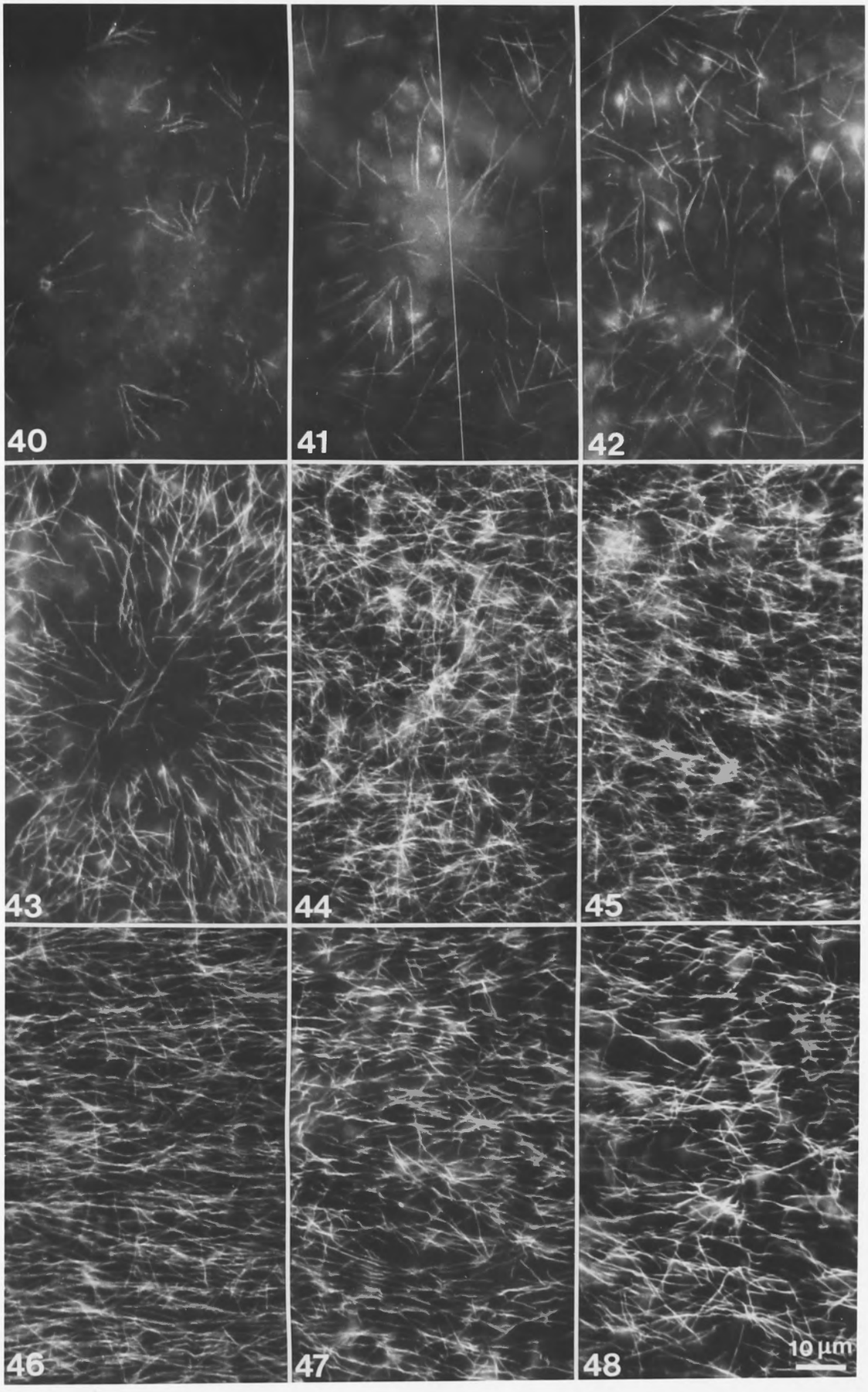
40
41
42
43
44
45
46
47
48
10 µm

Figs. 5.49 to 5.77. MT recovery in older, non-growing internodal cells from oryzalin-induced disassembly.

Figs. 5.49 to 5.51. 90 minutes recovery. MTs were first detected at discrete sites dispersed throughout the cortex. MTs at this stage are very short and generally contiguous with one or more MTs of similar length. In the lower part of Fig. 5.51, a more extensive branching assembly is visible.

Figs. 5.52 to 5.54. 100 minutes recovery: MTs arranged at sites in cortex. MTs rarely spread more than 90^{o} from individual focal points but assemblies themselves display no preferred orientation as illustrated in Fig. 5.52 where two nearby assemblies are 'pointed' in opposite directions.

Figs. 5.55 & 5.56. Herringbone-shaped assemblies of MTs at 160 minutes recovery. Individual assemblies retain their focussed appearance but MTs are no longer contiguous at a single site. Instead, some MTs 'branch' from what appear to be previously assembled MTs.

Fig. 5.57. Two fan-shaped branching assemblies at 160 minutes whose MTs are partially overlapping. Such a configuration could represent what would be expected for the the MT assemblies in Fig. 5.52 at later recovery time.

Figs. 5.58 & 5.59. Examples of branching assemblies which share a common focal point (160 minutes).

Fig. 5.60. Overlapping MTs from two nearby assemblies at 160 minutes recovery.

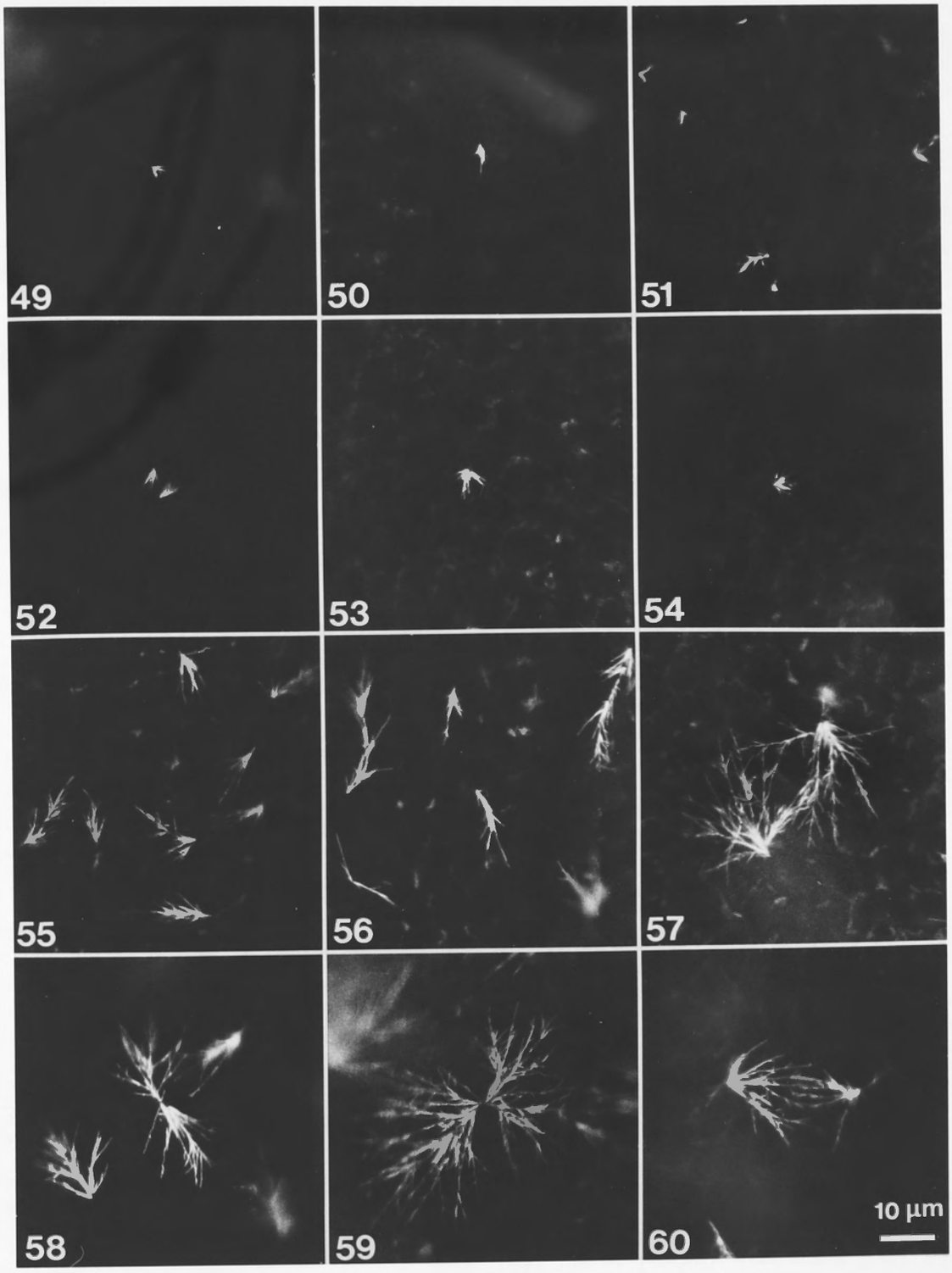
49
50
51
52
53
54
55
56
57
58
59
60
10 µm

Figs. 5.61 & 5.62. Spectacular star burst-shaped MT assemblies dispersed throughout the cortex (160 minutes recovery).

Figs. 5.63 to 5.68. 180 minutes recovery: The MT arrangement is variable but there is a general trend at this stage of recovery for assemblies to become disconnected.

Fig. 5.63. MT assemblies cover a greater area and component MTs appear to be of greater length than at earlier recovery times.

Fig. 5.64. MTs are no longer contiguous at a focal point suggesting that the earliest formed MTs have disassembled or become disconnected.

Figs. 5.65 to 5.68. These micrographs are all from the same cell and show various radial patterns of MT assembly.

Fig. 5.65. MTs radiate in every direction from the central region. MTs are still arranged in branching assemblies.

Fig. 5.66. Same field of view as Fig. 5.67 but lower plane of focus showing MTs projecting into the endoplasmic region.

Fig. 5.67. The same field of view as in Fig. 5.66 shows cortical MTs focussed around the same area from which MTs were seen at the lower plane of focus. The central area is mostly devoid of MTs.

Fig. 5.68. Another region of the same cell showing several branching assemblies positioned around an almost MT-free central zone.

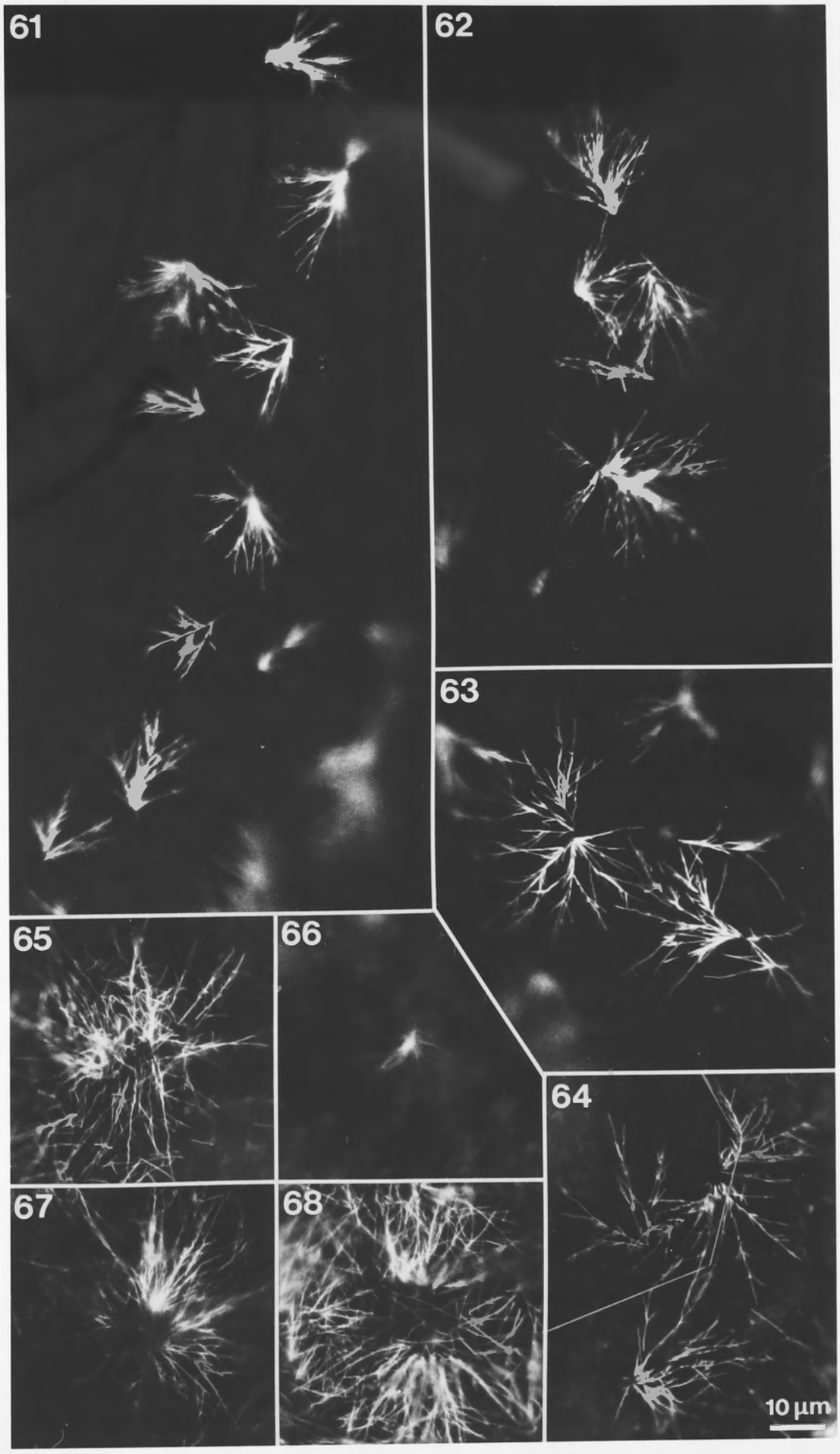
61
62
63
65
66
64
67
68
10 µm

Figs. 5.69 & 5.70. Two micrographs from different areas of the same cell (150 minutes recovery) showing very different MT patterns. In Fig. 5.69, the MTs are less abundant and mostly arranged in discrete branching assemblies. In contrast, the MTs in Fig. 5.70 are almost evenly dispersed and not as restricted to branching clusters. In addition to variation in organization within single cells, there was also considerable inconsistency in the degree of recovery between cells fixed at the same recovery times. Compare, for example the patterns of Figs. 5.55 and 5.70 which are from cells fixed after identical recovery times.

Figs. 5.71 to 5.77: 160, 170, 200, 220, 260, 270, 280 minutes respectively. MTs show increasingly even dispersal and branching assemblies become less conspicuous. At no stage during recovery do MTs show any preferred orientation.

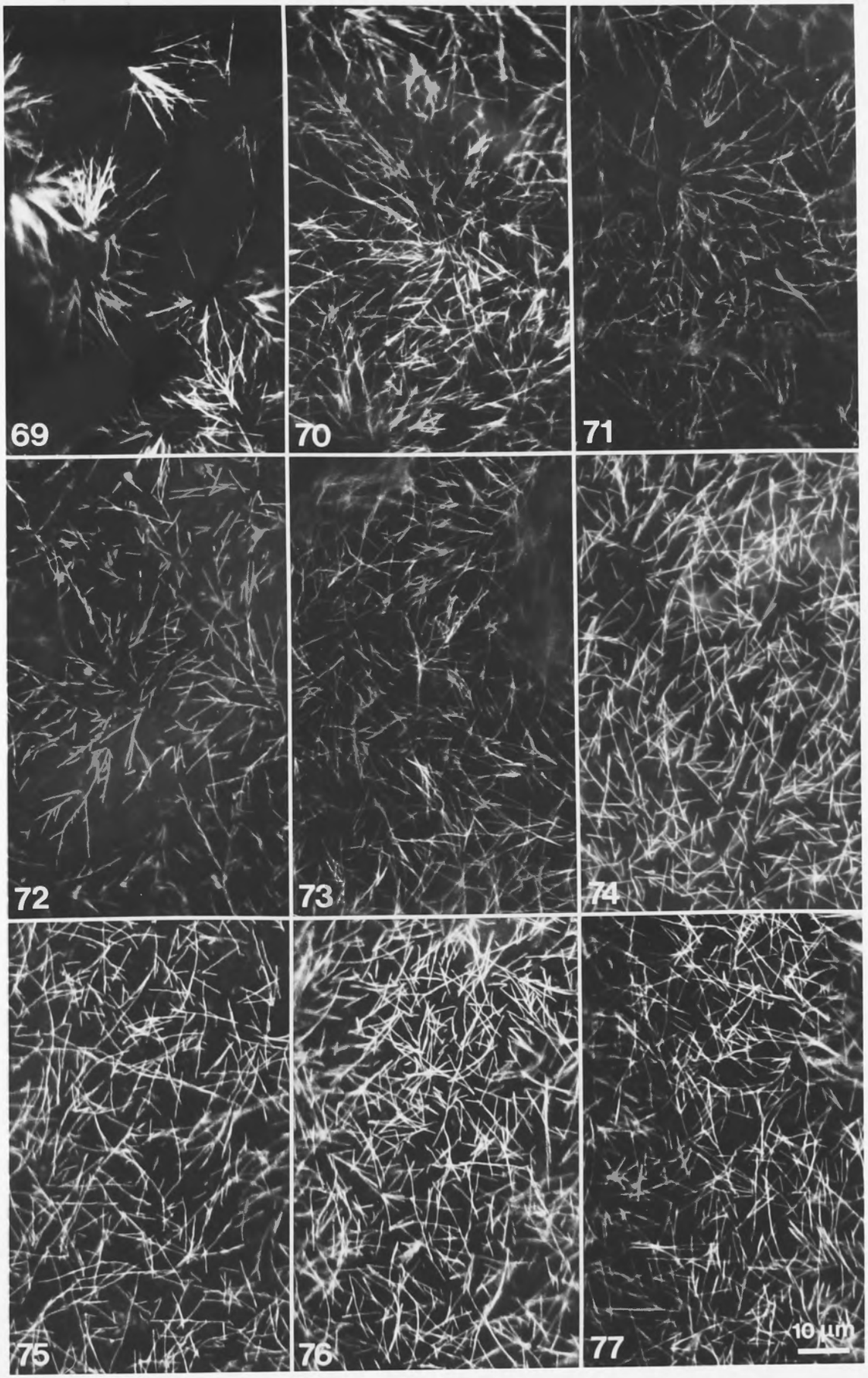
69
70
71
72
73
74
75
76
77
10 µm

Figs. 5.78 to 5.92. The occurence of MTs in the endoplasm of young, rapidly elongating internodal cells during recovery from oryzalin treatments. Cells were fixed after various recovery times and MT patterns in both the cortex and endoplasm analyzed. To avoid attenuation of fluorescence due to light absorption by the chloroplasts, single layer preparations were processed (as described in chapter 2) so that MTs could be viewed from alternate sides of the chloroplast layer. Thus better resolution of endoplasmic MTs was possible.

Figs. 5.78 to 5.80. Cortical (A) and endoplasmic (B) views of anti-tubulin-labelled internodal cells, fixed after various periods of recovery. In each case, the image shown in (A) is from approximately the same area as (B) but reversed because the cells have been viewed from opposite sides. C: Hoechst 33258-stained nuclei in the same field of view as B.

Fig. 5.78. 15 minutes recovery. No MTs detected in cortex (A) or in endoplasm (B). Nuclei (C) appear only faintly fluorescent with anti-tubulin immunofluorescence (B).

Fig. 5.79. After 50 minutes recovery, cortical MTs (A) are very abundant in the cortex (see also Fig. 5.8) but none are detected in the endoplasmic region (B). Bright patches of fluorescence on the nuclei (B) suggest tubulin-localization. These same sites are non-fluorescent with Hoechst staining (C) which indicates that either Hoechst labelling is impeded or the signal is blocked. This suggests the tubulin-specific sites are situated on the nuclear surface.

Figs. 5.80. 60 minutes recovery. As assembly in the cortex (A) reaches maximum levels (see Fig. 5.20), MTs are also detected on the endoplasmic side of the chloroplast layer (B). In this case, most of the MTs seen are aligned parallel to the subcotical actin cables but some are also associated with the endoplasmic nuclei (C). Some of the nuclei show a diffuse, tubulin-specific fluorescence.

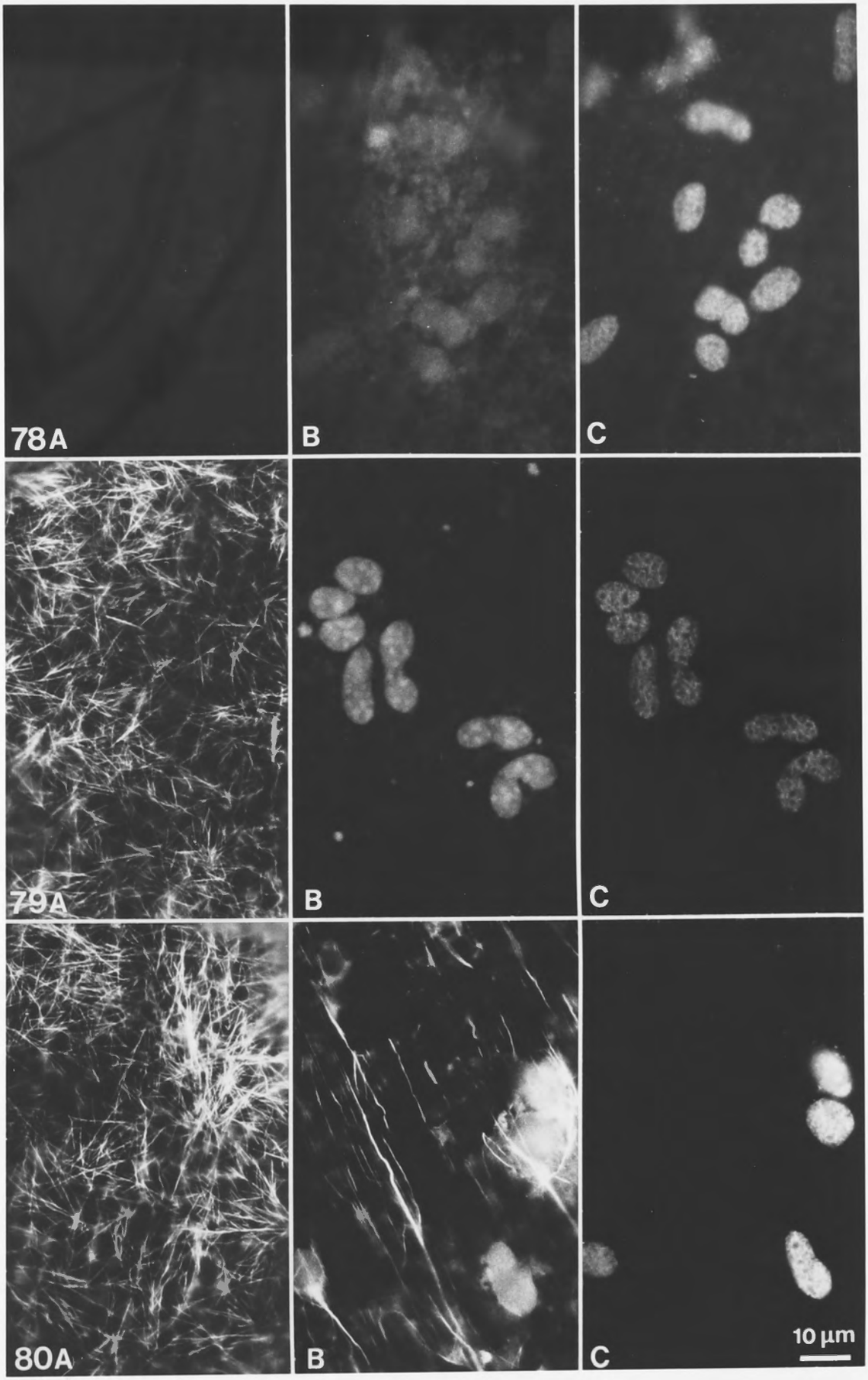
78A
B
C
79A
B
C
80A
B
C
10 µm

Figs. 5.81 to 5.85. Various arrangements of endoplasmic MTs observed at 60 minutes recovery.

Fig. 5.81. Through focus series showing (A) MTs against lower chloroplast layer (sub-cortex) and slightly deeper in the streaming endoplasm (B). In A, the MTs are mostly parallel to the chloroplast files. In B, MTs have formed a basket-like arrangement around one of the nuclei (located in the center of the photograph - compare with Hoechst-labelling pattern in C). Nuclei lack anti-tubulin-specific fluorescence.

Fig. 5.82. Through focus series showing (A) MTs against lower chloroplast layer (sub-cortex) and slightly deeper in the streaming endoplasm (B). As in previous figure, the subcortical MTs are mostly parallel to the chloroplast files but deeper in the endoplasm (B), they are oriented in a variety of patterns probably in association with nuclei.

Fig. 5.83. The majority of MTs in subcortical region are parallel to the chloroplast files and the actin cables but some divergence is sometimes observed.

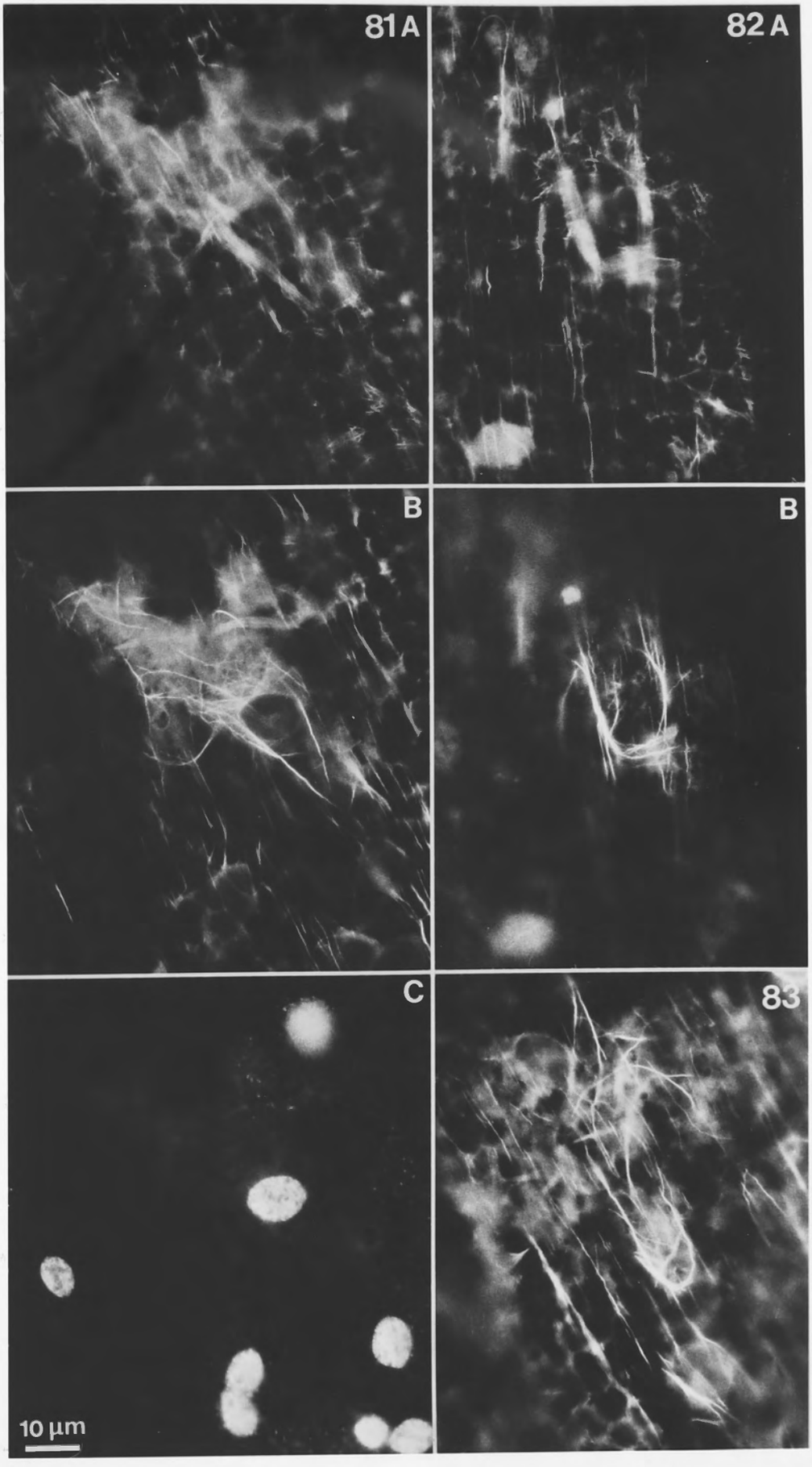
81 A
82 A
B
B
C
83
10 µm

Fig. 5.84. MTs associated with a large group of nuclei. **B:** MTs parallel to the chloroplast layer in the subcortical region. **B:** Deeper in the endoplasm, MTs form network around nuclei. **C:** Hoechst-labelling of nuclei.

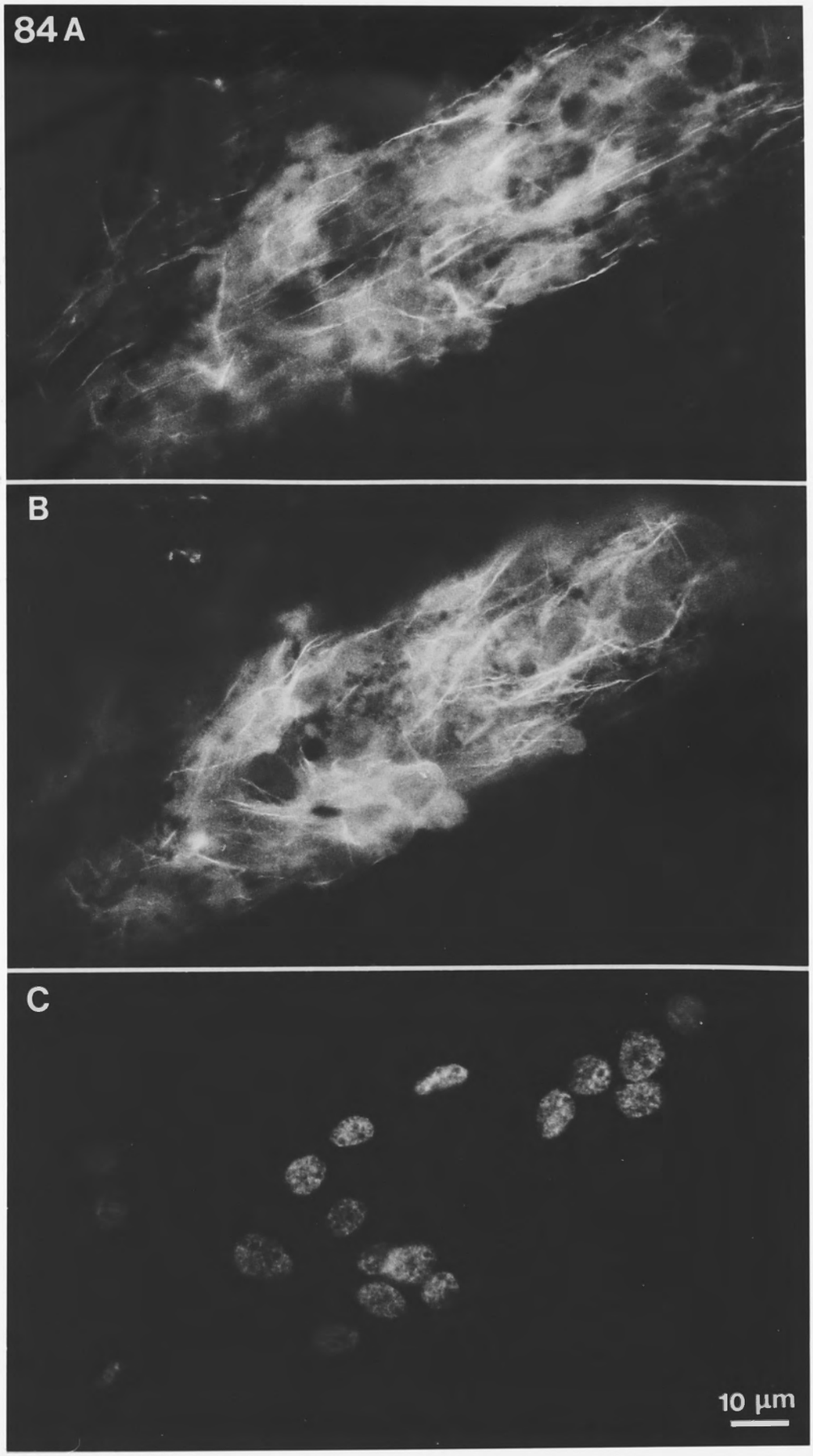
84 A
B
C
10 µm

Fig. 5.85. Network of MTs around a large group of nuclei. Slightly different planes of focus presented in A and B indicate depth of such an array. Comparing the MT pattern with the distribution of nuclei in C shows clearly the association of MTs with nuclei. The nuclei have no detectable anti-tubulin-specific fluorescence.

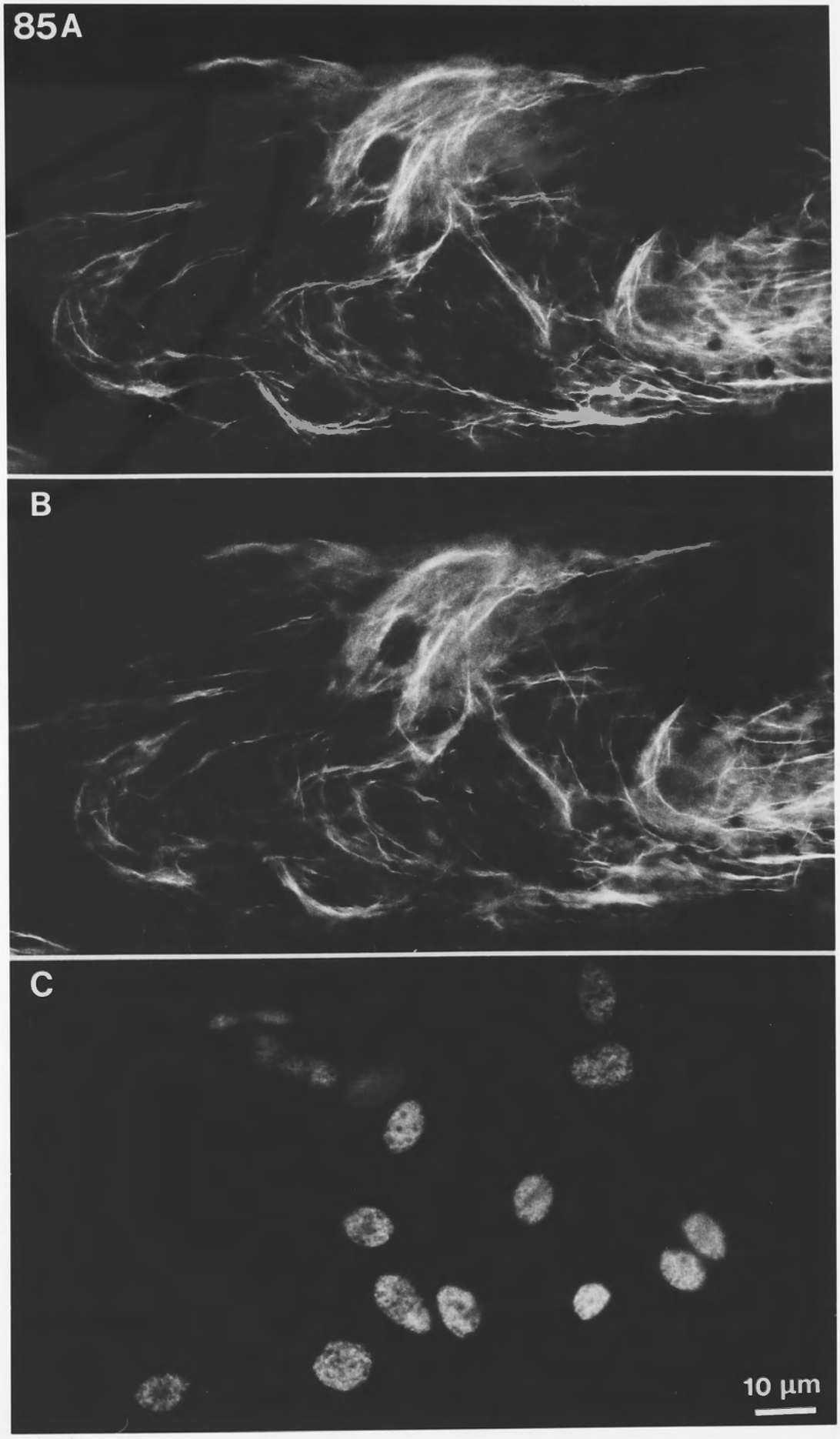
85A
B
C
10 µm

Fig. 5.86. Cortical MTs.

Fig. 5.87. Endoplasmic MTs in same cell as Fig. 5.86. MTs are still relatively long but are not arranged in networks around nuclei to the same extent as in cells sampled at 60 minutes.

Fig. 5.88. Subcortical MTs still present but are relatively short (compare with Figs. 5.80A and 5.83).

Fig. 5.89. Through focus series. A few MTs are seen close to the lower chloroplast layer (A and B) but only diffuse fluorescence is detected around nuclei (B and C).

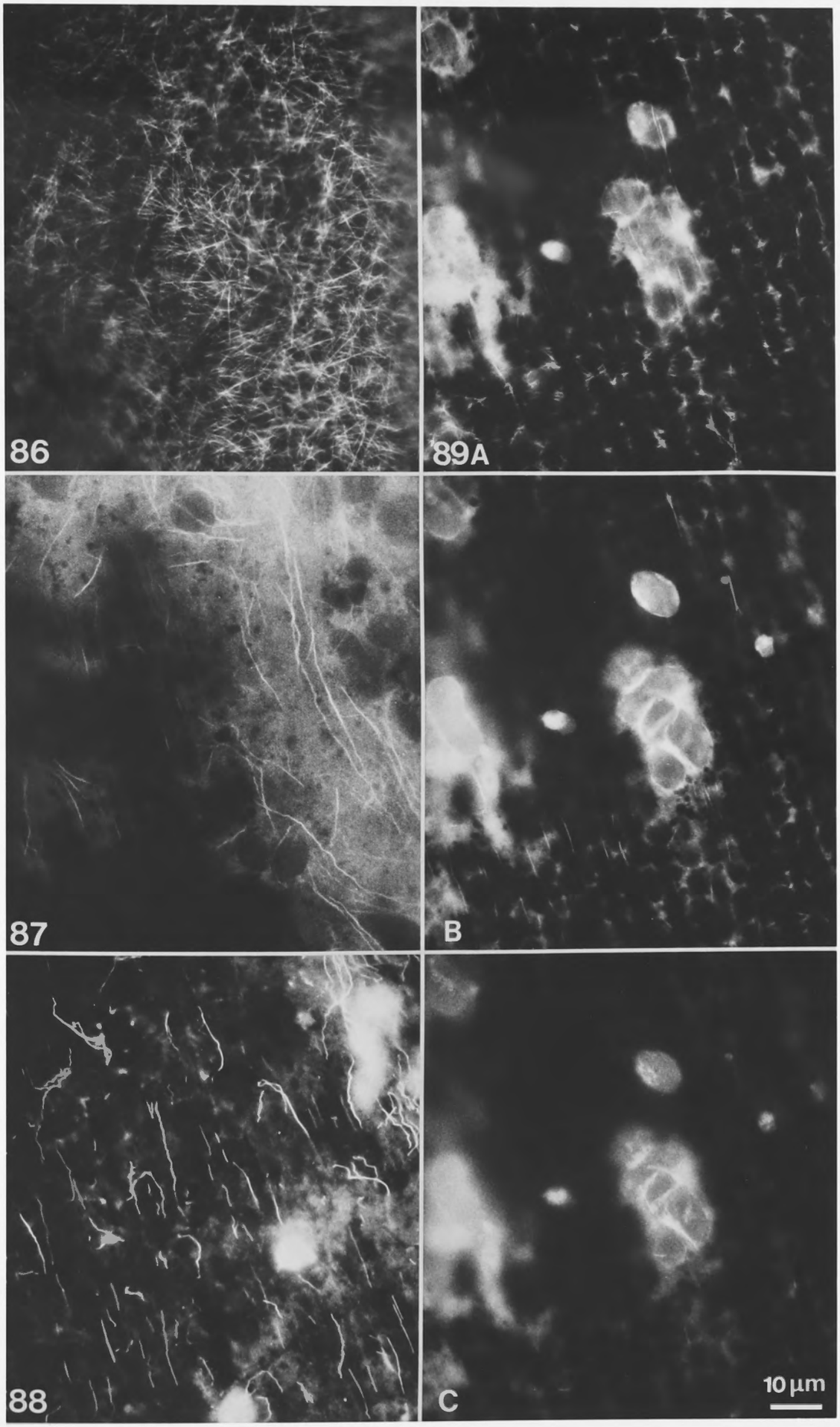
86
89A
87
B
88
C
10 µm

Figs. 5.90 to 5.92. Cortical (A) and endoplasmic (B) views of anti-tubulin-labelled internodal cells, fixed after various periods of recovery. In each case, the image shown in (A) is from approximately the same area as (B) but reversed because the cells have been viewed from opposite sides. **C:** Hoechst 33258-stained nuclei in the same field of view as B.

Fig. 5.90. 80 minutes recovery. Cortical MTs (A) are fully dispersed and starting to recover some degree of transverse order. No endoplasmic or subcortical MTs were found (B), but brightly fluorescent spots, similar to those detected at 50 minutes (Fig. 5.79B), were associated with the nuclei.

Figs. 5.91 & 5.92. 100 and 140 minutes recovery. Cortical MTs have resumed a mostly transverse order (A). In the endoplasm (B), nuclei display some patchy fluorescence but no MTs are detected.

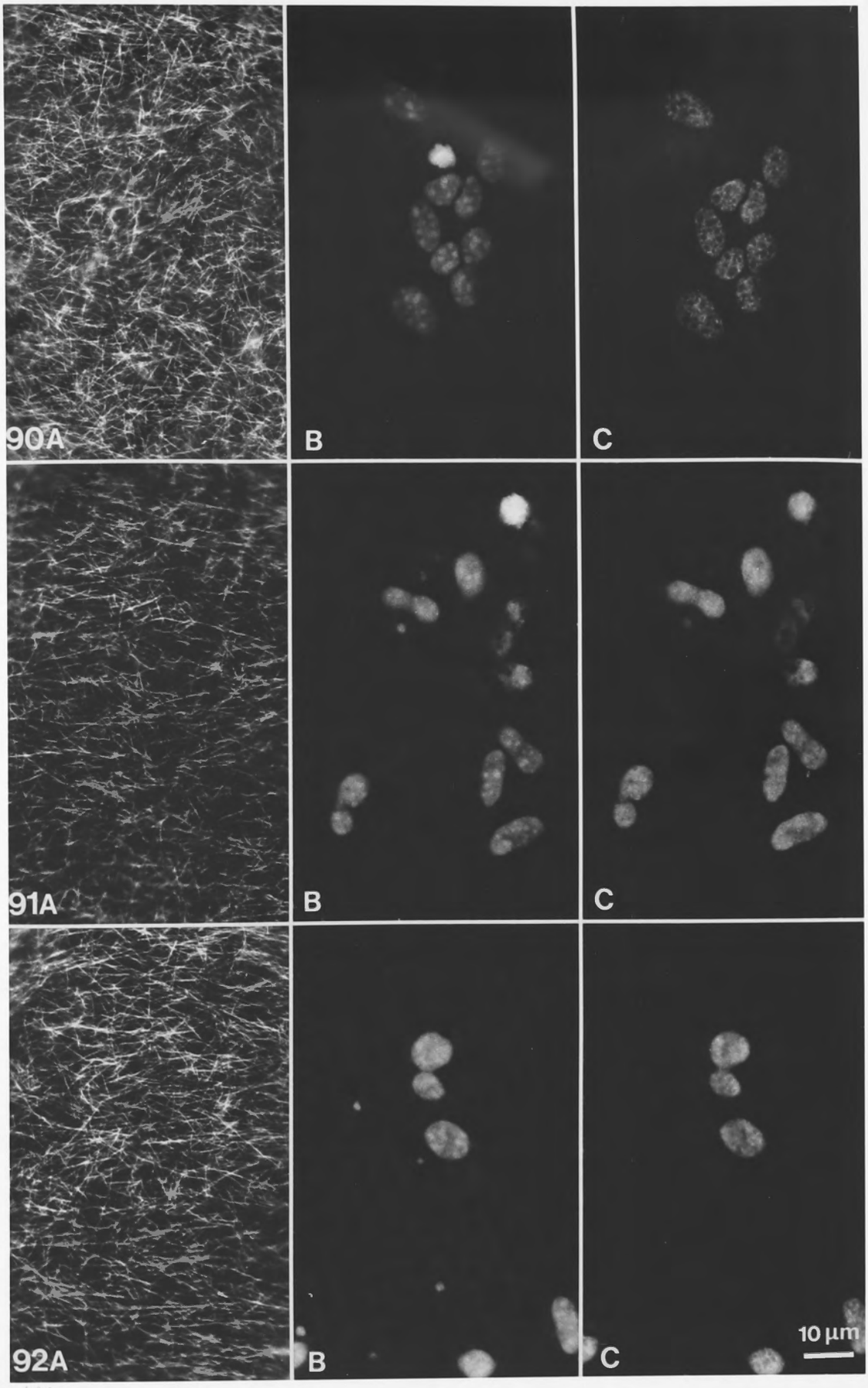
90A
B
C
91A
B
C
92A
B
C
10 µm

CHAPTER 6

IDENTIFICATION OF MICROTUBULE ASSEMBLY SITES IN *NITELLA* INTERNODAL CELLS USING A SEMI-*IN VITRO* ASSAY WITH PURIFIED EXOGENOUS TUBULIN

Some of the findings described in this chapter have been previously presented in a poster at the 4th International Congress of Cell Biology at Montreal in August 1988.

6.1 INTRODUCTION

Microtubule organizing center (MTOC) is a useful term for describing those sites within cells capable of regulating the behaviour of MTs. For clarification of what MTOCs can do and how they are believed to operate, a review of the section in Chapter 1 devoted to MTOCs (section 1.6) is recommended. MTOCs may be preferred assembly sites (*e.g.*, centrosomes, mitotic spindle pole bodies and basal body rootlets) but may also be the site of MT capture (*e.g.*, kinetochores). They frequently define the polarity and orientation of MTs and can regulate MT dynamics, stability, number, spatial distribution and length (for reviews see Tucker 1979; Brown *et al.* 1982; McIntosh 1983; Brinkley 1985). It is generally believed that MTOCs promote MT assembly by lowering the critical tubulin concentration or by facilitating the nucleation of MTs so that site specific MTs have a kinetic advantage over freely-assembled MTs. Alternatively, MTOCs are seen as MT stabilizers which can, through capping one end, prevent depolymerization.

MTOCs have been identified and studied in various ways. Any site in a cell from which MTs appear to radiate from or attach to is potentially a MTOC. Putative sites have been identified by observing the establishment of MT arrays at different stages of the cell cycle or after drug induced disassembly. A more reliable test of MT organizing capacity is the ability of a putative MTOC to stimulate MT assembly *in vitro*. In such assays, permeabilized cells or intact, isolated structures are supplied with purified, exogenous tubulin (Allen & Borisy 1974; Binder *et al.* 1975; Weisenberg & Rosenfeld 1975; Brinkley *et al.* 1981 a & b; Stearns & Brown 1981; Mitchison & Kirschner 1984a). If MTs are formed, the element is considered to have the capacity to nucleate MT assembly.

Some flagellated plant cells, in particular, the unicellular green algae *Chlamydomonas* (Goodenough & Weiss 1978) and *Polytomella* (Brown *et al.* 1976) have well defined MTOCs associated with the basal bodies. In other plant cells, which lack centrioles and a centrosomal region, MTOCs are less clearly

defined. Putative sites have been described at the nuclear envelope (De Mey *et al.* 1982, Clayton *et al.* 1985, Wick 1985, Ch. 5), along cell edges (Gunning *et al.* 1978), and at sites distributed throughout the cortical cytoplasm (Gunning 1980; Galatis *et al.* 1983; Falconer & Seagull 1986, 1987; Falconer *et al.* 1988; Hoffmann 1986; Hogetsu 1986; Cleary & Hardham 1988). MTOCs in non-flagellated plant cells are believed to be more numerous and more widely dispersed (Jackson & Doyle 1982) than those in animal cells. However, the existence of specific structures or pericentriolar-like material that could initiate MT assembly has not been conclusively demonstrated (Lloyd *et al.* 1985; Clayton *et al.* 1985; Wick 1985).

Immunofluorescence studies of MT distribution and orientation patterns in *Nitella* internodal cells (Ch. 2 & 3) have shown that whilst some endoplasmic MTs are closely associated with nuclei, cortical MTs normally show little evidence of association with any cell structures visible in the light microscope. Microtubule depolymerization/recovery experiments (Ch. 5) also showed an association of endoplasmic MTs with the with nuclei. Although this observation suggests that MTs may assemble at nuclei, it did not suggest that cortical MTs originate in the endoplasm (Ch. 5). Rather, before endoplasmic MTs appear, cortical MTs are seen at many discrete sites close to the plasma membrane. The reassembly process of cortical MTs can be divided into two distinct stages: (1) the initial appearance of single MTs and (2) the assembly of other MTs off (or very close to) the earlier formed MTs. Both stages could represent MTOC-initiated MT assembly. It is clearly of great interest to determine whether assembly-promoting material is associated with these sites.

Despite many years of plant MT research, there has not been any clear demonstration (apart from basal body MTOCs in flagellated algal cells) of sites in plant cells that can initiate MT assembly. The work described in this chapter provides a semi-*in vitro* experimental approach to defining structures in plant cells

that are capable of promoting the assembly of purified tubulin. The investigation involves the perfusion of *Nitella* internodal cells with tubulin purified from sheep brain tissue and subsequent evaluation of MT assembly with fluorescence microscopy.

6.2 MATERIALS AND METHODS

6.2.1 Plant Material and Culture Conditions

Shoots of *Nitella tasmanica* were cultured as described in Chapter 2. For all treatments, young, rapidly expanding internodal cells that were at least 1 cm in length were selected.

6.2.2 Tubulin Purification/ Biotinylation Method

Sheep brain tubulin was purified (with assistance from P.P. Jablonsky) by two cycles of assembly-disassembly and phosphocellulose chromatography using the method of Williams and Lee (1982). Purified tubulin was biotinylated using the method of Mitchison and Kirschner (1985a) except that biotinyl-aminocaproic acid N-hydroxysuccinimide ester was used. Biotinylated tubulin was subsequently purified by two cycles of assembly-disassembly. This method typically yielded tubulin at approximately 2 mg/ml (determined by P. P. Jablonsky). That biotinylation was successful was tested by electrophoresing a sample on an SDS gel, transferring to nitrocellulose and incubating with SA-horseradish peroxidase (F. Grolig's assistance). 200 µl aliquots were stored in 100mM PIPES buffer or MTAB (without GTP) at -80^{o}C for up to 6 weeks.

6.2.3 Perfusion Solutions

The standard solution used for the extraction of the central vacuole, tonoplast and some of the endoplasm prior to perfusion with purified tubulin was the 10^{-7}M free Ca^{2+} ATP-free solution (PS) of Williamson (1975) described in Chapter 2. For the promotion of MT assembly *in vitro*, a solution containing 2 M glycerol, 100 mM piperazine-N,N'-bis(2-ethanesulfonic acid) (PIPES) buffer with 2 mM ethyleneglycol-bis-(β-amino-ethyl ether)N,N,N',N'-tetraacetic acid (EGTA), 5 mM $MgCl_2$ and 1 mM GTP, pH 6.8, was used. Whilst this buffer, known as MT assembly buffer or MTAB, also promoted the assembly of MTs from purified

tubulin in perfusion, the cells were better preserved when the buffer was supplemented with 70 mM KCl, 1.48 mM $CaCl_2$ and 200 mM sucrose and the concentration of EGTA was increased to 5 mM [essentially the 10^{-7}M free Ca^{2+} ATP-free solution (PS) using 100 mM PIPES buffer (instead of 10 mM) and supplemented with 2 M glycerol and 1 mM GTP]. This solution, hereafter referred to as MTAB-2, promoted MT assembly and reduced the tendency for cells to become plasmolysed. Other experiments utilized a buffer that would not promote spontaneous assembly of MTs. This non-assembly buffer (NAB) consisted simply of 100 mM PIPES buffer with 200 mM sucrose and 1 mM GTP.

6.2.4 *In Vitro* Assays of Assembly-Promoting Capacity of Perfusion Solutions

Purified tubulin, supplied in MTAB and NAB was incubated directly on glass coverslips [coated with 2 µl poly- L-lysine; MW 306 kD (Sigma)] for 20 to 30 minutes at room temperature. Samples were fixed in 1% glutaraldehyde for 5 minutes, washed in PBS (see Ch 2) and labelled with SA-PE (see section 6.2.7) or processed for standard anti-tubulin immunofluorescence (Ch. 2, section 2.2.7). A turbidimetry assay (carried out by P. P. Jablonsky) measured the absorbance increase at 350 nm for 1ml reaction mixtures containing 1.2 to 2.0 $mg.ml^{-3}$ purified tubulin in MTAB or NAB. Reaction mixtures were kept on ice prior to the assay and tubulin polymerization initiated by incubation at 37°C after which absorbance was monitored continuously.

6.2.5 Microtubule Disassembly and Removal of Endogenous Microtubule Proteins

To follow the assembly of MTs from purified tubulin in the absence of any endogenous tubulin and associated proteins, cells were first treated with 10 µM oryzalin for 20 minutes (as described in Chapter 5) to depolymerize existing MTs and then perfused (the standard vacuolar perfusion technique described in Chapter 2, section 2.2.4) to wash out the soluble MT proteins. Although in some

experiments a MT destabilizing buffer containing high Ca^{2+} was used to ensure disassembly of all MTs, this step was found to be unecessary. When cells that had been perfused for 2 minutes with the standard 10^{-7} M ATP-free perfusion solution were incubated with tubulin-free MTAB, no MTs were detected. Thus, a 5 minute perfusion with either PS, MTAB or MTAB-2 after oryzalin treatment was sufficient to remove the endogenous MT proteins.

6.2.6 Perfusion and Fixation

After initial perfusion to remove vacuole, tonoplast and some of the endoplasm, cells were perfused with freshly thawed, purified tubulin in appropriate buffer solutions. For all experiments, GTP was added just prior to perfusion. Rather than continuous perfusion, the tubulin solutions were allowed to perfuse only to displace the previous solution. The height of liquid in each perfusion well was then adjusted to stop the flow of perfused solution. After incubating for specified periods of time, cells were briefly perfused (approx. 2 min.) with tubulin-free buffer in order to wash out unpolymerized tubulin and then fixed with 1% glutaraldehyde in the same buffer.

6.2.7 Visualization of Assembled Microtubules Using Fluorescence Microscopy

Fluorescence microscopy methods are described in Chapter 2, section 2.2.7. Since the purified tubulin that was supplied to the cells had been biotinylated, fluorescently-labelled streptavidin (SA) could be used to localize the assembled MTs. For this purpose, SA conjugated to both FITC (BIOMEDA F72-509) and phycoerythrin (PE) (Becton Dickinson 9023) was successful. The presence of residual endogenous MTs could be verified using standard anti-tubulin immunofluorescence (described in Ch 2, section 2.2.6). In experiments where oryzalin disassembly was not carried out prior to perfusion with purified tubulin,

the two populations of MTs could be distiguished with double labelling techniques (see Ch 2, section 2.2.7). MTs containing biotinylated tubulin were localized with SA-PE whereas all MTs could be identified with anti-tubulin and localized with a secondary antibody conjugated with FITC. Alternatively, biotinylated MTs were localized with SA-FITC and a secondary antibody, conjugated with PE was used to label the total set of MTs. The DNA-specific probe Hoechst 33258 was used exactly as described in Chapter 2 (section 2.2.7) for labelling nuclei.

6.3 RESULTS

The major achievement of this investigation was the successful application of a semi-*in vitro* tubulin assembly assay utilizing purified tubulin in an assembly-incompetent buffer. Other observations, regarding MT behaviour in assembly-promoting buffers, are also reported, but they should not obscure the primary objective of the research, which was to verify the existence of sites that are capable of initiating MT assembly. The results of this latter investigation, on which major emphasis should be placed, are described in section 6.3.6.

6.3.1 Effects of Microtubule Assembly Buffer on Existing Cortical Microtubules

Incubation of perfused internodal cells not exposed to oryzalin with MTAB prevented the disassembly of the cortical MT array for relatively long periods of time. Although such treatments did not cause any detectable change in the number of MTs, their arrangement was altered considerably (Figs. 6.1 to 6.4). Whereas cortical MTs are normally seen only in one narrow plane of focus near the plasma membrane, introduction of MTAB into the cells caused MTs to become distributed throughout the cortex. Through focussing was now required to observe all the MTs (see Fig. 6.1). In addition, the predominantly transverse orientation of MTs, expected in such rapidly growing cells, was less apparent after perfusion with MTAB. In some cases, the MT arrangement resembled that of non-growing cells (Fig. 6.2) with random MT orientation patterns except that the array was now also noticeably three-dimensional. In some cases, MTs were locally aligned in non-transverse directions (Fig. 6.3), possibly due to flow of buffer through the cell. Another feature of prolonged incubation of internodal cells with MTAB was the intense labelling of endoplasmic nuclei after anti-tubulin immunofluorescence (Fig. 6.4). This buffer clearly favored the maintenance of MTs but not their highly ordered arrangement.

6.3.2 *In Vitro* Microtubule Assembly

To test the ability of the purified tubulin to polymerize in the chosen assembly buffer, biotinylated tubulin in MTAB with 1 mM GTP was applied to poly-L-lysine[1] -coated coverslips and incubated for up to 30 minutes. After fixation in 1% glutaraldehyde and labelling with SA-PE, a fine meshwork of filaments, presumed to be MTs, was observed by fluorescence microscopy (Fig. 6.5). Anti-tubulin immunofluorecence gave identical labelling patterns. This experiment verified that the assembly buffer would support spontaneous MT assembly at that tubulin concentration. In contrast, biotinylated tubulin did not produce MTs under identical conditions when diluted in NAB with 1 mM GTP. A turbidimetric assay of MT assembly conducted by P. P. Jablonsky verified that tubulin polymerization occurred in MTAB but not in NAB. There was a substantial increase in absorbance when biotinylated and purified tubulin was incubated in MTAB but no significant change in NAB.

6.3.3 Microtubule Assembly Patterns in Cells Perfused with Purified Tubulin in Assembly-Promoting Buffer

In order to observe assembly patterns of purified tubulin in internodal cells in the presence of an assembly-promoting buffer, oryzalin-treated cells were perfused and incubated for up to 90 minutes with biotinylated tubulin in MTAB. SA-PE was used for the detection of MTs assembled from biotinylated tubulin. GTP was found to be essential for MT assembly. Assembly patterns varied but MTs were most abundant in the endoplasm (Figs. 6.6 to 6.10). Cells incubated for 20 minutes showed fairly extensive arrays of MTs. These contained MTs of highly variable

---

1. Poly-L-lysine is known to promote tubulin polymerization but apparently only in the presence of MAPs (Erickson & Voter 1976; Murphy *et al.* 1977). Since MAP-free tubulin was used, poly-L-lysine-induced polymerization should not be a problem.

orientations (Figs. 6.6 to 6.8). Although some "free" MTs were observed, MTs associated with nuclei seemed to be predominant. Nuclei generally had a diffuse fluorescence and almost invariably were surrounded by some short MTs (Figs. 6.9 & 6.10).

MTs were rarely detected in the cortex and only when cells were incubated for over 1 hour. These MTs generally did not resemble typical *Nitella* cortical MTs (Figs. 6.11 & 6.13); they tended to appear as rather short thick filamentous structures. After 1 hour incubation, nuclei still had a diffuse fluorescence but endoplasmic MTs were scarce (Figs. 6.12 to 6.14).

6.3.4 Effects of ATP on Microtubule Assembly

Cytoplasmic streaming, a ubiquitous property of living internodal cells, can be re-induced in perfused *Chara* internodes when ATP is added to the perfusion solution (Williamson 1975). ATP was therefore included in the MTAB-2 to simulate *in vivo* conditions during incubation with purified brain tubulin. Under these conditions, cytoplasmic streaming was maintained at a very slow rate (probably due to the high viscosity of the glycerol in the buffer) and very unusual networks of MTs were formed. In some cases when nuclei were lost (presumably by streaming) from the perfused cells, MT assemblies were still observed in the endoplasm (Fig. 6.19) and also to some extent in the cortex (Fig. 6.18). This suggests that nuclei are not required for MT assembly in MTAB. MTs formed tightly-organized, net-like arrays. Where nuclei remained in the cells, MT networks were generally more extensive but did not associate exclusively with nuclei.

6.3.5 Assembly of Microtubules from Purified Tubulin Without Removal of the Existing Array

Although most of the experiments performed in this study involved the initial disassembly of MTs and subsequent removal of the soluble MT proteins by perfusion, it was also of interest to see how assembly of MTs from purified tubulin would occur if the original array was still present. It was also thought that the introduced tubulin might co-assemble with the existing MTs. To minimize disassembly of the existing MTs during the incubation of the cell with biotinylated tubulin, the purified tubulin was introduced in MTAB-2 after a very short initial perfusion. By double labelling, it was possible to distinguish the MTs that contained biotin-tagged tubulin molecules from the endogenous MT population and thereby identify sites of MT assembly.

After such treatments, MTs were observed in the cortex but there was no labelling with SA-FITC to suggest that these MTs comprised biotinylated tubulin. Rather they appeared to include only non-biotinylated tubulin (Fig. 6.15d). On the other hand, MTs that were observed in the endoplasm were apparently assembled from the purified, biotinylated tubulin introduced by perfusion (Fig. 6.15a,b & c). It therefore seems that although the purified tubulin was able to assemble into MTs, it probably did not associate with the original MTs nor did it undergo assembly in the cortex. The MTs that did assemble in the endoplasm under these conditions tended to have a strong association with nuclei (Fig. 6.16) and MTs containing biotinylated tubulin often extended from the periphery of nuclei. The surface of nuclei also tended to label strongly with SA-fluorochromes after incubation with biotinylated tubulin, even when no MTs were detected (Fig. 6.17).

6.3.6 Assembly of Microtubules in Internodal Cells in a Non-Assembly Buffer

The most important part of this study involved the investigation of MT assembly after perfusion of purified tubulin in a buffer that would not, on its own,

promote MT assembly. When purified tubulin was incubated *in vitro* in NAB (see section 6.3.2) MT assembly did not occur. In contrast, the perfusion of such a solution into internodal cells resulted in considerable MT assembly in both the endoplasm and cortex especially when cells were perfused for long periods of time (*i.e.*, up to 2 hours). The location and configuration of the MTs assembled depended to a large extent on the degree to which the chloroplast array remained intact. Normally MTs were only observed in the endoplasm. These either formed extensive, swirling bundles of MTs (Figs. 6.25 & 6.26) that had no apparent association with a particular structure or else they formed interconnected networks of MTs running between nuclei (Figs. 6.28 & 6.29). Occasionally, MT clusters centered at the chloroplast layer extended partially into the cortex (Figs. 6.27 & 6.30).

When the chloroplast layer was disrupted by rapid initial flow of PS, MT assembly in the cortex was usually detected. In cases where complete removal of large areas of chloroplasts occurred, MTs of unusual, wiggly form that were apparently appressed to the plasma membrane were found (Figs. 6.21 to 6.23). Where only partial removal of the chloroplast array was achieved, massive MT assembly occurred between the plasma membrane and the chloroplast layer (Figs. 6.24 & 6.27). Occasionally some of these MTs extended from beneath the chloroplast layer into the chloroplast-free zones (Figs. 6.24 & 6.27).

In some cases, large numbers of MTs appeared to radiate out from foci (Figs. 6.31a, 6.32a & 6.33a). Such foci were fairly evenly distributed throughout the cortex but almost invariably were located near a site of damage to the chloroplast layer (see Figs. 6.31b, 6.32b & 6.33b). MTs that assembled at such sites usually did not show any sign of preferred orientation. Occasional realignment of MTs, shown, for example in Fig. 6.31, may have been simply caused by the flow of perfusion solution through the cell (possibly getting under the chloroplast layer in some areas).

6.3.7 Perinuclear Fluorescence

Strong perinuclear fluorescence was commonly observed after perfusion with biotinylated tubulin (see Figs. 6.9, 6.10, 6.12 to 14, 6.16, 6.17 & 6.29). Whether this labelling was due to the affinity of the nuclei for tubulin or biotin was examined in two ways. Firstly, cells were perfused with purified, non-biotinylated tubulin. Anti-tubulin immunofluorescence showed strong (qualitatively stronger than normal perinuclear fluorescence observed with anti-tubulin immunofluorescence) labelling of nuclei suggesting binding of tubulin. Secondly, internodal cells were perfused with a biotinylated, non-specific antibody (to goat IgG) followed by SA-PE. While the resulting nuclear fluorescence was considerably less than that seen after incubation with biotinylated tubulin, the nuclei showed fluorescence above that of SA-PE only controls. It is therefore possible that at least some of the binding of biotinylated tubulin to the nuclei was due to nuclear affinity for biotin. This investigation was merely preliminary; more exhaustive experiments will be applied to determine the exact nature of both tubulin and biotin binding to the nucleus.

6.4 DISCUSSION

6.4.1 Experimental Objectives

The principal objective of this investigation was to identify MT assembly sites by perfusing cells with purified exogenous tubulin. The experiments were of two types: those utilizing MT assembly buffers (MTAB & MTAB-2) and those utilizing a buffer that would not on its own, support MT assembly (NAB). Only those experiments with NAB can be considered truly diagnostic for MT assembly sites since MTAB may also support some spontaneous assembly.

The experimental approach is of course limited in the extent to which it can simulate *in vivo* assembly conditions. Soluble proteins that normally bind to MTs or MTOCs are probably removed from the cell during perfusion, especially after the endogenous MTs have been disassembled with drug treatments. Although MT assembly should still occur at intact assembly sites, their arrangement is unlikely to resemble the *in vivo* assembly pattern. Biotinylation of the purified tubulin may also introduce abnormal assembly behaviour and biotin itself may have binding properties that affect the distribution of the tubulin subunits. There was, for example, some suggestion that biotin has an affinity for the surface of nuclei that is independent of tubulin's apparent affinity for the same site.

6.4.2 Selection of Suitable Assembly Buffers

Vacuolar perfusion was used for the introduction of purified exogenous tubulin to internodal cells. This technique removes the tonoplast and central vacuole (Smith & Walker 1981; Williamson 1975) along with proteases (Moriasu & Tazawa 1986) so that the contents of the endoplasm can be quickly replaced with a buffer containing the purified tubulin. The buffers in which the exogenous tubulin was supplied to the internodal cells were similar in composition to the 10^{-7}M free Ca^{2+} ATP-free solution (PS) of Williamson (1975) which prevents plasmolysis, causes minimal distortion to the components of the cortical cytoplasm

(Williamson 1975, 1985) and maintains the plasma membrane in a functional condition (Smith & Walker 1981). GTP (1 mM), which is necessary for MT polymerization (Weisenberg *et al.* 1968; Jameson & Caplow 1980; Carlier *et al.* 1981, 1987; Schilstra *et al.* 1987; Hesse *et al.* 1987; Martin & Bayley 1987) was included in the buffer solutions.

6.4.3 Stability of Endogenous Cortical Microtubule Array in Assembly Buffer

By modifying the perfusion solution, disassembly of the cortical MT array can be delayed considerably. In Chapter 2 it was shown that extended perfusion with the standard 10^{-7}M free Ca^{2+} ATP-free solution (PS) led to almost complete loss of MTs within 20 minutes. NAB causes a similar effect. In contrast, MT disassembly and loss is greatly impeded when MTAB (or MTAB-2) is used instead of PS or NAB. This observation is important because it indicates that the MTAB favors MT stability in perfused cells for considerable lengths of time and it therefore should be useful for stabilizing the MTs that are assembled from an exogenous source of tubulin.

Although MTAB clearly delayed disassembly of endogenous MTs, it did not maintain their transverse arrangement in the cortex. This observation is extremely interesting with regard to MT organization. Under *in vivo* conditions, cortical MTs are (apparently) constrained to lie close to the plasma membrane and in elongating cells to be oriented predominantly transverse to the major axis of expansion. In Chapter 3 it was suggested that this transverse orientation might result from selective disassembly of non-transverse MTs. By perfusing cells with MTAB, the control over MT orientation was apparently lost and MTs became distributed throughout the cortex and oriented in many directions. This effect might be attributed to the MT-stabilizing properties of MTAB. Thus, the idea that MT arrangement relies on variable stability based in part on location (*i.e.* close to the

plasma membrane) and orientation is supported. By permitting unconditional stability, MT order seems to be lost.

There are, however, other plausible explanations for the change in MT orientation that was observed. If the orienting mechanism is influenced by the rate of expansion, as suggested in previous chapters, perfusion - by eliminating turgor pressure - would eliminate a necessary cue for transverse MT alignment. Perfusion undoubtedly depletes the cell of factors such as MAPs that are likely to be involved in MT orientation. If transverse alignment relies on the formation of cross-bridges of MTs with each other and to the plasma membrane, perfusion with MTAB could cause breakdown of such linkages. If ATP is required for cross-bridge formation (McIntosh 1973; Gibbons 1977; Sale & Satir 1977), its removal from the cell by perfusion could result in rapid loss of MT order. Alternatively, glycerol, which was present in the assembly buffer may have caused disruption of MT order just as it did (albeit at much higher concentrations) when applied to internodal cells in the form of a stabilizing buffer in Chapter 2. Glycerol is known to alter membrane properties (Willison 1975) so may have disrupted normal associations between MTs and the plasma membrane.

Whether such changes in MT distribution and orientation are due to realignment of stabilized MTs or because new MTs are assembled from the tubulin pool in other locations is uncertain. Glycerol can promote spontaneous MT assembly (Mitchison & Kirschner 1984b; Rothwell *et al.* 1986; Kristofferson *et al.* 1986) in the absence of MAPs (Na & Timasheff 1981), but the assembly products are frequently abnormal (Matsumura & Hayashi 1976). Glycerol acts primarily as a stabilizer rather than a promoter of MT assembly since it decreases the rate of tubulin association and dissociation but does not lower the critical tubulin concentration (Keates 1980). It therefore seems more likely that MTAB would favor the process of MT reorientation over disassembly/ reassembly.

6.4.4 The Nature of Putative Microtubule Assembly Sites in Internodal Cells

The observation that purified tubulin can assemble into MTs when perfused into internodal cells of *Nitella* - even in the presence of a buffer that would not, on its own, support MT assembly - suggests that there are elements present which favor MT initiation. The ability to promote the assembly of purified brain tubulin under conditions it would not otherwise be able to has been considered diagnostic for MTOCs (Allen & Borisy 1974; Binder *et al.* 1975; Weisenberg & Rosenfeld 1975; Brinkley *et al.* 1981 a & b; Stearns & Brown 1981; Mitchison & Kirschner 1984a). For the first time, such activity has been demonstrated in a non-flagellated plant cell.

The MTs formed after perfusion of purified brain tubulin in NAB are not merely randomly assembled but appear to be arranged in specific locations, especially around the nuclei in the endoplasm and also from sites in the cortex. These resemble the same sites deduced from oryzalin recovery experiments (Ch. 5) to be the location of MT assembly. It will be important to establish with certainty that the cortical sites in the perfused cell cortex are the same as cortical assembly sites in oryzalin-recovering cells.

Characterization of the assembly-promoting elements located in internodal cells is now a realistic goal. It could be achieved by adding back to the tubulin solution various cytoplasmic fractions isolated from internodal cells to see if specific proteins can produce assembly patterns that more closely resemble those of recovering cells. Similar use of common agents of tubulin assembly could also be valuable. In the present investigation, for example, the inclusion of ATP in assembly buffer caused net-like arrays to be formed. This may be significant, with regard to intertubule crosslinking which may require energy in the form of ATP (McIntosh 1973; Gibbons 1977; Sale & Satir 1977; Green 1980).

It is possible that the putative MTOCs of *Nitella* internodal cells favor MT assembly in a manner that is similar to other MTOCs, that is, by lowering the

critical tubulin concentration necessary for MT initiation, (De Brabander *et al.* 1980), by capping of the slow growing end of MTs (Euteneuer & McIntosh 1981a) or by conferring a kinetic advantage to MTs by promoting nucleation (Mitchison & Kirschner 1984a). Although the putative assembly sites have not yet been identified and characterized, it is now almost certain that specialized elements exist even if they are not associated with specific cell structures. In this regard, it is interesting that some animal cells have peripherally-organized MTs that do not associate with classic MTOCs. Some examples include the MTs of nerve axons (Bray & Bunge 1981; Sasaki *et al.* 1983) and the cortical MTs of certain insect epidermal cells which in many respects resemble the cortical arrays of plant cells (Tucker 1979; Mogensen & Tucker 1987). The recent demonstration that MT assembly and organization can occur in centrosome-free fragments of teleost melanophores (McNiven & Porter 1988) is convincing evidence that non-centralized MT assembly is possible. The fact that MT assembly at centrosomes appears to be initiated from pericentriolar material rather than from centrioles (Gould & Borisy 1977; Berns & Richardson 1977) suggests, in any case, that the well defined MTOCs may merely represent the sites at which nucleating elements are anchored.

6.4.5 Patterns of Microtubule Assembly at Sites in the Endoplasm

Endoplasmic MTs were most frequently associated with nuclei, either clustered around single nuclei or forming extensive, interconnected arrays incorporating one or more nuclei. Diffuse fluorescent labelling of nuclei indicated that there was an affinity for tubulin. Non-biotinylated control perfusions suggested that most of this fluorescence could not be attributed to a specificity of the nucleus for the biotin attached to tubulin subunits. Prolonged incubation of internodal cells with MTAB without exogenous tubulin also promoted intense labelling of nuclei (see Fig. 6.4). This observation suggests that the endogenous

tubulin may also have an affinity for the surface of nuclei. Such affinity for tubulin supports the idea that the nuclear surface may also promote MT assembly. That the nucleus is a site for MT assembly in plant cells has already been suggested (Bajer & Molè-Bajer 1986b; Bakhuizen *et al.* 1985; De Mey *et al.* 1982; Schmit *et al.* 1983; Dickinson & Sheldon 1984; Clayton *et al.* 1985; Wick & Duniec 1984; Wick 1985; Ch 5). The results of this perfusion assay provide further supporting evidence.

MTs without apparent organizing loci were also observed in the endoplasm even when NAB was applied. These arrays, which in some cases formed extensive swirling bundles of MTs (*e.g.* Fig. 6.25 & 6.26) may have been nucleated by non-nuclear sites that are not visible with light microscopy. Alternatively they might have assembled at sites that subsequently became detached from the nuclear surface. These assemblies of MTs were unlike those seen in the endoplasm of untreated cells in that they often displayed MT bundling and branching. Such unusual characteristics are not unexpected. The properties of MTs assembled from purified exogenous tubulin could reflect differences in tubulin isoforms, the depletion or removal of endogenous MAPs or other assembly agents from the cell or a change in physiological conditions, all of which can affect the morphology of MTs (Brinkley 1985).

6.4.6 Limitations of Microtubule Assembly in the Cortex

MT assembly from purified tubulin in NAB was not detected in the cortical cytoplasm unless some disruption of the chloroplast layer had taken place. The abundance of MTs between the chloroplast layer and the plasma membrane suggests that this location is favorable for MT assembly and stability. By comparison, relatively few MTs were observed if the chloroplast layer was removed completely.

Why does the assembly of MTs in the cortex from purified brain tubulin take place only when the chloroplast layer is disrupted? It may be that chloroplasts collapse against the plasmalemma when the soluble cortical material is extracted by perfusion. Partial disruption to the chloroplast layer might reintroduce the space necessary for MT assembly. Alternatively, localized damage might stimulate tubulin assembly in the same way that localized damage might induce a wound response *in vivo*.

6.4.6 Future Experiments

The assembly of MTs from purified tubulin in the internodal cells of *Nitella* demonstrates the existence of assembly-promoting factors. This represents a major achievement in the understanding of MT organization in plant cells. To refine the data described in this investigation, it will be necessary to:

(1) define the nature of biotin labelling of nuclei and repeat the perfusion assembly experiment with non-biotinylated tubulin,

(2) add inactive competitor protein to compete for nuclear assembly sites,

(3) examine the apparent correlation between chloroplast disruption and stimulation of cortical MT assembly, possibly by wounding living cells,

(4) establish whether the cortical assembly sites seen in perfused cells are the same as those induced by oryzalin treatments,

(5) characterize the structural aspects, if any, of the endoplasmic and cortical assembly sites by using electron microscopy,

(6) determine the polarity of MTs radiating from assembly sites using hook decoration techniques,

(7) characterize the biochemical aspects of MT assembly and orientation by adding cytoplasmic fractions to tubulin preparations *in vitro* and in perfusion,

(8) repeat the tubulin perfusion experiments with purified plant tubulin,

(9) investigate the importance of tubulin concentration to MT organization by perfusing known concentrations of tubulin into internodal cells after partial recovery from drug induced MT disassembly.

6.5 CONCLUSION

MT assembly patterns have been observed after *Nitella* internodal cells were perfused with exogenous tubulin in various buffers. The demonstration that MT assembly in internodal cells can occur in a buffer that would not normally support MT assembly establishes that there are sites present that are capable of promoting MT assembly. These sites, located in the cortex and in the endoplasm, bear considerable resemblance to those deduced from oryzalin recovery experiments. Although this method is limited to the identification of preferred sites of MT assembly, it has nonetheless established, for the first time, that such sites are present in non-flagellated plant cells.

CHAPTER 6 - FIGURES

In all figures, except 6.21 to 6.23, photographs are presented so that their relative orientation with respect to the cell axis and to each other is preserved. Thus, the long axis of each photograph parallels the vertical axis of the cell from which it was taken. All cells were viewed from the cortical side of the chloroplast layer so that some resolution of MTs in the endoplasm is lost. Unless otherwise stated, micrographs represent fluorescent images.

Figs. 6.1 to 6.3. Effects of perfusion of MT assembly buffer on MTs of *Nitella* internodal cells. All cells were perfused for 40 minutes with MTAB with 1 mM GTP and processed for anti-tubulin immunofluorescence.

Fig. 6.1. Through focus series of cortical MT array localized with anti-tubulin immunofluorescence. The photographs are from the same field of view and include the MTs closest to the plasma membrane (A) in mid focus (B) and some in lower focus (C) that are close to the chloroplast layer.

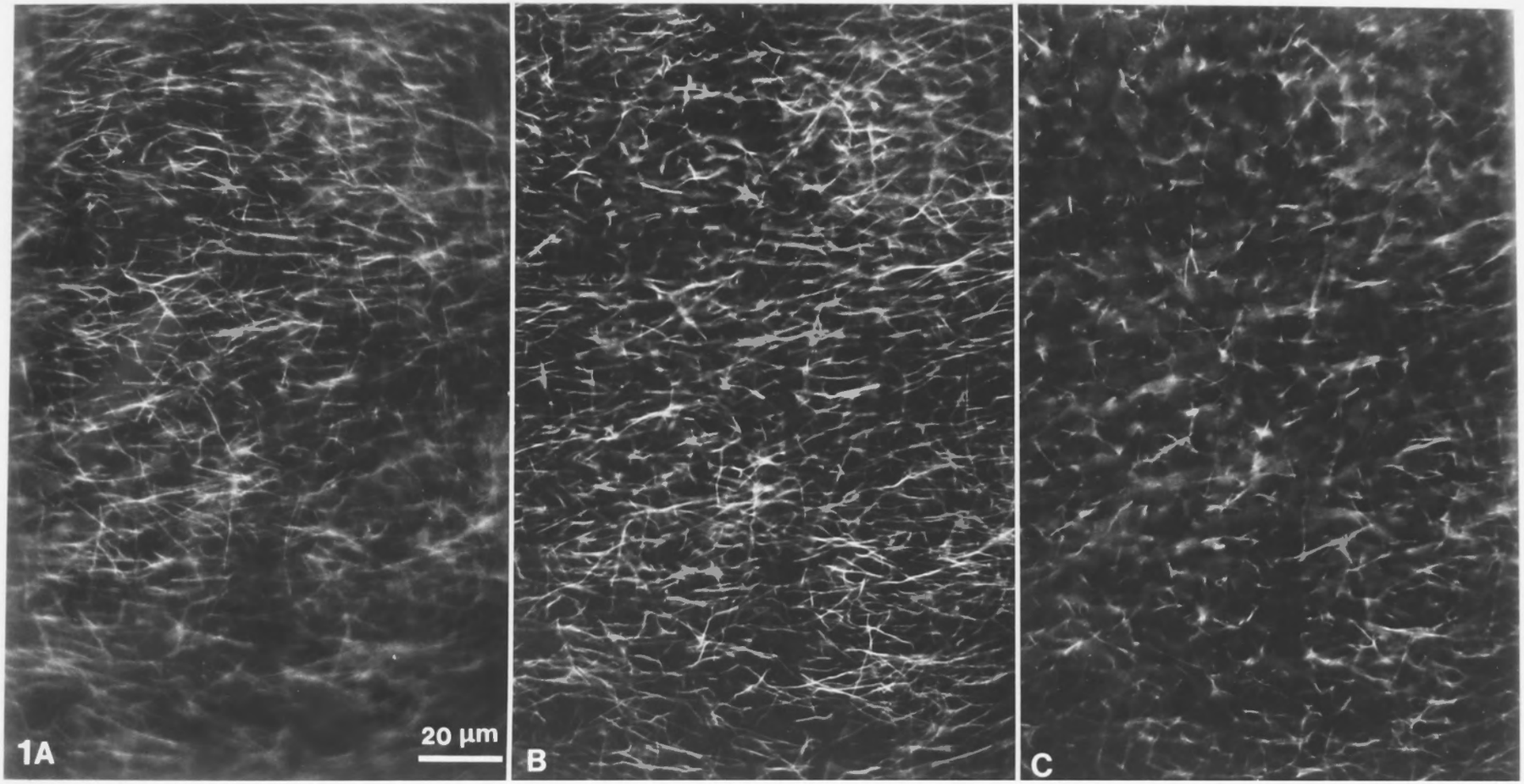
1A
20 µm
B
C

Fig. 6.2. Examples of randomization of cortical MTs after perfusion with MTAB. Different views from the same cell are shown in A, B and C. The neutral line region is seen in C.

Fig. 6.3. Orientation of cortical MTs at neutral line. Through focus series showing MTs to the left (A), at (B) and to the right (C) of the neutral line. **A:** Upper focus showing cortical MTs to left of neutral line have retained their transverse orientation. **B:** At neutral line, many MTs are oriented parallel to the chloroplast files. **C:** To the right of the neutral line, the MTs again show distinct orientation.

Fig. 6.4. Effect of perfusion of MTAB on anti-tubulin perinuclear fluorescence. **A:** Anti-tubulin immunofluorescence in cortex shows cortical MTs. Out of focus nuclei are also visible. **B:** Endoplasmic focus shows extremely intense anti-tubulin nuclear fluorescence. **C:** Nuclei labelled with Hoechst 33258.

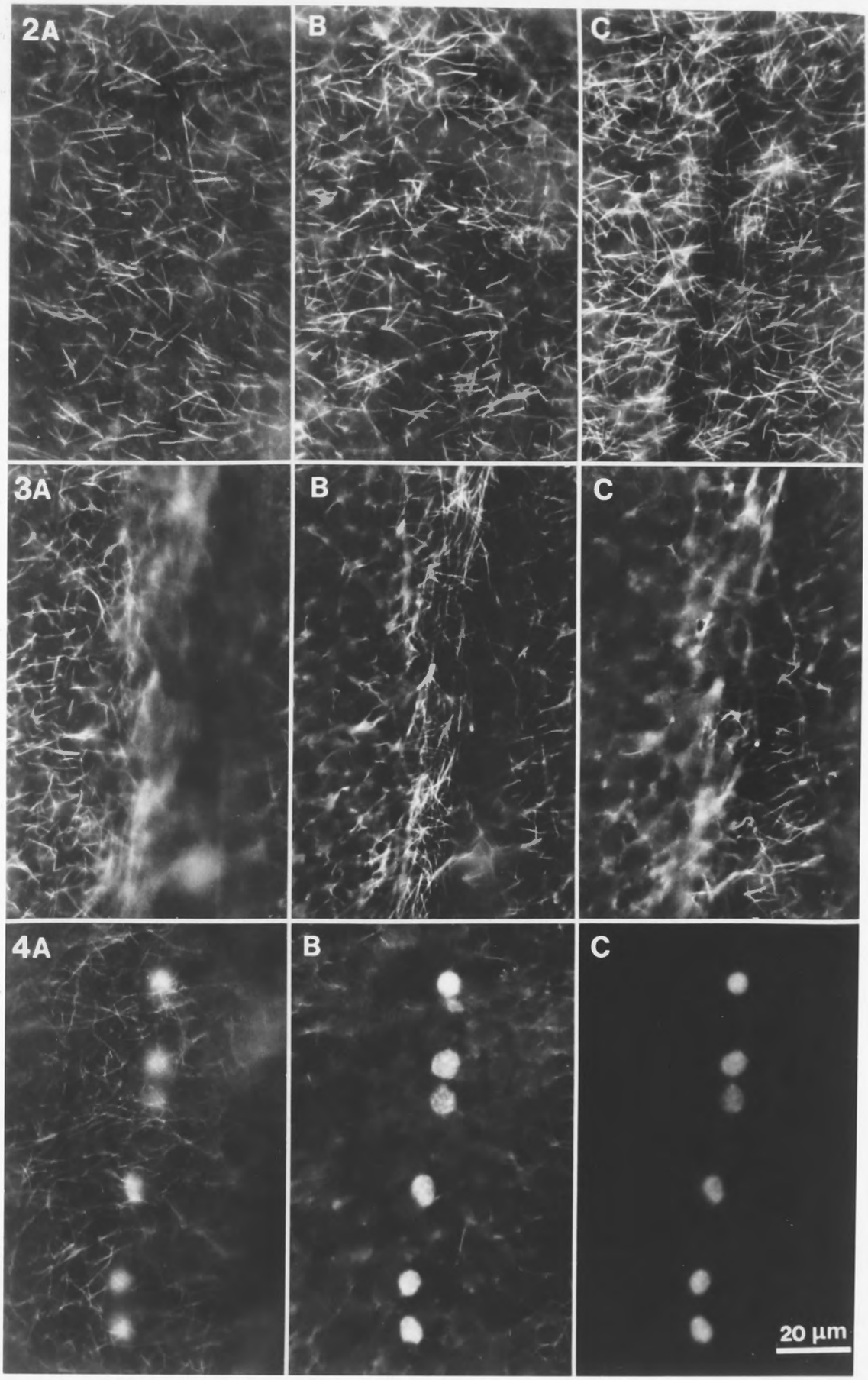
2A
B
C
3A
B
C
4A
B
C
20 µm

Fig. 6.5. *In vitro* assembly of purified and biotinylated tubulin in MTAB. Biotinylated tubulin, localized with streptavidin-phycoerythrin has formed a meshwork of filamentous structures that are presumably MTs. Since the preparation was not washed prior to fixation, the blotchy labelling may be in part due to unpolymerized tubulin.

Figs. 6.6 to 6.14. MT assembly in cells perfused with purified sheep brain tubulin in MTAB after removal of endogenous MT proteins. Biotinylated tubulin has been localized with streptavidin-phycoerythrin.

Fig. 6.6 to 6.10. 20 minute incubation.

Fig. 6.6. Small, fan-shaped cluster of MTs in the endoplasm.

Fig. 6.7. A large cluster of MTs in the endoplasm. Most of these MTs are longitudinally-oriented, possibly due to flow alignment.

Fig. 6.8. Through focus series of endoplasmic MT array. Most of these MT appear to radiate from a focus in the upper left corner with "cross-bridging" MTs also observed.

Fig. 6.9. MTs associated with two nuclei. Perinuclear fluorescence is very bright and a few short MTs, projecting from the nuclear surface are visible. **A & B:** MTs seen in two focal planes. **C:** Bright field view of nuclei, positioned in the neutral line.

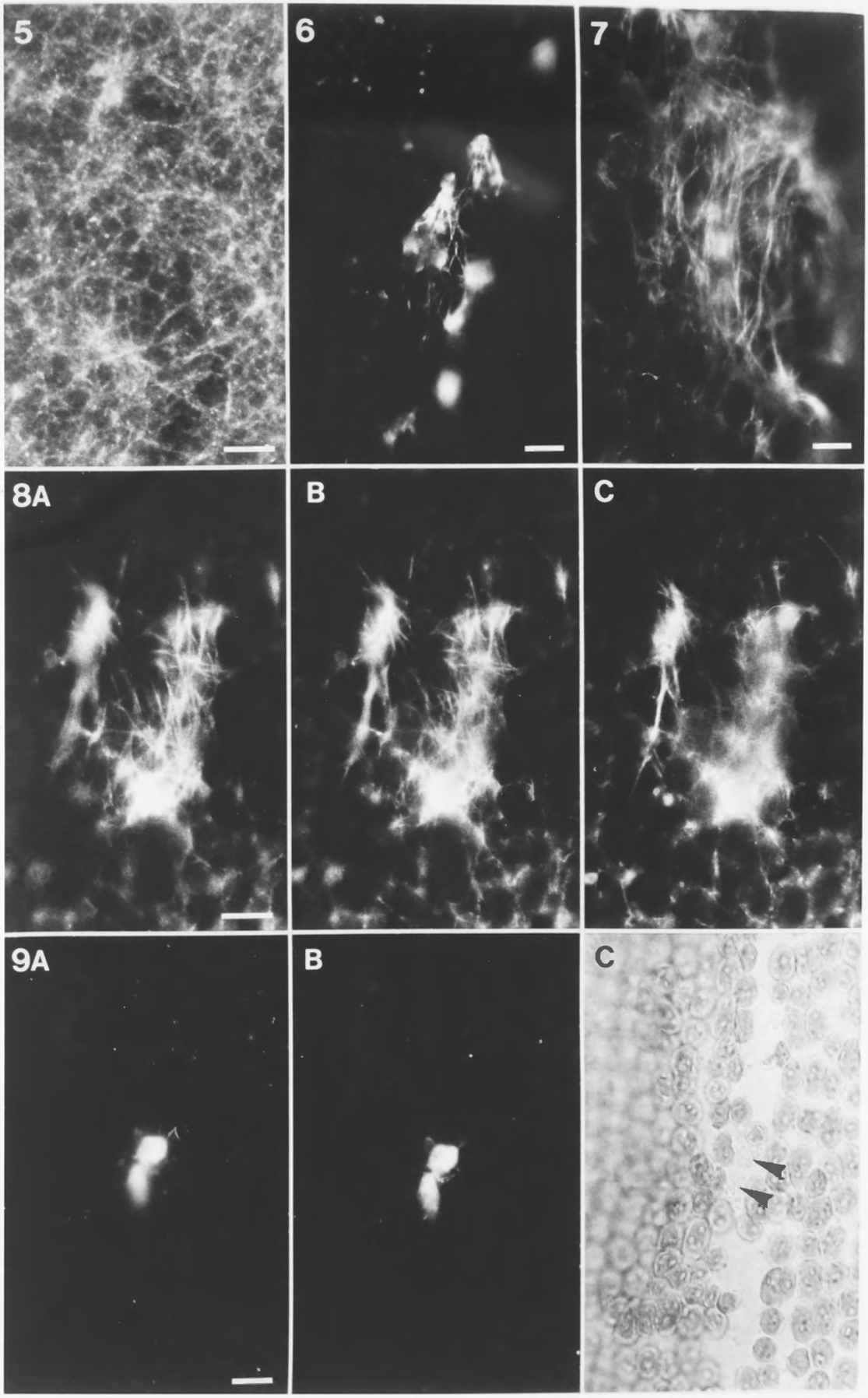
5
6
7
8A
B
C
9A
B
C

Fig. 6.10. Preferential assembly of MTs around nuclei. **A, B & C:** Through focus series in endoplasm showing MT assembly from 5 nuclei. **D:** Nuclei (arrows) visible through chloroplasts which are slightly out of focus. Bright Field image.

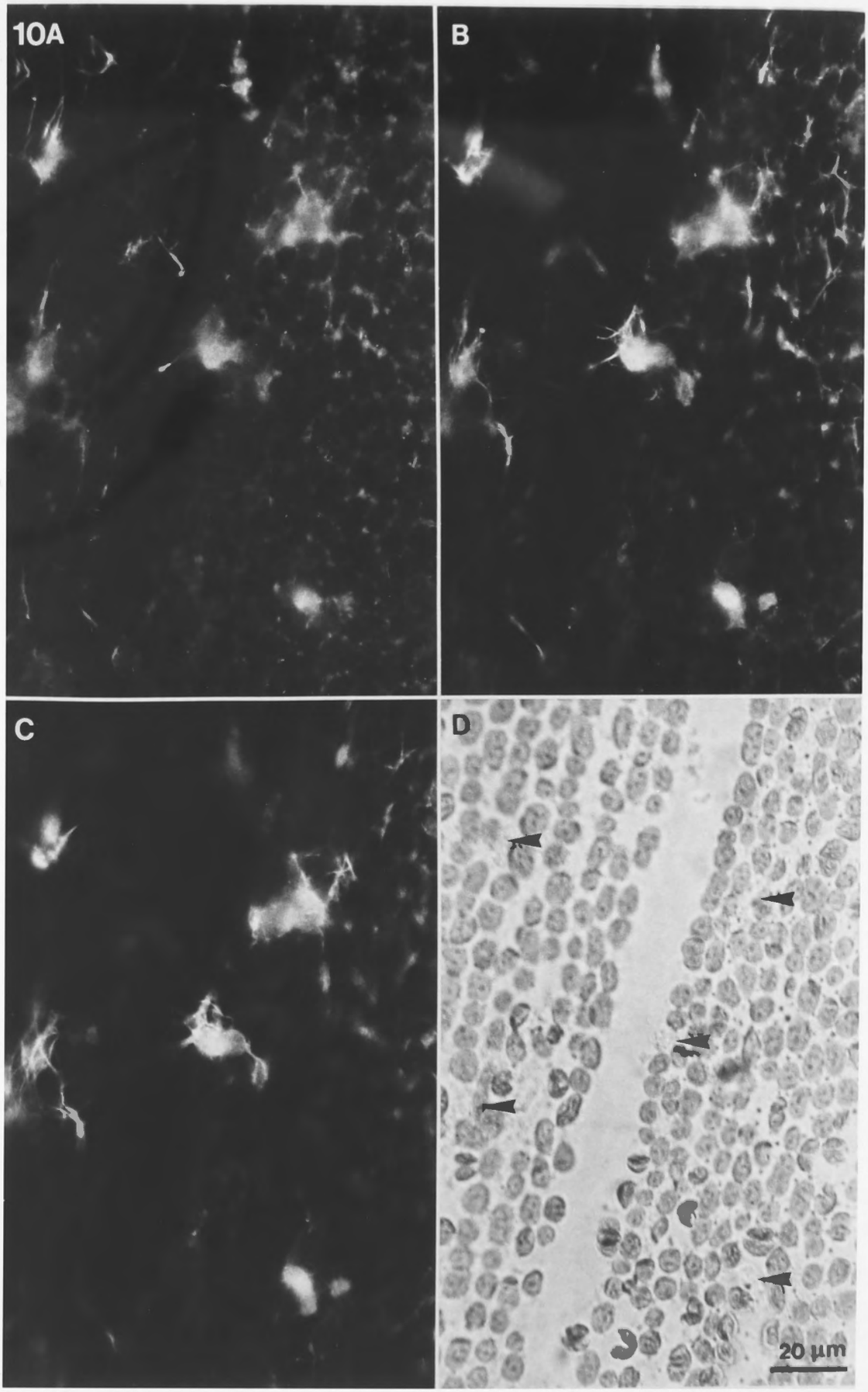
10A
B
C
D
20 µm

Fig. 6.11 to 6.14. 75 minutes incubation of purified tubulin in MTAB.

Fig. 6.11. MTs in the cortex are relatively short and arranged in branched patterns. Speckled fluorescence is also observed in the cortex.

Fig. 6.12. After 75 minutes incubation, nuclei remain very bright but no perinuclear MTs are observed. **A:** Nuclei are heavily labelled with SA-PE, suggesting that the biotinylated tubulin has great affinity to the nuclear surface. **B:** Nuclei labelled with Hoechst 33258.

Fig. 6.13. **A:** A small cluster of endoplasmic MTs close to the chloroplast layer (center) and a brightly-labelled nucleus (upper right). **B:** Nucleus labelled with Hoechst 33258. **C:** Bright field image of chloroplast array showing considerable disruption.

Fig. 6.14. Affinity of biotinylated tubulin for nuclear surface. **A:** SA-PE labelling of biotinylated tubulin located near the nuclear surface. **B:** Hoechst 33258 **C:** Bright Field and fluorescent image combined to show chloroplasts and nucleus respectively.

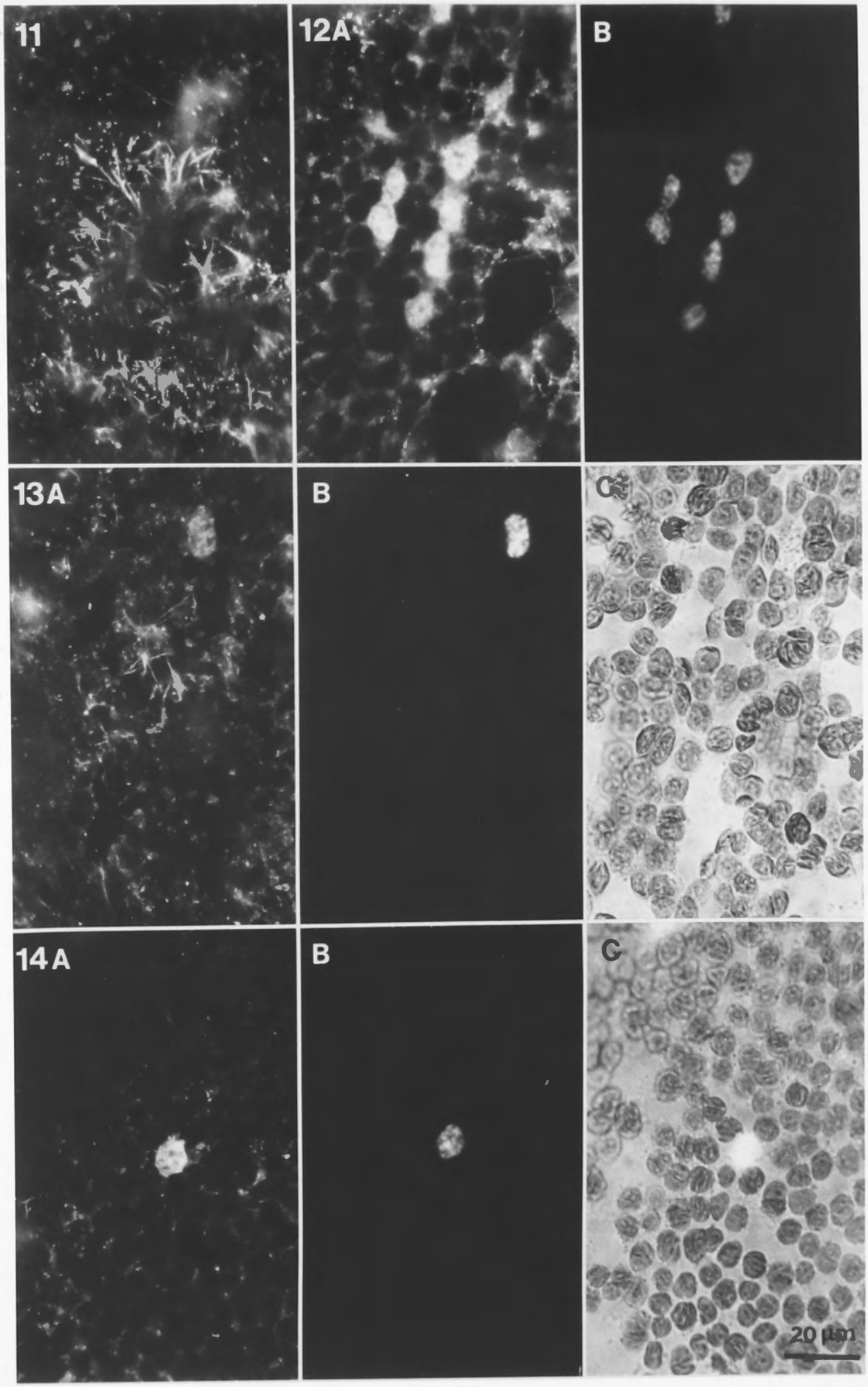
11
12A
B
13A
B
C
14A
B
C
20 µm

Figs. 6.15 & 6.16. Assembly of MTs from purified tubulin in internodal cells without prior removal of MT proteins. Cells were perfused for 1 hour with purified tubulin in MTAB-2.

Fig. 6.15. A, B & C: Through focus series of endoplasmic MTs labelled with SA-FITC. **D:** Anti-tubulin immunofluorescence using a phycoerythrin-conjugated secondary antibody localized cortical MTs that were not visible with the FITC filter combination. There was no FITC signal from the cortical region. This suggests that the exogenous purified tubulin only assembled into MTs in the endoplasm and that the cortical MTs were residual endogenous MTs.

Fig. 6.16. Under these conditions, the MTs assembled in the endoplasm were generally associated with nuclei. **A:** SA-FITC. MTs connected to nuclei which also show specificity for biotinylated tubulin. **B:** Hoechst 33258.

Fig. 6.17. Comparison of distribution of biotinylated and total tubulin in a cell perfused for 90 minutes with purified tubulin in MTAB-2. **A:** Biotinylated tubulin, localized with SA-FITC. Tubulin is found only at the nuclear surface. **B:** Anti-tubulin immunofluorescence using PE-conjugated secondary antibody. In this cell, MTs are found predominantly in the cortex (not in focus) whereas endoplasmic labelling with anti-tubulin is diffuse and located around the nuclei as in a. **C:** Hoechst 33258.

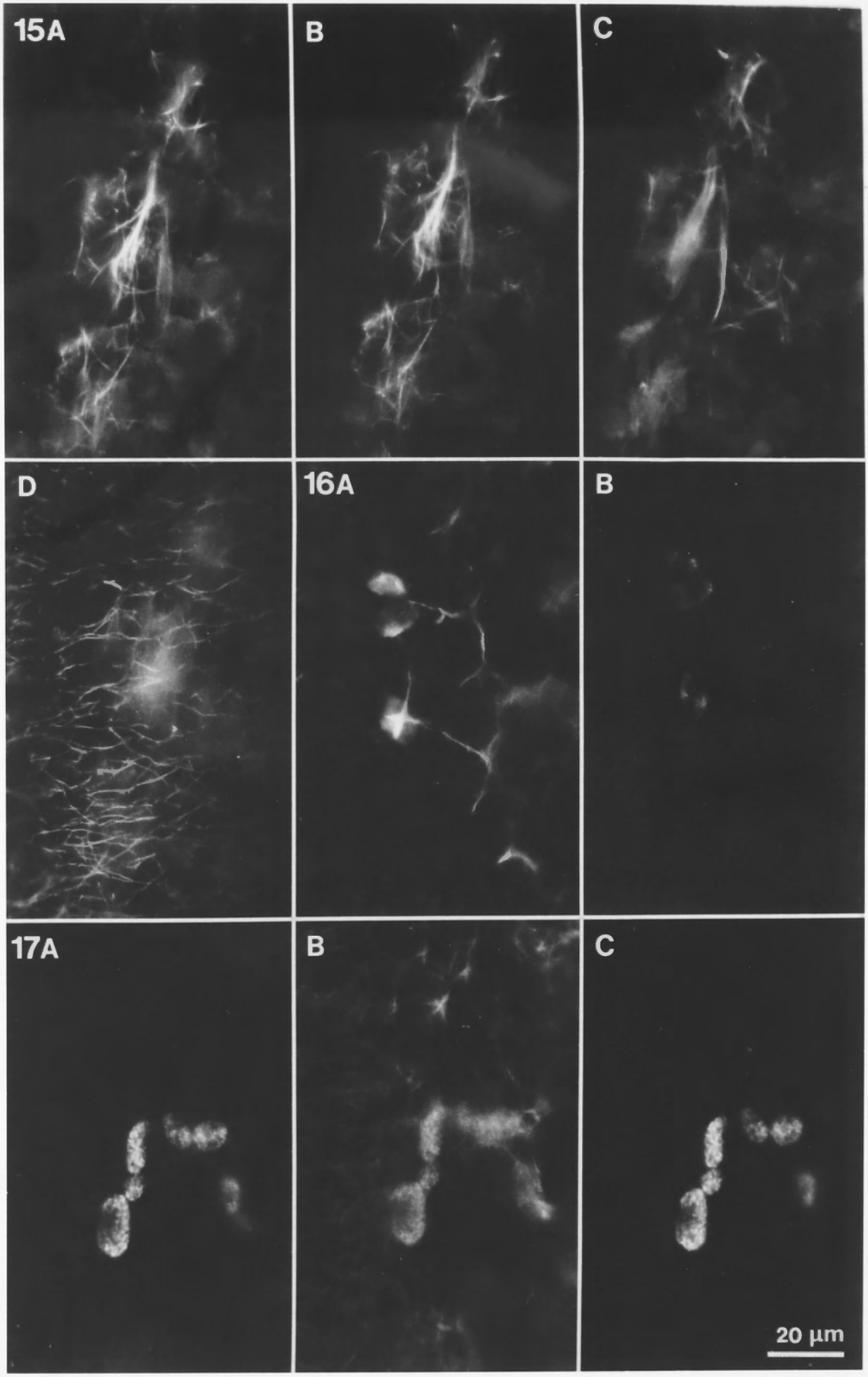
15A
B
C
D
16A
B
17A
B
C
20 µm

Figs. 6.18 to 6.20. Assembly patterns of purified tubulin in MTAB-2 with 1 mM ATP.

Fig. 6.18. MT cluster in the cortex.

Fig. 6.19. Net-like MT assemblies in the endoplasm.

Fig. 6.20. Extensive MT assemblies in the endoplasm and associated nuclei. **A:** MTs have formed a spreading, net-like array. **B:** Hoechst 33258.

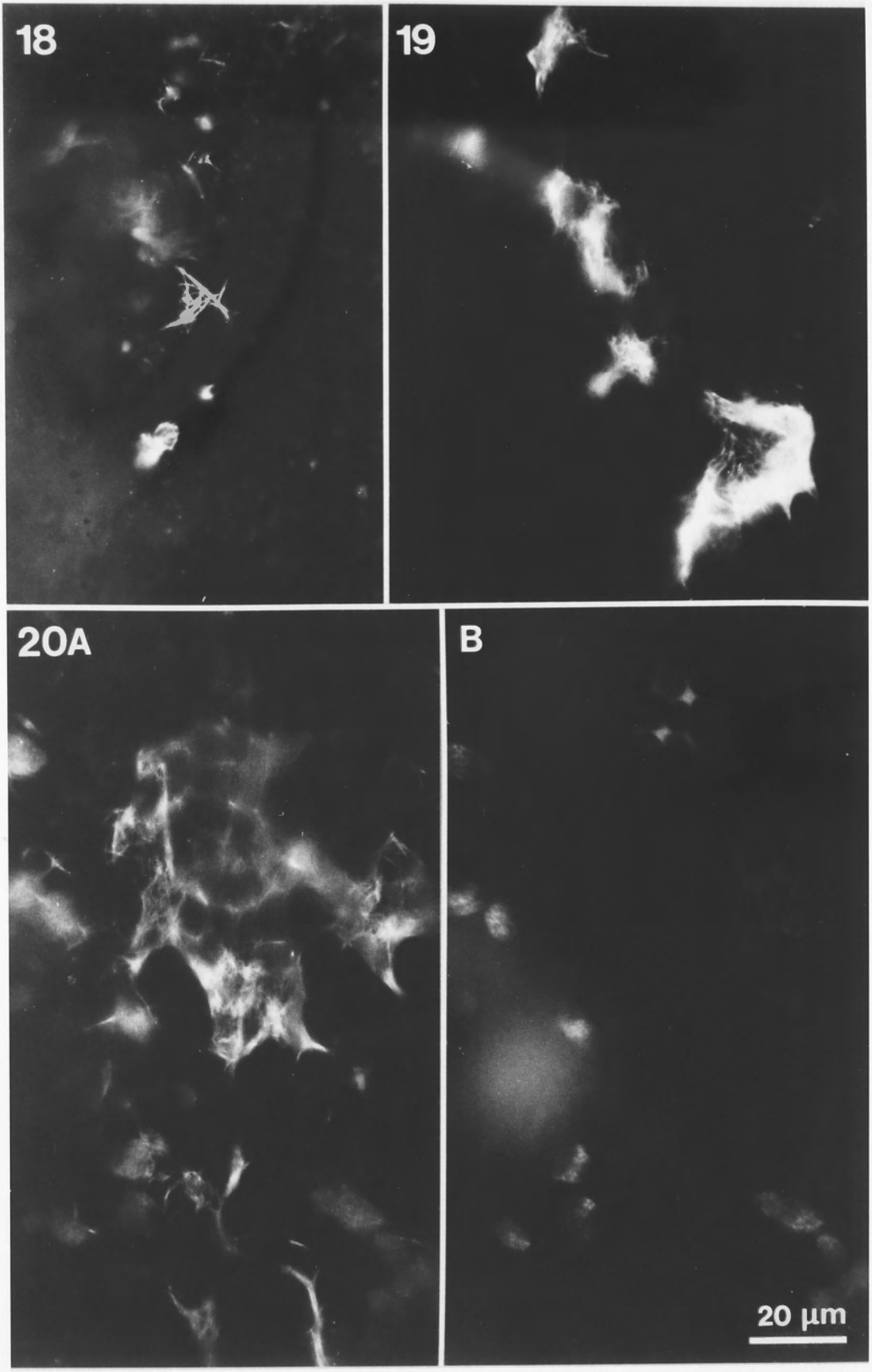
18
19
20A
B
20 µm

Figs. 6.21 to 6.33. MT assembly from purified brain tubulin after perfusion into *Nitella* internodal cells in non-assembly promoting buffer (NAB). The photographs shown in the following figures are from cells that were incubated for 2 hours. Biotinylated tubulin was localized with SA-FITC.

Figs. 6.21 to 6.23. MTs that appear to be attached to the plasma membrane. The chloroplast layer which normally separates the cortex from the endoplasm has been removed by rapid initial perfusion. These MTs are of very unusual twisted morphology.

Fig. 6.24A, B & C. Through focus series from same field showing vast number of MTs radiating from a common area in the cortex (upper right). **D:** Bright Field image shows partial removal of chloroplast array. MT distribution is largely restricted to the region of the cortex where the chloroplast array is still intact.

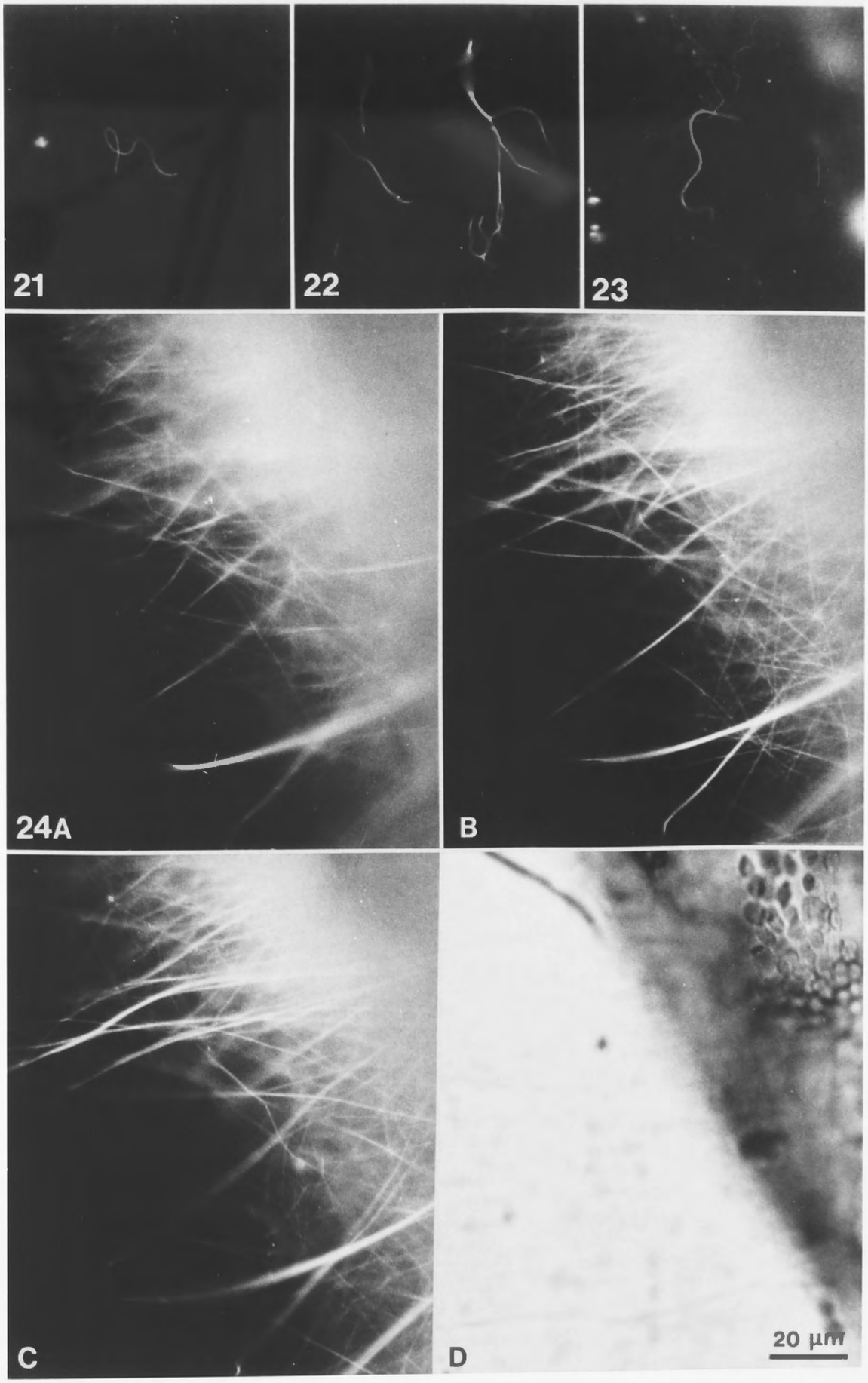
21
22
23
24A
B
C
D
20 µm

Figs. 6.25 & 6.26. Coiled bundles of MTs assembled in the endoplasm. These arrays of MTs show no obvious attachment to any structure visible in the light microscope.

Fig. 6.27. In a region where partial removal of the chloroplast array has taken place, as indicated by the bright field image (B), MTs (A) are seen near the chloroplast layer. In the upper left of the photograph (A) MTs appear to run between chloroplasts. The MTs in the central region of 6.27A have formed an extensive network.

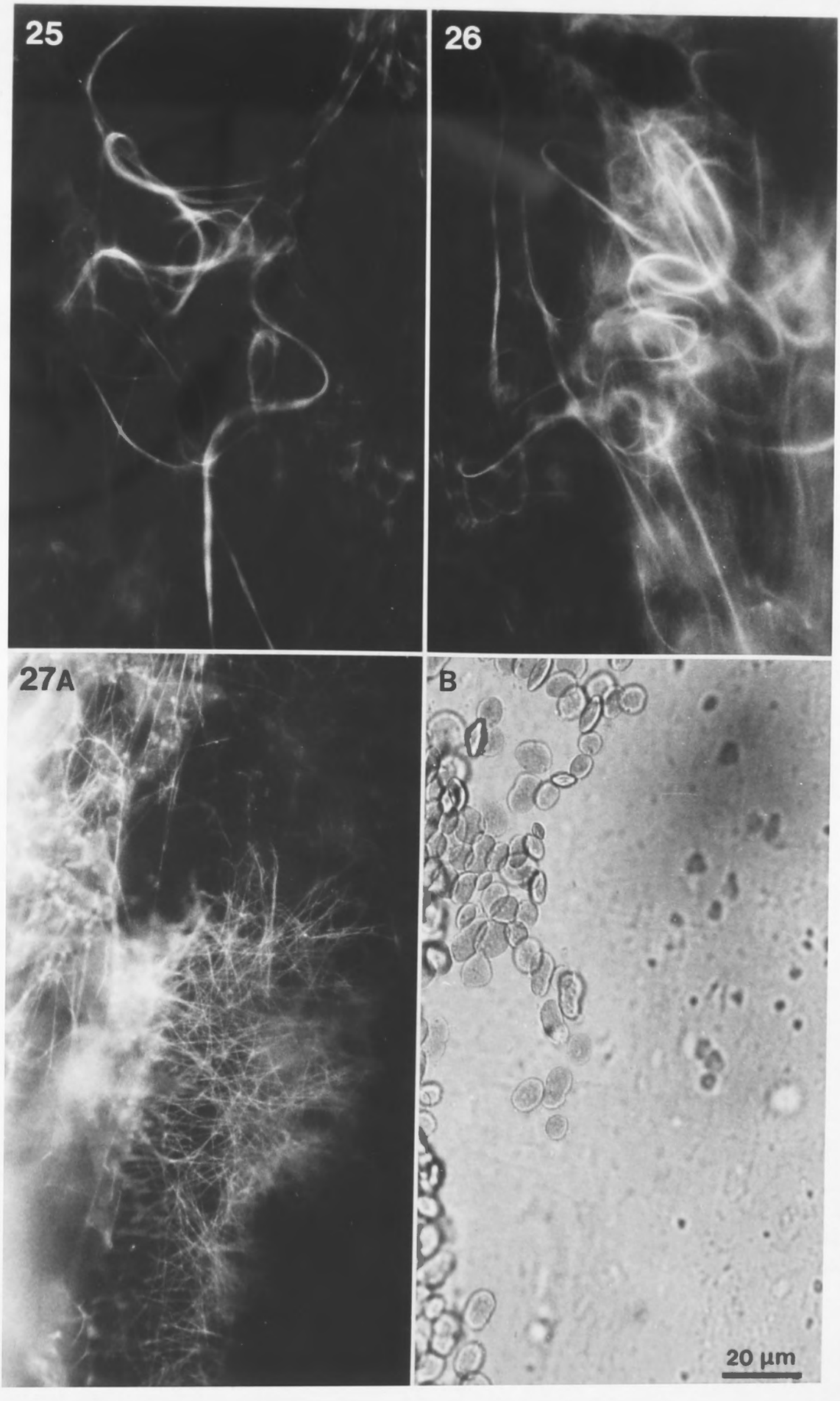
25
26
27A
B
20 µm

Fig. 6.28. Interconnected network of MTs in the endoplasm.

Fig. 6.29A. MTs in endoplasm forming a network between nuclei which have biotinylated tubulin-specific fluorescence. **B:** Hoechst stained nuclei.

Fig. 6.30. Through focus series of MTs radiating from a focus near the chloroplast layer. **A:** Upper focus shows MTs in cortex (left side of photograph). **B:** Mid focus shows MTs at level of chloroplast layer. The long MT running down is below the chloroplast layer; the overlying chloroplasts have produced the periodic attenuation along its length. **C:** Lower focus shows MTs mainly in endoplasm.

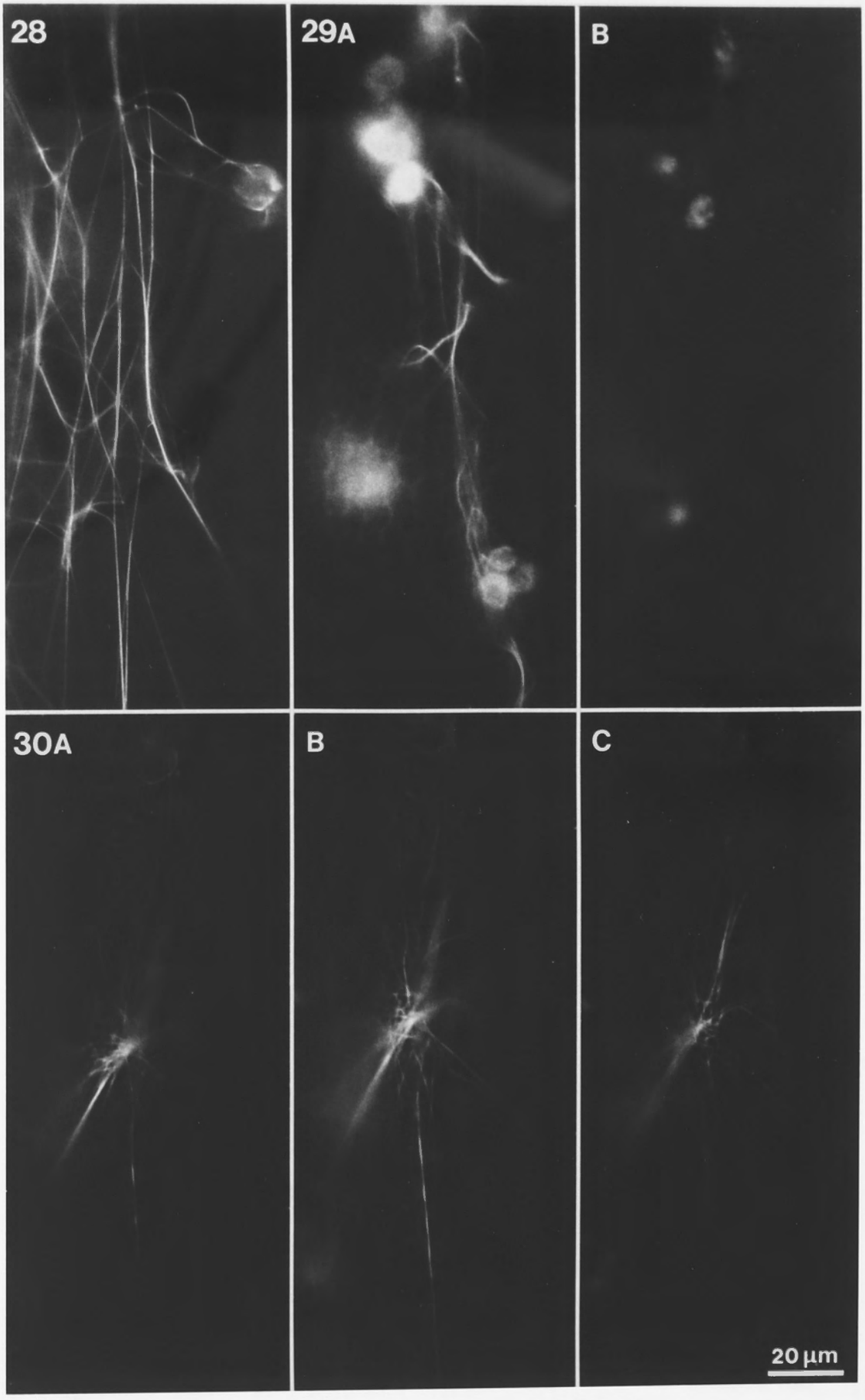
28
29A
B
30A
B
C
20 µm

Figs. 6.31 to 6.33. Cortical MTs assembled from purified tubulin. Three assemblies of MTs from adjacent regions of the same cell (A) all appear to radiate from foci located in the cortex. Some MTs appear to have become realigned (see right side of Fig. 6.31A). Presumably this realignment has occurred by the flow of perfusion solution and not through binding for actin in which case and oblique orientation would be expected. The chloroplasts visualized with Bright Field (B) have been disrupted by rapid initial flow of perfusion solution so that gaps have been created.

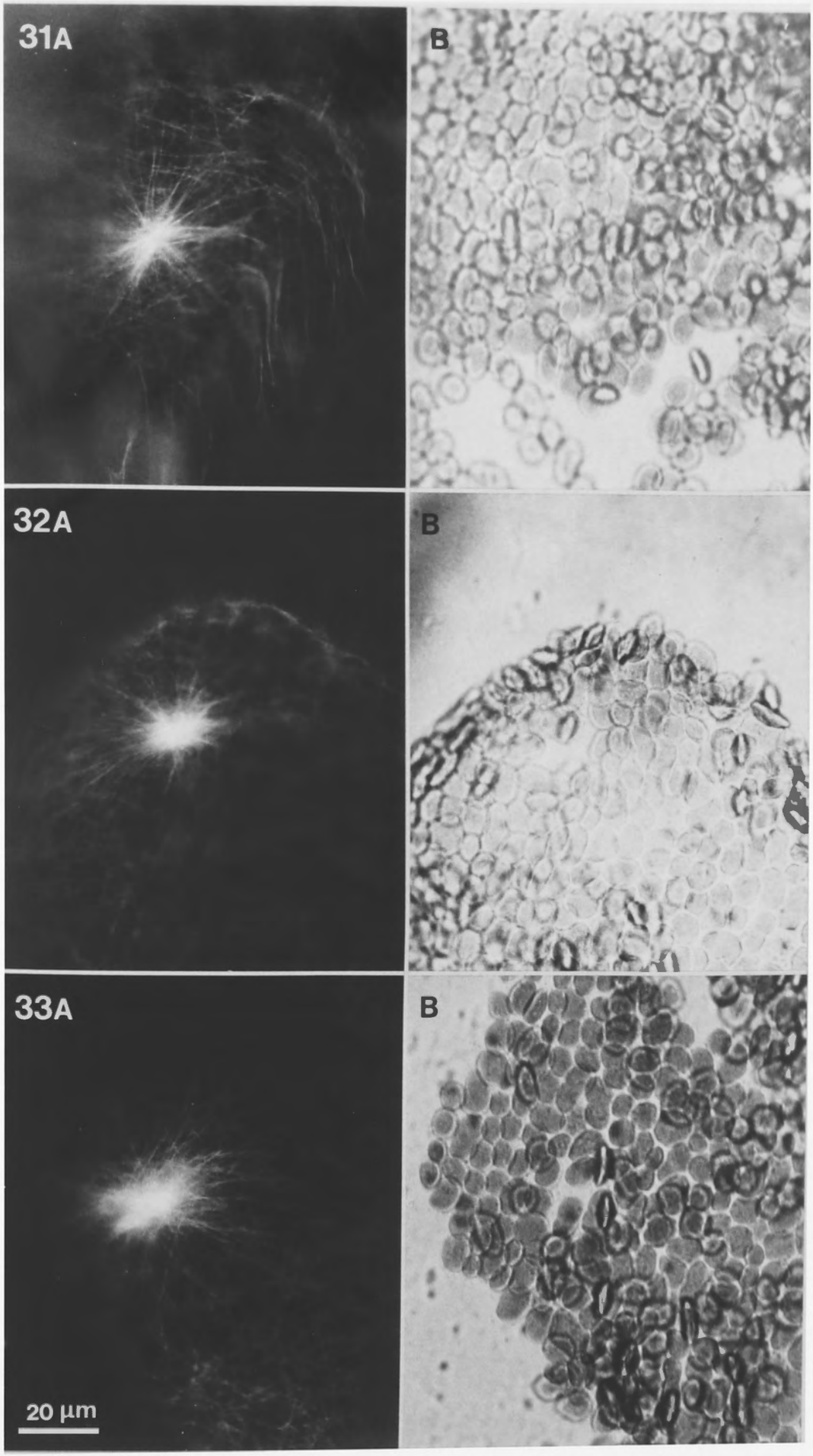
31A
B
32A
B
33A
B
20 µm

CHAPTER 7

MICROTUBULE ORGANIZATION IN CHARACEAN INTERNODAL CELLS:

A CONCLUDING DISCUSSION

Indeed, any hypothesis which possesses a sufficient degree of plausibility to account for a number of facts will help us to arrange those facts in proper order and will suggest to us proper experiments either to confirm or refute it.

Charles Babbage, 1815.

7.1 INTRODUCTION

Over a quarter of a century has passed since Green proposed that "proteins of spindle fiber nature exist in the cortical cytoplasm (of plant cells) and are active in the control of wall texture and cell form" (Green 1962). Subsequent confirmation that "microtubules" were indeed located in the cortical cytoplasm of plant cells and the observation that these structures had the same orientation as wall microfibrils (mfs) (Ledbetter & Porter 1963; Hepler & Newcomb 1964) inspired a quest to understand the involvement of MTs in wall deposition and cell morphogenesis. Progress has been slow and even today, despite substantial supporting evidence, there is still some resistance to Green's proposal (see, for example, the recent review by Preston 1988). This is largely due to the discovery that MTs are not always involved in wall deposition (Neville & Levy 1984) and partly because none of the many proposed mechanisms by which MTs could control mf orientation (Heath 1974; Seagull & Heath 1980; Hepler & Fosket 1971; Schnepf 1974; Herth 1980; Mueller & Brown 1980) has been fully substantiated.

Although electron microscopy was indispensable for all early work, the development of immunofluorescence microscopy and the rapid progress in MT biochemistry has dramatically changed our concept of MTs in plant cells. The early impression was that cortical MTs are relatively static elements, comprising "hoops" that encircle the cell just inside the plasma membrane. However, it is now generally believed that MTs exist as a population of separate, dynamic elements that can behave as an integrated unit to regulate morphogenesis (as well as other processes throughout the cell cycle) under potentially variable conditions. Whilst the involvement of MTs in wall deposition remains unresolved, much attention has shifted to the crucial question of how MTs are organized.

The work presented in the preceding chapters of this thesis was carried out to provide a better description of MT arrangement in the cortex of elongating plant cells. It is appropriate that the internodal cells of *Nitella* were selected as a system

for this work since it was observations with these cells that led to Green's postulation that elements of this nature are involved in wall patterning. Since then, characean internodal cells have contributed relatively little to the field of cortical MT research because of the problems of fixation for electron microscopy (Nagai & Rehbun 1966). This contrasts with their extensive use in studying actin's role in motility (Kamiya 1986). Through the successful application of immunofluorescence microscopy for studying MTs in these cells it was possible to make many observations about MT organization. The remaining discussion will summarize and consider the significance of these observations.

7.2 MICROTUBULE DISTRIBUTION IN INTERNODAL CELLS

Early observations with electron microscopy (Nagai & Rehbun 1966; Pickett-Heaps 1967a) verified the presence of cortical MTs in characean internodal cells. When immunofluorescence microscopy was applied (Ch. 2), it was possible to observe not only the arrangement of cortical MTs throughout the length of entire cells but also to carry out a survey of MT distribution in non-cortical regions. Thus, in addition to the prominent sub-plasmalemmal cortical MT array, MTs were also localized in the sub-cortical region running parallel to the actin cables and associated with the endoplasmic nuclei.

7.3 MICROTUBULE ASSEMBLY SITES

In addition to characterizing the distribution of MTs in internodal cells, it was of interest to define sites capable of promoting MT assembly. Two approaches were used:

(1) *in vivo* assembly of MTs after drug-induced depolymerization (Ch. 5) and

(2) a semi-*in vitro* assay of MT assembly in cells perfused with purified exogenous tubulin (Ch. 6).

The results of these studies suggest that MT assembly sites occur in both the cortex and in the endoplasm.

Many researchers (De Mey *et al.* 1982; Bakhuizen *et al.* 1984; Wick & Duniec 1984; Bajer & Molè-Bajer 1986b; Sheldon & Dickinson 1986) have suggested that the nucleus serves as a nucleating site for MTs and that MTs assembled at the nuclear envelope radiate towards the plasma membrane where it is thought (Lloyd 1987) they can be subsequently and independently organized. Disassembly/recovery experiments (Ch. 5) with multinucleate *Nitella* internodal cells detected MTs around nuclei only after considerable assembly had already taken place in the cortex. It therefore seems likely that the nuclei of *Nitella* are sites for MT nucleation but that the MTs of the endoplasmic and cortical arrays are independently nucleated and organized. Perfusion of exogenous tubulin into internodal cells (Ch. 6) resulted in MT assembly around nuclei and at sites in the cortex, supporting the idea that MT nucleation can occur in both locations. The cortical sites, however, were not as clearly defined as in disassembly/recovery experiments.

7.4 MICROTUBULE ASSEMBLY PATTERNS

During recovery from oryzalin-induced depolymerization (Ch. 5), cortical MTs were arranged in assemblies whose branching patterns suggested that MTs were assembled at sites along existing MTs. The arrangement of MTs was very consistent; MTs abutted at acute angles so that the angular dispersion of "branch" MTs at the fringes of such assemblies was much greater than that of earlier assembled "trunk" MTs. MT arrangements like these have not been previously documented in cortical arrays of plant cells. The MT "fir trees" of kinetochore fibres observed in *Haemanthus* endosperm cells (Inoué *et al.* 1985; Bajer & Molè-Bajer 1986b), onion root cells (Palevitz 1988) and in the alga *Oedogonium* (Schibler & Pickett-Heaps 1987), may be arranged in a similar way. As recovery

proceeded, branching assemblies became less extensive and were less conspicuous amidst the predominantly transverse array of young cells but could still be recognized in fully recovered cells. On examining untreated cells more closely, branching assemblies were also recognized. Thus, these configurations could represent a sub-population of MTs that are continuously assembled at a variety of angles, possibly for incorporation into the transverse MT array of elongating cells.

Interestingly, MTs in branching clusters were selectively labelled with an anti-tubulin monoclonal antibody (Ch. 2) that was raised against purified plant tubulin. Since the transverse MTs are not detected with this antibody, it is likely that they are modified antigenically in the process of being oriented transversely. Although this investigation is still at a early stage, it provides the first evidence that MT orientation may involve a change in the MT antigenicity. Possible modifications include the binding of MAPs to the MT surface or the cross-linking of MTs to the plasma membrane which could obscure the antigenic site recognized in newly assembled MTs. It would be interesting to apply this antibody to partially recovered cells (which should be enriched with MTs in branching assemblies) to see if the newly assembled MTs are labelled. The nature of MT-MT interaction in these branching clusters could also profitably be studied with electron microscopy.

7.5 MICROTUBULE CO-LOCALIZATION WITH ACTIN

Recently there has been much attention directed to the possible co-localization of MTs with actin filaments. Advances in preparation methods for electron microscopy such as dry-cleavage and freeze substitution have resulted in the preservation of fine filaments amongst cortical MTs (Hawes 1985; Traas 1984; Traas *et al.* 1985; Lancelle *et al.* 1986; Tiwari *et al.* 1984). Similarly, phalloidin labelling of filaments in the cortex of plant cells has been achieved with specialized preparation methods for fluorescence microscopy (Traas *et al.* 1987; Kakimoto & Shibaoka 1987b). Anti-actin immunofluorescence has also been successfully used

to demonstrate MT-actin filament co-alignment in *Bryopsis* (Menzel & Schliwa 1986).

The distribution of actin in internodal cells of *Chara* has been examined with anti-actin immunofluorescence (Williamson & Toh 1979; Williamson *et al.* 1987) and fluorescently-coupled phallacidin (Barak *et al.* 1980) but these studies have only described the prominent actin cables that are involved in cytoplasmic streaming and are located almost exclusively in the sub-cortical region. No cortical arrays of actin filaments such as those described in other plant cells (Traas *et al.* 1987; Kakimoto & Shibaoka 1987a) have been observed. As reported in Chapter 2, a survey of actin distribution in internodal cells of *Nitella tasmanica* was negative for such filaments. Anti-actin in aldehyde-fixed cells identified sub-cortical cables and, for the first time, filamentous rings on the nuclei but did not show any sign of actin filaments co-aligning with the cortical MTs. A non-fixation method was also attempted whereby fluorescently-coupled phalloidin was perfused into cells in a stabilizing buffer (not shown). This also resulted in labelling of the actin cables but was negative for cortical filaments. Interestingly, whilst actin co-localization with cortical MTs was not observed, a small number of MTs appeared to be co-aligned with the sub-cortical actin cables. While this observation does not provide evidence that actin filaments co-localize with cortical MTs, it does suggest that actin-MT interaction can occur in characean internodal cells.

7.6 CORTICAL MICROTUBULE ORIENTATION, CELL MORPHOGENESIS AND DEVELOPMENT

The supposition that MTs influence the orientation of wall mfs and therefore, the direction of cell expansion has been supported by observations in many plant cells of parallel alignment of MTs and mfs. Preliminary examination of cortical MTs in *Nitella* internodal cells with immunofluorescence and inner wall replicas with electron microscopy (Ch. 2) indicated that the orientation of MTs and newly

deposited mfs was similar. In young, rapidly elongating cells, MTs and mfs were transverse but in older, non-growing cells, the MTs and mfs appeared to be randomly-oriented.

Owing to their enormous size and predictable growth pattern, it is possible to accurately measure internodal cells and follow their growth throughout development. This made it possible to document the MT orientation patterns of *Nitella* internodal cells at different stages of development in the same way Green (1958) documented changes in wall texture. It was also possible to carry out computer-assisted quantitative analysis of MT images due to the excellent resolution achieved with the vacuolar perfusion method of immunofluorescence and because large areas of cortical MT array could be photographed. Thus, unprecedented data on MT orientation, length distribution and density were collected and correlated with cell age and growth rates.

The results of this part of the study are discussed in detail in Chapter 3 but they will be briefly summarized for the present discussion. In young, rapidly elongating internodal cells, MTs are predominantly transverse and as the rate of elongation decreases towards growth cessation, MTs become increasingly dispersed about the cell's long axis until in non-growing cells they appear to be arranged randomly. While mf orientation in *Nitella axillaris* (Green 1958; Richmond 1983) undergoes similar changes throughout development, it is not certain that it is always controlled by MTs. A survey of MT orientation patterns in internodal cells of *Chara corallina* (Ch. 4) revealed a different arrangement of MTs around the time of growth cessation. It seems possible that MTs may lose their control over mf orientation when growth cessation is at hand. This is consistent with the recent claim that the wall of *Nitella* internodal cells is organized as a helicoid (Neville & Levy 1984) which is believed to arise through self-assembly of mfs (Neville *et al.* 1976), not co-alignment with MTs. Contrary to Neville & Levy's (1984) claim, however, it is unlikely that a helicoidal wall pattern

exists in elongating cells. Apart from the difficulty understanding how such a wall could regulate directed cell expansion, treatment of growing cells with the herbicide oryzalin, which specifically causes MT disassembly, resulted in isodiametric growth (Fig. 1.1; *cf.* Green 1962, 1963 for colchicine and Green *et al.* 1970 for trifluralin). Thus MTs appear to be required for the direction of mf orientation in growing internodal cells but might lose this function in later stages of development, particularly in non-expanding cells.

Future investigations should include a correlative survey of MT and mf orientation for cells at known stages of development to establish, with certainty, at what stages and to what extent MTs control wall deposition. Immunofluorescence and electron microscopy could be carried out for the same cells to compare MT and mf orientation respectively.

7.7 MICROTUBULE STABILITY AND DYNAMICS

One of the greatest puzzles of plant cell morphogenesis is how a MT array can be maintained in a transverse orientation while the cell is expanding. The earliest impression, from electron micrographs, was that MTs formed unbroken, static hoops (Ledbetter & Porter 1963; Hepler & Newcomb 1964). It was not until the late 70's, owing largely to the painstaking serial sectioning work of Hardham (1978) that cortical MTs were no longer considered to be complete hoops. Rather, MT arrays appeared to be "composed of overlapping, component MTs, which are short relative to the dimensions of the cell" (Hardham & Gunning 1978). Such an arrangement of MTs has the advantage of being capable of rapid adjustment, through MT growth or shrinkage, assembly or disassembly. Green (1980) suggested that such short MTs could be oriented transversely by maximizing overlaps between adjacent MTs, thus forming a self-cinching loop whose most stable position of minimum circumference is transverse. Recently, this model has been modified to account for the variety of orientations from transverse through

oblique to longitudinal that are observed in certain higher plant cells when the technique of whole cell immunofluorecence is applied. Lloyd & Seagull's dynamic spring model (1985) proposes that MTs are organized as a helix that can change direction as an integral rather than fragmentary array through inter-tubule sliding. This model relies on the occurrence of cross-bridging between MTs and the ability of MTs to undergo changes in direction by a mechanism that has not been clearly specified but with minimal assembly or disassembly.

The MT organization in characean internodal cells does not accord with the dynamic spring model. Quantitative analysis of MT orientation in *Nitella* showed that although oblique and longitudinal MTs were often present, at no stage of development could the array be described as helical (despite conspicuous helical features of the cell). The array would be better described as fragmentary with relatively short MTs showing considerable local angular variation while contributing to an overall orientation. Furthermore, in early recovery from oryzalin-induced disassembly (Ch. 5), the first MTs to assemble were well dispersed yet had transverse orientation. It seems unlikely that such alignment could be the result of intertubule cross-bridging. Even in *Chara*, which at about the time of growth cessation displays local shifts in orientation from transverse to longitudinal (Ch. 4) while maintaining the MTs in reasonably parallel order, the array can not be described as helical since it does not form a continuous spiral. Although MTs are locally parallel, they never remain oriented consistently while circumscribing the cell but instead the array exhibits sudden shifts in orientation that contradict the image of an array controlled by a spring-like mechanism based on sliding between adjacent MTs.

The emerging picture of MT organization in characean internodal cells is one of a fragmented rather than integrated array. The maintenance of transverse orientation throughout the extensive (about 30 day) period of elongation does not appear to rely so heavily on interaction between MTs as has been proposed for

other plant cells. Perhaps cross-bridging of MTs to the plasma membrane (also considered a potential mediator of MT orientation) plays a major role in the organization of MTs in these cells. Such linkages could mediate orientation from a plasma membrane-based template. They could also confer stability to MTs so that transverse MTs, through capping, would be less prone to catastrophic disassembly than unlinked, non-transverse MTs. Thus, the process of dynamic instability (which has been documented in living cells [Schulze & Kirschner 1986, 1987]) could be involved in the regulation of MT orientation in these cells. The changes in orientation seen at later stages of development could easily result from disassembly-reassembly rather than MT pivoting. Similarly, the changes in orientation observed in the "helical" MT arrays of higher plant cells could also result from disassembly-reassembly. Direct evidence that intertubule sliding takes place is still lacking.

7.8 FACTORS CONTROLLING MICROTUBULE ORIENTATION

MT orientation is related to cell development. Rapid expansion correlates with transverse orientation and as the rate of growth declines so does the proportion of transversely-oriented MTs. In cells that are no longer growing, MTs are apparently randomly oriented. Thus, a factor that controls growth might also affect MT orienting mechanisms. The possibility that MT orientation is based on interaction with the plasma membrane has been considered in the previous section (7.7). Changes in membrane fluidity affect the ability of epithelial cells to organize sub-plasma membrane MT cytoskeletons (Sauk *et al.* 1987) so membrane fluidity could be one property that is adjusted to affect MT organization. The possibility that MT orientation is somehow regulated by strain has also been discussed in Chapter 3. Whilst it is plausible that MT behaviour (for example, MT-plasma membrane cross-linking) might respond to changes in the strain environment of the plasma membrane or cytosol, such a mechanism does not adequately account for

how the orientation of MTs could be regulated. Transverse MT orientation was achieved in recovery experiments (Ch. 5), even after the direction of strain could be expected to have been altered by 24 hour oryzalin treatments and even in slowly growing, older cells in which strain would be almost negligible. Future work should include an investigation of MT recovery in physically-constrained cells and under conditions of reduced turgor.

Electrical activity is well documented in plant cells, especially characean internodal cells (Walker & Smith 1977; Toko *et al.* 1985, 1987, 1988) where the electric potential across the plasma membrane can fluctuate along the length of the cell as proton extruding and importing bands are set up. Electrical currents could be one factor involved in the regulation of MT orientation. White and co-workers (personal communication) have recently demonstrated that if regenerating *Mougeotia* protoplasts are held in an electrical field, the cells will all elongate in the same direction, parallel to the gradient with MTs, therefore, perpendicular to it. Whether this response is due to a direct effect on MTs has not been determined but it is not unreasonable to assume that the orientation of MTs - which themselves are inherently polar structures - could be influenced by such a force.

7.9 FUTURE EXPERIMENTS

The characean internodal cell has once again proven to be a valuable biological specimen. Cortical MT organization and recovery has been described quantitatively in unprecedented detail and for the first time, the existence of sites that are capable of initiating the assembly of exogenous tubulin in plant cells has been documented. The aims of future investigations include:

(1) following MT behaviour *in vivo*, in real time, under normal conditions and in the presence of various physical and chemical constraints, utilizing microinjection of fluorescently-coupled tubulin and low light video fluorescence microscopy,

(2) examining the nature of MT-MT and MT-plasma membrane interaction with electron microscopy and

(3) carrying out an investigation of MAPs, their localization and function in the organization of the cortical MT array.

Although these plans are ambitious, their achievement would represent a major contribution to MT research and plant cell biology. The concept of cortical MTs in plant cells arose from work exploiting the valuable features of characean internodal cells (Green 1962); those same features should assist the return of charophytes to the forefront of MT research using contemporary cell biological techniques.

BIBLIOGRAPHY

Akashi, T., and H. Shibaoka. 1987. Effects of gibberellin on the arrangement and the cold stability of cortical microtubules in epidermal cells of pea internodes. Plant Cell Physiol. 28: 339.

Allen, C., and G. G. Borisy. 1974. Structural polarity and directional growth of microtubules of *Chlamydomonas* flagella. J. Mol. Biol. 90: 381.

Amos, L. A. 1979. Structure of microtubules. In: Microtubules, Roberts, K. Hyams, J. S., Eds., pp. 1-64. London. Academic Press.

Andrews, M., S. McInroy, and J. A. Raven. 1984. Culture of *Chara hispida*. Br. phycol. 19: 277.

Apelbaum, A., and S. P. Burg. 1971. Altered cell microfibrillar orientation in ethylene-treated *Pisum sativum* stems. Pl. Physiol. 48: 648.

Arai, T., and Y. Kaziro. 1977. Role of GTP in the assembly of microtubules. J. Biochem. 82: 1063.

Arce, C. A., M. E. Hallak, J. A. Rodriguez, H. S. Barra, and R. Caputto. 1978. Capabitity of tubulin and microtubules to incorporate and to release tyrosine and phenylalanine and the effect of the incorporation of these amino acids on tubulin assembly. J. Neurochem. 31: 205.

Argaraña, C. E., H. S. Barra, and R. Caputto. 1980. Tubulinyl-tyrosine carboxypeptidase from chicken brain: properties and partial purification. J. Neurochem. 34(1): 114.

Asai, D. J., W. C. Thompson, L. Wilson, C. F. Dresden, H. Schulman, and D. L. Purich. 1985. Microtubule-associated proteins (MAPs): a monoclonal antibody to MAP1 decorates microtubules in *vitro* but stains stress fibers and not microtubules *in vivo*. Proc. Natl Acad. Sci. USA. 82: 1434.

Ashton, F. M., O. T. De Villiers, R. K. Glenn, and W. B. Duke. 1977. Localization of metabolic sites of action of herbicides. Pestic. Biochem. Physiol. 7: 122.

Bajer, A. S., and J. Molè-Bajer. 1986a. Drugs with colchicine-like effects that specifically disassemble plant but not animal microtubules. In Dynamic Aspects of Microtubule Biology. editor D. Soifer. Ann. N.Y. Acad. Sci. 466: 767.

Bajer, A. S., and J. Molè-Bajer. 1986b. Reorganization of microtubules in endosperm cells and cell fragments of the higher plant *Haemanthus in vivo*. J. Cell Biol. 102: 263.

Bakhuizen, R., P. C. Van Spronsen, F. A. J. Sluiman-den Hertog, C. J. Venverloo, and L. Goosen-de Roo. 1985. Nuclear envelope radiating microtubules in plant cells during interphase mitosis transition. Protoplasma. 128: 43.

Barak, L. S., R. R. Yocum, E. A. Nothnagel, and W. W. Webb. 1980. Fluorescence staining of the actin cytoskeleton in living cells with 7-nitrobenz-2-oxa-1,3-diazole-phallacidin. Proc. Natl. Acad. Sci. 77: 980.

Barton, J. S., D. L. Vandivort, D. H. Heacock, J. A. Coffman, and K. A. Trygg. 1987. Microtubule assembly kinetics. Biochem. J. 247: 505.

Bayer, D. E., C. L. Foy, T. E. Mallory, and E. G. Cutter. 1967. Morphological and histological effects of triflurlin on root development. Amer. J. Bot. 54: 945.

Ben-Ze'ev, A., S. R. Farmer, and S. Penman. 1979. Mechanisms of regulating tubulin synthesis in cultured mammalian cells. Cell. 17: 319.

Bergen, L. G., and G. G. Borisy. 1980. Head-to-tail polymerization of microtubules *in vitro*. J. Cell Biol. 84: 141.

Bergen, L. G., R. Kuriyama, and G. G. Borisy. 1980. Polarity of microtubules nucleated by centrosomes and chromosomes of chinese hamster ovary cells *in vitro*. J. Cell Biol. 84: 151.

Bergfeld, R., V. Speth, and P. Schopfer. 1988. Reorientation of microfibrils and microtubules at the outer epidermal wall of maize coleoptiles during auxin-mediated growth. Bot. Acta. 101: 57.

Berkowitz, S. A., and J. Wolff. 1981. Intrinsic calcium sensitivity of tubulin polymerization. The contribution of temperature, tubulin concentration and associated proteins. J. Biol. Chem. 256: 11216.

Berns, M., and S. M. Richardson. 1977. Continuation of mitosis after selective microbeam destruction of the centriolar region. J. Cell Biol. 75: 977.

Binder, L. I., W. L. Dentler, and J. L. Rosenbaum. 1975. Assembly of chick brain tubulin onto flagellar microtubules from *Chlamydomonas* and sea urchin sperm. Proc. Natl Acad. Sci. USA. 72: 1122.

Blakeslee, A. 1937. Dédoublement du nombre de chromosomes chez les plantes par traitment chimique. C. R. Acad. Sci. (Paris). 205: 476.

Böhm, K. J., W. Vater, H. Fenske, and E. Unger. 1984. Effect of microtubule-associated proteins on the protofilament number of microtubules assembled *in vitro*. Biochim. Biophys. Acta. 800: 119.

Bonne, D., and D. Pantaloni. 1982. Mechanism of tubulin assembly: guanosine 5'-triphosphate hydrolysis decreases the rate of microtubule depolymerization. Biochemistry. 21: 1075.

Bordas, J., E. M. Mandelkow, and E. Mandelkow. 1983. Stages of tubulin assembly and disassembly studied by time-resolved synchrotron X-ray scattering. J. Mol. Biol. 164: 89.

Borisy, G. G., J. M. Marcum, J. B. Olmsted, D. B. Murphy, and K. A. Johnson. 1975. Purification of tubulin and associated high molecular weight proteins from porcine brain and characterization of microtubule assembly *in vitro*. Ann, NY Acad. Sci. 253: 107.

Borisy, G. G., and E. W. Taylor. 1967a. The mechanism of action of colchicine. Colchicine binding to sea-urchin eggs and the mitotic apparatus. J. Cell Biol. 34: 535.

Borisy, G. G., and E. W. Taylor. 1967b. The mechanism of action of colchicine. Binding of colchicine ^{3}H to cellular protein. J. Cell Biol. 34: 525.

Bradley, M. O. 1973. Microfilaments and cytoplasmic streaming: inhibition of streaming by cytochalasin. J. Cell Sci. 12: 327.

Bray, D. 1979. Stops and starts in microtubules. Nature. 280: 537.

Bray, D., and M. B. Bunge. 1981. Serial analysis of microtubules in cultured rat sensory axons. J. Neurocytol. 10: 589.

Brinkley, B. R. 1985. Microtubule organizing centers. Ann. Rev. Cell Biol. 1: 145.

Brinkley, B. R., S. M. Cox, and S. H. Fistel. 1981a. Organizing centers for cell processes. Neurosci. Res. Prog. Bull. 19: 106.

Brinkley, B. R., S. M. Cox, D. A. Pepper, L. Wible, S. L. Brenner, and R. L. Pardue. 1981b. Tubulin assembly sites and the organization of cytoplasmic microtubules in cultured mammalian cells. J. Cell Biol. 90: 557.

Brinkley, B. R., G. M. Fuller, and D. P. Highfield. 1976. Tubulin antibodies as probes for microtubules in dividing and nondividing mammalian cells. In: Cell Motility, , Goldman, R., Pollard, T., Rosenbaum, J., Eds., pp. 435-456. Cold Spring Harbor, NY. Cold Spring Harbor Lab.

Brower, D. L., and P. K. Hepler. 1976. Microtubules and secondary wall deposition in xylem: the effects of isopropyl N-phenylcarbamate. Protoplasma. 87: 91.

Brown, D. L., and G. B. Bouck. 1974. Microtubule biogenesis and cell shape in *Ochromonas*. III. Effects of the herbicidal mitotic inhibitor isopropyl N-phenylcarbamate on shape and flagellum regeneration. J. Cell Biol. 61: 514.

Brown, D. L., A. Massalski, and R. Patenaude. 1976. Organization of the flagellar apparatus and associated cytoplasmic microtubules in the quadriflagellate alga *Polytomella agilis*. J. Cell Biol. 69: 106.

Brown, D. L., M. E. Stearns, and T. H. MacRae. 1982. Microtubule organizing centres. In: The Cytoskeleton in Plant Growth and Development, Lloyd, C. W., Ed., pp. 55-83. London. Academic Press.

Bryan, J., and L. Wilson. 1971. Are cytoplasmic microtubules heteropolymers? Proc. Natl Acad. Sci. USA. 68: 1762.

Bulinski, J. C., J. E. Richards, and G. Piperno. 1988. Posttranslational modification of α-tubulin: detyrosination and acetylation differentiate populations of interphase microtubules in cultured cells. J. Cell Biol. 106: 1213.

Burns, R. 1987. Tubulin's terminal tyrosine. Nature. 327: 103.

Burton, P. R., and R. H. Himes. 1978. Electron microscope studies of pH effects on assembly of tubulin free of associated proteins. Delineation of substructure by tannic acid staining. J. Cell Biol. 77: 120.

Busby, C. H., and B. E. S. Gunning. 1983. Orientation of microtubules against transverse cell walls in roots of *Azolla pinnata* R. Br. Protoplasma. 116: 78.

Busby, C. H., and B. E. S. Gunning. 1984. Microtubules and morphogenesis in stomata of the water fern *Azolla*: An unusual mode of guard cell and pore development. Protoplasma. 122: 108.

Buttlaire, D. H., B. A. Czuba, and T. H. Stevens. 1980. Manganous ion binding to tubulin. J. Biol. Chem. 255: 2164.

Calarco-Gillam, P. D., M. C. Siebert, R. Hubble, T. Mitchison, and M. Kirschner. 1983. Centrosome development in early mouse embryos are defined by an autoantibody against pericentriiolar material. Cell. 35: 621.

Cambray-Deakin, M. A., and R. D. Burgoyne. 1987. Posttranslational modifications of α-tubulin: acetylated and detyrosinated forms in axons of rat cerebellum. J. Cell Biol. 104: 1569.

Cambray-Deakin, M. A., and R. D. Burgoyne. 1987. Posttranslational modifications of α-tubulin: acetylated and detyrosinated forms in axons of rat cerebellum. J. Cell Biol. 104: 1569.

Caplow, M., G. M. Langford, and B. Zeeberg. 1982. Concerning the efficiency of the treadmilling phenomenon with microtubules. J. Biol. Chem. 257: 15012.

Caplow, M., J. Shanks, and B. P. Brylawski. 1985. Concerning the location of the GTP hydrolysis site on microtubules. Can. J. Biochem. Cell Biol. 63: 422.

Carlier, M.-F. 1988. Role of nucleotide hydrolysis in the polymerization of actin and tubulin. Cell Biophysics. 12: 105.

Carlier, M.-F., T. Hill, and Y.-D. Chen. 1984. Interference of GTP hydrolysis in the mechanism of microtubule assembly: An experimental study. Proc. Natl. Acad. Sci. USA. 81: 771.

Carlier, M. F., R. Melki, D. Pantaloni, T. L. Hill, and Y. Chen. 1987. Synchronous oscillations in microtubule polymerization. Proc. Natl. Acad. Sci. USA. 84: 5257.

Carlier, M. F., and D. Pantaloni. 1978. Kinetic analysis of cooperativity in tubulin polymerization in the presence of guanosine di- or triphosphate nucleotides. Biochemistry. 17: 1908.

Carlier, M. F., and D. Pantaloni. 1982. Assembly of microtubule protein: role of guanine di- and triphosphate nucleotides. Biochemistry. 21: 1215.

Carlier, M. F., and D. Pantaloni. 1985. Role of nucleoside-triphosphate hydrolysis in the dynamics of microtubules and microfilaments assembly. In: Microtubules and microtubule inhibitors, Ed., pp. 61-69. Amsterdam. Elsevier.

Caron, J. M., A. L. Jones, and M. W. Kirschner. 1985. Autoregulation of tubulin synthesis in hepatocytes and fibroblasts. J. Cell Biol. 101: 1763.

Cavalier-Smith, T. 1975. The origin of nuclei and of eukaryotic cells. Nature. 256: 463.

Cavalier-Smith, T. 1978. The evolutionary origin and phylogeny of microtubules, mitotic spindles and eukaryotic flagella. BioSystems. 10: 93.

Chalfie, M., and J. N. Thomson. 1982. Structural and functional diversity in neuronal microtubules of *Caenorhabditis elegans*. J. Cell Biol. 93: 15.

Clayton, L., C. M. Black, and C. W. Lloyd. 1985. Microtubule nucleating sites in higher plant cells identified by an auto-antibody against pericentriolar material. J. Cell Biol. 101: 319.

Clayton, L., and C. W. Lloyd. 1985. Actin organisation during the cell cycle in meristematic plant cells. Actin is present in the cytokinetic phragmoplast. Exp. Cell Res. 156: 231.

Cleary, A. L., and A. R. Hardham. 1988. Depolymerization of mictrotubule arrays in root tip cells by oryzalin, and their recovery with modified nucleation patterns. Can. J. Bot. (in press).

Cleveland, D. W. 1983. The tubulins: form DNA to RNA to protein and back again. Cell. 34: 330.

Cleveland, D. W., M. A. Lopata, P. Sherline, and M. W. Kirschner. 1981. Unpolymerized tubulin modulates the level of tubulin mRNAs. Cell. 25: 537.

Cleveland, D. W., M. F. Pittenger, and J. R. Feramisco. 1983. Elevation of tubulin levels by microinjection suppresses new tubulin synthesis. Nature (London). 305: 738.

Cleveland, D. W., and K. F. Sullivan. 1985. Molecular biology and genetics of tubulin. Ann. Rev. Biochem. 54: 331.

Correia, J. J., L. T. Baty, and R. C. Williams, Jr. 1987. Mg^{2+} dependence of guanine nucleotide binding to tubulin. J. Biol. Chem. 262: 17278.

Cote, R. H., L. G. Bergen, and G. G. Borisy. 1980. Head-to-tail polymerization of microtubules *in vitro*: a review. In: Microtubules and microtubule inhibitors De Brabander, M., De Mey, J., Eds., pp. 325-338. Amsterdam. Elsevier/North.

Cote, R. H., and G. G. Borisy. 1981. Head-to-tail polymerization of microtubules *in vitro*. J. Mol. Biol. 150: 577.

Cyr, R. J., and B. A. Palevitz. Microtubule-binding proteins from carrot. I. Initial characterization and microtubule bundling. Planta. In Press.

David-Pfeuty, T., and P. Huitorel. 1980. Tubulin polymerization in the presence of GMP-PCP. Biochem. Biophys. Res. Comm. 95: 535.

Davis, C., and K. Gull. 1983. Protofilament number in microtubules in cells of two parasitic nematodes. J. Parisitol. 69: 1094.

De Brabander, M., G. Geuens, J. De Mey, and M. Joniau. 1981. Nucleated assembly of mitotic microtubules in living PTK2 cells after release from Nocodazole treatment. Cell Motility. 1: 469.

De Brabander, M., G. Geuens, R. Nuydens, R. Willebrords, and J. De Mey. 1980. The microtubule nucleating and organizing activity of kinetochores and centrosomes in living PTK2-cells. In: Microtubules and Microtubule Inhibitors 1980, De Brabander, M., De Mey, J., Eds., pp. 255-268. Amsterdam. Elsevier/North.

Deery, W. J., and B. R. Brinkley. 1983. Cytoplasmic microtubule assembly-disassembly from endogenous tubulin in Brij-lysed cell models. J. Cell Biol. 96: 1631.

De Mey, J., A. M. Lambert, A. S. Bajer, M. Moeremans, and M. De Brabander. 1982. Visualization of microtubules in interphase and mitotic plant cells of *Haemanthus* endosperm with the immuno-gold staining method. Proc. Natl. Acad. Sci. USA. 79: 1898.

De Mey, J., M. Moeremans, G. Geuens, R. Nuydens, H. Van Belle, and M. De Brabander. 1980. Immunocytochemical evidence for the association of calmodulin with microtubules of the mitotic apparatus. In: Microtubules and Microtubule Inhibitors, De Brabander, M., De Mey, J., Eds., pp. 227-241. Amsterdam. Elsevier/North.

Derksen, J., G. Jeucken, J. A. Traas, and A. A. M. Van Lammeren. 1986. The microtubular skeleton in differentiating root tips of *Raphanus sativus* L. Acta Bot. Neerl. 35: 223.

Derksen, J., E. S. Pierson, and J. A. Traas. 1985. Microtubules in vegetative and generative cells of pollen tubes. Eur. J. Cell Biol. 38: 142.

Dickinson, H. G., and J. M. Sheldon. 1984. A radial system of microtubules extending between the nuclear envelope and the plasma membrane during early male haplophase in flowering plants. Planta. 161: 86.

Diggins, M. A., and W. F. Dove. 1987. Distribution of acetylated alpha-tubulin in *Physarum polycephalum*. J. Cell Biol. 104: 303.

Dustin, P. 1984. Microtubules, 2nd Edn. pp. 482. Berlin, Heidelberg, New York, Tokyo. Springer.

Eagle, G. R., R. R. Zombola, and R. H. Himes. 1983. Tubulin-zinc interactions: binding and polymerization studies. Biochemistry. 22: 221.

Edde, B., C. Jeantet, and F. Gros. 1981. One β tubulin subunit accumulates during neurite outgrowth in mouse neuroblastoma cells. Biochem. Biophys. Res. Commun. 3: 1035.

Eichenlaub-Ritter, U., and J. B. Tucker. 1984. Microtubules with more than 13 protofilaments in the dividing nuclei of ciliates. Nature. 307: 60.

Emons, A. M. C. 1982. Microtubules do not control microfibril orientation in a helicoidal cell wall. Protoplasma. 113: 85.

Emons, A. M. C., and A. M. C. Wolters-Arts. 1983. Cortical microtubules and microfibril deposition in the cell wall of root hairs of *Equisetum hyemale*. Protoplasma. 117: 68.

Erickson, H. P., and W. A. Voter. 1976. Polycation-induced assembly of purified tubulin. Proc. Natl Acad. Sci. USA. 73: 2813.

Euteneuer, U., W. T. Jackson, and J. R. McIntosh. 1982. Polarity of spindle microtubules in *Haemanthus* endosperm. J. Cell Biol. 94: 644.

Euteneuer, U., and J. R. McIntosh. 1980. The polarity of midbody and phragmoplast microtubules. J. Cell Biol. 87: 509.

Euteneuer, U., and J. R. McIntosh. 1981a. Polarity of some motility-related microtubules. Proc. Natl Acad. Sci. USA. 78: 372.

Euteneuer, U., and R. J. McIntosh. 1981b. Structural polarity of kinetochore microtubules in PtK1 cells. J. Cell Biol. 89: 338.

Evans, L., T. Mitchison, and M. Kirschner. 1985. The influence of the centrosome on the structure of the nucleated microtubule. J. Cell Biol. 100: 1185.

Falconer, M. M., G. Donaldson, and R. W. Seagull. 1988. MTOCs in higher plant cells: an immunofluorescent study of microtubule assembly sites following depolymerization by APM. Protoplasma. 144:46.

Falconer, M. M., and R. W. Seagull. 1985a. Immunofluorescent and calcofluor white staining of developing tracheary elements in *Zinnia elegans* L. suspension cultures. Protoplasma. 125: 190.

Falconer, M. M., and R. W. Seagull. 1985b. Xylogenesis in tissue culture: taxol effects on microtubule reorientation and lateral association in differentiating cells. Protoplasma. 128: 157.

Falconer, M. M., and R. W. Seagull. 1986. Xylogenesis in tissue culture II: microtubules, cell shape and secondary wall patterns. Protoplasma. 133: 140.

Falconer, M. M., and R. W. Seagull. 1987. Amiprophos-methyl(APM): a rapid, reversible, anti-microtubule agent for plant cell cultures. Protoplasma. 136: 118.

Farrell, K. W., and M. A. Jordan. 1982. A kinetic analysis of assembly-disassembly at opposite microtubule ends. J. Biol Chem. 257: 3131.

Farrell, K. W., M. A. Jordan, H. P. Miller, and L. Wilson. 1987. Phase dynamics at microtubule ends: the coexistence of microtubule length changes and treadmilling. J. Cell Biol. 104: 1035.

Fellous, A., J. Francon, A.-M. Lennon, and J. Nunez. 1977. Microtubule assembly *in vitro*. Euro. J. Biochem. 78: 167.

Forsberg, C. 1965. Nutritional studies of *Chara* in axenic cultures. Physiologia Pl. 18: 275.

Fujiwara, K., and R. W. Link. 1982. The use of tannic acid in microtubule research. In: Methods in Cell Biology, Vol 24, The Cytoskeleton, Part A, Cytoskeletal Proteins, Isolation and Characterisation, Wilson, L., Ed., pp. 217-233. New York. Academic Press.

Fulton, C., and P. A. Simpson. 1976. Selective synthesis and utilization of flagellar tubulin. The multitubulin hypothesis. In: Cell Motility, Goldman, R., Pollard, T., Rosenbaum, J., Eds., pp. 987-1005. New York. Cold Spring Harbour Publications.

Galatis, B. 1982. The organization of microtubules in guard cell mother cells of *Zea mays*. Can. J. Bot. 60:1148.

Galatis, B., P. Apostolakos, and C. H. R. Katsaros. 1983. Microtubules and their organizing centres in differentiating guard cells of *Adiantum capillus veneris*. Protoplasma. 115:176.

Galway, M. E., and A. R. Hardham. 1986. Microtubule reorganization, cell wall synthesis and establishment of the axis of elongation in regenerating protoplasts of the alga *Mougeotia*. Protoplasma. 135:130.

Gard, D. L., and M. W. Kirschner. 1985. A polymer-dependent increase in phosphorylation of β-tubulin accompanies differentiation of a mouse neuroblastoma cell line. J. Cell Biol. 100: 764.

Gard, D. L., and M. W. Kirschner. 1987. A microtubule-associated protein from *Xenopus* eggs that specifically promotes assembly at the plus end. J. Cell Biol. 105: 2203.

Gaskin, F., C. R. Cantor, and M. L. Shelanski. 1974. Turbidimetric studies of the *in vitro* assembly and disassembly of porcine neurotubules. J. Mol. Biol. 89: 737.

Gaskin, F., and Y. Kress. 1977. Zinc ion-induced assembly of tubulin. J. Biol. Chem. 252: 6918.

Geahlen, R. L., and B. E. Haley. 1979. Use of GTP photoaffinity probe to resolve aspects of the mechanism of tubulin polymerization. J. Biol. Chem. 254: 11982.

Gertel, E. T., and P. B. Green. 1977. Cell growth pattern and wall microfibrillar arrangement. Experiments with *Nitella*. Plant Physiol. 60: 247.

Geuens, G., G. G. Gundersen, R. Nuydens, F. Cornelissen, J. C. Bulinski, and M. DeBrabander. 1986. Ultrastructural colocalization of tyrosinated and detyrosinated α-tubulin in interphase and mitotic cells. J. Cell Biol. 103: 1883.

Gibbons, I. R. 1977. Structure and function of flagellar microtubules. In: International Cell Biology. 1976-1977, Brinkley, B. R., Porter, K. R., Eds., pp. 348-357. New York. Rockefeller Univ. Press. USA.

Giddings, T. H., Jr., and L. A. Staehelin. 1988. Spatial relationship between microtubules and plasma-membrane rosettes during the deposition of primary wall microfibrils in *Closterium* sp. Planta. 173: 22.

Giloh, H., and J. W. Sedat. 1982. Fluorescence microscopy: reduced photobleaching of rhodamine and fluorescein protein conjugates by n-propyl gallate. Science. 217: 1252.

Goodenough, U. W., and R. L. Weiss. 1978. Interrelationships between microtubules, a striated fiber, and the gametic mating structure of *Chlamydomonas reinhardi*. J. Cell Biol. 76: 430.

Gorter, C. 1945. De invloed van colchicine of den groei van den celwand van wortelharen. Proc. K. Ned. Akad. Wet. 48: 3.

Gould, R. R., and G. G. Borisy. 1977. The pericentriolar material in Chinese hamster cells nucleates microtubule formation. J. Cell Biol. 73: 601.

Green, P. B. 1954. The spiral growth pattern of the cell wall in *Nitella axillaris*. Am. J. Bot. 41: 403.

Green, P. B. 1958. Structural characteristics of developing *Nitella* internodal cell walls. J. Biophysic. and Biochem. Cytol. 4: 505.

Green, P. B. 1960. Multinet growth in the cell wall of *Nitella*. J. Biophysic. and Biochem. Cytol. 7(2): 289.

Green, P. B. 1962. Mechanism for plant cellular morphogenesis. Science. 138: 1404.

Green, P. B. 1963. On mechanisms of elongation. In: Cytodifferentiation and Macromolecular Synthesis, Locke, M., Ed., pp. 203-234. NewYork. Academic Press Inc.

Green, P. B. 1964. Cinematic observations on the growth and division of chloroplasts in *Nitella*. Amer. J. Bot. 51: 334.

Green, P. B. 1968. Growth physics in *Nitella*: a method for continuous *in vivo* analysis of extensibility based on a micro-manometer technique for turgor pressure. Plant Physiol. 43: 1169.

Green, P. B. 1980. Organogenesis- a biophysical view. Ann. Rev. Plant Physiol. 31: 51.

Green, P. B. 1984. Shifts in plant cell axiality: histogenic influences on cellulose orientation in the succulent, *Graptopetalum*. Dev. Biol. 103: 18.

Green, P. B., and G. B. Chapman. 1955. On the development and structure of the cell wall in *Nitella*. Am. J. Bot. 42: 685.

Green, P. B., and J. C. W. Chen. 1960. Concerning the role of wall stresses in the elongation of the *Nitella* cell. Z. wiss. Mikroscop. 64: 482.

Green, P. B., R. O. Erickson, and J. Buggy. 1971. Metabolic and physical control of cell elongation rate. *In vivo* studies in *Nitella*. Plant Physiol. 47: 423.

Green, P. B., R. O. Erickson, and P. A. Richmond. 1970. On the physical basis of cell morphogenesis. Ann. New York Acad. Sci. 175: 712.

Green, P. B., and A. King. 1966. A mechanism for the origin of specifically oriented textures in development with special reference to *Nitella* wall texture. Aust. J. Biol. Sci. 19: 421.

Griffith, L. M., and T. D. Pollard. 1982. The interaction of actin filaments with microtubules and microtubule-associated proteins. J. Biol. Chem. 257: 9143.

Grimm, I., H. Sachs, and D. G. Robinson. 1976. Structure, synthesis and orientation of microfibrils. II. The effects of colchicine on the wall of *Oocystis solitaria*. Cytobiologie. 14: 61.

Gundersen, G. G., and J. C. Bulinski. 1986a. Distribution of tyrosinated and nontyrosinated α-tubulin during mitosis. J. Cell Biol. 102: 1118.

Gundersen, G. G., and J. C. Bulinski. 1986b. Microtubule arrays in differentiated cells contain elevated levels of a post-translationally modified form of tubulin. Eur. J. Cell Biol. 42:288.

Gundersen, G. G., M. H. Kalnoski, and J. C. Bulinski. 1984. Distinct populations of microtubules: Tyrosinated and nontyrosinated alpha tubulin are distributed differently *in vivo*. Cell. 38: 779.

Gundersen, G. G., S. Khawaja, and J. C. Bulinski. 1987. Postpolymerization detyrosination of α-tubulin: a mechanism for subcellular differentiation of microtubules. J. Cell Biol. 105: 251.

Gunning, B. E. S. 1980. Spatial and temporal regulation of nucleating sites for arrays of cortical microtubules in root tip cells of the water fern *Azolla pinnata*. Eur. J. Cell Biol. 23: 53.

Gunning, B. E. S. 1981. Microtubules and cytomorphogenesis in a developing organ: The root primordium of *Azolla pinnata*. In: Cytomorphogenesis in Plants, Kiermayer, O., Ed., pp. 301-325. Wein. Springer.

Gunning, B. E. S., and A. R. Hardham. 1982. Microtubules. Ann. Rev. Plant Physiol. 33: 651.

Gunning, B. E. S., A. R. Hardham, and J. E. Hughes. 1978. Pre-prophase bands of microtubules in all categories of formative and proliferative cell division in *Azolla* roots. Planta. 143: 145.

Gunning, B. E. S., and S. M. Wick. 1985. Preprophase bands, phragmoplasts and spatial control of cytokinesis. J. Cell Sci. Suppl. 2: 157.

Gyenes, M., and R. Saxena. 1985. Existence of a membrane between the chloroplast layer and the moving cytoplasm in the cells of *Nitellopsis obtusa* and *Nitella transluscens*. Biophysics. 30: 901.

Haimo, L. T., B. R. Telzer, and J. L. Rosenbaum. 1979. Dynein binds to and crossbridges cytoplasmic microtubules. Proc. Natl Acad. Sci. U.S.A. 76: 5759.

Hammel, E., A. A. Del Campo, M. C. Lowe, P. G. Waxman, and C. M. Lin. 1982. Effects of organic acids on tubulin polymerization and associated guanosine 5'-triphosphate hydrolysis. Biochemistry. 21: 503.

Hardham, A. R., P. B. Green, and J. M. Lang. 1980. Reorganization of cortical microtubules and cellulose deposition during leaf formation in *Graptopetalum paraguayense*. Planta. 149:181.

Hardham, A. R., and B. E. S. Gunning. 1978. Structure of cortical microtubule arrays in plant cells. J. Cell Biol. 77: 14.

Hardham, A. R., and B. E. S. Gunning. 1980. Some effects of colchicine on microtubules and cell division in roots of *Azolla pinnata*. Protoplasma. 102: 31.

Harper, J. D. I., J. M. Mitchison, R. E. Williamson, and P. C. L. John. 1989. Does the autoimmune serum 5051 specifically recognize microtubule organising centres in plant cells? Manuscript in Preparation. :.

Haskins, K. M., R. R. Zombola, J. M. Boling, Y. C. Lee, and R. H. Himes. 1980. Tubulin assembly induced by cobalt and zinc. Biochem. Biophys. Res. Comm. 95: 1703.

Hawes, C. R. 1985. Conventional and high voltage electron microscopy of the cytoskeleton and cytoplasmic matrix of carrot (*Daucus carota* L.) cells grown in suspension culture. Eur. J. Cell Biol. 38: 201.

Hayashi, M., and F. Matsumura. 1975. Calcium binding to bovine brain tubulin. FEBS Lett. 58: 222.

Heath, I. B. 1974. A unified hypothesis for the role of membrane bound enzyme complexes and microtubules in plant cell wall synthesis. J. Theor. Biol. 48: 445.

Heath, I. B., and R. W. Seagull. 1982. Oriented cellulose fibrils and the cytoskeleton: a critical comparison of models. In: The Cytoskeleton in Plant Growth and Development, Lloyd, C. W., Ed., pp. 163-182. London. Academic Press.

Heidemann, S. R., and J. R. McIntosh. 1980. Visualization of the structural polarity of microtubules. Nature. 286: 517.

Hepler, P. K., and D. E. Fosket. 1971. The role of microtubules in vessel number differentiation in *Coleus*. Protoplasma. 72: 213.

Hepler, P. K., and E. H. Newcomb. 1964. Microtubules and fibrils in the cytoplasm of *Coleus* cells undergoing secondary wall deposition. J. Cell Biol. 20: 529.

Hepler, P. K., and B. A. Palevitz. 1974. Microtubules and microfilaments. Ann. Rev. Plant Physiol. 25: 309.

Hertel, C., and D. Marme. 1983. Herbicides and fungicides inhibit Ca^{2+} uptake by plant mitochodria: a possible mechanism of action. Pestic. Biochem. Physiol. 19: 282.

Herth, W. 1980. Calcofluor white and congo red inhibit chitin microfibril assembly of *Poterioochromonas*. Evidence for a gap between polymerization and microfibril formation. J. Cell Biol. 87: 442.

Herth, W. 1985. Plasma-membrane rosettes involved in localized wall thickening during xylem formation of *Lepidium sativum* L. Planta. 164: 12.

Hesse, J., M. Thierauf, and H. Ponstingl. 1987. Tubulin sequence region β155-174 is involved in binding exghangeable guanosine triphosphate. J. Biol. Chem. 262: 15472.

Heusele, C., D. Bonne, and M.-F. Carlier. 1987. Is microtubule assembly a biphasic process? A fluorimetric study using 4',6-diamidino-2-phenylindole as a probe. Eur. J. Biochem. 165: 613.

Hill, T. L., and M.-F. Carlier. 1983. Steady-state theory of the interference of GTP hydrolysis in the mechanism of microtubule assembly. Proc. Natl Acad. Sci. USA. 80: 7234.

Hill, T. L., and M. W. Kirschner. 1982. Bioenergetics and kinetics of microtubule and actin filament assembly-disassembly. Int. Rev. Cytol. 78: 1.

Himes, R. H., P. R. Burton, and J. M. Gaito. 1977. Dimethyl sulfoxide-induced self-assembly of tubulin lacking associated proteins. J. Biol. Chem. 252: 6222.

Himes, R. H., P. R. Burton, R. N. Kersey, and G. B. Pierson. 1976. Brain tubulin polymerization in the absence of microtubule-associated proteins. Proc. Natl. Acad. Sci. USA. 73: 4397.

Himes, R. H., Y. L. Lee, G. R. Eagle, K. M. Haskins, S. D. Babler, and J. Ellermeier. 1982. The relationship between cobalt binding to tubulin and the stimulation of assembly. J. Biol. Chem. 257: 5839.

Hoffmann, F. 1986. Formation and reorientation of cortical microtubular lattices in cultured protoplasts. Plant Physiol. 80: 69s.

Hogan, C. J. 1987. Microtubule patterns during meiosis in two higher plant species. Protoplasma. 138: 126.

Hogetsu, T. 1986. Re-formation of microtubules in *Closterium ehrenbergii* Meneghini after cold-induced depolymerization. Planta. 167: 437.

Hogetsu, T., and Y. Oshima. 1985. Immunofluorescence microscopy of microtubule arrangement in *Closterium acerosum* (Schrank) Ehrenberg. Planta. 166: 169.

Hogetsu, T., and H. Shibaoka. 1978. Effects of colchicine on cell shape and on microfibril arrangement in the cell wall of *Closterium acerosum*. Planta. 140: 15.

Hollenbeck, P. J., and K. Chapman. 1986. A novel microtubule-associated protein from mammalian nerve shows ATP-sensitive binding to microtubules. J. Cell Biol. 103: 1539.

Hope, A. B., and N. A. Walker. 1975. The physiology of giant algal cells. pp. 201. London:. Cambridge University Press.

Horio, T., and H. Hotani. 1986. Visualization of the dynamic instability of individual microtubules by dark-field microscopy. Nature. 321: 605.

Hotchkiss, A. T., Jr., and R. M. Brown, Jr. 1987. The association of rosette and globule terminal complexes with cellulose microfibril assembly in *Nitella translucens var. Axillaris* (Charophyceae). J. Phycol. 23: 229.

Huber, G., G. Pehling, and A. Matus. 1986. The novel microtubule-associated protein MAP3 contributes to the *in vitro* assembly of brain microtubules. J. Biol. Chem. 261: 2270.

Hyams, J. S. 1982. Microtubules. In: The Cytoskeleton in Plant Growth and Development, Lloyd, C. W., Ed., pp. 31-53. London. Academic Press.

Inoué, S., J. Molè-Bajer, and A. S. Bajer. 1985. Three-dimensional distribution of microtubules in *Haemanthus* endosperm cells. In: Microtubules and microtubule inhibitors 1985, DeBrabander, M., DeMey, J., Eds., pp. 269-276. Amsterdam. Elsevier Science Publishers.

Itoh, T., and K. Shimaji. 1976. Orientation of microfibrils and microtubules in cortical parenchyma cells of poplar during elongation growth. Bot. Mag. Tokyo. 89: 291.

Jackson, W. T., and B. G. Doyle. 1982. Membrane distribution in dividing endosperm cells of *Haemanthus*. J. Cell Biol. 94: 637.

Jacobs, M. 1979. Tubulin and nucleotides. In: Microtubules, , Roberts, K., Hyams, J. S., Eds., pp. 255-277. London, New York, Toronto, Sydney, San Francisco. Academic Press.

Jacobs, M., and M. Caplow. 1976. Microtubular protein reaction with nucleotides. Biophys. Biochem. Res. Comm. 68: 127.

Jacobs, M., and P. Huitorel. 1979. Tubulin-associated nucleoside diphosphokinase. Eur. J. Biochem. 99: 613.

Jacobs, M., H. Smith, and E. W. Taylor. 1974. Tubulin: nucleotide binding and enzyme activity. J. Molec. Biol. 89: 455.

Jameson, L., and M. Caplow. 1980. Effect of guanosine diphosphate on microtubule assembly and stability. J. Biol Chem. 255: 2284.

Jameson, L., T. Frey, B. Zeeberg, F. Dalldorf, and M. Caplow. 1980. Inhibition of microtubule assembly by phosphorylation of microtubule-associated proteins. Biochemistry. 19: 2472.

Jemiolo, D. K., and C. M. Grisham. 1982. Divalent cation-nucleotide complex at the exchangeable nucleotide binding site of tubulin. J. Biol. Chem. 257: 8148.

Job, D., M. Pabion, and R. L. Margolis. 1985. Generation of microtubule stability subclasses by microtubule-associated proteins: Implications for the microtubule "dynamic instability" model. J. Cell Biol. 101: 1680.

Johnson, K. A., and G. G. Borisy. 1977. Kinetic analysis of microtubule self-assembly *in vitro*. J. Mol. Biol. 117: 1.

Jones, J. C. R., and J. B. Tucker. 1981. Microtubule-organizing centres and assembly of the double-spiral microtubule pattern in certain heliozoan axonemes. J. Cell Sci. 50: 259.

Joshi, H. C., T. J. Yen, and D. W. Cleveland. 1987. *In vivo* coassembly of a divergent β-tubulin subunit (cb6) into microtubules of different function. J. Cell Biol. 105: 2179.

Kakimoto, T., and H. Shibaoka. 1987a. Actin filaments and microtubules in the preprophase band and phragmoplast of tobacco cells. Protoplasma. 140:151.

Kakimoto, T., and H. Shibaoka. 1987b. A new method for preservation of actin filaments in higher plant cells. Plant Cell Physiol. 28:1581.

Kakiuchi, S., and K. Sobue. 1981. Ca^{2+}- and calmodulin-dependent flip-flop mechanism in microtubule assembly-disassembly. FEBS Lett. 132: 141.

Kamiya, N. 1962. Protoplasmic streaming. In: Handbuch der Pflanzenphysiologie, vol. 17 part 2, Ruhland, W., Ed., pp. 979-1035. Berlin, Gottingen, Heidelberg. Springer.

Kamiya, N. 1986. Cytoplasmic streaming in giant algal cells: a historical survey of experimental approaches. Bot. Mag. Tokyo. 99: 441.

Karr, T. L., D. Kristofferson, and D. L. Purich. 1980a. Calcium ion induces end-wise depolymerization of bovine brain microtubules. J. Biol. Chem. 255: 11853.

Karr, T. L., D. Kristofferson, and D. L. Purich. 1980b. Mechanism of microtubule depolymerization. J. Biol. Chem. 255: 8560.

Karr, T. L., A. E. Podrasky, and D. L. Purich. 1979. Participation of guanine nucleotides in nucleation and elongation steps of microtubule assembly. Proc. Natl. Acad. Sci. USA. 76: 5475.

Karr, T. L., and D. L. Purich. 1979. A microtubule assembly/disassembly model based on drug effects and depolymerization kinetics after dilution. J. Biol. Chem. 254: 10885.

Keates, R. A. B. 1980. Effects of glycerol on microtubule polymerization kinetics. Biochem. Biophys. Res. Comm. 95: 1163.

Kemphues, K., T. C. Kaufmann, R. A. Raff, and E. C. Raff. 1982. The testis specific β-tubulin subunit in Drosophila melanogaster has multiple functions in spermatogenesis. Cell. 31: 655.

Khan, M., and Y. S. R. K. Sarma. 1984. Cytogeography and Cytosystematics of Charophyta. In: Systematics of the Green Algae, Irvine, D. E. G., John, D. M., Eds., pp. 303-330. London and Orlando. Academic Press.

Khawaja, S., G. G. Gundersen, and J. C. Bulinski. 1988. Enhanced stability of microtubules enriched in detyrosinated tubulin is not a direct function of detyrosination level. J. Cell Biol. 106: 141.

Kilmartin, J. V., B. Wright, and C. Milstein. 1982. Rat monoclonal antitubulin antibodies derived by using a new nonsecreting rat cell line. J. Cell Biol. 93: 576.

Kirsch, M., and L. R. Yarbrough. 1981. Assembly of tubulin with nucleotide analogs. J. Biol Chem. 256: 106.

Kirschner, M., and T. Mitchison. 1986. Beyond self-assembly: from microtubules to morphogenesis. Cell. 45: 329.

Kirschner, M. W. 1980. Implications of treadmilling for the stability and polarity of actin and tubulin polymers *in vivo*. J. Cell Biol. 86: 330.

Kirschner, M. W., R. C. Williams, M. Weingarten, and J. C. Gerjart. 1974. Microtubules from the mammalian brain: some properties of their depolymerization products and a proposed mechanism of assembly and disassembly. Proc. Natl Acad. Sci. USA. 71: 1159.

Kobayashi, H., H. Fukuda, and H. Shibaoka. 1987. Reorganization of actin filaments associated with the differentiation of tracheary elements in *Zinnia* mesophyll cells. Protoplasma. 138: 69.

Kobayashi, T. 1975. Nucleotides bound to brain tubulin and reconstituted microtubules. J. Biochem. (Tokyo). 76: 201.

Kodowaki, T., Y. Fujita-Yamaguchi, E. Nishida, F. Takuka, T. Akiyama, S. Kathuria, Y. Akanuma, and M. Kasuga. 1985. Phosphorylation of tubulin and microtubule-associated proteins by the purified insulin receptor kinase. J. Biol. Chem. 260: 4016.

Koszka, C., R. Foisner, H. M. Seyfert, and G. Wiche. 1987. Isolation of a Ca^{2+}-protease resistant high Mr microtubule binding protein from mammalian brain: characterization of properties partially expected for a dynein-like molecule. Protoplasma. 138: 54.

Kreis, T. E. 1987. Microtubules containing detyrosinated tubulin are less dynamic. EMBO J. 6: 2597.

Kristofferson, D., T. Mitchison, and M. Kirschner. 1986. Direct observation of steady-state microtubule dynamics. J. Cell Biol. 102: 1007.

Kumagai, H., and E. Nishida. 1979. The interactions between calcium-dependent regulator protein of cyclic nucleotide phosphodiesterase and microtubule proteins. II. Association of calcium-dependent regulator protein with tubulin dimer. J. Bichem. 85: 1267.

Kumar, N., and M. Flavin. 1981. Preferential action of a brain detyrosinolating carboxypeptidase on polymerized tubulin. J. Biol. Chem. 256: 7678.

Kumar, N., and M. A. Flavin. 1982. Modulation of some parameters of assembly of microtubules *in vitro* by tyrosinolation of tubulin. J. Biochem. 128: 215.

Kunicki-Goldfinger, W. J. H. 1980. Evolution and endosymbiosis. In: Endocytobiology. Endosymbiosis and Cell Biology, Schwemmler, W., Schenk, H.E.A., Eds., pp. 969-984. Berlin, New York. Walter de Gruyter.

Kuriyama, R. 1975. Further studies ontubulin polymerization *in vitro*. J. Biochem. (Tokyo). 77: 23.

Kuriyama, R., and T. Miki-Nomoura. 1975. LIght microscopic observations of individual microtubules reconstituted from brain tubulin. J. Cell Sci. 19: 607.

Kuroda, K. 1964. The behaviour of naked cytoplasmic drops isolated from plant cells. In: Primitive Motile Systems in Cell Biology, Allen, R. D., Kamiya, N., Eds., pp. 31-41. New York, London. Academic Press.

Kuznetsov, S. A., V. I. Rodionov, V. I. Gelfand, and V. A. Rosenblat. 1981. Microtubule-associated protein MAP1 promotes microtubule assembly *in vitro*. FEBS Lett. 135: 241.

L'Hernault, S. W., and J. L. Rosenbaum. 1983. *Chlamydomonas* α-tubulin is posttransationally modified in the flagella during flagellar assembly. J. Cell Biol. 97: 258.

L'Hernault, S. W., and J. L. Rosenbaum. 1985a. *Chlamydomonas* α-tubulin is posttransationally modified by acetylation on the ε-group of a lysine. Biochemistry. 24: 473.

L'Hernault, S. W., and J. L. Rosenbaum. 1985b. Reversal of the posttranslational modification on *Chlamydomonas* flagellar α-tubulin occurs during flagellar resorption. J. Cell Biol. 100: 457.

La Claire, J. W., II. 1987. Microtubule cytoskeleton in intact and wounded coenocytic green algae. Planta. 171: 30.

Lambert, A. M. 1980. The role of chromosomes in anaphase trigger and nuclear envelope activity in spindle formation. Chromosoma. 76: 295.

Lancelle, S. A., D. A. Callaham, and P. K. Hepler. 1986. A method for rapid freeze fixation of plant cells. Protoplasma. 131: 153.

Lancelle, S. A., M. Cresti, and P. K. Hepler. 1987. Ultrastructure of the cytoskeleton in freeze-substituted pollen tubes of *Nicotiana alata*. Protoplasma. 140:141.

Lang, J. M., W. R. Eisinger, and P. B. Green. 1982. Effects of ethylene on the orientation of microtubules and cellulose microfibrils in pea epicotyl cells with polylamellate cell walls. Protoplasma. 110: 5.

Larsson, H., M. Wallin, and A. Edstrom. 1976. Induction of a sheet polymer of tubulin by Zn^{2+}. Exp. Cell Res. 100: 104.

Ledbetter, M. C. 1967. The disposition of microtubules in plant cells during interphase and mitosis. Symp. Int. Soc. Cell Biol. 6: 55.

Ledbetter, M. C., and K. R. Porter. 1963. A "microtubule" in plant cell fine structure. J. Cell. Biol. 19: 239.

LeDizet, M., and G. Piperno. 1986. Cytoplasmic microtubules containing acetylated α-tubulin in *Chlamydomonas reinhardtii*: spatial arrangement and properties. J. Cell Biol. 103: 13.

Lee, J. C., and S. N. Timasheff. 1975. The reconstitution of microtubules from purified calf brain tubulin. Biochemistry. 14: 5183.

Lee, J. C., and S. N. Timasheff. 1977. *In vitro* reconstitution of calf brain microtubules: effects of solution variables. Biochemistry. 16: 1754.

Lemischka, I., and P. A. Sharp. 1982. The sequence of an expressed rat α-tubulin gene and pseudogene with an inserted repetitive element. Nature. 300: 330.

Levi, A., M. Cimino, D. Mercanti, and P. Calissano. 1974. Studies on the binding of GTP to the microtubule protein. Biochim. Biophys. Acta. 365: 450.

Levy, S. 1987. A 3-D computer representation of helicoidal superstructures in biological materials, exemplified by the *Nitella* cell wall. Eur. J. Cell Biol. 44: 27.

Lin, B. -L., and J. A. Jernstedt. 1987. Microtubule organization in root cortical cells of *Hyacinthus orientalis*. Protoplasma. 140: 13.

Lloyd, C. W. 1984. Toward a dynamic helical model for the influence of microtubules on wall patterns in plants. Int. Rev. Cytol. 86: 1.

Lloyd, C. W. 1987. The plant cytoskeleton: the impact of fluorescence microscopy. Ann. Rev. Plant Physiol. 38: 119.

Lloyd, C. W., Ed. 1982. The Cytoskeleton in Plant Growth and Development. pp. 457. London, New York. Academic Press.

Lloyd, C. W., L. Clayton, P. J. Dawson, J. H. Doonan, J. S. Hulme, I. N. Roberts, and B. Wells. 1985. The cytoskeleton underlying side walls and cross walls in plants: Molecules and macromolecular assemblies. J. Cell Sci. 2: 143.

Lloyd, C. W., S. B. Lowe, and G. W. Peace. 1980a. The mode of action of 2,4-D in counteracting the elongation of carrot cells grown in culture. J. Cell Sci. 45: 257.

Lloyd, C. W., K. J. Pearce, D. J. Rawlins, R. W. Ridge, and P. J. Shaw. 1987. Endoplasmic microtubules connect the advancing nucleus to the tip of legume root hairs, but F-actin is involved in basipetal migration. Cell Motil. Cytoskel. 8: 27.

Lloyd, C. W., and R. W. Seagull. 1985. A new spring for plant cell biology: microtubules as dynamic helices. Trends in Biochem. Sci. 10: 476.

Lloyd, C. W., A. R. Slabas, A. J. Powell, and S. B. Lowe. 1980b. Microtubules, protoplasts and plant cell shape. Planta. 147: 500.

Lloyd, C. W., A. R. Slabas, A. J. Powell, G. MacDonald, and R. A. Badley. 1979. Cytoplasmic microtubules of higher plant cells visualised with anti-tubulin antibodies. Nature. 279: 239.

Lloyd, C. W., and B. Wells. 1985. Microtubules are at the tips of root hairs and form helical patterns corresponding to inner wall fibrils. J. Cell Sci. 75: 225.

Ludueña, R. F. 1979. Biochemistry of tubulin. In: Microtubules, , Roberts, K., Hyams, J. S., Eds., pp. 65-116. London. Academic.

Ludueña, R. F., A. Fellous, J. Francon, J. Nunez, and L. McManus. 1981. Effect of tau on the vinblastine-induced aggregation of tubulin. J. Cell Biol. 89: 680.

Maccioni, R. B., and N. W. Seeds. 1982. Residual nucleotide and tubulin's ability to polymerize with nucleotide analogs. J. Biol. Chem. 257: 3334.

Maccioni, R. B., and N. W. Seeds. 1983. Affinity labelling of tubulin's exchangeable guanosine 5'-triphosphate binding site. Biochemistry. 22: 1572.

MacNeal, R. K., and D. L. Purich. 1978. Chromium (III)-nucleotide complexes as probes of the guanosine 5'-triphosphate-induced microtubule assembly. Arch. Biochem. Biophys. 191: 233.

Mandelkow, E.-M., G. Lange, A. Jagla, U. Spann, and E. Mandelkow. 1988. Dynamics of the microtubule oscillator: role of the nucleotides and tubulin - MAP interactions. EMBO J. 7: 357.

Mandelkow, E., J. Thomas, and C. Cohen. 1977. Microtubule structure at low resolution by x-ray diffraction. Proc. Natl. Acad. Sci. USA. 74: 3370.

Mandelkow, E. M., A. Harmsen, E. Mandelkow, and .. Bordas. 1980. X-ray kinetic studies of microtubule assembly using synchrotron radiation. Nature. 287: 595.

Mandelkow, E. M., and E. Mandelkow. 1979. Junctions between microtubule walls. J. Mol. Biol. 129: 135.

Marchant, H. J. 1979. Microtubules, cell wall deposition and the determination of plant cell shape. Nature. 278: 167.

Marcum, J. M., and G. G. Borisy. 1978. Characterization of microtubule protein oligomers by analytical ultracentrifugation. J. Biol. Chem. 253: 2825.

Margolis, R. L. 1981. Role of GTP hydrolysis in microtubule treadmilling and assembly. Proc. Natl Acad. Sci. USA. 78: 1586.

Margolis, R. L., and Wilson. L. 1979. Regulation of the microtubule steady state *in vitro* by ATP. Cell. 18: 673.

Margulis, L., D. Chase, and L. To. 1979. Possible evolutionary significance of spirochetes. Proc. R. Soc. London. B 204: 189.

Margulis, L., L. To, and D. Chase. 1978. Microtubules in prokaryotes. Science. 200: 1118.

Margulis, L., L. To, and D. Chase. 1981. Microtubules, undulipodia and pillotina spirochetes. Ann. N. Y. Acad. Sci. 361: 356.

Martin, S. R., and P. M. Bayley. 1987. Effects of GDP on microtubules at steady state. Biophys. Chem. 27: 67.

Martin, S. R., F. M. M. Butler, D. C. Clark, J.-M. Zhou, and P. M. Bayley. 1987. Magnesium ion effects on microtubule nucleation *in vitro*. Biochim. Biophys. Acta. 914: 96.

Matsumura, F., and M. Hayashi. 1976. Polymorphism of tubulin assembly. *In vitro* formation of sheet, twisted ribbon and microtubule. Biochem. Biophys. Acta. 453: 162.

Matus, A., B. Riederer, and G. Huber. 1987. Influence of monoclonal antibodies on microtubule assembly. J. Neurochem. 49: 714.

Mazia, D. 1984. Centrosomes and mitotic poles. Exper. Cell Res. 153: 1.

McEwen, B., and S. J. Edelstein. 1980. Evidence for a mixed lattice in microtubules reassembled *in vitro*. J. Mol. Biol. 139: 123.

McGill, M., and B. R. Brinkley. 1975. Human chromosomes and centrioles as nuceating sites for the *in situ* assembly of microtubules from bovine brain tubulin. J. Cell Biol. 67: 189.

McIntosh, J. R. 1973. The axostyle of *Saccinobaculus*. II. Motion of the microtubule bundle and a structural comparison of straight and bent axostyles. J. Cell Biol. 56: 324.

McIntosh, J. R. 1981. Microtubule polarity and interaction in mitotic spindle function. In: International Cell Biology, 1980-81, Schweiger, H. G., Ed., pp. 359-368. Berlin. Springer.

McIntosh, J. R. 1984. Microtubule catastrophe. Nature. 312: 196.

McNiven, M. A., and K. R. Porter. 1986. Microtubule polarity confers direction to pigment transport in chromatophores. J. Cell Biol. 103: 1547.

McNiven, M. A., and K. R. Porter. 1988. Organization of microtubules in centrosome-free cytoplasm. J. Cell Biol. 106: 1593.

McNiven, M. A., M. Wang, and K. R. Porter. 1984. Microtubule polarity and the direction of pigment transport reverse simultaneously in surgically severed melanophore arms. Cell. 37: 753.

Menzel, D., and M. Schliwa. 1986. Motility in the siphonous green alga *Bryopsis*. I. Spatial organization of the cytoskeleton and organelle movement. Eur. J. Cell Biol. 40: 275.

Métraux, J.-P. 1982. Changes in cell-wall polysaccharide composition of developing *Nitella* internodes. Analysis of walls of single cells. Planta. 155: 459.

Métraux, J.-P., P. A. Richmond, and L. Taiz. 1980. Control of cell elongation in *Nitella* by endogenous cell wall pH gradients: multiaxial extensibility and growth studies. Plant Physiol. 65: 204.

Métraux, J.-P., and L. Taiz. 1978. Transverse viscoelastic extension in *Nitella*. I. Relationship to growth rate. Plant Physiol. 61: 135.

Mita, T., and M. Katsumi. 1986. Gibberellin control of microtubule arrangement in the mesocotyl epidermal cells of the d5 mutant of *Zea mays* L. Plant & Cell Physiol. 27: 651.

Mita, T., and H. Shibaoka. 1983. Changes in microtubules in onion leaf sheath cells during bulb development. Plant & Cell Physiol. 24: 109.

Mitchison, T., L. Evans, E. Schulze, and M. Kirscher. 1986. Sites of microtubule assembly and disassembly in the mitotic spindle. Cell. 45: 515.

Mitchison, T., and M. Kirschner. 1984a. Microtubule assembly nucleated by isolated centrosomes. Nature. 312: 232.

Mitchison, T., and M. Kirschner. 1984b. Dynamic instability of microtubule growth. Nature. 312: 237.

Mitchison, T. J., and M. W. Kirschner. 1985a. Properties of the kinetochore *in vitro*. I. Microtubule nucleation and tubulin binding. J. Cell Biol. 101: 755.

Mitchison, T. J., and M. W. Kirschner. 1985b. Properties of the kinetochore *in vitro*. II. Microtubule capture and ATP-dependent translocation. J. Cell Biol. 101: 766.

Mizuhira, U., and Y. Futaesaku. 1972. Acta Histochem. Cytochem. 5: 233.

Mogensen, M. M., and J. B. Tucker. 1987. Evidence for microtubule nucleation at plasma membrane-associated sites in *Drosophila*. J. Cell Sci. 88: 95.

Mohri, H. 1968. Amino-acid composition of "tubulin" constituting microtubules of sperm flagella. Nature. 217: 1053.

Monasterio, O. 1987. ^{19}F Nuclear Magnetic resonance measurement of the distance between the ε-site GTP and the high-affinity Mg^{2+} in tubulin. Biochemistry. 26: 6099.

Monasterio, O., and N. Timasheff. 1987. Inhibition of tubulin self-assembly and tubulin-colchicine GTPase activity by guanosine 5-(γ-fluorotriphosphate). Biochemistry. 26: 6091.

Monteiro, M. J., and R. A. Cox. 1987. Primary structure of an α-tubulin gene of *Physarum polycephalum*. J. Molec. Biol. 193: 427.

Morejohn, L. C., T. E. Bureau, and D. E. Fosket. 1983. Oryzalin binds to plant tubulin (T) and inhibits taxol-induced microtubule (MT) assembly *in vitro*. J. Cell Biol. 97: 211a.

Morejohn, L. C., T. E. Bureau, L. P. Tocchi, and D. E. Fosket. 1987a. Resistance of *Rosa* microtubule polymerization to colchicine results from a low-affinity interaction of colchicine and tubulin. Planta. 170: 230.

Morejohn, L. C., T. E. Bureau, J. Molè-Bajer, A. S. Bajer, and D. E. Fosket. 1987b. Oryzalin, a dinitroaniline herbicide, binds to plant tubulin and inhibits microtubule polymerization *in vitro*. Planta. 172: 252.

Morejohn, L. C., and D. E. Fosket. 1984. Taxol-induced rose microtubule polymerization *in vitro* and its inhibition by colchicine. J. Cell Biol. 99: 141.

Morejohn, L. C., and D. E. Fosket. 1986. Tubulins from plants, fungi, and protists. In: Cell and Molecular Biology of the Cytoskeleton, Shay, J. W., Ed., 257-321. New York, London. Plenum Press.

Moreland, D. E., F. S. Farmer, and G. G. Hussey. 1972. Inhibition of photosynthesis and respiration by substituted 2,6-dinitroaniline herbicides. I. Effects on chloroplast and mitochodrial activities. Pestic. Biochem. Physiol. 2: 342.

Moriyasu, Y., and M. Tazawa. 1986. Distribution of several proteases inside and outside the central vacuole of *Chara australis*. Cell Struct. Funct. 11: 81.

Mueller, S. C., and R. M. Brown. 1982. The control of cellulose microfibril deposition in the cell wall of higher plants. II. Freeze-fracture microfibril patterns in maize seedling tissues following experimental alteration with colchicine and ethylene. Planta. 154: 501.

Murata, T., A. Kadota, T. Hogetsu, and M. Wada. 1987. Circular arrangement of cortical microtubules around the subapical part of a tip-growing fern protenema. Protoplasma. 141: 135.

Murphy, D. B., and G. G. Borisy. 1975. Association of high-molecular weight proteins with microtubules and their role in microtubule assembly *in vitro*. Proc. Natl Acad. Sci. USA. 72: 2696.

Murphy, D. B., K. A. Johnson, and G. G. Borisy. 1977. Role of tubulin-associated proteins in microtubule nucleation and polymerization. J. Mol. Biol. 117: 33.

Murthy, A. S. N., G. T. Bramblett, and M. Flavin. 1985. The sites at which brain microtubule-associated protein 2 is phosphorylated *in vivo* differ from those accesible to cAMP-dependent kinase *in vitro*. J. Biol. Chem. 260: 4364.

Murthy, A. S. N., and M. Flavin. 1983. Microtubule assembly using the microtubule-associated protein MAP-2 prepared in defined states of phosphorylation with protein kinase and phosphatase. Eur. J. Biochem. 137: 37.

Na, G. C., and S. N. Timasheff. 1981. Interaction of calf brain tubulin with glycerol. J. Mol. Biol. 151: 165.

Nagai, R., and L. I. Rebhun. 1966. Cytoplasmic microfilaments in streaming *Nitella* cells. J. Ultrastruct. Res. 14: 571.

Neville, A. C., D. C. Gubb, and R. M. Crawford. 1976. A new model for cellulose architecture in some plant cell walls. Protoplasma. 90: 307.

Neville, A., and S. Levy. 1984. Helicoidal orientation of cellulose microfibrils in *Nitella opaca* internode cells: ultrastructure and computed theoretical effects of strain reorientation during wall growth. Planta. 162: 370.

Newcomb, E. H. 1969. Plant microtubules. Ann. Rev. Plant Physiol. 20: 253.

Nishida, E., H. Kumagai, I. Ohtsuki, and H. Sakai. 1979. The interactions between calcium-dependent regulator protein of cyclic nucleotide phosphodiesterase and microtubule proteins. I. Effect of calcium-dependent regulator protein on the calcium sensitivity of microtubule assembly. J. Biochem. 85: 1257.

O'Brien, T., W. A. Voter, and H. P. Erickson. 1987. GTP hydrolysis during microtubule assembly. Biochemistry. 26: 4148.

Ockleford, C. D., and J. B. Tucker. 1973. Growth, breakdown, repair and rapid contraction of microtubular axopodia in the heliozoan *Actinophrys sol*. J. Ultrastruct. Res. 44: 369.

Okamura, S. 1979. Effects of colchicine, griseofulvin and caffeine on cell shape in septum formation of cultured carrot cells in suspension. Cell Structure and Function. 4: 11.

Okuda, K., and S. Mizuta. 1987. Modification in cell shape un-related to cellulose microfibril orientation in growing thallus cells of *Chaetomorpha moniligera*. Plant Cell Physiol. 28: 461.

Olmsted, J. B., and G. G. Borisy. 1973. Characterization of microtubule assembly in porcine brain extracts by viscometry. Biochemistry. 12: 4282.

Olmsted, J. B., and G. G. Borisy. 1975. Ionic and nucleotide requirements for microtubule polymerization *in vitro*. Biochemistry. 14: 3996.

Olmsted, J. B., J. M. Marcum, K. A. Johnson, C. Allen, and G. G. Borisy. 1974. Microtubule assembly: some possible regulatory mechanisms. J. Supramol. Struct. 2: 429.

Oosawa, F., and M. Kasai. 1962. A theory of linear and helical aggregations of macromolecules. J. Mol. Biol. 4: 10.

Palevitz, B. A. 1987. Actin in the preprophase band of *Allium cepa*. J. Cell Biol. 104: 1515.

Palevitz, B. A. 1988. Microtubular fir-trees in mitotic spindles of onion roots. Protoplasma. 142: 74.

Palevitz, B. A., and P. K. Hepler. 1976. Cellulose microfibril orientation and cell shaping in developing guard cells of *Allium*. The role of microtubules and ion accumulation. Planta. 132: 71.

Pantaloni, D., M. F. Carlier, C. Simon, and G. Batelier. 1981. Mechanism of tubulin assembly: role of rings in the nucleation process and of associated proteins in the stabilization of microtubules. Biochemistry. 20: 4709.

Parameswaran, N., and W. Liese. 1981. Occurrence and structure of polylamellate walls in some lignified cells. In: Cell Walls '81, Robinson, D. G., Quader, H., Eds., pp. 171-188. Stuttgart. Wissenschaftliche Verlagsgesellschaft.

Parysek, L. M., J. J. Wolosewick, and J. B. Olmsted. 1984. MAP4: a microtubule-associated protein specific for a subset of tissue microtubules. J. Cell Biol. 99: 2287.

Pearson, P. J., and J. B. Tucker. 1977. Control of shape and pattern during the assembly of a large microtubule bundle. Evidence for a microtubule-nucleating-template. Cell Tissue Res. 180: 241.

Penningroth, S. M., D. W. Cleveland, and M. W. Kirschner. 1976. *In vitro* studies of the regulation of microtubule assembly. In: Cell motility, Goldman, R., Pollard, T., Rosenbaum, J., Eds., Cold Spring Harbour Lab.

Penningroth, S. M., and M. W. Kirschner. 1977. Nucleotide binding and phosphorylation in microtubule assembly *in vitro*. J. Mol. Biol. 115: 643.

Pepper, D. A., and B. R. Brinkley. 1979. Microtubule initiation at kinetochores and centrosomes in lysed mitotic cells: Inhibition of site specific nucleation by tubulin antibody. J. Cell Biol. 82: 585.

Pernice, B. 1889. Sulla cariocinesi delle epitheliali e dell'endotellio dei vasi della mucosa dello stomaco et dell'intestino, nelle studio della gastroenterite sperimentale (nell'avvelenamento per colchico). Sicilia Med. 1: 265.

Pickett-Heaps, J. D. 1967a. Ultrastructure and differentiation in *Chara sp.* I. Vegetative cells. Aust. J. biol. Sci. 20: 539.

Pickett-Heaps, J. D. 1967b. The effects of colchicine on the ultrastructure of dividing plant cells, xylem wall differentiation and distribution of cytoplasmic microtubules. Devel. Biol. 15: 206.

Pickett-Heaps, J. D. 1969. The evolution of the mitotic apparatus: an attempt at comparative ultrastructural cytology in dividing plant cells. Cytobios. 1: 257.

Pickett-Heaps, J. D. 1974. Plant Microtubules. In: Dynamic aspects of plant ultrastructure, Robards, A. W., Ed., pp. 219-255. London, New York. McGraw Hill.

Pickett-Heaps, J. D., D. H. Tippit, and K. R. Porter. 1982. Rethinking mitosis. Cell. 29: 729.

Pierson, G. B., P. R. Burton, and R. H. Himes. 1978. Alterations in number of protofilaments in microtubules assembled *in vitro*. J. Cell Biol. 76: 223.

Pierson, G. B., P. R. Burton, and R. H. Himes. 1979. Wall substructure of microtubules polymerized *in vitro* from tubulin of crayfish nerve cord and fixed with tannic acid. J. Cell Sci. 39: 89.

Piperno, G., and M. T. Fuller. 1985. Monoclonal antibodies for an acetylated form of α-tubulin recognize the antigen in cilla and flagella from a variety of organisms. J. Cell Biol. 101: 2085.

Piperno, G., M. LeDizet, and X. Chang. 1987. Microtubules containing acetylated α-tubulin in mammalian cells in culture. J. Cell Biol. 104: 289.

Pollard, T. D., S. C. Selden, and P. Maupin. 1984. Interaction of actin microfilaments with microtubules. J. Cell Biol. 99: 33s.

Pollard, T. D., and A. G. Weeds. 1984. The rate constant for ATP hydrolysis by polymerized actin. FEBS Lett. 170: 94.

Ponstingl, H., E. Krauhs, and M. Little. 1983. Tubulin amino acid sequence and consequences. J. Submicrosc. Cytol. 15: 359.

Porter, M. E., J. M. Scholey, D. L. Stemple, G. P. A. Vigers, R. D. Vale, M. P. Scheetz, and J. R. McIntosh. 1987. Characterization of the microtubule movement produced by sea urchin egg kinesin. J. Biol. Chem. 262: 2794.

Preston, R. D. 1974. The Physical Biology of Plant Cell Walls. pp. 491. London. Chapman and Hall.

Preston, R. D. 1988. Cellulose-microfibril-orienting mechanisms in plant cell walls. Planta. 174: 67.

Probine, M. C. 1963. Cell growth and the structure and mechanical properties of the wall in internodal cells of *Nitella opaca*. III. Spiral growth and cell wall structure. J. exp. Bot. 14: 101.

Probine, M. C., and N. F. Barber. 1966. The structure and plastic properties of the cell wall of *Nitella* in relation to extension growth. Aust. J. Biol. Sci. 19: 421.

Probine, M. C., and R. D. Preston. 1958. Protoplasmic streaming and wall structure in *Nitella*. Nature. 182: 1657.

Probine, M. C., and R. D. Preston. 1961. Cell growth and the structure and mechanical properties of the wall in internodal cells of *Nitella opaca*. J. Exp. Bot. 12: 261.

Probine, M. C., and R. D. Preston. 1962. Cell growth and the structure and mechanical properties in internode cells of *Nitella opaca*. II. Mechanical properties of the walls. J. Exp. Bot. 13: 111.

Purich, D. L., B. J. Terry, R. K. Macneak, and T. L. Karr. 1982. Characterization of tubulin and microtubule-associated protein interactions with guanine nucleotides and their non-hydrolyzable analogs. In: Methods in cell biology, Vol 25. The cytoskeleton. Part B. Structural and contractile proteins, Wilson, L., Ed., pp. 416-432. New York, London. Academic Press.

Quader, H., I. Wagenbreth, and D. G. Robinson. 1978. Structure, synthesis and orientation of microfibrils. V. On the recovery of *Oocystis solitaria* from microtubule inhibitor treatment. Cytobiologie. 18: 39.

Raff, E. C. 1984. Genetics of microtubule systems. J. Cell Biol. 99: 1.

Raudaskoski, M., H. Astrom, K. Pertilla, I. Virtanen, and J. Louhelainen. 1987. Role of the microtubule cytoskeleton in pollen tubes: an immunocytochemical and ultrastructural approach. Biol. Cell. 61: 177.

Raybin, D., and M. Flavin. 1977. Enzyme which specifically adds tyrosine to the α-chain of tubulin. Biochemistry. 16: 2189.

Regula, C. S., J. R. Pfeiffer, and R. D. Berlin. 1981. Microtubule assembly and disassembly at alkaline pH. J. Cell Biol. 89: 45.

Richmond, P. A. 1983. Patterns of cellulose microfibril deposition and rearrangement in *Nitella: in vivo* analysis by a birefringence index. J. Appl. Polymer Science: Appl. Polymer Symp. 37: 107.

Richmond, P. A., S. Lukens, and C. Ericsson. 1988. A comparison of microtubule arrangements in young and mature *Nitella* internodes. The American Society for Cell Biology Summer Research Conference: Algal Experimental Systems in Cell Biological Research. The American Society for Cell Biology, 9650 Rockville Pike, Bethesda, MD 20814, pp. Abstract No. 46.

Richmond, P. A., J-P. Métraux, and L. Taiz. 1980. Cell expansion patterns and directionality of wall mechanical properties in *Nitella*. Plant Physiol. 65: 211.

Rieder, C. L., and G. G. Borisy. 1981. The attachment of kinetochores to the pro-metaphase spindle in PtK1 cells Recovery from low temperature treatment. Chromosoma. 82: 693.

Riederer, B., R. Cohen, and A. Matus. 1986. MAP5: a novel brain microtubule-associated protein under strong developmental regulation. J. Neurocytol. 15: 763.

Roberts, I. N., C. W. Lloyd, and K. Roberts. 1985. Ethylene-induced microtubule reorientations: mediation by helical arrays. Planta. 164: 439.

Roberts, L. W., and S. Baba. 1968. IAA-induced xylem differentiation in the presence of colchicine. Plant Cell Physiol. 9: 315.

Robinson, D. G., I. Grimm, and H. Sachs. 1976. Colchicine and microfibril orientation. Protoplasma. 89: 375.

Robinson, D. G., and H. Quader. 1980. Structure, synthesis and orientation of microfibrils. VII. Microtubule reassembly in vivo after cold treatment in *Oocystis* and its relevance to microfibril orientation. Eur. J. Cell Biol. 21: 229.

Robinson, D. G., and H. Quader. 1982. The microtubule-microfibril syndrome. In: The Cytoskeleton in Plant Growth and Development, Lloyd, C. W., Ed., pp. 109-126. London. Academic Press.

Roland, J. C. 1981. Comparison of arced patterns in growing and non-growing polylamellate cell walls of higher plants. In: Cell Walls '81, Robinson, D. G., Quader, H., Eds., pp. 162-170. Stuttgart. Wissenschaftliche Verlagsgesellschaft.

Roland, J. C., and M. Mosiniak. 1983. On the twisting pattern, texture and layering on the secondary cell walls of lime wood. Proposals of an unifying model. IAWA Bull. 4: 15.

Roland, J. C., D. Reis, M. Mosiniak, and B. Vian. 1982. Cell wall texture along the growth gradient of mung bean hypocotyl: ordered assembly and dissipative processes. J. Cell Sci. 56: 303.

Rosenbaum, J. L., and F. M. Child. 1967. Flagellar regeneration in protozoan flagellates. J. Cell Biol. 34: 345.

Rothwell, S. W., W. A. Grasser, and D. B. Murphy. 1986. End-to-end annealing of microtubules *in vitro*. J. Cell Biol. 102: 619.

Saito, K., and K. Hama. 1982. Structural diversity of microtubules in the supporting cells of the sensory epithelium of guinea pig organ of Corti. J. Electron Microsc. 31: 278.

Sale, W. S., J. C. Besharse, and G. Piperno. 1988. Distribution of acetylated α-tubulin in retina and in *in vitro*-assembled microtubules. Cell Motil. Cytoskeleton. 9: 243.

Sale, W. S., and P. Satir. 1977. Direction of active sliding of microtubules in *Tetrahymena* cilia. Proc. Natl. Acad. Sci. 74: 2045.

Sammak, P. J., and G. G. Borisy. 1988. Direct observation of microtubule dynamics in living cells. Nature. 332: 724.

Sammak, P. J., G. J. Gorbsky, and G. G. Borisy. 1987. Microtubule dynamics *in vivo*: a test of mechanisms of turnover. J. Cell Biol. 104: 395.

Sandoval, I. V., J. L. Jameson, J. Niedel, E. McDonald, and P. Cuatrecasas. 1978. Role of nucleotides in tubulin polymerization. Effect of guanosine 5'-methylene diphosphate. Proc. Natl. Acad. Sci. USA. 75: 3178.

Sandoval, I. V., and K. Weber. 1979. Polymerization of tubulin in the presence of colchicine or podophyllotoxin. Formation of a ribbon structure induced by guanylyl-5'-methylene diphosphate. J. Mol. Biol. 134: 159.

Sasaki, S., J. K. Stevens, and N. Bodick. 1983. Serial reconstruction of microtubular arrays within dendrites of the cat retinal ganglion cell: the cytoskeleton of a vertebrate dendrite. Brain Res. 259: 193.

Sasse, R., M. C. P. Glyn, C. R. Birkett, and K. Gull. 1987. Acetylated α-tubulin in *Physarum*: Immunological characterization of the isotype and its usage in particular microtubular organelles. J. Cell Biol. 104: 41.

Satir, P., J. Wais-Steider, S. Lebduska, A. Nasr, and J. Avolio. 1981. The mechanochemical cycle of the dynein arm. Cell Motility. 1: 303.

Sattilaro, R. F., W. L. Dentler, and E. L. LeCluyse. 1981. Microtubule-associated proteins (MAPs) and the organization of actin filaments *in vitro*. J. Cell Biol. 90: 467.

Sauk, J. J., M. Krumwiede, D. Cocking-Johnson, and J. G. White. 1987. Alterations in lipid fluidity induced by cholesterol and cholesterol hemisuccinate modulate the organization of microtubule skeletons in epithelial cells. J. Oral Pathol. 16: 69.

Saxton, W. M., M. E. Porter, S. A. Cohn, J. M. Scholey, E. C. Raff, and J. R. McIntosh. 1988. *Drosophila* kinesin: characterization of microtubule motility and ATPase. Proc. Natl. Acad. Sci. USA. 85: 1109.

Scheele, R. B., L. G. Bergen, and G. G. Borisy. 1982. Control of the structural fidelity of microtubules by initiation sites. J. Mol. Biol. 154: 485.

Schibler, M. J., and J. D. Pickett-Heaps. 1987. The kinetochore fiber structure in the acentric spindles of the green alga *Oedogonium*. Protoplasma. 137: 29.

Schiff, P. B., J. Fant, and S. B. Horwitz. 1979. Promotion of microtubule assembly *in vitro* by taxol. Nature. 277: 665.

Schilstra, M. J., S. R. Martin, and P. M. Bayley. 1987. On the relationship between nucleotide hydrolysis and microtubule assembly: studies with a GTP-regenerating system. Biochem. Biophys. Res. Comm. 147: 588.

Schliwa, M., U. Euteneuer, J. C. Bulinski, and J. G. Izant. 1981. Calcium lability of cytoplasmic microtubules and its modulation by microtubule-associated proteins. Proc. Natl Acad. Sci. USA. 78: 1037.

Schmit, A.-C., M. Vantard, J. De Mey, and A.-M. Lambert. 1983. Aster-like microtubule centers establish spindle polarity during interphase-mitosis transition in higher plant cells. Plant Cell Rep. 2: 285.

Schneider, B., and W. Herth. 1986. Distribution of plasma membrane rosettes and kinetics of cellulose formation in xylem development of higher plants. Protoplasma. 131: 142.

Schnepf, E. 1974. Microtubules and cell wall formation. Port. Acta Biol. Ser. A. 14: 451.

Schnepf, E., G. Deichgraber, and N. Ljubesic. 1976. The effects of colchicine, ethionine and deuterium oxide on microtubules in young *Sphagnum* leaflets. A quantitative study. Cytobiology. 13: 341.

Schroeder, M., J. Wehland, and K. Weber. 1985. Immunofluorescence microscopy of microtubules in plant cells; stabilization by dimethylsulfoxide. Eur. J. Cell Biol. 38: 211.

Schulze, E., D. J. Asai, J. C. Bulinski, and M. Kirschner. 1987. Posttranslational modification and microtubules stability. J. Cell Biol. 105: 2167.

Schulze, E., and M. Kirschner. 1986. Microtubule dynamics in interphase cells. J. Cell Biol. 102: 1020.

Seagull, R. W. 1983. The role of the cytoskeleton during oriented microfibril deposition. I. Elucidation of the possible interaction between microtubules and cellulose synthetic complexes. J. Ultrastruct. Res. 83: 168.

Seagull, R. W. 1986. Changes in microtubule organization and wall microfibril orientation during *in vitro* cotton fiber development: an immunofluorescent study. Can. J. Bot. 64: 1373.

Seagull, R. W., M. M. Falconer, and C. A. Weerdenburg. 1987. Microfilaments: dynamic arrays in higher plant cells. J. Cell Biol. 104: 995.

Seagull, R. W., and I. B. Heath. 1980. The organization of cortical microtubule arrays in the radish root hair. Protoplasma. 103: 205.

Segaar, P. J., and G. M. Lokhorst. 1988. Dynamics of the microtubular cytoskeleton in the green alga *Aphanochaete magna* (Chlorophyta). I. Late mitotic stages and the origin and development of the Phycoplast. Protoplasma. 142: 176.

Shelanski, M. L., and E. W. Taylor. 1967. Isolation of a protein subunit from microtubules. J. Cell Biol. 34: 549.

Sheldon, J. M., and H. G. Dickinson. 1986. Pollen wall formation in *Lilium*: The effect of chaotropic agents, and the organization of the microtubular cytoskeleton during pattern development. Planta. 168: 11.

Sherwin, T., A. Scheider, R. Sasse, T. Seebeck, and K. Gull. 1987. Distinct localization and cell cycle dependence of COOH terminally tyrosinated α-tubulin in the microtubules of *Trypanosoma brucei brucei*. J. Cell Biol. 104: 439.

Simmonds, D., G. Setterfield, and D. L. Brown. 1983. Organization of microtubules in dividing and elongating cells of *Vicia hajastana* Grossh. in suspension culture. Eur. J. Cell Biol. 32: 59.

Simmonds, D. H., and G. Setterfield. 1986. Aberrant microtubule organization can result in genetic abnormalities in protoplast cultures of *Vicia hajastana*. Protoplasma. 167: 460.

Slautterback, D. B. 1963. Cytoplasmic microtubules. I. *Hydra*. J. Cell Biol. 18: 367.

Smith, P. T., and N. A. Walker. 1981. Studies on the perfused plasmalemma of *Chara corallina*: I. Current-voltage curves: ATP and potassium dependence. J. Memb. Biol. 60: 223.

Sobue, K., M. Fujita, and Y. K. Muramoto, S. 1981. The calmodulin-binding protein in microtubules is Tau-factor. FEBS Lett. 132: 137.

Soltys, B. J., and G. G. Borisy. 1985. Polymerizatin of tubulin *in vivo*: Direct evidence for assembly onto microtubule ends and from centrosomes. J. Cell Biol. 100: 1682.

Srivastava, L. M., V. K. Sawhney, and M. Bonettemaker. 1977. Cell growth, wall deposition and correlated fine structure of colchicine treated lettuce hypocotyl cells. Can J. Bot. 55: 902.

Stearns, M. E., and D. L. Brown. 1979. Purification of a microtubule-associated protein based on its preferential association with tubulin during microtubule initiation. FEBS Lett. 101: 15.

Stearns, M. E., and D. L. Brown. 1981. Microtubule organizing centers (MTOCs) of the alga *Polytomella* exert spatial control over microtubule initiation in vivo and in vitro. J. Ultrastruct. Res. 77: 366.

Strachan, S. D., and F. D. Hess. 1983. The biochemical mechanism of action of the dinitroaniline herbicide oryzalin. Pestic. Biochem. Physiol. 20: 141.

Summers, K. E., and M. W. Kirschner. 1977. The effect of polarity and capping on microtubule stability *in vitro* as observed by darkfield light microscopy. J. Cell. Biol. 75: 296a.

Szathmary, E. 1987. Early evolution of microtubules and undulipodia. BioSystems. 20: 115.

Taiz, L. 1984. Plant cell expansion: Regulation of cell wall mechanical properties. Ann. Rev. Plant Physiol. 35: 585.

Takeda, K., and H. Shibaoka. 1981. Effects of gibberellin and colchicine on mf arrangement in epidermal cell walls of *Vigna angularis* Ohwi et Ohashi epicotyls. Planta. 151: 393.

Taylor, E. W. 1965. The mechanism of colchicine inhibition of mitosis. I. Kinetics of inhibition and the binding of H^3-colchicine. J. Cell Biol. 25: 145.

Telzer, B. R., and L. T. Haimo. 1981. Decoration of spindle microtubules with dynein: evidence for uniform polarity. J. Cell Biol. 89: 373.

Terry, B. J., and D. L. Purich. 1979. Nucleotide release from tubulin and nucleoside-5'-diphosphate kinase action in microtubule assembly. J. Biol. Chem. 254: 9469.

Terry, B. J., and D. L. Purich. 1980. Assembly and disassembly of microtubules formed in the presence of GTP, 5'-guanylyl imidodiphosphate and 5'-guanylyl methylenediphosphate. J. Biol. Chem. 255: 10532.

Tewinkel, M., and D. Volkmann. 1987. Observations on dividing plastids in the protenema of the moss *Funaria hygrometrica* Sibth. Arrangement of microtubules and filaments. Planta. 172: 309.

Tiwari, S. C., S. M. Wick, R. E. Williamson, and B. E. S. Gunning. 1984. The cytoskeleton and integration of cellular function in cells of higher plants. J. Cell Biol. 99: 63s.

Tjio, J. H., and A. Levan. 1956. The chromosome number of man. Hereditas. 42: 1.

Toko, K., H. Chosa, and K. Yamafuji. 1985. Dissipative structure in the *Characeae*: spatial pattern of proton flux as a dissipative structure in characean cells. J. Theor. Biol. 114: 127.

Toko, K., T. Fujiyoshi, K. Ogata, H. Chosa, and K. Yamafuji. 1987. Theory of electric dissipative structure in characean internode. Biophys. Chem. 27: 149.

Toko, K., K. Hayashi, T. Yoshida, T. Fujiyoshi, and K. Yamafuji. 1988. Oscillations of electric spatial patterns emerging from the homogeneous state in characean cells. Eur. Biophys. J. 16: 11.

Traas, J. A. 1984. Visualization of the membrane bound cytoskeleton and coated pits of plant cells by means of dry cleaving. Protoplasma. 119: 212.

Traas, J. A., P. Braat, A. M. C. Emons, H. M. T. Meekes, and J. W. M. Derksen. 1985. Microtubules in root hairs. J. Cell Sci. 76: 303.

Traas, J. A., P. Braat, and J. W. Derksen. 1984. Changes in microtubule arrays during the differentiation of cortical root cells of *Raphanus sativus*. Eur. J. Cell Biol. 34: 229.

Traas, J. A., J. H. Doonan, D. J. Rawlins, P. J. Shaw, J. Watts, and C. W. Lloyd. 1987. An actin network is present in the cytoplasm throughout the cell cycle of carrot cells and associates with the nucleus. J. Cell Biol. 105: 387.

Tsukita, S., and H. Ishihawa. 1981. The cytoskeleton in myelinated axons: serial section study. Biomed. Res. 2: 424.

Tucker, J. B. 1977. Shape and pattern specification during microtubule bundle assembly. Nature (London). 266: 22.

Tucker, J. B. 1979. Spatial organization of microtubules. In: Microtubules , Roberts, K., Hyams, J. S., Eds., pp. 315-358. London. Academic Press.

Tucker, J. B. 1984. Spatial organization of microtubule-organizing centers and microtubules. J. Cell Biol. 99: 55s.

Unger, E., K. J. Böhm, and W. Vater. 1986. Factors regulating microtubule structure - A minireview. Acta histochemica. Suppl.-Band XXXIII: S. 85.

Upadhyaya, M. K., and L. D. Nooden. 1977. Mode of dinitroaniline herbicide action I. Analysis of the colchicine-like effects of dinitroaniline herbicides. Plant Cell Physiol. 18: 1319.

Upadhyaya, M. K., and L. D. Nooden. 1980. Mode of dinitroaniline herbicide action II. Characterization of [^{14}C]oryzalin uptake and binding. Plant Physiol. 66: 1048.

Vale, R. D., T. S. Reese, and M. P. Sheetz. 1985. Identification of a novel force-generating protein, kinesin, involved in microtubule-based motility. Cell. 42: 39.

Vale, R. D., B. J. Schnapp, T. Mitchison, E. Steur, T. S. Teese, and M. P. Sheetz. 1985. Different axoplasmic proteins generate movement in opposite directions along microtubules *in vitro*. Cell. 43: 623.

Vale, R. D., and Y. Y. Toyoshima. 1988. Rotation and translocation of microtubules *in vitro* induced by dyneins from *Ttetrahymena* cilia. Cell. 52: 459.

Valenzuela, P., M. Quiroga, J. Zaldivar, W. J. Rutter, M. W. Kirschner, and D. W. Cleveland. 1981. Nucleotide and corresponding amino acid sequences encoded by α and β tubulin mRNAS. Nature. 289: 650.

Vallee, R. B. 1980. Structure and phosphorylation of microtubule-associated protein-2 (MAP2). Proc. Natl Acad. Sci. USA. 77: 3206.

Vallee, R. B. 1982. A taxol-dependent procedure for the isolation of microtubules and microtubule-associated proteins (MAPs). J. Cell Biol. 92: 435.

Vallee, R. B., and G. G. Borisy. 1978. The non-tubulin component of microtubule protein oligomers. Effect on self-association and hydrodynamic properties. J. Biol. Chem. 253: 2834.

Van Der Valk, P., P. J. Rennie, J. A. Connolly, and L. C. Fowke. 1980. Distribution of cortical microtubules in tobacco protoplasts. An immunofluorescence microscopic and ultrastructural study. Protoplasma. 105: 27.

Van Lammeren, A. A. M., C. J. Keijzer, M. T. M. Willemse, and H. Kieft. 1985. Structure and function of the microtubular cytoskeleton during pollen development in *Gasteria verrucosa* (Mill.) H. Duval. Planta. 165: 1.

Vater, W., K. Böhm, and E. Unger. 1983. Effects of DNA on the taxol-stimulated *in vitro* assembly of microtubule protein from porcine brain. Stud. biophys. 97: 49.

Vera, J., C. Rivas, and R. B. Maccioni. 1988. Antibodies to synthetic peptides from the tubulin regulatory domain interact with tubulin and microtubules. Proc. Natl. Acad. Sci. USA. 85: 6763.

Viklicky, V., P. Oraber, J. Hasek, and J. Bartek. 1982. Production and characterization of a monoclonal antitubulin antibody. Cell Biol. Int. Rep. 6: 725.

Villasante, A., J. Dela Torre, R. Manso-Martinez, and J. Avila. 1980. Microtubule-associated protein MAP 1 is not implicated in the polymerization of microtubules. Eur. J. Biochem. 112: 611.

Wacker, I., H. Quader, and E. Schnepf. 1988. Influence of the herbicide oryzalin on cytoskeleton and growth of *Funaria hygrometrica* protenemata. Protoplasma. 142: 55.

Wadsworth, P., and E. D. Salmon. 1986. Analysis of the treadmilling model during metaphase of mitosis using fluorescence redistribution after photobleaching. J. Cell Biol. 102: 1032.

Walker, N. A., and F. A. Smith. 1977. Circulating electric currents between acid and alkaline zones associated with HCO3- assimilation in *Chara*. J. Exp. Bot. 28: 1190.

Walker, R. A., N. K. Pryer, L. U. Cassimeris, M. Soboeiro, and E. D. Salmon. 1986. Axoneme-nucleated MAP-free microtubules exhibit polarity-dependent dynamic instability: a real time observation. J. Cell Biol. 103: 432a.

Wallin, M., H. Larsson, and A. Edstrom. 1977. Tubulin sulfhydryl groups and polymerization *in vitro*. Expl Cell Res. 107: 219.

Wandosell, F., L. Serrano, and J. Avila. 1987. Phosphorylation of α-tubulin carboxyl-terminal tyrosine prevents its incorporation into microtubules. J. Biol. Chem. 262: 8268.

Wardrop, A. B. 1962. Cell wall organization in higher plants. I. The primary wall. Bot. Rev. 28: 241.

Wasteneys, G. O., and R. E. Williamson. 1987. Microtubule orientation in developing internodal cells of Nitella: a quantitative analysis. Eur. J. Cell Biol. 43: 14.

Waxman, P. G., A. A. Del Campa, M. C. Lowe, and E. Hamel. 1981. Induction of polymerization of purified tubulin by sulfonate buffers. Marked differences between 4-morpholineethanesulfonate (Mes) and 1,4-piperazineethanesulfonate (Pipes). Eur. J. Biochem. 120: 129.

Webster, D. R., G. G. Gundersen, J. C. Bulinski, and G. G. Borisy. 1986. Cellular detyrosinated microtubules turn over slowly. J. Cell Biol. 103: 1009a.

Webster, D. R., G. G. Gundersen, J. C. Bulinski, and G. G. Borisy. 1987a. Assembly and turnover of detyrosinated tubulin *in vivo*. J. Cell Biol. 105: 265.

Webster, D. R., G. G. Gundersen, J. C. Bulinski, and G. G. Borisy. 1987b. Differential turnover of tyrosinated and detyrosinated microtubules. Proc. Natl Acad. Sci. USA. 84: 9040.

Wehland, J., and K. Weber. 1987. Turnover of the carboxy-terminal tyrosine of a-tubulin and means of reaching elevated levels of detyrosination in living cells. J. Cell Sci. 88: 185.

Weingarten, M. D., A. H. Lockwood, Hwo S.-Y., and M. W. Kirschner. 1975. A protein factor essential for microtubule assembly. Proc. Natl Acad. Sci. USA. 72: 1858.

Weisenberg, R. C. 1972. Microtubule formation *in vitro* in solutions containing low calcium concentrations. Science. 177: 1104.

Weisenberg, R. C. 1981. The role of nucleotide triphosphate in actin and tubulin assembly and function. Cell Motility. 1: 485.

Weisenberg, R. C., G. G. Borisy, and E. W. Taylor. 1968. The colchicine-binding protein of mammalian brain and its relation to microtubules. Biochemistry. 7: 4466.

Weisenberg, R. C., and W. J. Deery. 1976. Role of nucleotide hydrolysis in microtubule assembly. Nature. 263: 792.

Weisenberg, R. C., W. J. H. Deery, and P. Dickinson. 1976. Nucleotide interactions during polymerization and depolymerization of tubulin. In: Cell motility, Goldman, P., Pollard, T., Rosenbaum, J., Eds., pp. 1123-1132. Cold Spring Harbor Lab.

Weisenberg, R. C., and A. C. Rosenfeld. 1975. *In vitro* polymerization of microtubules into asters and spindles in homogenates of surf clam eggs. J. Cell Biol. 64: 146.

White, H. D., B. A. Coughlin, and D. L. Purich. 1980. Adenosine triphosphate activity of bovine brain microtubule protein. J. Biol Chem. 255: 486.

Wick, S. M. 1985. The higher plant mitotic apparatus: redistribution of microtubules, calmodulin and microtubule initiation material during its establishment. Cytobios. 43: 285.

Wick, S. M., and J. Duniec. 1983. Immunofluorescence microscopy of tubulin and microtubule arrays in plant cells. I. Preprophase band development and concomitant appearance of nuclear envelope-associated tubulin. J. Cell Biol. 97: 235.

Wick, S. M., and J. Duniec. 1984. Immunofluorescence microscopy of tubulin and microtubule arrays in plant cells. II. Transition between the pre-prophase band and the mitotic spindle. Protoplasma. 122: 45.

Wick, S. M., and J. Duniec. 1986. Effects of various fixatives on the reactivity of plant cell tubulin and calmodulin in immuofluorescence microscopy. Protoplasma. 133: 1.

Wick, S. M., R. W. Seagull, M. Osborn, K. Weber, and B. E. S. Gunning. 1981. Immunofluorescence microscopy of organized microtubule arrays in structurally stabilized meristematic plant cells. J. Cell Biol. 89: 685.

Williams, R. C., and J. C. Lee. 1982. Preparation of tubulin from brain. In: Methods in Cell Biology, Vol. 25. The cytoskeleton, Part B. Structural and contractile proteins, Wilson, L., Ed., pp. 376-384. New York, London. Academic Press.

Williamson, R. E. 1975. Cytoplasmic streaming in *Chara*: a cell model activated by ATP and inhibited by cytochalasin B. J. Cell Sci. 17: 655.

Williamson, R. E. 1985. Immobilisation of organelles and actin bundles in the cortical cytoplasm of the alga *Chara corallina* Klein ex. Wild. Planta. 163: 1.

Williamson, R. E., U. A. Hurley, and J. L. Perkin. 1984. Regeneration of actin bundles in *Chara*: polarised growth and orientation by endoplasmic flow. Eur. J. Cell Biol. 34: 221.

Williamson, R. E., D. W. McCurdy, U. A. Hurley, and J. L. Perkin. 1987. Actin of *Chara* giant internodal cells. Plant Physiol. 85: 268.

Williamson, R. E., J. L. Perkin, and U. A. Hurley. 1985. Selective extraction of *Chara* actin bundles: identification of actin and two coextracting proteins. Cell Biol. Int. Reports. 9: 547.

Williamson, R. E., and B. H. Toh. 1979. Motile models of plant cells and the immunofluorescent localization of actin in a motile *Chara* cell model. In: Cell motility: molecules and organisation, Hatano, S, Ishikawa, H., Sato, H., Eds., Tokyo. University of Tokyo Press.

Willison, J. H. M. 1975. Plant cell wall disposition revealed by freeze-fractured plasmalemma not treated with glycerol. Planta. 126: 93.

Yamauchi, P. S., and D. S. Purich. 1987. Modulation of microtubule assembly and stability by phosphatidylinositol action on microtubule-associated protein-2. J. Biol. Chem. 262: 3369.

Yamauchi, T., and H. Fujisawa. 1988. Regulation of the interaction of actin filaments with microtubule-associated protein 2 by calmodulin-dependent protein kinase II. Biochimica et Biophysica Acta. 968: 77.

Yocum. 1980. Measurement of photophosphorylation associated with photosystem II. Methods in Enzymology. 69: 576.

Zabrecky, J. R., and R. D. Cole. 1980. ATP-induced aggregates of tubulin rings. J. Biol. Chem. 255: 11981.

Zabrecky, J. R., and R. D. Cole. 1982. Effect of ATP on the kinetics of microtubule assembly. J. Biol Chem. 257: 4633.

Zeeberg, B., J. Check, and M. Caplow. 1980. Exchange of tubulin dimmer into rings in microtubule assembly-disassembly. Biochemistry. 19: 5078.